Polymers, Metal Compounds and New Materials

Vasile Gutsanu

Polymers, Metal Compounds and New Materials

Polymers, Metal Compounds and New Materials

By

Vasile Gutsanu

Cambridge
Scholars
Publishing

Polymers, Metal Compounds and New Materials

By Vasile Gutsanu

This book first published 2020

Cambridge Scholars Publishing

Lady Stephenson Library, Newcastle upon Tyne, NE6 2PA, UK

British Library Cataloguing in Publication Data
A catalogue record for this book is available from the British Library

ISBN (10): 1-5275-4308-0
ISBN (13): 978-1-5275-4308-9

CONTENTS

PREFACE

The monograph stands for an investigation of the interaction of strongly basic anion exchangers with some metal cations, a theoretically improbable process since such anionites have affinity towards anions. These polymers are produced at an industrial scale and are widely used in various chemical and technical operations, but most of all in the treatment of water at thermal and atomic power stations. Their interaction with metal cations, especially with iron, an unpredictable and uncontrollable process, leads to their intoxication and rapid exhaustion. However, if the interaction of these polymers with cations is controlled, then in the polymer phase, ultra-fine particles of the compounds are formed, that radically change their physical and chemical properties. These composites become selective sorbents and catalysts with good hydro and aerodynamic properties to conduct processes in flow, a key factor in technology. This is proven by patents on water purification from chromates, nitrate/nitrite, sulphides and air purification from iodine and hydrogen sulfide. These composites can be used to make anti-gas masks that would protect the personnel of atomic stations. The monograph shows for the first time that cations Fe^{3+}, Cr^{3+}, Al^{3+}, Ga^{3+}, In^{3+}, lanthanide (III) in the phase of strongly basic anion exchangers form compounds of the jarosite mineral type. Bismuth (III) forms another type of compound. The compounds in the polymer phase, coordinating with polydentate ligands, allow the construction of various composite holding active multi-centres, which is very important, and not only for catalysis.

The jarosite is formed in the aqueous medium. That is why the discovery of the jarosite on Mars led to the discovery of water on the planet. Investigating the jarosite on Earth could give us much information about the evolution of the processes on some heavenly bodies. The catalytic properties of polymers modified with metallic compounds have not been practically studied. A wide field of activity opens up. The monograph shows that such composites can fix nitrogen from the air under normal conditions.

The monograph can be useful for chemists, technologists, environmentalists, specialists in the water treatment industry, chemical engineers, students and even mineralogists and others.

INTRODUCTION

What happens if a cross linked ionic polymer having strongly basic groups $-N(CH_3)_3Cl$ were to be placed in an electrolyte solution? Any chemist and not only chemists will say that there will be only a reversible and non-selective process of anion exchange: $R_4NCl + A^- \leftrightarrow R_4NA + Cl^-$. Due to this process such polymers are widely used in technologies of substances separation, concentration and water treatment. The positive aspect of these polymers is their ability to remove from solution all negatively charged particles regardless of their nature. This property, along with the property of the strongly acid cation exchangers to remove all particles with positive charges, is widely used to obtain deionized liquids, first of all water. The downside of the strongly basic polymers is that they are not selective. But the advanced technologies, especially in the chemical industry, medicine, analytical chemistry and environmental protection, need new adsorbents and catalysts with selective properties. The properties of polymers, containing strongly basic groups, would change essentially if they could be synthesized using metal compounds in their phase. However, their polymer matrix does not contain negatively charged or electron-donor atoms and, theoretically, they cannot interact with cations. Surprisingly, our investigation showed that under certain conditions these polymers can interact with metal cations from solutions such as Fe^{3+}, Cr^{3+}, Al^{3+} and others.

In this book the research findings of the interaction of cations containing Fe(III), Cr(III), Al(III), Ga(III), In(III) , Lanthanides (III) and BI(III) are discussed. In fact, hydroxocations, rather than hydrated metal cations, interact with functional groups of polymers. The processes, involving ionic cross-linked polymers containing strongly basic groups, were performed using the Mössbauer spectroscopy. In the second part of the book the results of applied research with the use of polymers containing metal compounds into their phase, using FTIR and EPR spectroscopy, SEM, powder X-ray diffraction and thermogravimetric analysis are presented. The book contains research findings of some unusual and incredible processes.

PART I.

METAL COMPOUNDS IN THE POLYMER PHASE

I.

IRON (III) COMPOUNDS IN THE POLYMERS PHASE

1.1. Historic

How did we get the idea to do such researches, the results of which are presented in this book? Was it mere chance or regularity? Firstly, we investigated the sorption of metal cations on different cross-linked ionic polymers [1-3]. We investigated the sorption of Zr(IV), Cr(III), Al(III), Fe(III), Fe(II), Co(II), Ni(II), and Cu(II) containing cations on different polymers (sulfocationites KU 1, KU 2, carboxylic cation exchangers KB-2, KB-4 , exchangers containing amino groups AV-16, EDE-10P, AN-2FN, AN-31 and strongly basic exchanger AV-17 [4]) in a wide range of pH of the solution with the use of so-called "nuclear filter" [5-7]. We have observed that the sorption, in the function of the pH, passes through maximum, which is usually in the range of pH in which existed hydroxide precipitate. Most of the research has been devoted to the complexation processes of metal cations with amine groups of the polymers. It was proved that sorption of Cu^{2+} ions from mixtures of metallic cations on the polymers that contain amine groups is contrary to the Langmuir sorption model. For example, the Cu^{2+} ions sorption by the polymer EDE-10P in solutions containing mixtures of $ZnSO_4$ and $CdSO_4$ is much higher than in their absence, although cations Zn^{2+} and Cd^{2+} also coordinates the amine groups [8-10]. It was shown that the nature and concentration of anions (SO_4^{2-}, NO_3^-, ClO_4^- F^-, Cl^-, Br^-) significantly influence the complexation of Cu^{2+} ions with the amine groups of the polymers [11-16]. Some anions influence positively and others negatively, the metallic cations sorption (complexation) on the polymers holding amine groups. Who could believe that anions can influence, especially negatively, complexation of the cations with amine groups of the polymers? Because of this, in many works the influence of the nature and concentration of the anions on the sorption of metal cations by amine polymers was neglected. Our research has shown that the influence of the nature and concentration of ions on the processes of complexing in the amine polymers phase is manifested in two ways. Anions influence the degree of protonation-deprotonating of amine groups and complexation can occur only with deprotonated groups [17, 18]. On the other hand, some anions coordinate the cations which are already linked to the amine groups. These processes correlate with each other. The investigation, conducted using EPR spectroscopy, showed that in the phase of amine polymers the anions SO_4^{2-}, F^-, Cl^- and cations Cu^{2+} form different isomeric complexes [18]. It also was seen that the nature and concentration of the anions affects differently the process of complexation of Al (III) and Fe (III) having cations with the carboxylic acid groups of the polymers [19-21].

Studying the influence of the anions on the complexation of metal cations with amine groups, we asked whether cations are retained in the polymer phase due to the formation of complexes with negative charges. To answer this question, we introduced a monofunctional cross-linked ionic polymer sample, which held groups of the type $-N(CH_3)_3Cl$ in a solution of $Fe_2(SO_4)_3$.

As known, strongly basic anion exchangers do not hold negatively charged or electron donor atoms in their matrix and, theoretically, they cannot interact with metal cations. They can retain only particles with negative charges. The decision to choose the electrolyte $Fe_2(SO_4)_3$ was determined by the fact that the sorption process can be investigated using Mössbauer spectroscopy that allows us to find whether the sorption occurs through anion exchange or by formation of coordinative bonds. The results of these tests will be depicted in the following paragraphs.

1.2. Iron compounds formed in phase of strongly basic anion exchanger

1.2.1. Transformations in Fe(III)-containing polymer on heating in air

Surprisingly, we have observed [21], that at room temperature cross linked ionic polymer AV-17(Cl) containing quaternary ammonium groups, can sorb Fe(III)-containing cations from sulfate solution, but not from chloride (in the absence of $[FeCl_4]^-$ in the solution) or nitrate solutions. The effects of Cl^-, SO_4^{2-} and other factors on Fe(III)-containing cations sorption by AV-17(Cl) [22-24] were evaluated by mathematical statistical techniques (the response surface methodology-the E.P.Box and K.B.Wilson method) [25]. The Student criterion of the coefficients significance in the regression equations (b_{sig}) was calculated at a level of significance of 5 % and number degree of freedom f =7. These effects are expressed by Equation (1-1), where Y is adsorbed iron (mg Fe/g):

$$Y = 3.074+1.566\ X_1–0.840\ X_2 +0.969\ X_3–1.139\ X_4 + 0.790\ X_5,\ B_{sig.}= t.s\{b_i\} = 0.1759 \quad (1\text{-}1)$$

The following notations are used with the variation intervals given in parentheses: X_1 = pH (1.6-2.0); X_2 = t (30-40°C); $X_3 = K_2SO_4$ (0.03-0.1 N); X_4= KCl (0.03-0.1N); X_5 = acetone (5-10 vol.%); X_6 = ethanol (5-10 vo.%) and X_7 = duration of polymer contact with solution (8-12 h).

An increase in the pH (X_1) and the concentration of SO_4^{2-} (X_3) and acetone (X_5) has a positive effect on Fe(III)-containing cations sorption by AV-17. On the other hand, an increase in the temperature (X_2) and the Cl^- concentration (X_4) has a negative effect on Fe(III)-containing cations sorption. The insignificance of the coefficient X_7 indicates that sorption equilibrium is almost set up after 10 h of polymer-solution contact. To elucidate the nature of the compounds that are formed in the polymer phase in contact with the solution of $Fe_2(SO_4)_3$, the following investigations were made. A commercial strongly basic anion exchanger [AV-17X8, holding $-N(CH_3)_3^+$ groups] in Cl form was used. The gel-type resin had a polystyrene – divinylbenzene matrix. Its full exchange capacity is 3.5– 4.0 mEq/g [4]. Dried polymer samples of 1 g were contacted with 500 mL of 0.01M $Fe_2(SO_4)_3$ solution for 24 h at room temperature, which was enough to set up equilibrium. The pH of the solution-sample systems was 2.0 ± 0.1. Following the contact with the solution, the samples were filtered, washed with distilled water, dried in air, and used for investigations. The Fe(III) content in the samples (12.5 mg/g ± 0.3 mg) was determined by the photo-colorimetry method [14] using 2,2-dipyridine after desorption with a solution of 1–1.5M HCl.

Samples of Fe(III)-containing polymer were heated in air at 100, 120, 140, 160, 180, and 200°C for 6–7 h. These samples were investigated by using Mössbauer, IR, and EPR spectroscopies. To modify the nature, content, and sizes of the Fe-containing particles of compounds in the polymer phase, several sorption– boiling in water cycles with samples of the exchanger were carried out. These samples were also investigated using Mössbauer spectroscopy. The EPR spectra were recorded at 300 K on a RE-1307 radio spectrometer with a 3-cm wavelength. The IR spectra were recorded at 300 K over the 400–4000 cm^{-1} interval on a SPECORD M-70 spectrometer. The Mössbauer spectra were obtained at 300 and 80 K.

NOTE: Here and further, the Mössbauer spectra were recorded on an ICA-70 spectrometer in the accelerated dynamic regime, and ^{57}Co in a Cr matrix was employed as the γ-ray source. In the case of spectra in the form of a doublet for determination of parameters such as isomeric shift (δ), quadrupole splitting (ΔE_Q), left line width (Γ_l), and right line width (Γ_r) of the doublet, sodium nitroprusside was used as the reference. In the case of spectra in the form of a sextet, metallic iron was used as a reference. The error of the intensity on the iron nuclei magnetic field ($H_{ef.}$) was ±5 kOe and for the other parameters was ±0.04 mm/s. All δ values are expressed relative to sodium nitroprusside.

Metallic compounds formed in the phase of strongly basic anion exchangers in contact with $Fe_2(SO_4)_3$ solutions are not $Fe(OH)_3$ or FeOOH. The Mössbauer spectra of the Fe(III)-containing strongly basic anion exchangers show large values of quadrupole splitting (ΔE_Q - 1 mm/s) [26] whereas they are less for $Fe(OH)_3$ or FeOOH (about 0.7 mm/s). We suggest that the sorption of Fe(III)-containing ions from $Fe_2(SO_4)_3$ solutions on strongly basic anion exchangers takes place through formation in the polymer phase of $FeOHSO_4$ or jarosite mineral-type compounds $R_4N[Fe_3(OH)_6(SO_4)_3]$ and $H_3O[Fe_3(OH)_6(SO_4)_2]$ [27-29].

During thermal dehydration of $FeOHSO_4$, the ΔE_Q value increases from 0.97 to 1.5 mm/s at 298 K. Jarosite type compounds are stable to about 230 °C [30, 31]. One of the decay products at 230 °C is $FeOHSO_4$, which is stable up to 450–500 °C. However, when boiled in water, jarosite-type compounds of Fe(III) are transformed into highly dispersed particles of α-FeOOH [29] in the superparamagnetic state and the value of ΔE_Q decreases. Thus, the different behaviour of jarosite-type and $FeOHSO_4$ compounds on heating in air or boiling in water permit us to identify the nature of Fe(III) compounds in the polymer phase.

The Mössbauer spectra of the Fe(III)-containing samples of AV-17 heated at different temperatures present a doublet at 300 and 80 K [32]. Their parameters (Table 1-1) show that the Fe(III) states when heated to 160°C remain practically unchanged. Some changes observed in the spectral parameters of heated samples in the temperature interval from 120 to 160°C are conditioned by dehydration processes. In the heated samples transformations commenced at t >160°C, which resulted in partial reduction of Fe(III) to Fe(II) at 200 °C.

Table 1-1. Parameters of Mössbauer spectra of heated in air Fe(III)-containing AV-17 polymer

Temperature		Spectra parameters, mm/s			
Heating (^{0}C)	Spectrum recorder (K)	δ	ΔE_Q	Γ_l	Γ_r
120	300	0.62	0.88	0.59	0.56
	80	0.80	0.89	0.64	0.53
140	300	0.59	0.96	0.60	0.59
	80	0.74	0.94	0.55	0.56
160	300	0.51	0.99	0.74	0.63
	80	0.93	0.62	0.47	0.76
180	300	Unresolved spectrum			
	80	0.71	1.00	0.68	0.53
200	300	Unresolved spectrum			
	80	0.51	0.59	0.86	0.86
		1,35	2.72	0.53	0.53

Thus, the main conclusion of this part of the investigation is that the Fe(III) compound in the AV-17 phase is not $FeOHSO_4$, but it is probably a jarosite type compound. The reduction of Fe(III) to Fe(II) in the resin indicates mutual influences of Fe(III) compounds and the polymer on their thermal stability. Unresolved Mössbauer spectra of samples recorded at 300 K (Table 1-1) may be due to the breakimg of the polymer chain involving a large amplitude of the Fe(III)-containing particle vibrations. Supplementary information about changes taking place in the Fe(III)-containing polymer phase on heating in the air was obtained from EPR and IR spectra. In the EPR spectra of all heated samples, there are three spectral lines: one at g = 4.3 and two lines at g = 2.003. One of the lines at g = 2.003 is large, and another is narrow. The width of a large line is about 800 Oe for samples heated at $t \leq 140$ °C and decreases to 400 Oe for samples heated at t >140 °C. The signals at g = 4.3 and 2.003 (wide line) are attributed to the Fe(III) ions in rhombic and octahedral surroundings, respectively [33]. As is known, jarosite-type compounds consist of octahedrons. The narrow signal at g = 2.003 is attributed to a stable radical, probably a semiquinone [34]. Its intensity increases with the increase of the heating temperature of the Fe(III)-containing polymer samples.

The IR spectra of the heated Fe(III)-containing samples of AV-17 (Fig.1-1), were interpreted according to Nakamoto [35] and Bellami [36]. In the IR spectrum of the sample heated at 120 °C a new absorption band at 1730 cm^{-1} appeared, and in the spectrum of the sample heated at 140 °C another band appeared at 1695 cm^{-1}. These bands were attributed to ν(C=O) of ketone groups. We suggest that the bands at 1730, 1105, 620, 550 and 420 cm^{-1} correspond to an aromatic ketone type:

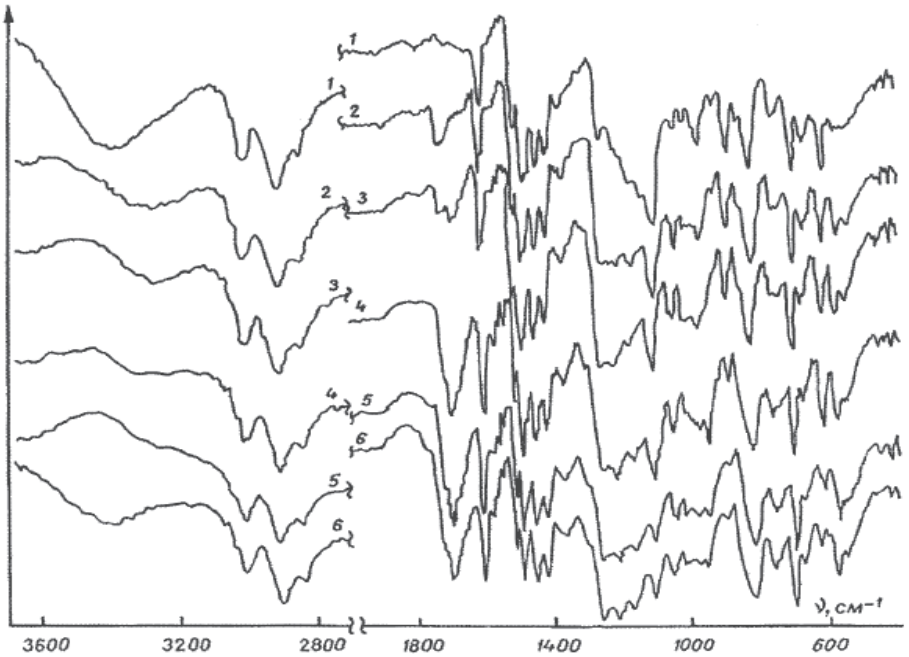

Figure 1-1. IR spectra of the Fe(III)-containing AV-17 after heating in air at 100 (spectrum 1), 120 (spectrum 2), 140 (spectrum 3), 160 (spectrum 4), 180 (spectrum 5), and 200°C (spectrum 6).

The absorption band at 1695 cm^{-1} corresponds to C=O groups in an aromatic nucleus, that is, to a quinone-type ketone. If this is true, the frequency of the valence vibrations of atoms in the C=C and C–H groups of the aromatic nucleus must be changed. Upon increasing the temperature of the heated samples, ν (C = C) moves from 2990 to 3010 cm^{-1}; ν(C–H) moves from 1610 to 1595 cm^{-1}; and band widening at 820, 970 and 1045 cm^{-1} takes place. In the IR spectrum of the sample heated at 200°C, a large absorption band of valence vibrations of an OH group appeared at 3500–3300 cm^{-1} and a band of ν(C=O) of a carboxylic group appeared at 1715 cm^{-1}. This fact and the growing intensity band at 1260 cm^{-1} [ν(C–O) of a carboxylic group] that increases with temperature permit us to suggest that carboxylic groups are formed on heating in the Fe(III)-containing polymer. It is also confirmed by the appearance in the IR spectra of an intensive band at 945 cm^{-1} (OH group), which increases with temperature at $t \geq 140°C$. The essential decreasing of the intensity of the band at 890 cm^{-1} in the IR spectra of the samples heated at $t \geq 160°C$ shows that the $-N(CH_3)_3^+$ groups undergo changes [37]. According to Karrer [38] on heating in the air the tetraalkylammonium bases are transformed into methanol and tertiary amines. The bands in the IR spectra at 1050 and 1160 cm^{-1} can be attributed to alcohol OH groups and at 1040 and 1680 cm^{-1} to aldehyde groups (Fig.1-1). The absorption bands at 1100 and 615 cm^{-1} show that the Fe(III)-containing polymer samples also contain a considerable amount of SO_4^{2-} anions.

It is reasonable to compare the obtained results with those studying the thermal behaviour of an AV-17 exchanger in the absence of Fe(III) compounds in its phase. The results of these investigations are reported by Tulupov and Grebeni [39] and Ugleanskaya et al. [40]. According to Tulupov and Grebeni [39] on heating an AV-17(Cl) exchanger in air, the following processes are carried out:

$$2RCH_2N(CH_3)_3Cl + H_2O \rightarrow RCH_2NH(CH_3)_2Cl + (CH_3)_4NCl + RCH_2OH \quad (1\text{-}2)$$

$$RCH_2N(CH_3)_3Cl + RCH_2NH(CH_3)_2Cl + HOH \rightarrow RCH_2NH_2CH_3Cl +$$

$$+ (CH_3)_4NCl + RCH_2OH. \quad (1\text{-}3)$$

As shown in [39], processes (1-2) and (1-3) take place in the polymer phase on heating at $t \geq 150$ °C. Ugleanskaya et al. [40], mention that air dried AV-17 is stable up to 200 °C, and degradation begins at 230 [AV-17(Cl)] or 220 °C [AV-17(OH)]. The results of our investigations show that the existence of Fe(III) compounds in the phase of a strongly basic anion exchanger influences not only the thermal stability of the polymer but also the mechanism of thermochemical processes.

1.2.2. Transformations in Fe(III)-containing polymer on boiling in water

When boiled in water, jarosite compounds are known [29] to be converted to highly dispersed particles of FeOOH in a superparamagnetic state. The Mössbauer spectra of β-, γ-, and α-FeOOH in the superparamagnetic state show only one doublet and each modification of FeOOH cannot be identified. However, when several cycles of sorption– boiling in water are carried out, large FeOOH particles in the polymer phase are obtained. The large FeOOH particles become magnetically ordered, which allows identification of their modification using Mössbauer spectroscopy.

The Mössbauer spectra of the AV-17 sample after one cycle of sorption– boiling in water are a doublet at 300 and 80 K (Fig.1-2).

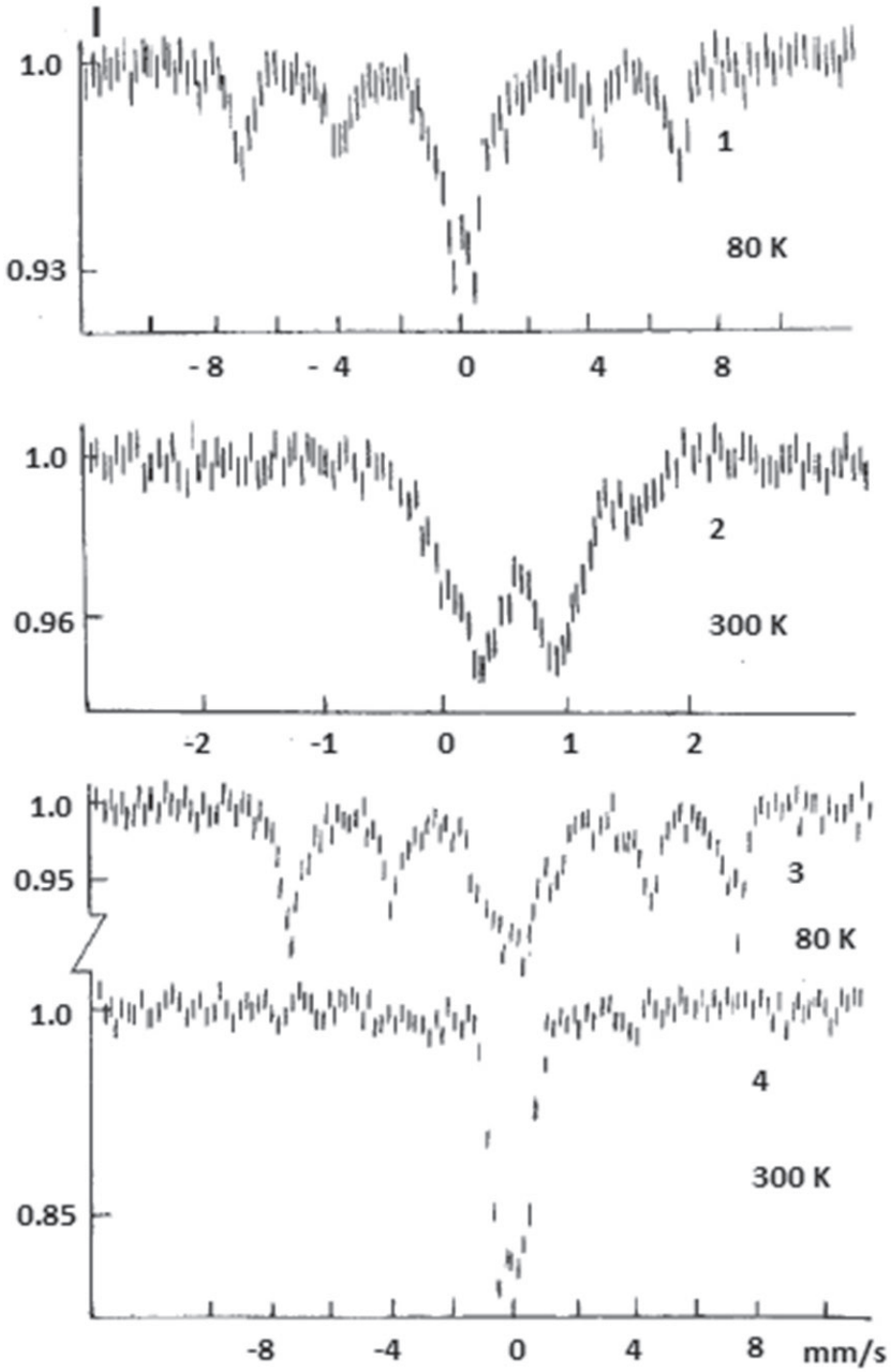

Figure 1-2. Mössbauer spectra of the Fe(III)-containing AV-17 after 3 (spectra 1 and 2) and 6 (spectra 3 and 4) sorption-boiling in water cycles

Mössbauer spectra of samples after two or more cycles of sorption– boiling in water present a doublet at 300 K and a sextet with a doublet in the centre of the spectrum at 80 K. The appearance of a sextet in the Mössbauer spectrum indicates the existence in the polymer phase of relatively massive and magnetically ordered Fe(III)-containing particles. The parameters of the sextet (Tab.1-2) correspond to β-FeOOH particles with varied sizes [42-43]. The massive particles of β-FeOOH are paramagnetic at room temperature and antiferromagnetic at T< 283 K [44]. The structure of the particles depends on the nature of anions presented in the medium of β-FeOOH formation [45-47].

Table 1-2. Parameters of Mössbauer spectra of AV-17 exchanger after different numbers of sorption-boiling in water cycles

No. cycles	Temp. (K)	Spectrum shape	Mössbauer parameters (mm/s)				H_{ef} (kOe)	Fe content (mg Fe/g sempe)
			δ	ΔE_Q	Γ_l	Γr		
1	300 80	Doublet Doublet	0.58 0.72	0.72 0.79	0.56 0.58	0.49 0.68	0 0	12.5
2	300 80	Doublet Doublet Sextet	0.65 0.80 0.80	0.72 0.94 o.18	0.52 0.84 -	0.62 0.84 -	- - 462	20,07
3	300 80	Doublet Doublet Sextet	0.61 0.66 0.74	0.72 0.76 -0.23	0.57 0.61 -	0.42 0.61 -	0 0 479	25.8
4	300 80	Doublet Doublet Sextet	0.59 0.69 0.66	0.69 0.77 -0.19	0.55 0.77 -	0.55 0.77 -	0 0 456	45,6
5	300 80	Doublet Doublet Sextet	0.63 0.82 0.68	0.72 0.87 -0.14	0.43 0.77 -	0.51 0.77 -	0 0 454	57.8
6	300 80	Doublet Doublet Sextet	0.61 0.68 0.66	0.71 0.70 -0.18	0.51 0.70 -	0.48 0.77	0 0 450	65.2

The doublet in the centre of the sextet is attributed to highly dispersed β-FeOOH in the superparamagnetic state, which stays in the narrow pores of the exchanger. With an increasing number of sorption– boiling in water cycles, the amount of massive β-FeOOH particles in the polymer phase grows. Jarosite-type compounds boiled in water are converted into α-FeOOH [29], but in the investigated polymer they are converted into β-FeOOH. The AV-17 exchanger was in Cl^- form and the formation of β-FeOOH may be conditioned by Cl^- anions still being in the polymer phase. According to several studies [45-49], β-FeOOH is formed in the presence of Cl^- or F^- anions in solution. The Cl^- anions are contained in the β-FeOOH structure and may participate in the anion exchange process [50]. The exchange capacity of the β-FeOOH depends on the concentration of anions and the pH of the solutions, being 1 mmol Cl^- /g at pH 3.0 [51]. However, Goncharov et al. [43], reported that β-FeOOH may be obtained in the absence of Cl^- or F^- anions. It is possible that the formation of FeOOH modifications depends on the size of the particles, which is analogous to the suggestion of α-, γ-Fe_2O_3 formation [52]. According to this suggestion, the Fe_2O_3 modifications depend on the critical diameter (d_{cr}) of the particles. Paramagnetic *x*-Fe_2O_3 exists when $d_{cr}= 8 \pm 2$ nm, ferromagnetic γ-Fe_2O_3 exists when d_{cr} = 8–30 nm, and antiferromagnetic α-Fe_2O_3 exists when $d_{cr} > 30$ nm. When *d* becomes more than d_{cr}, paramagnetic *x*-Fe_2O_3 particles spontaneously become magnetically ordered [54].

Thus, the transformations of the Fe(III)-containing compounds in the AV-17 phase when boiled in an aqueous medium permit us to suggest that the sorption of metallic cations from $Fe_2(SO_4)_3$ solutions on strongly basic anion exchangers takes place through formation of the jarosite-type compounds $R_4N[Fe_3(OH)_6(SO_4)_2]$ and $H_3O[Fe_3(OH)_6(SO_4)_2]$.

1.2.3. Chemisorption of Fe(III)- containing cations on strongly basic cross-linked polymers

The retaining of Fe(III)-containing cations from sulfate solutions takes place not only on AV-17(Cl) but on any polymer containing strongly basic groups. To confirm this, the sorption of Fe (III) containing cations from sulfate solution was performed not only on AV-17(Cl), containing - $N(CH_3)_3Cl$, but also on the commercial polymer Varion-AD, containing functional groups - $[N(CH_3)_2CH_2CH_2OH]Cl$ [53]. The full exchange capacity of the Varion-AD is 4.0 mEq/g [4].

Dried samples (0.2 g) of the polymers were placed in contact with 200 ml of $Fe_2(SO_4)_3$ solution for 24 h. The pH of the solution-sample systems was kept at 2.0±0.1 by using either H_2SO_4 or KOH solution. The temperature dependence of the sorption of Fe(III) containing ions in $2x10^{-2}$ M $Fe_2(SO_4)_3$ solutions was investigated over the temperature range of 20–70°C. The system temperature was kept at a constant with an error of ±1°C. There was no evidence of the resins degrading at these temperatures.

As is shown in Figure 1-3, the sorption of Fe(III) containing ions from the $Fe_2(SO_4)_3$ solution on strongly anion exchangers AV-17 and Varion-AD depending on temperature passes through a maximum at about 50°C.

The first important conclusion from the temperature dependence of the Fe(III) containing - ions retaining on polymers is that the sorption is not a physical but a chemical process. This fact excludes ion exchange as a possible process for the sorption of Fe(III) containing ions. It also excludes sorption due to the formation of an Fe(OH) precipitate in the polymer phase. As it is known [54], the degree of hydrolysis of ions in the exchange phase differs from that in solution. We suggest that the retention of the Fe(III) containing ions on the strongly basic anion

exchangers is due to the formation of jarosite type compounds in the polymer phase.

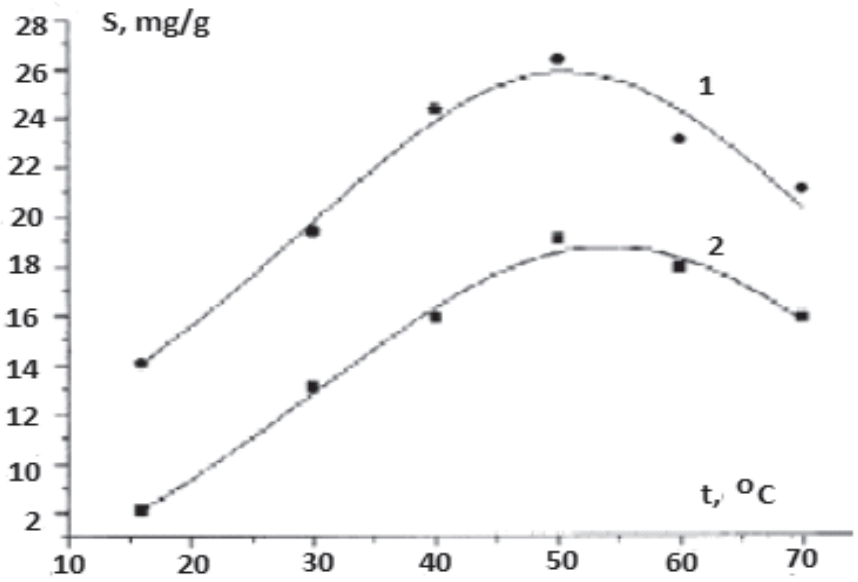

Figure 1-3. Temperature dependence of the Fe(III) containing ions' sorption on anion exchangers Varion-AD (1) and AV-17 (2).

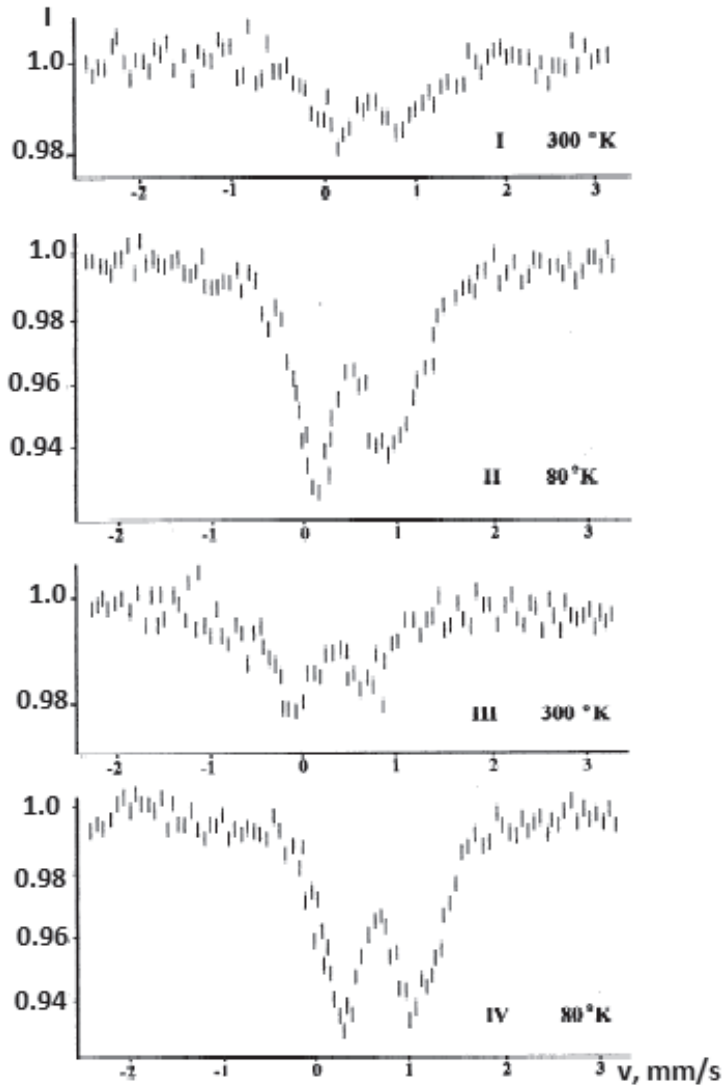

Figure 1-4. Mössbauer spectra of the anion exchanger Varion-AD after retaining Fe(III)-containing ions from $Fe_2(SO_4)_3$ solution at 30 (I, II) and 50^0C (III, IV).

The appearance of a maximum on the temperature dependence of sorption shows that in the polymer–$Fe_2(SO_4)_3$ solution system processes occur with opposing influences on sorption. These processes could take place in the polymer phase or in solution. To detect the existence of different Fe(III) compounds in the polymer phase we investigated Fe(III) containing samples of Varion-AD obtained at 30 and 50°C using Mössbauer spectroscopy. The resulting Mössbauer spectra are presented in Figure 1-4 and their parameters are listed in Table 1-3.

Table 1-3. Parameters of the Mössbauer spectra of anion-exchanger Varion-AD retaining Fe(III) containing ions from $Fe_2(SO_4)_3$ solutions at different temperatures

T, K	δ, mm/s	ΔE_Q, mm/s	Γ_l, mm/s	Γr, mm/s
			Samples obtained at 30°C	
300	0.56	0.71	0.62	0.69
80	0.66	0.86	0.60	0.70
			Samples obtained at 50°C	
300	0.65	0.77	0.68	0.64
80	0.54	0.79	0.63	0.70

They show that in the polymer phase there are only Fe(III) ions in the high spin state. A visible amount of Fe(II) ions is not detected, which indicates the absence of reducing centres in the polymers. The electronic state of Fe(III) ions in Varion-AD is almost the same as in AV-17 [26]. Perhaps some of the OH groups of Varion-AD coordinate with Fe(III) ions affect the symmetry of the compound. The shape of the spectra is important along with their characteristic values, showing that in the polymer phase there is only one type of Fe(III) compound. So, the Fe(III) containing ions sorption temperature dependence maximum (Fig. 1-3) is probably a result of the change which takes place in the $Fe_2(SO_4)_3$ solution on heating. It is known that in aqueous solutions Fe^{3+} ions hydrolyse.

The presence of some compounds such as Fe^{3+}, $FeOH^{2+}$, $Fe_2(OH)_2^{4+}$, $Fe_3(OH)_4^{5+}$, $Fe(OH)_2^{+}$, $Fe(OH)_3$ and $Fe(OH)_4^{-}$ will affect the influence of the concentration of the iron salt, pH, temperature and ionic strength of the solution on the sorption properties. The relative content of Fe(III)-containing ions in the solution we used, according to Refs. [55, 56] may be estimated as about 25% $[Fe(H_2O)_6]^{3+}$, 50% $[FeOH(H_2O)_5]^{2+}$ and 25% $[Fe_2(OH)_2(H_2O)_8]^{4+}$. Not all of these cations are able to participate in the formation of the Fe(III) compounds in the exchanger phase. While the pH increases, the concentration of $[Fe(H_2O)_6]^{3+}$ cations in solution decreases, but sorption of the Fe(III) ions on polymers containing R_4N^+ grows [57]. From solutions of pH ≤ 1.5, the sorption of Fe(III) ions is absent. So, $[Fe(H_2O)_6]^{3+}$ cations do not take part in the formation of Fe(III) compounds in the polymer phase. While the temperature equilibrium (1-4) shifts to the right and in the absence of precipitate formation the concentration of $[Fe_2(OH)_2(H_2O)_8]^{4+}$ cations in solution increases [56]. But as is seen in Figure 3, at t >50°C sorption of Fe(III)-containing ions on the polymers decreases. Therefore the participation of the $[Fe_2(OH)_2(H_2O)_8]^{4+}$ cations in the Fe(III) compounds formation in the polymer phase is unlikely. On heating, the $[Fe_2(OH)_2(H_2O)_8]^{4+}$ cations are transformed into $[(H_2O)_5Fe–O–Fe(H_2O)_5]^{4+}$ ions. These dimer cations cannot easily be restructured to form new units [58], and they have not been detected in the polymer phase by Mössbauer spectroscopy. During the formation process of the Fe(III) compounds in the polymer phase, it is probable that the $[FeOH(H_2O)_5]^{2+}$ cations participate. When studying the effect of pH, the concentration of $[FeOH\ (H_2O)_5]^{2+}$ ions in the solution passed through a maximum [55]. The position and value of the maximum depends also on the concentration of iron ions, ionic strength and temperature. The degree of hydrolysis of Fe^{3+} ions in the polymer phase differs from the one in solution. The hydrolysis processes taking place in the resin may result in local changes in the $[H^+]$:$[OH^-]$ ratio, creating conditions for compounds to be formed according to Equation (1-5):

$$2[Fe(H_2O)_6]^{3+} \leftrightarrow 2[FeOH(H_2O)_5]^{2+} + 2H^+ \leftrightarrow [FeOH(H_2O)_8]^{4+} + 2H^+ + 2H_2O \quad (1\text{-}4)$$

$$3[FeOH(H_2O)_5]^{2+} + 3OH^- + 2SO_4^{2-} \leftrightarrow [Fe_3(OH)_6(SO_4)]^- + 15H_2O \quad (1\text{-}5)$$

The complex anions polymerize themselves to form a solid-phase [59]. Equilibrium (1-5), and therefore the formation of jarosite type compounds, does not take place in the liquid phase of the systems we were using. The conditions of the formation of jarosite-type compounds in solution are described in Refs. [59, 60]. The experimentally obtained isotherms of Fe(III) ions sorption on anion exchangers AV-17 and Varion-AD were analysed using the Freund lich, Temkin and Langmuir sorption models.

Freundlich Sorption Model. The Freundlich nonlinear isotherm [61] is described by Equation (1-6) and the linear isotherm is described by Equation (1-7):

$$\boldsymbol{S_F = K_F * C^{1/n}}, \quad (1\text{-}6),$$

$$\boldsymbol{\ln S_F = \ln K_F + 1/n * \ln C} \quad (1\text{-}7)$$

where: S_F is the sorption value at equilibrium (mg Fe/g), K_F is the Freundlich isotherm constant, C is the concentration of Fe(III) ions in solution at equilibrium (mg Fe/mL). The a and n are constants the physical and

chemical nature of which was not identified. The *1/n* is a measure of the nature and strength of the adsorption process and of the distribution of active sites. If *1/n* >1, bond energies increase with the surface density; if *1/n* < 1, bond energies decrease with the surface density; and when *1/n* = 1, all surface sites are equivalent.

Temkin Sorption Model. Ignoring very low and very large values of concentration, the Temkin equation is shown as Equation (1-8) [62, 63]:

$$S_T = a + b \ln C, \tag{1-8}$$

where *a* and *b* are constants, the nature of which is not defined, and S_T is the sorption value at equilibrium (mg Fe/g) and C is as in Equation (1-6).

Langmuir Sorption Model. The Langmuir nonlinear isotherm [64] is described by Equation (1-9) and the linear isotherm is described by Equation (1-10):

$$S = S_L K_L C/(1 + K_L C) \tag{1-9},$$

$$1/S = 1/S_L K_L + C/S_L \tag{1-10}$$

where: *S* is as S_F the same as in Equation (1-6), S_L is the monolayer capacity of the sorbent (mg Fe/g); K_L is the Langmuir isotherm constant (mL/mg), and *C* is the Fe^{3+} concentration at sorption equilibrium (mg Fe/mL).

The application of the Langmuir equation suggests that the sorption energy is constant and does not depend on the degree of occupation of the active centres of a sorbent. For sorption on the sorbents having two energetically distinct kinds of sorption centres, Langmuir proposed the following Equation (1-11) of the isotherm:

$$S = S'_L K_L' C/(1 + K'_L C) + S''_L K_L'' C/(1 + K_L'') \tag{1-11}$$

where the constants K_L' and K_L'' characterize the centres with more and less affinity, respectively.

Under finite conditions the sorption may take place only on centres with low affinity, the high-affinity centres being completed. In this case the Langmuir Equation (1-12) is applied:

$$S = S'''_L + S''_L K_L'' C/(1 + K_L'' C) \tag{1-12}$$

There are some methods to resolve Equations (1-8) to (1-12). Most efficient is the method of non-linear regressions [16–18]. The isotherms obtained experimentally and calculated are shown in Figures 1-5 and 1-6, and their parameters are shown in Table 1-4.

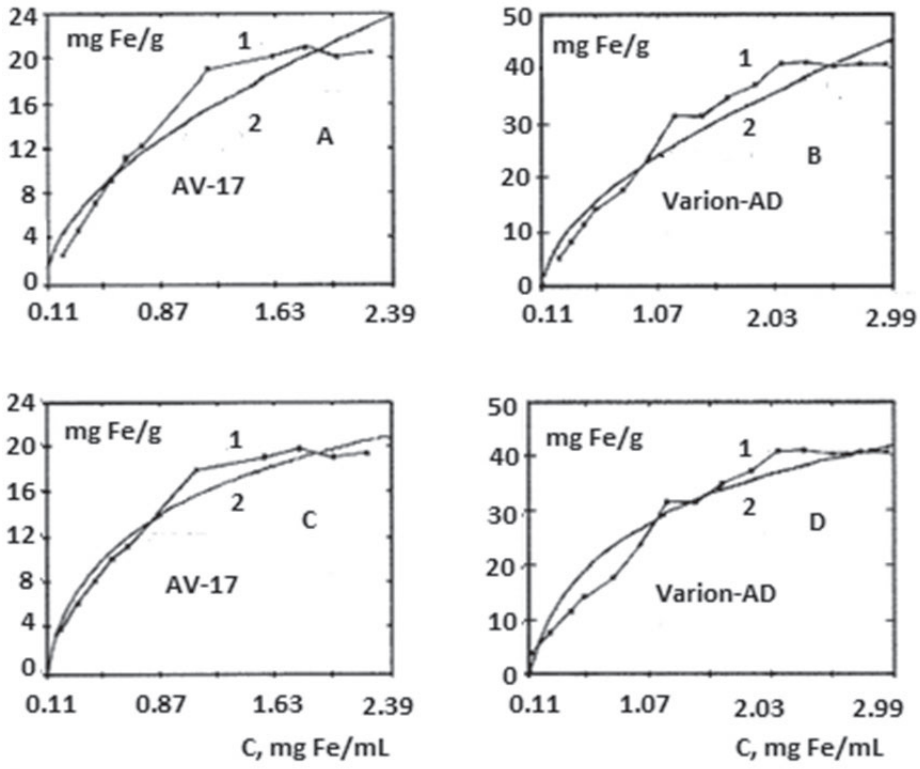

Figure 1-5. Experimental (1) and calculated (2) isotherms of Fe(III) containing cations' sorption on polymer AV-17 and Varion-AD using Freundlich (A, B) and Temkin (C, D) equations.

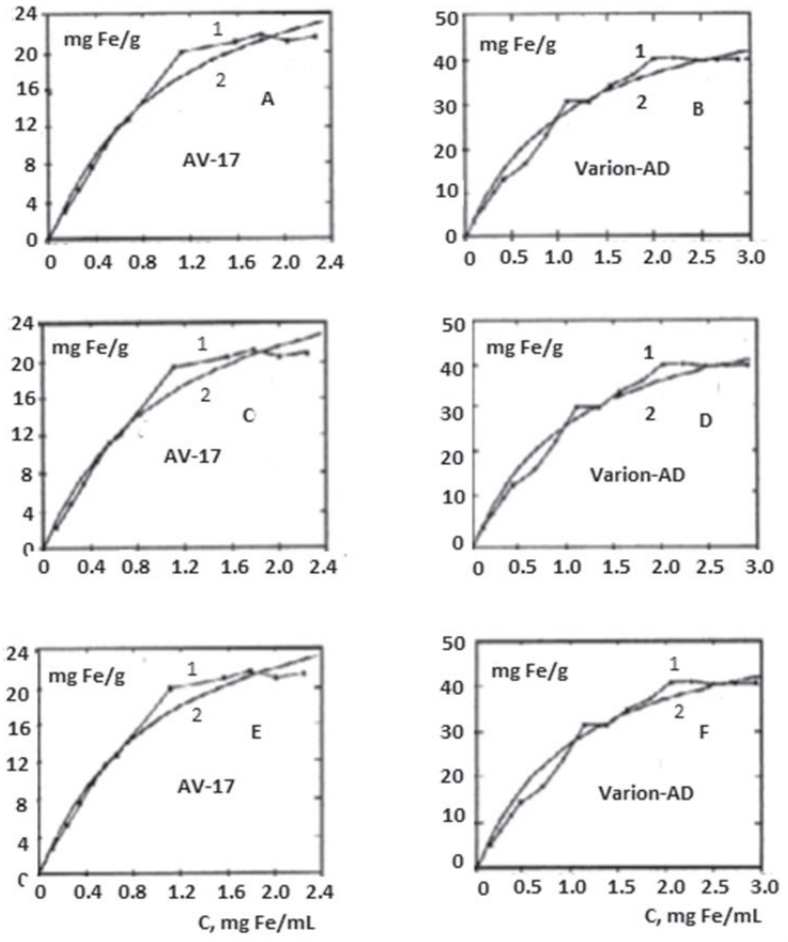

Figure 1-6. Experimental (1) and calculated (2) isotherms of Fe(III) containing cations' sorption on anion exchangers AV-17 and Varion-AD using Langmuir Eq. (1-9) (A, B), Eq. (1-11) (C, D), and Eq. (1-12) (E, F).

Statistical analysis and approximation of the experimental and calculated isotherms show that the Langmuir equations describe the Fe(III) ions sorption isotherms on the AV-17 and Varion-AD polymers more adequately than the Freundlich or Temkin equations. Equations (1-9), (1-11) and (1-12) show the same affinity of the less active sorption centres. These equations also describe identically the sorption capacities of polymers which are determined by the low-affinity sorption centres. The higher affinity sorption centres constitute only about 0.04–0.09% according to Eq.(1-12) or 0.03–0.04% according to Equation (1-11). This means that all active centres of polymers AV-17 and Varion-AD are energetically the same. These active centres of the polymers cannot be other than R_4N^+. So, R_4N^+ groups take part in the formation of metallic compounds in the polymer phase.

Table 1-4. Parameters of Freundlich, Temkin and Langmuir equations for Fe(III) containing ions' sorption isotherms on polymers AV-17 and Varion-AD

AV-17	Varion-AD
Freundlich. Eq. 1-6.	
K_F =14.72, n =1.788	K_F =24.06, n =1.731
Temkin. Eq. 1-8.	
α =16.09, b =7.11	α =27.14, b = 13.05
Langmuir. Eq. 1-9.	
K_L = 0.926 ml/mg, S_L = 32.91 mg/g	K_L = 0.907 ml/mg, S_L = 56.24 mg/g
Langmuir. Eq. 1-11.	
K'_L = 9.010 ml/mg, S'_L = 0.013 mg/g K''_L = 0931 ml/mg, S''_L = 32.970 mg/g	K'_L = 9.030 ml/mg, S'_L = 0.018 mg/g K''_L = 0.901 ml/mg, S''_L = 56.520 mg/g
Langmuir. Eq. 1-12.	
K''_L=0.924 ml/mg, S''_L=32.92 mg/g, S'''_L=0.015 mg/g	K''_L=0.902 ml/mg, S''_L= 56.34 mg/g, S'''_L=0.051 mg/g

1.2.4. Iron compounds in the polymer phase as precursors for the obtaining of sorbents and catalysts

The sorption of Fe(III) containing cations from sulfate solutions takes place through the formation in the polymer phase of the jarosite mineral type compounds: $R_4N[Fe_3(OH)_6(SO_4)_2]$ and some $H_3O[Fe_3(OH)_6(SO_4)_2$, where R_4N^+ is a functional group of the polymer. The jarosite mineral type compounds are formed as layers of 3 or 6 octahedral cycles [58]. The OH^- groups are in the equatorial plane, forming a bridge between metal ions, and SO_4^{2-} groups are in axial position, each coordinate 3 metal ions of 3 octahedra. Between the jarosite polymer layers there are mobile R_4N^+, H_3O^+ and other cations retained by Coulomb's electrostatic interactions. The jarosite mineral type compounds in the polymers phase change significantly their physical-chemical properties. In the previous investigation [33], the Fe(III)-containing cations sorption on AV-17(Cl) took place at the room temperature and iron content in the polymer phase has constituted only about 12 mg Fe/g. For obtaining effective and selective sorbents and catalysts the polymers must have a more consistent number of metallic compounds in their phase. It is also necessary to know and have a possibility to change the morphology and composition of structural units of ultrafine particles, their distribution on the surface and in the volume of polymer granule, a method to change particles sizes. In the

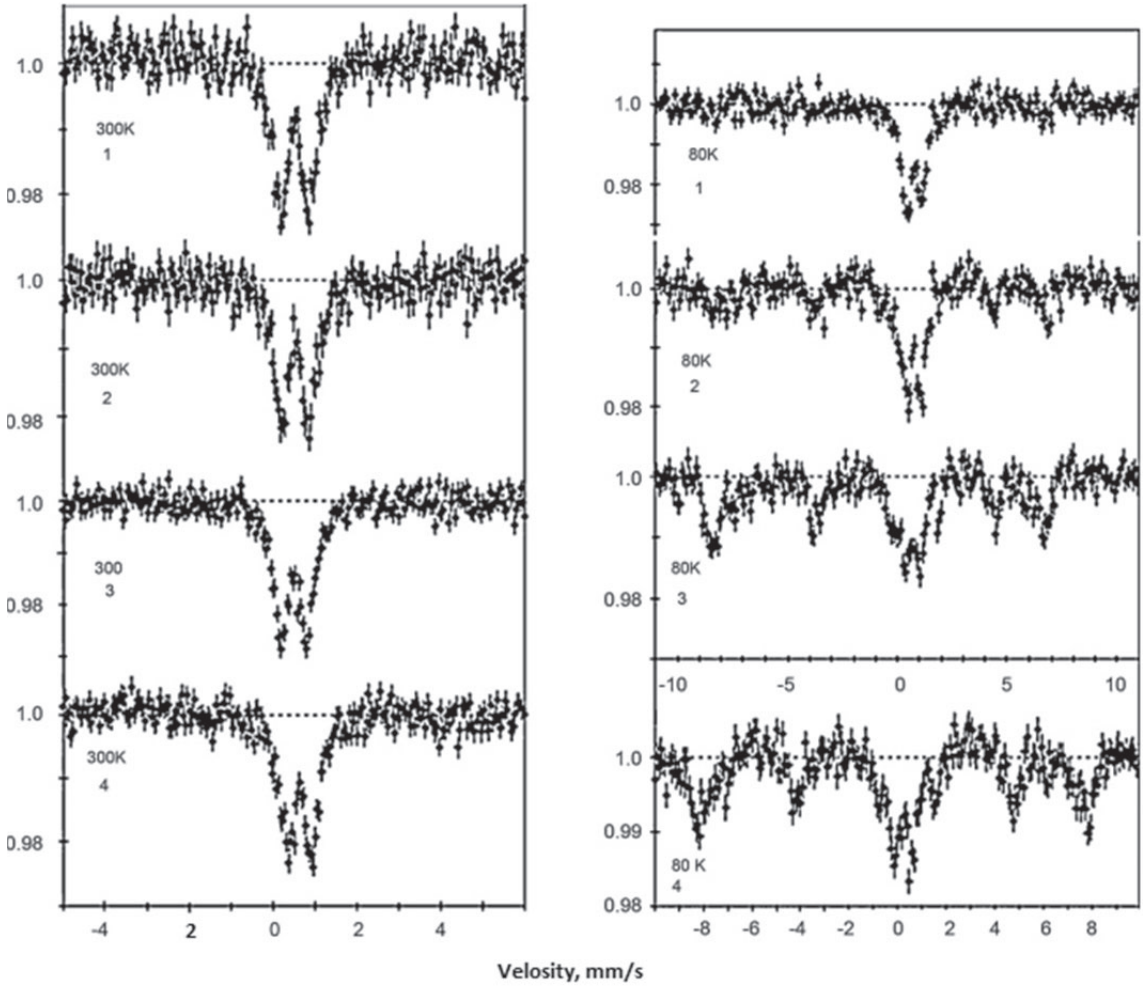

Figure 1-7. Mössbauer spectra recorded at 300 and 80 K of the Fe(III)-containing AV-17 after 2 (1), 4 (2), 6 (3) and 8 h (4) of heating in the water in a boiling water bath.

investigation [64], the samples of the AV-17 polymer had a much higher amount of Fe (Tabs.1-5 and 1-6). The Mössbauer spectra of the AV-17 polymer samples after contacting with $Fe_2(SO_4)_3$ solution are doublets both at 300 and 80 K. The isomeric shift of these spectra is 0.70 and 0.83 mm/s and quadrupole splitting is 0.79 and 0.88 mm/s, respectively at 300 and 80 K (Tab.1-6, cycle 0). The values of the quadrupole splitting are smaller than in Ref. [33]. As it is seen in Figure 1-7, the Mössbauer spectra of the Fe(III) compounds in the AV-17 polymer phase after 2 h of heating in the water in a boiling water bath are doublets at 300 and 80 K. The ΔE_Q values of these doublets are much smaller (Tab.1-5), in comparison with that of the jarosite type compounds (Tab.1-6, cycle 0). It means that after 2 h of heating in the water, the jarosite type compounds in the polymer phase are transformed into FeOOH ultrafine particles in the superparamagnetic state. We cannot conclude what modification of FeOOH is formed in the polymer phase after 2 h of heating in the water of the jarosite-containing AV-17. The Mössbauer spectra of α-, β-, γ- or δ-FeOOH in the superparamagnetic state (nanoparticles), are doublets both at 300 and 80 K [65].

Table 1-5. Parameters of the Mössbauer spectra of the Fe(III) containing AV-17 after heating in water

Heating duration, h	T, K	Spectrum shape	Mössbauer parameters, mm/s				H_{eff}, kOe	Fe content, mg/g
			δ	ΔE_Q	Γ_l	Γ_r		
2	300	Doublet	0.76	0.57	0.57	0.48	0	39.7
	80	Doublet	0.62	0.66	0.40	0.40	0	
4	300	Doublet	0.60	0.63	0.42	0.38	0	31.6
	80	Doublet	0.76	0.57	0.57	0.48	0	
		Sextet	0.36	-	-	-	450	
6	300	Doublet	0.60	0.61	0.42	0.42	0	31.9
	80	Doublet	0.71	0.66	0.28	0.38	0	
		Sextet	o.33	-	-	-	450	
8	300	Doublet	0.63	0.55	0.41	0.43	0	31.3
	80	Doublet	0.70	0.73	0.32	0.24	0	
		Sextet	0.74	-	-	-	460	

Table 1-6. Parameters of the Mössbauer spectra of the Fe(III) containing AV-17 after some "Fe(III) – sorption – heating in water" cycles

No. cycles	T, K	Spectrum shape	Mössbauer parameters, mm/s				H_{eff}, kOe	Fe content, mg/g
			δ	ΔE_Q	Γ_l	Γ_r		
0*	300	Doublet	0.70	0.70	0.49	0.32	0	24.9
	80	Doublet	0.83	0.88	0.57	0.51	0	
1	300	Doublet (a)	0.68	0.91	0.23	0.23	0	24.5
		Doublet (b)	0.67	0.42	0.19	0.19	0	
	80	Doublet (a)	0.77	1.27	0.33	0.33	0	
		Doublet (b)	0.88	0.55	0.28	0.28	0	
2	300	Doublet	0.78	0.53	0.48	0.44	0	45.4
	80	Doublet	0.70	0.74	0.63	0.63	0	
		Sextet	o.36	-	-	-	480	

To find the modification of the FeOOH using Mössbauer spectroscopy it is necessary to have massive particles of the compound. The Mössbauer spectrum of the Fe(III)-containing compounds in the polymer phase after 4 h of heating in the water medium is a doublet at 300 K and a sextet with a doublet in the centre of the spectrum at 80 K (Fig.1-7). The appearance of a sextet in the Mössbauer spectrum indicates the existence in the polymer phase of relatively massive and magnetically ordered particles of Fe(III)-containing compounds. The parameters of the sextet (Tab.1-5) correspond to β-FeOOH particles [42-44]. The massive particles of β-FeOOH are paramagnetic at $T > 283$ K (a doublet in the Mössbauer spectrum) and antiferromagnetic at $T < 283$ K (a sextet) [45]. So, we conclude that after 2 h of heating in water jarosite type compounds in the polymer phase are converted into highly dispersed particles of β-FeOOH in a superparamagnetic state.

As it is seen in Figure 1-7, with the increasing of the duration ($\tau > 2$ h) of heating in water of the polymer containing the jarosite, the spectral lines of the sextet in the Mössbauer spectra become more pronounced. It means that with the increasing duration of heating in water of the jarosite-containing polymer, more β-FeOOH particles become massive and the magnetically ordered. The doublet in the centre of the sextet in the spectra recorded at 80 K belongs to highly dispersed β-FeOOH particles in the superparamagnetic state which remain in the narrow pores of the polymer. Under heating of the jarosite-containing polymer in water medium in the water boiling bath the processes (1-13) and (1-14) take place:

$$2R_4N[Fe_3(OH)_6(SO_4)_2] \rightarrow 6(\beta\text{-FeOOH}) + (R_4N)_2SO_4 + 3H_2SO_4 \quad (1\text{-}13)$$

$$H_3O[Fe_3(OH)_6(SO_4)_2] \rightarrow 3(\beta\text{-FeOOH}) + 2H_2SO_4 + H_2O \quad (1\text{-}14)$$

The analysis of the experimental data shows a correlation between the amount of the Fe(III) in the polymer phase and samples heating in water duration to appear the β-FeOOH particles in a magnetically ordered state. So, when in the polymer phase is about 40 mg Fe/g, relatively massive magnetically ordered β-FeOOH particles appear after 4 h of heating in water medium in a boiling water bath (Fig.1-7, Tab.1-5). If the polymer has 25 mg Fe/g, magnetically ordered particles of β-FeOOH do not appear after 4 h of heating in water (Fig.1-8, Tab.1-6, cycle 1). In this case, after 4 h of heating in water of the jarosite-containing polymer, two doublets appear in the Mössbauer spectra (Fig.1-8).

The doublet (a) with a larger quadrupole splitting belongs to jarosite-type compounds particles and another doublet (b) belongs to β-FeOOH ultrafine particles in the superparamagnetic state. The Mössbauer spectra parameters (Tab.1-6, cycle 1) show that when heating in water of AV-17, ΔE_Q of jarosite type compounds in the polymer phase increases significantly from 0.79 and 0.88 to 0.91 and 1.27 mm/s (that is characteristic for jarosite) correspondingly at 300 and 80 K. This fact shows that during heating in water a part of the jarosite type compounds is converted into β-FeOOH in the superparamagnetic state and another part of jarosite becomes more structured. Unstructured jarosite type compounds in the polymer phase may be the explanation of the observed low values of the quadrupole splitting in some studies [53, 66].

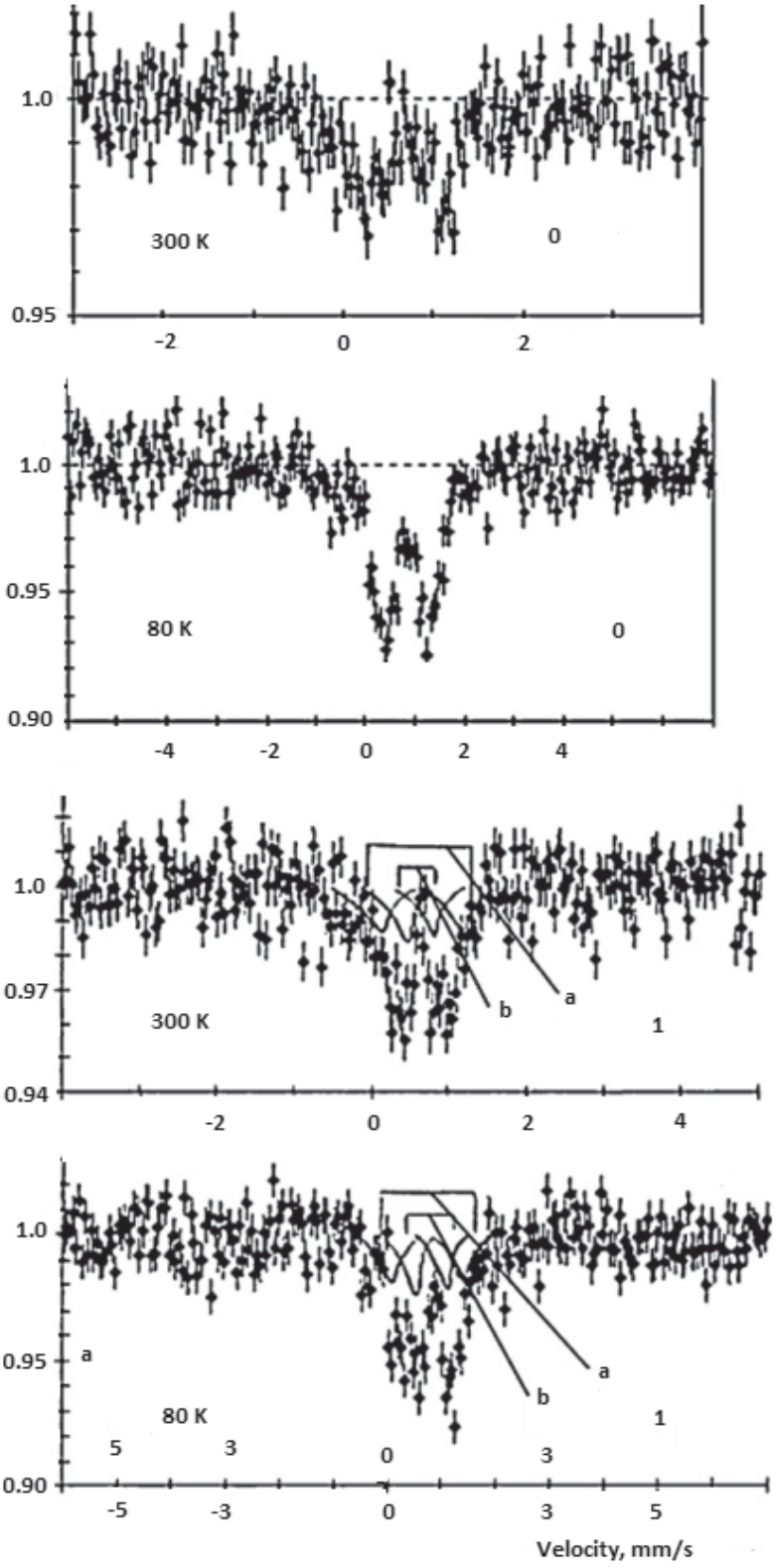

Figure 1-8. Mössbauer spectra of the jarosite containing AV-17 before (0) and after 4 h heating in water (1).

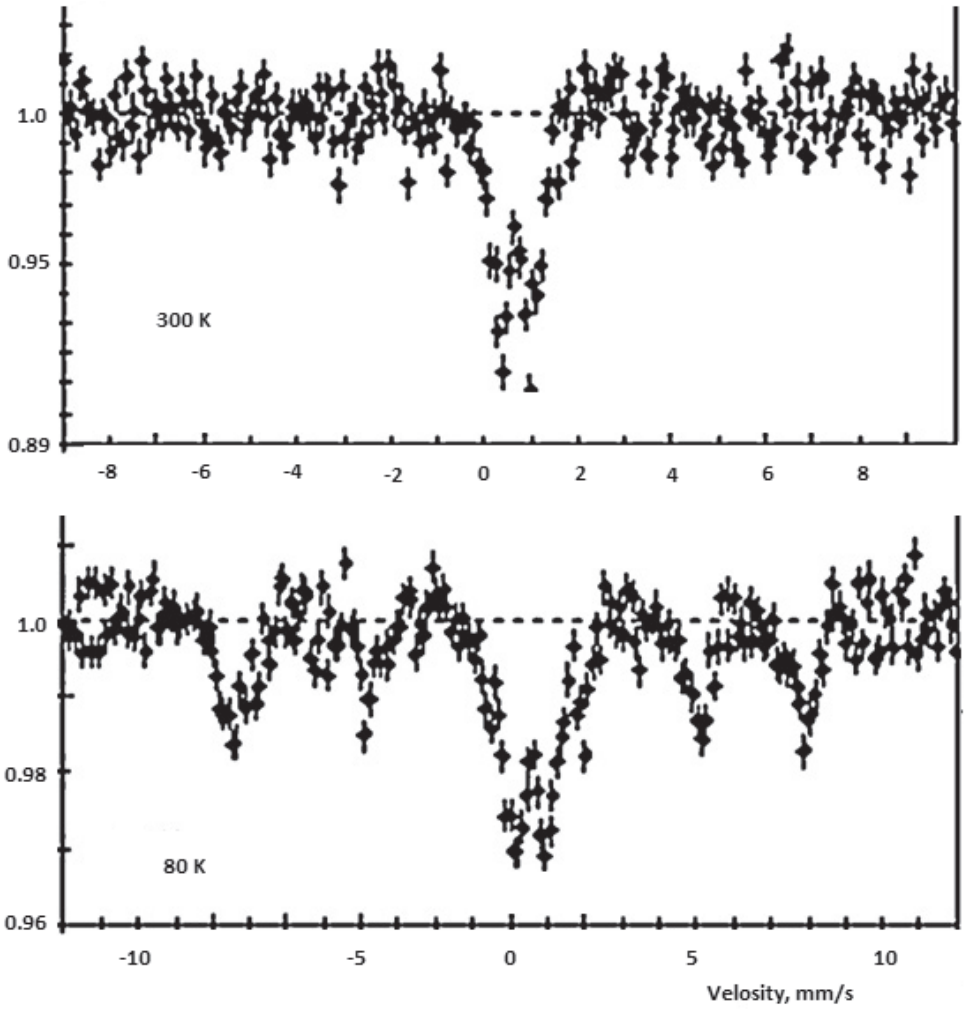

Figure 1-9. Mössbauer spectra of the Fe(III)-containing AV-17 after 2 cycles of "Fe(III) sorption – 4 h heating in the water".

When the polymer contains more Fe^{3+} (45.4 mg Fe/g), that was achieved after 2 cycles "Fe(III) sorption – heating in water for 4 h", jarosite type compounds in the polymer phase are completely transformed into β-FeOOH both relatively massive, magnetically ordered and in the superparamagnetic state particles (Fig.1-9; Tab.1-6, cycle 2).

The ideas mentioned above about jarosite transformation on boiling in water of the Fe(III)-containing AV-17 are confirmed by SEM investigation. The SEM images on the surface and in the volume of the jarosite-containing AV-17 polymer granule (cycle 0) are presented in Figure 1-10. These images confirm that jarosite type compounds in the polymer phase are in the form of ultra-dispersed particles.

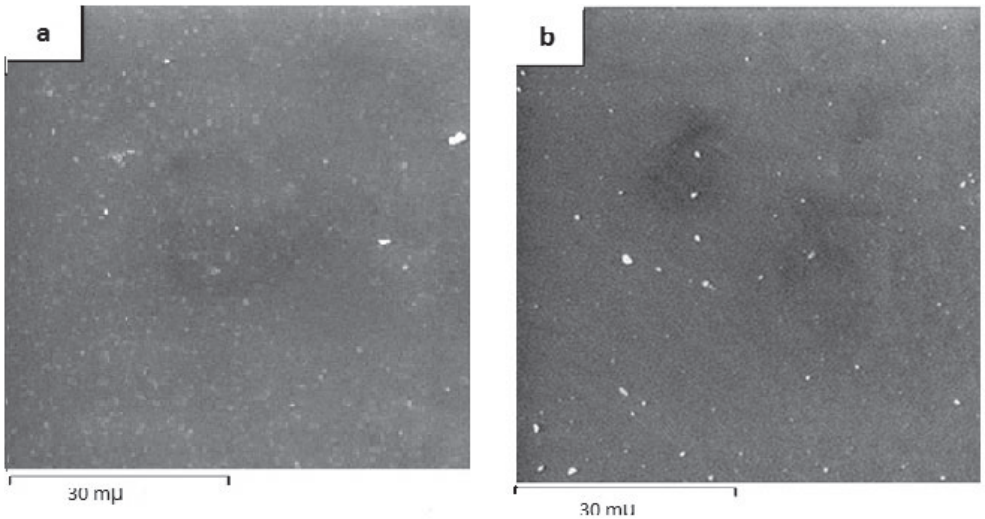

Figure 1-10. SEM images of the jarosite particles on the surface (a) and in the volume (b) of an AV-17 polymer granule.

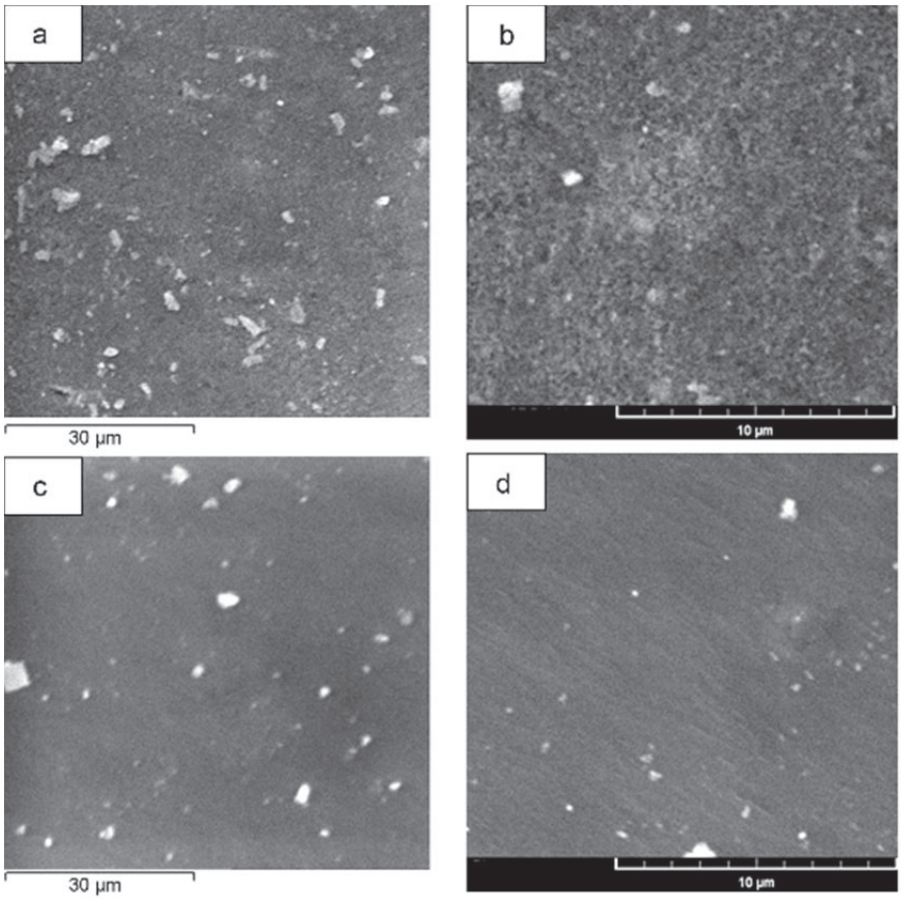

Figure 1-11. SEM images of the Fe(III)-containing compound particles on the surface (a, b) and in the volume of a polymer granule (c, d) after 2 h heating in water of jarosite containing AV-17.

The elemental composition of the Fe(III)-containing structural units were obtained by SEM –EDX investigation. Using the elemental composition of the Fe(III)-containing structural units, the brut formulas of the Fe(III)-containing structural units were calculated and constituted as $Fe_1O_{18\text{-}3}Cl_{1.8}S_{3.56}C_{88.0}$ (on the granule surface) and $Fe_1O_{18.1}Cl_{2.1}S_{3.5}C_{103.5}$ (in the volume of the polymer granule). These formulas show that composition of the Fe(III)-containing structural units on the surface and in the volume of the polymer granule is practically identical. Taking into consideration that the content of O and S atoms in the jarosite type compounds is less than in the Fe(III)-containing structural units in the polymer phase and that jarosite does not contain Cl and C atoms we suggest that jarosite particles in the polymer phase are situated on $[–N(CH_3)_3]_2SO_4$ and $–N(CH_3)_3Cl$ groups. As it is seen in Figure 1-11, after 2 h of heating in the water in the boiling water bath of jarosite- containing AV-17, highly dispersed particles of the Fe(III) compounds are observed both on the surface and in the polymer granule volume.

In the volume of the polymer granule, particles of the Fe(III)-containing compounds are fewer but larger than on the surface. It means that on heating in water a part of the Fe(III)-containing particles migrate up to the surface of the polymer granule. This is confirmed by the elemental composition data of the Fe(III)-containing structural unit. The brut formula of an Fe(III)-containing structural unit on the surface of the polymer granule is $Fe_1O_{8.2}Cl_{0.17}S_{0.86}C_{10.6}$ and in the volume $–Fe_1O_{11.1}Cl_{0.38}S_{1.21}C_{57.9}$. The elemental composition of the Fe(III)-containing structural unit is approximate because its composition includes a part of the polymer chain and atoms of functional groups. On the other hand, these structural units are statistically equally distributed both on the surface and in the volume of the polymer granule. It is known from Mössbauer spectroscopy data that the polymer phase comprised β-FeOOH compounds. Furthermore, SEM images confirmed the existence of β-FeOOH particles in a highly dispersed form. The existence of $Cl^–$ ions in the β-FeOOH structure has also been confirmed. Some of the $Cl^–$ ions could belong to R_4NCl groups because of the equilibrium (1-15), when the polymer contacts with $Fe_2(SO_4)_3$ solution:

$$2R_4NCl + SO_4^{2–} \leftrightarrow (R_4N)_2SO_4 + 2Cl^- \quad (1\text{-}15)$$

The content of oxygen atoms in the brut formulas is much higher than corresponding to FeOOH. Taking into consideration that the AV-17 polymer matrix does not contain O and S atoms in its composition, it may be concluded that β-FeOOH particles are situated on $[–N(CH_3)_3]_2SO_4$ groups. A part of atoms of these groups is included in the composition of Fe(III)-containing structural units.

After 6 h of heating in water of the jarosite-containing polymer, both highly dispersed and massive particles of β-FeOOH are formed on the polymer granule surface [(Fig.1-12 (a)]. In the volume of the polymer granule

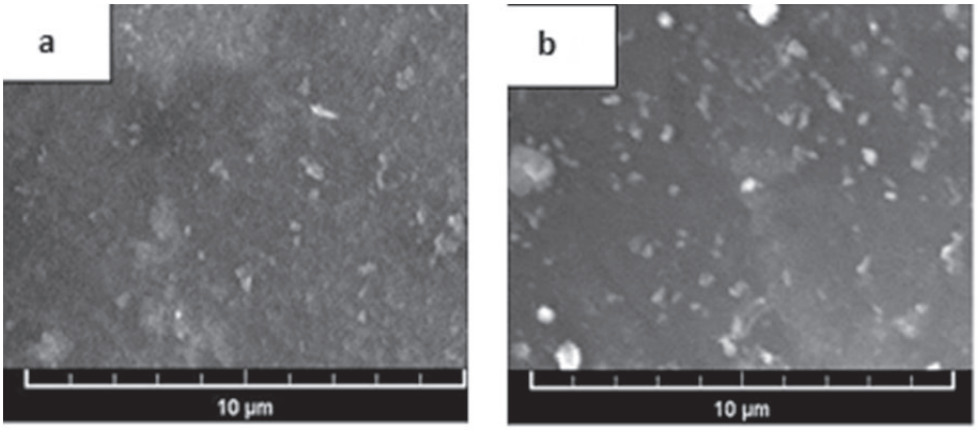

Figure 1-12. SEM images of the Fe(III)-containing compound particles on the surface (a) and in the volume of a polymer granule (b) after 6 h heating in water of jarosite containing AV-17.

there are only highly dispersed β-FeOOH particles [(Fig.1-12 (b)]. The brut formula of the Fe(III)-containing structural units on the polymer granule surface is $Fe_1O_{16.8}Cl_{0.25}S_{2.12}C_{68.3}$ and in the granule volume – $Fe_1O_{44.7}Cl_{0.36}S_{3.17}C_{206.6}$. The high content of O, C and S atoms in the brut formula confirms that β-FeOOH particles are situated on the $–N(CH_3)_3Cl$ and $[–N(CH_3)_3]_2SO_4$ groups, and on the $–CH_2-$ polymer chain. When the jarosite-containing polymer has been heated in water for 8 h, almost all Fe(III)-containing compounds were situated on the polymer granule surface (Fig.1-13).

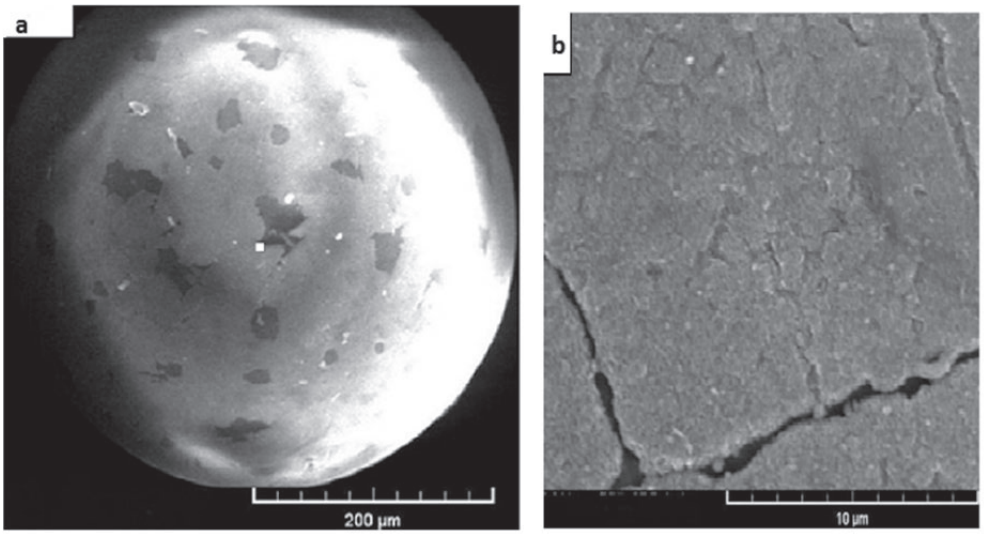

Figure 1-13. SEM images of the Fe(III)-containing compound particles on the surface (a, b) after 8 h heating in water of jarosite containing AV-17

There are many more relatively massive pieces of β-FeOOH on the polymer granule surface than in the case of 6 h of heating in water of jarosite-containing AV-17. This may create kinetic problems when using this sample of the Fe(III)-containing polymer as a sorbent or catalyst. The elemental composition of the Fe(III)-containing structural units on the surface and into the polymer granule of the jarosite containing AV-17 after 8 h of heating in water permits us to calculate the brut formula of the structural units. The brut formula of the Fe(III)- containing structural unit on the surface is $Fe_1O_{11}C_{l0.12}S_{0.83}C_{15.4}$ and in the volume of the polymer granule – $Fe_1O_{111}C_{l0.76}S_{6.38}C_{357}$. As in the cases described above, the particles of β-FeOOH are situated on the polymer's functional groups. Usually β-FeOOH and natural or synthetic jarosite are in the crystalline state, but there are jarosite compounds in an amorphous state as well [58]. Powder X-ray diffraction testing showed that both jarosite type compounds and β-FeOOH in the investigated polymer samples are in an amorphous state. In Ref. [67] it is shown that β-FeOOH and sulfated β-FeOOH particles have different morphologies. Obviously high SO_4^{2-} and Cl^- anion concentration in the polymer phase influences the morphology and crystallinity of jarosite and β-FeOOH particles.

To apply the Fe(III)-containing polymer as a sorbent or catalyst it is necessary to know its behaviour in different media. For that purpose, there was an investigation of thermal behaviour in the nitrogen medium of the Fe(III)-containing AV-17 and for comparison, thermal behaviour in the same conditions of the AV-17 in the form of SO_4^{2-} (AV-17(SO_4)).

From the literature [58], it is known that on heating in air in the range 220–450 ˚C synthetic jarosite loses water from its structure. The initial temperature of endothermic effects for $NH_4[Fe_3(OH)_6(SO_4)_2]$ is observed at 230, 350, 480, 515, 630°C [68] and for $H_3O[Fe_3(OH)_6(SO_4)_2]$ – at 230, 405, 515, 620, 660°C [69] or at 290, 370 and 510°C [58]. The thermogravimetric investigation of $NH_4[Fe_3(OH)_6(SO_4)_2]$ jarosite showed five mass loss steps at 120, 260, 389, 510 and 541◦C [70].

The thermal treatment in air of β-FeOOH showed endothermic peaks at 230, 260 (a shoulder) and 275 °C, and an exothermic peak (small intensity) at 455°C. Endothermic effects correspond to dihydroxylation of β-FeOOH and the exothermic effect to the recrystallization of α-Fe_2O_3 [51]. The DTA curve of sulfated β-FeOOH showed two endothermic peaks at 275 and 350°C and an exothermic peak at 550°C. The jarosite and β-FeOOH compounds in the polymer phase were formed in conditions of high concentrations of SO_4^{2-} and Cl^- ions and their thermal behaviour is expected to differ from the thermal behaviour of $NH_4[Fe_3(OH)_6(SO_4)_2]$ and $H_3O[Fe_3(OH)_6(SO_4)_2]$. It was shown [33] that the polymer matrix influenced the thermal behaviour in the air of the Fe(III)-containing compounds, and metallic compounds influenced the thermal behaviour of the polymer.

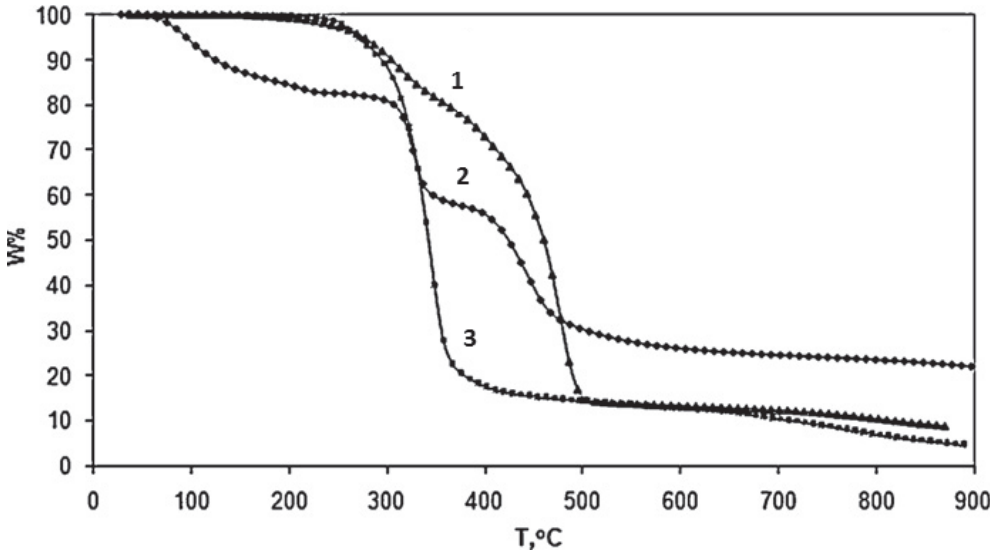

Figure 1-14. TG curves of the samples AV-17(Fe) (1), AV-17(SO_4) (2) and AV-17(FeOOH) (3).

The thermal stability of the compounds was evaluated by dynamic TGA in a nitrogen atmosphere. The TG curves of the samples are presented in Figure 1-14. According to the thermograms the thermal degradation runs in two, three or four stages, being accompanied by endothermic effects. Hence, the TG, DTG and DTA curves of the polymer samples, under an inert atmosphere, indicate a complex degradation pathway of these novel materials. The TGA data for AV-17 in SO_4^{2-} form – AV(SO_4) sample, the jarosite containing polymer – AV(Fe) sample and the heated in water jarosite containing polymer – AV(FeOOH) sample, included T_{onset} – the initial temperatures of thermal degradation, T_{peak} – the temperature corresponding to the maximum degradation rate, T_{endset} – the final temperature at which the degradation process for each stage ends and mass loss (wt.%) for nitrogen atmosphere, which are listed in Table 1-7.

The surveys were extended with the kinetic processing of thermogravimetric data. The Freemann–Caroll [71] method application is based on Equation (1-16) and considers incremental differences in (dα/dT), (1−α) and (1/T):

$$\frac{\Delta \ln(\frac{d\alpha}{dT})}{\Delta \ln(1-\alpha)} = n - \frac{E_\alpha}{R} x \frac{\Delta(\frac{1}{T})}{\Delta \ln(1-\alpha)} \quad (1\text{-}16)$$

where, α is a normalized fractional conversion defined as (1-17):

$$\alpha = \frac{m_i - m(t)}{m_i - m_f} \quad (1\text{-}17)$$

m(t) is the mass at any time *t*, and m_i and m_f, respectively, are the initial and final sample mass; *Ea* is activation energy; *n* is the reaction order; *R* is the universal constant of gases and *T* is the absolute temperature in *K*. By plotting the graph of Δln(dα/dT)/Δln(1-α) dependent on Δ(1/T)/Δln((1-α) from the line slope we can compute the activation energy *Ea* and from origin of interception, we get the reaction order *n*. The pre-exponential factor is computed by Equation (1-18):

$$\frac{d\alpha}{dT} = \frac{1}{a} A exp(\frac{-Ea}{RT}) f(\alpha) \quad (1\text{-}18)$$

Table 1-7. Thermogravimetric and kinetic data of the samples $AV(SO_4)$, AV(Fe) and AV(FeOOH)

Sample	Stage	$T_{onset,,}$ °C	$T_{peac,}$ °C	$T_{endset,}$ °C	W, %	Rezidue, %	Ea , kJ/ mol	n	Ln A
$AV(SO_4)$	I	70	91	133	13.98	19.09	54.35±0.98	1.87±0.003	13.23±0.34
	II	161	210	274	3.74		-	-	-
	III	315	326	339	25.53		555.8±6.97	2.80±0.003	108.94±1.43
	IV	409	440	539	37.66		209.9±2.07	1.62±0.001	31.18±0.36
AV(Fe)	I	256	311	339	19.33	7.58	95.90±0.86	1.48±0.001	14.54±0.19
	II	389	398	444	19.07		82.94±2.38	0.43±0.002	9.09±0.44
	III	444	476	498	54.02		185.4±8.24	0.52±0.004	24.63±1.37
AV (FeOOH)	I	251	263	299	8.26	3.71	98.85±5.29	0.70±0.006	16.46±1.21
	II	298	343	372	88.26		155.3±0.89	0.75±0.008	25.33±0.18

Table 1-7 reveals the kinetic characteristics data such as: *Ea* – the apparent activation energy, *n* – the reaction order and *lnA* –the pre-exponential factor corresponding to each stage. The first step (70–133°C) for the $AV(SO_4)$ sample, is assigned to the water loss from their structures. The temperature corresponding to the maximum degradation rate in the next stages for this sample is seen at 210, 326 and 440°C, respectively. The thermal degradation of the jarosite-containing polymer – AV(Fe) sample, takes place in three stages, with different mass loss percentages. For this compound, the most important mass loss has been recorded in the last stage of the thermal degradation, at onset temperatures over 444°C. The thermal degradation in nitrogen atmosphere of AV(FeOOH) indicated two endothermic peaks at 263 and 344°C. For this sample, the degradation processes are almost complete, a small residue being left (3.71 wt.%). From the data of the thermal analysis we can conclude that the sorbent (catalyst) obtained by forming the Fe-jarosite compounds of the strongly basic polymers is stable up to about 250°C. It is also stable up to about 250°C and the adsorbent (catalyst) is made up of polymer and β-FeOOH.

As a result of the research, the sorbent (catalyst) AV-17 (Fe-jarosite) was obtained [72, 73] which is selective for the removal of CN^-, NCS^-, NCO^- ions from the solutions [74].

1.2.5. Iron compounds in the phase of polyfunctional polymers

1.2.5.1. Iron compounds in polymers also containing groups that can participate in anion exchange processes

In the earlier paragraphs, we discussed the processes for the formation of iron compounds in the phase of monofunctional polymers containing ammonium quaternary nitrogen. In such polymers, Fe^{3+} cations form jarosite-type compounds under certain conditions. Can jarosite type compounds be formed in polymers containing ammonium quaternary nitrogen and electron donor atoms? To answer this question, polymers with various functional groups were obtained (Cornelia Luca PhD and Violeta Neagu PhD," Petru Poni" Institute of Macromolecular Chemistry, Iassy, Romania) and investigated [75, 76]. 4-vinylpyridine: divinylbenzene copolymer (4-VP: DVB) was investigated with a different cross-linking degree (for comparison) and a chemically modified copolymer. The preparation of the copolymer samples is described in detail in [75].

The interaction of 4-VP: DVB copolymers with the aqueous solution of $Fe_2(S0_4)_3$ was performed. Copolymer samples of 0.2 g were contacted with a 200 mL solution of 0.01M $Fe_2(SO_4)_3$ for 7 days. The pH of the sample-solution system was kept at 2.0 by use of a solution of either H_2S0_4 or KOH.

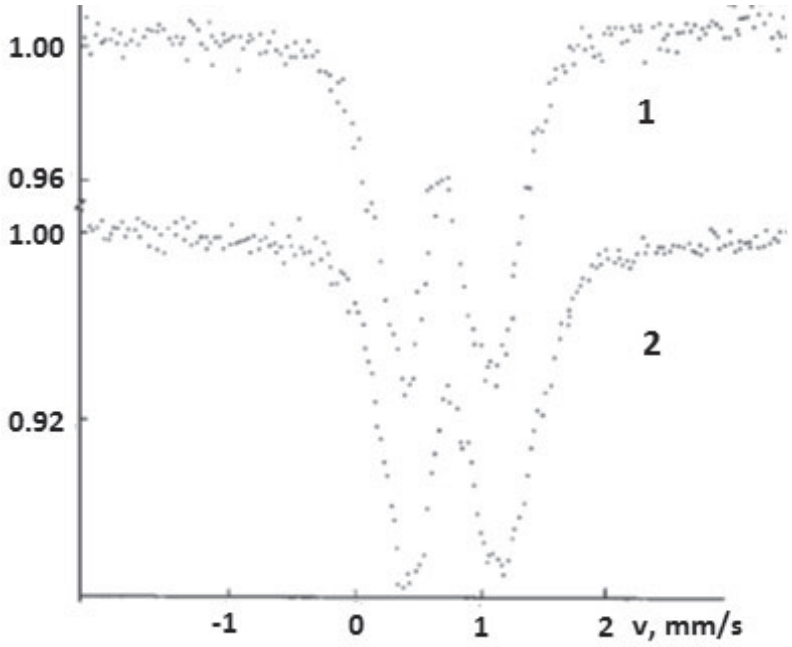

Figure 1-15. Mössbauer spectra of 4-VP: 10% DVB gel-type copolymer-Fe(III) complexes obtained at 300 (1) and 80 K (2).

Figures 1-15 and 1-16 present some typical Mössbauer spectra appearing as doublets. The parameters of the Mössbauer spectra, along with the retained amounts of Fe(III), are listed in Table 1-8. It can be noticed that the form of the spectra together with their characteristics values indicates the presence of Fe^{3+} ions in the high spin state and the octahedral configuration, as well as the absence of Fe^{2+} ions, i.e. the absence of a reducing agent in the copolymers.

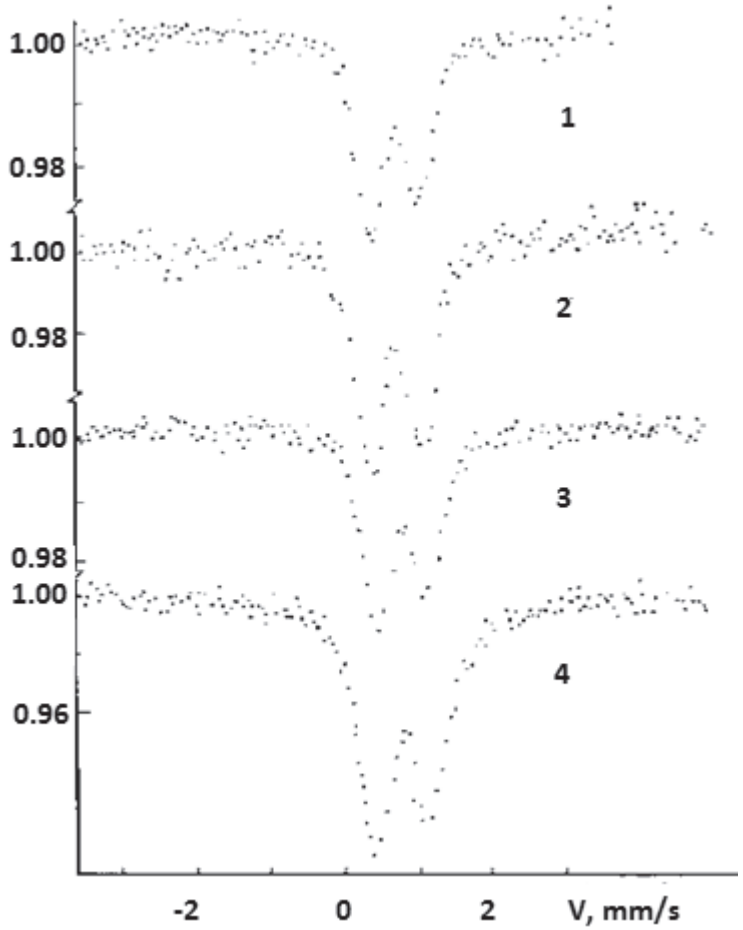

Figure 1-16. Mössbauer spectra of 4-VP: 2% DVB-Fe(III) complexes at 300 (1) and 80 K (2) and of 4-VP: 15% DVB toluene-modified copolymer-Fe(III) complexes at 300 (3) and 80 K (4).

Also, Table 1-8 shows that the determination of the spectra at 80 K induces a slight increase of the quadrupole splitting, with the increase of the cross-linking degree, meaning that the electronic state of Fe^{3+} in the copolymer hardly depends on the DVB content. The tendency of increasing the isomeric shifting with the increase of the crosslinking degree may also be observed, indicating a decrease of the covalent linking of the metal to the ligand. The line width in the studied spectra is higher as compared to that of crystalline structures; yet lower than that of ion exchangers retaining either iron cations or iron complex anions as a result of electrostatic interaction [77, 78]. The **Γ** values change with temperature, similar to those of the Fe^{3+} ions coordinated with the amine groups in weak basic anion exchangers [79]. For the samples containing 2 and 6% DVB, respectively, the width of the spectral lines does not depend on temperature. However, for the copolymers with ≥ 10% DVB, a certain dependence of **Γ** on temperature may be noticed, as a result of the spin-network type relaxation processes. The value of the probability (f ') of the Mössbauer Effect provides information on the oscillation of the coordinating centre of the macromolecular chain. As one can see from Table 1-8, the values of the f'_{300}/f'_{80} ratios (where f'_{300} *and* f'_{80} represent the probability of the Mössbauer Effect at 300 and 80 K**,** respectively) for the gel-type copolymers with 6 and 10% DVB and also for the copolymers synthesized in the presence of toluene, with 10% DVB, indicate a slight dependence of the Mössbauer Effect on temperature. The parameters of the Mössbauer spectra and their dependence on temperature support the conclusion that sorption of the Fe^{3+} ions on the 4-VP: DVB copolymer is conditioned, as expected, by the coordination process of cations with pyridinic nitrogen, the electronic state of Fe^{3+} ions in the copolymer depending, nevertheless, only slightly on their crosslinking degree. It has been also observed that in the complexed copolymers no complex ions of the $[Fe(H_2O)_6]^{3+}$, $[Fe_2(OH)_2(H_2O)_6]^{4+}$ and $[Fe(OH)(H_2O)_5]^{2+}$ types are formed. Consequently, as a result of the Fe(III) complexation with pyridinic nitrogen, destruction of the aqua-hydroxylic and dimeric complexes of Fe^{3+} occurs. From a quantitative point of view, Fe(III) is retained in the same order of magnitude by all 4-VP : DVB copolymers; the Fe(III) retention is significant, although sorption has been performed from an aqueous solution of $Fe_2(SO_4)_3$ and water is a poor solvent for the polyvinylpyridine chains.

The complexation of Fe^{3+} ions with the pyridinic groups of the 4-VP:DVB copolymers was confirmed by the IR spectra (Fig.1-17***).*** As known, complexation of polyvinylpyridine with ions of transitional metals is accompanied by an increase of the frequency of the C = N bond. The IR spectra (Fig.1-17***)*** evidence, besides the absorption band at 1600 cm^{-1}, attributed to the noncomplexed pyridinic rings, an intense band at about 1635 cm^{-1}, due to the nitrogen-metal bond; the analysis of some previous data shows that this absorption band is also present in quaternary ammonium containing polymers based on poly(4-vinylpyridine), i.e., compounds in which the pair of nitrogen-free electrons is occupied [80].

Table 1-8. Influence of the structure of 4-VP: DVB networks on quantitative and qualitative Fe(III) retaining complexes

Copolymer	Nitrogen, %	Fe, mg/g	T, K	Mössbauer parameters, mm/s				f_{300}/f_{80}
				δ	**ΔE_Q**	**Γ_l**	**Γ_r**	
4-VP: 2% DVB, gel type	10.80	16.24	300 80	0.62 0.73	0.70 0.68	0.47 0.47	0.47 0.47	0.37
4-VP: 6% DVB, gel type	10.25	20.71	300 80	0.70 0.75	0.70 0.73	0.57 0.52	0.57 0.57	0.67
4-VP: 10% DVB, gel type	10.30	19.94	300 80	0.68 0.77	0.72 0.77	0.44 0.49	0.52 0.64	0.66
4-VP: 10% DVB, toluene modified, $f_v = 0.7$	9.30	19.66	300 80	0.70 0.75	0.75 0.75	0.55 0.57	0.55 0.57	0.49
4-VP: 15% DVB, toluene modified, $f_v = 0.045$	9.35	19.14	300 80	0.62 0.65	0.68 0.73	0.49 0.62	0.55 0.62	0.22

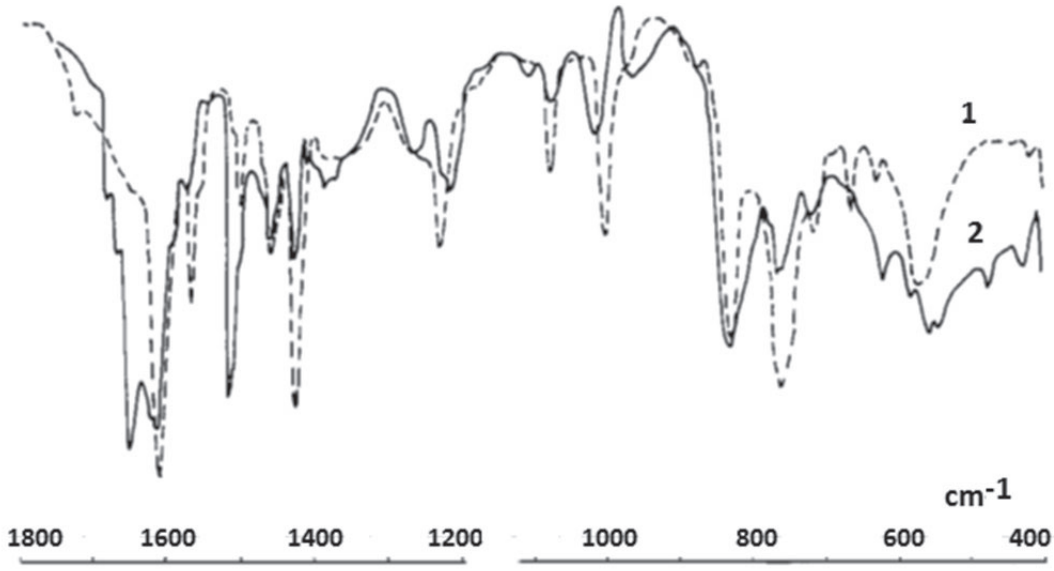

Figure 1-17. IR spectra 4-VP-8% DVB gel type copolymer (1) and 4-VP: 8% DVB gel-type copolymer – Fe(III) complex (2).

To obtain bifunctional polymers, the chemical modification of 4-VP: 8% DVB copolymers was carried out by the addition reaction of the copolymer to the carbon-carbon double bond of some electrophilic ethylenic compounds, such as acrylamide (AM), acrylonitrile (AN), and methyl vinyl ketone (MVK). The capacity of anion exchange ($Cl^- \leftrightarrow SO_4^{2-}$) and the sorption capacity (S) of cations (Fe^{3+}) from $Fe_2(SO_4)_3$ solution with pH 2.0 of modified copolymers were determined (Tab.1-9)

The 4-VP: DVB copolymers significantly change their nature upon modification. Consequently, the electron-donor pyridinic nitrogen is transformed into ammonium quaternary nitrogen, unable of forming donor-acceptor bonds. Also, in the chemically modified products appear functional groups having nitrogen and/or oxygen atoms, able of forming donor-acceptor bonds. It is assumed that such modifications essentially change the properties and, especially, the sorption mechanism of the Fe^{3+} cations. Table 1-9 shows some data on the chemically modified copolymer as compared to the precursor copolymer. The values presented in this table evidence distinct aspects: 1. The addition reaction of the 4-VP: DVB copolymer to ethylenic electrophilic compounds leads to unconventional strongly basic anion exchanger structures having exchange capacities with values close to those of common strong basic anion exchangers and - 2. The new crosslinked ionic structures retain Fe^{3+} cations in amounts close to the parent copolymer but much higher than the three-dimensional structures with benzyltrimethylammonium chloride or benzyldimethyl-2-hydroxyammonium chloride groups corresponding to strongly basic anion exchangers of types I or II**,** respectively.

Table 1-9. . Mössbauer parameters of synthesized ionic polymers-Fe(III) complexes

Code	Temperature, K	Mössbauer parameters, mm/s			
		δ	**ΔE_Q**	**Γ_l**	**Γ_r**
4-VP: 8% DVB + AN	300 80	0.79 0.87	0.94 0.90	0.37 0.46	0.57 0.75
4-VP: 8% DVB + AM	300	0.74	0.92	0.49	0.77
4-VP: 8% DVB + MVK	300	0.73	0.84	0.50	0.61

Figure 1-18 plots the Mössbauer spectra of the ionic polymer-Fe(III) complexes; the Mössbauer spectra appear as a doublet. From the values of the Mössbauer spectra (Tab.1-10), one can observe that the state of the Fe^{3+} cations in ionic polymers is different from that in the 4-VP: DVB copolymers, namely, that the values of quadrupole splitting corresponding to the state of Fe^{3+} cations in jarosite-type compounds, formed in strongly basic anion exchangers.

Table 1-10. Some characteristics of 4-VP: 8% DVB chemically modified copolymers as well as of the parent copolymer

Code	Structure ionic unit	Exchange capacity		S,
		meq/g	meg/mL	mg Fe/g
4-VP: 8% DVB	\\ /N	-	-	25.0
4-VP: 8% DVR + AN	\\ / N+-CH2-CH2-CN, Cl-	4.00	1.80	40.56
4-VP: 8% DVB + AM:	\\ / N+-CH,-CH2-CONH, Cl-	2.20	1.34	57.15
4-VP: 8% DVB + AM	\\ / N+-CH2-CH,-CO-CH3, Cl-	2.23	1.30	63.76

At the same time, the Mössbauer spectra show that in the synthesized ionic polymers the Fe^{3+} cations appear in a single electronic state, i.e., they form a single type of compounds.

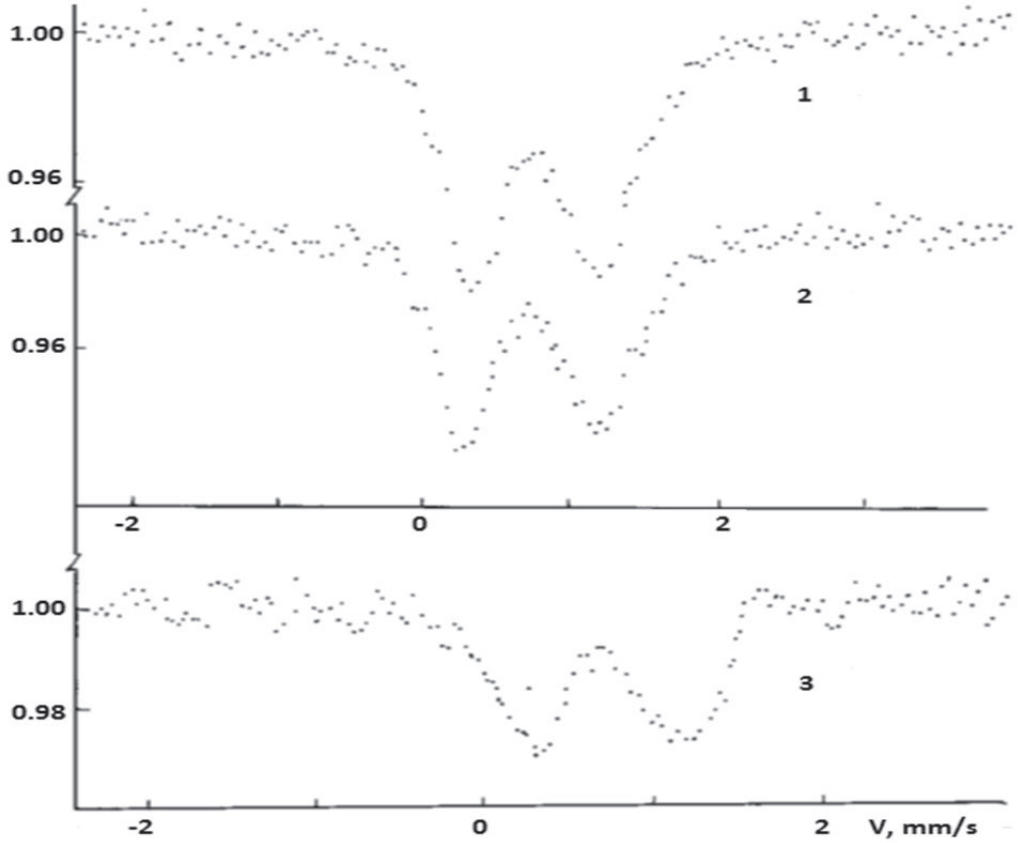

Figure 1-18. Mössbauer spectra of complexes of Fe^{3+} with 4-VP-8% DVB chemically modified copolymer with AN (1), AM (2) and MVK (3). All spectra were registered at 300 K.

Consequently, the amidic, ketonic, and nitrile functional groups do not participate through their nitrogen and/or oxygen atoms to complexation with Fe^{3+} cations. Additional proof of such an assertion is provided as well by IR spectroscopy (Figs.1-19 and 1-20).

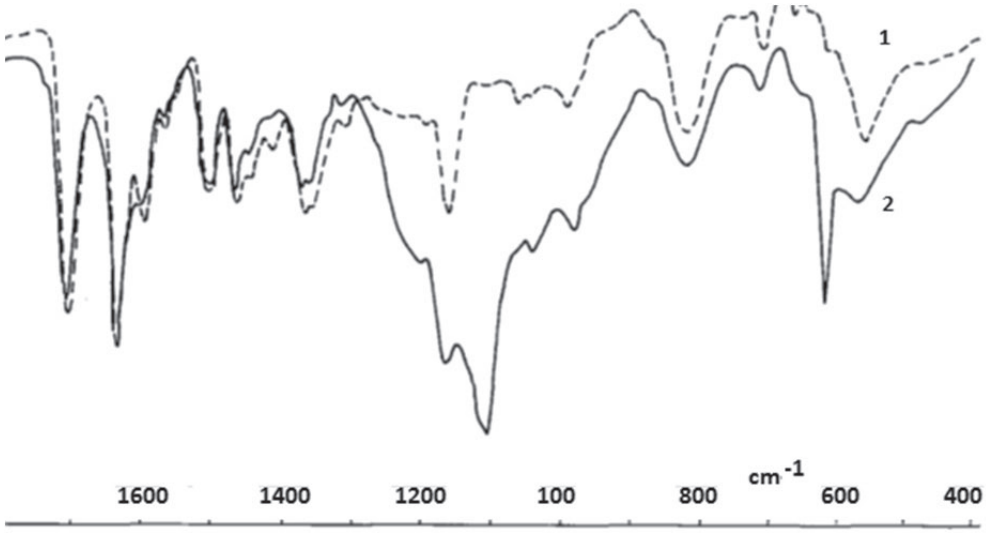

Figure 1-19. IR spectra of 4-VP: 8% DVB + MVK (1) sample and 4-VP: 8% DVB + MVK-Fe(III) complex (2).

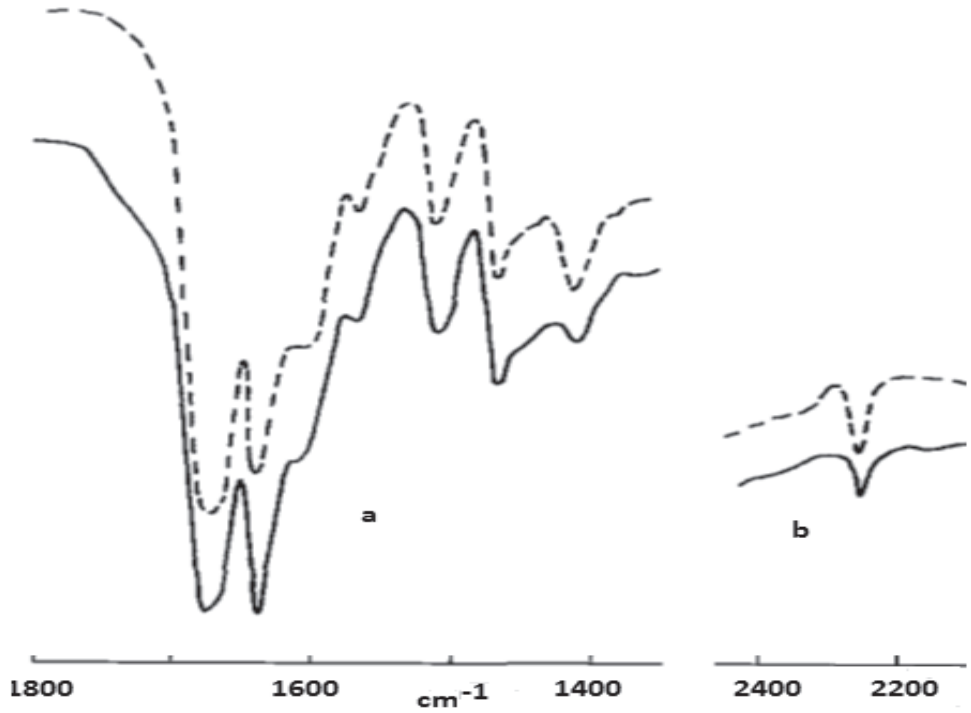

Figure 1-20. Characteristic absorption bands of IR spectra for (a) 4-VP: 8% DVB + AN sample and its Fe(III) complex, and (b) 4-VP: 8% DVB + AM sample and its Fe(II1) complex. Broken lines represent the initial samples while the complexes are represented by full lines.

The IR spectra of the chemically modified copolymers having Fe^{3+} ions evidence absorption bands at 1100, 870, and 620 cm^{-1}, belong to the free SO_4^{2-} ions. The absorption bands at 1200 and 1300-1130 cm^{-1} belong to SO_4^{2-} coordinated with three metallic ions while the absorption band at about 480 cm-' is assigned to the ***v*** (M - O) metal-oxygen bond from SO_4^{2-}, OH^- and H_2O [81].

Another aspect of the IR spectra of the ionic polymer - Fe(III) complexes is worth mentioning here. The bands characteristic to the amidic, ketonic, and nitrile functional groups are not subjected to any shift. They may be found at the following values: ***v*** (CN) = 2250 cm^{-1}, ***v*** (CO) = 1710 cm^{-1}, and ***v*** (CONH) = 1670 cm^{-1}, similarly to the situation in ionic polymers without Fe(III). All these observations lead to the conclusion that the Fe^{3+} cations are kept by the synthesized ionic polymers not through the ionic exchange, due to the quaternary nitrogen atoms, retention occurring in the form of the jarosite-type compounds. It was also seen that, although having atoms able to form donor-acceptor bonds, the functional groups do not participate in complexation. Probably, the presence of the nitrogen quaternary atom with an inductive effect *(-I)* reduces the electron density from the donor atoms of the functional groups, preventing their complexation with metallic ions. Additional evidence supporting the retention of the Fe^{3+} cations by the synthesized ionic structures by jarosite-type compounds formation consists in the fact that they do not retain the metal from $FeCl_3$, but only from $Fe_2(SO_4)_3$.

1.2.5.2. Iron compounds in polymers also containing groups that can participate in cations exchange processes

The synthesis of the copolymer 4-vinylpyridine divinylbenzene (4-VP : 8% DVB) chemically modified by monochloroacetic and acrylic acids was investigated, and the study of its interactions with Fe^{3+} cations [79]. Fe(III)-containing samples of the modified copolymer were prepared as follows: copolymer samples of 1 g were contacted at 50°C with a 500 ml solution (pH 2.0) of 0.02 M $Fe_2(SO_4)_3$ for 12 h.

The IR spectra of the copolymer modified by acrylic acid (Fig.1-21) include a series of absorption bands of carboxylic groups. The absorption band ν (COO) = 1710 cm^{-1} is attributed to the carboxylic group in the $\geq N^+–CH_2 – CH_2 –COOH$ fragment, and bands ν_{as} (COO) =1596 cm^{-1} and ν_s (COO) = 1413 cm^{-1} are attributed to the ionized carboxylic group [36]. The IR spectra confirm that almost all carboxylic groups in the modified copolymer are ionized. We suggest that the absorption band at 1636 cm^{-1} represents a superposition of the $\delta(H_2O)$ and ν(C⎓O) bands of ionized carboxylic groups interacting electrostatically with quaternary ammonium groups.

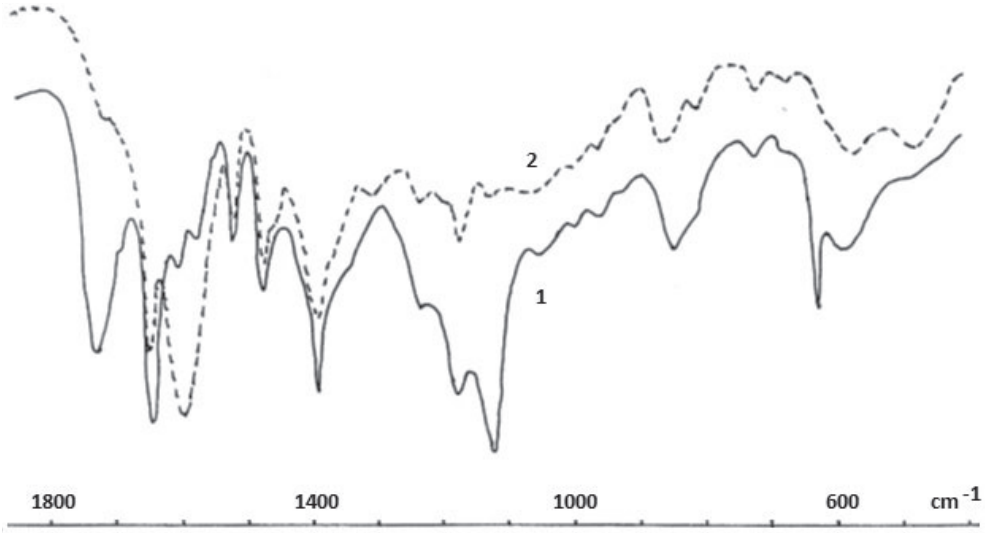

Figure 1-21. IR spectra of copolymer modified by acrylic acid with (1) and without (2) Fe^{3+} ions.

The IR spectrum of the Fe(III)-containing polymer is essentially different (Fig.1-21). The increase of the absorption band at 1724 cm^{-1} indicates that some of the carboxylic groups of the polymer become protonated during treatment with $Fe_2(SO_4)_3$ solution. The decrease of the band intensity at 1596, 1450 and 1413 cm^{-1} and the appearance of new bands at 1575 and 1538 cm^{-1} are due to the complexation of Fe^{3+} cations with carboxylic groups of the polymer. According to the IR spectra (Figs.1-21 and 1-22) in the copolymer chemically modified by monochloroacetic acid, Fe^{3+} cations may form complexes of types I and II (Scheme 1-1).

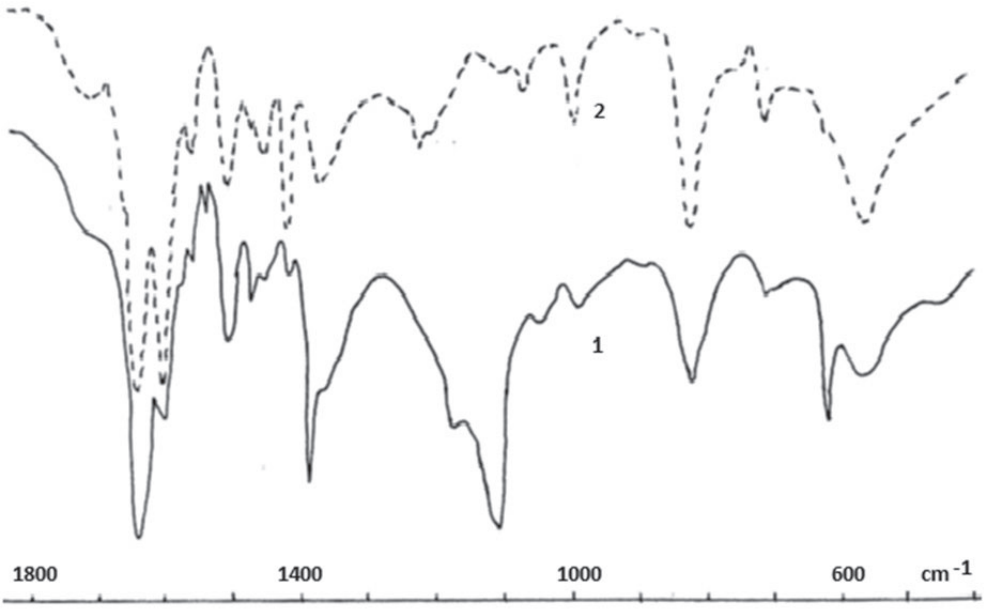

Figure 1-22. IR spectra of copolymer modified by monochloracetic acid with (1) and without (2) Fe(III) compounds.

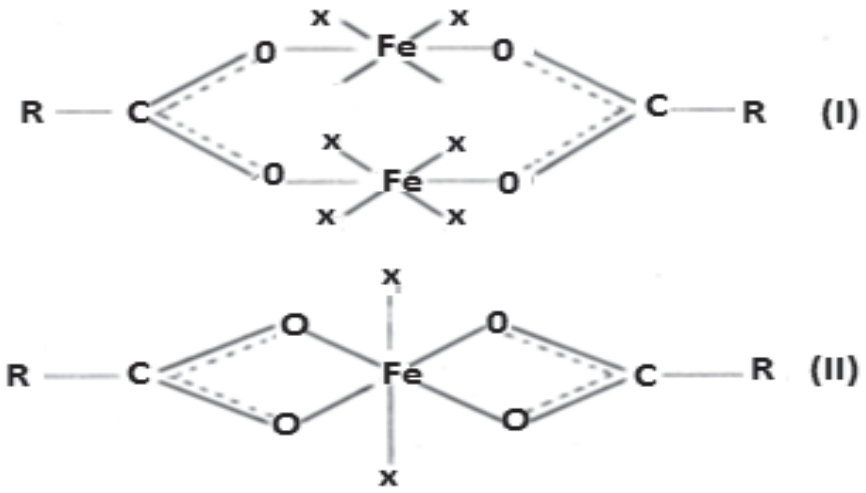

Scheme 1-1. Types of Fe(III) compounds, where x can be SO_4^{2-} and H_2O.

The absorption bands at 1105 and 615 cm^{-1} (Figs.21 and 22) show that the Fe(III)-containing polymers also contain a considerable amount of SO_4^{2-} anions. The superposition bands at about 1100 cm^{-1} do not allow us to identify the SO_4^{2-} anions in the jarosite-type compounds.

The IR spectra of the chemically modified copolymers containing Fe^{3+} ions display absorption bands at 1105 and 615 cm^{-1} indicative of free SO_4^{2-} anions.

The absorption bands at about 1200, 1230 and 1130 cm^{-1} are probably due to SO_4^{2-} anions in the jarosite-type compounds.

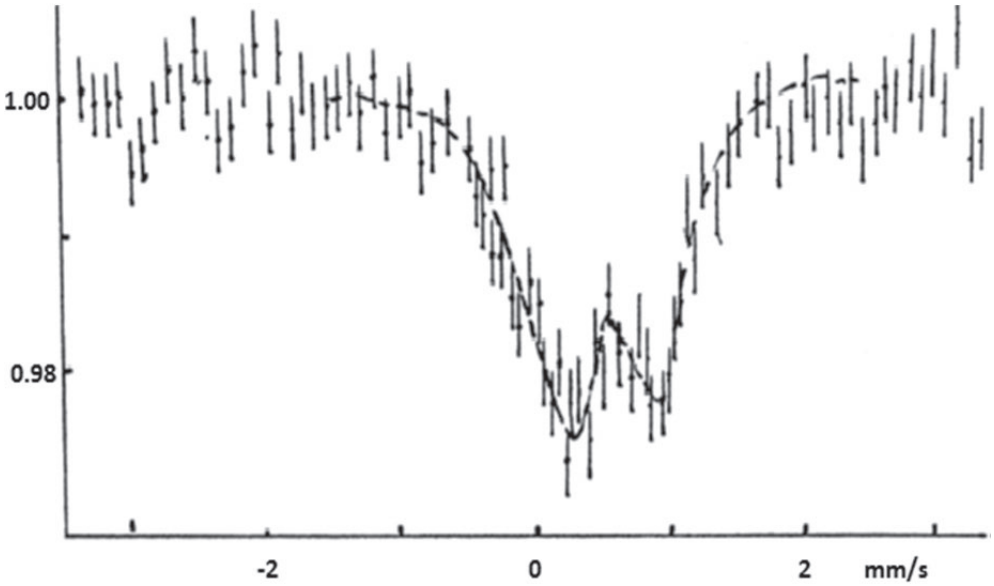

Figure 1-23. Mössbauer spectrum at 300 K of copolymer modified by acrylic acid that has retained Fe^{3+} ions from $Fe(NO_3)_3$ solution.

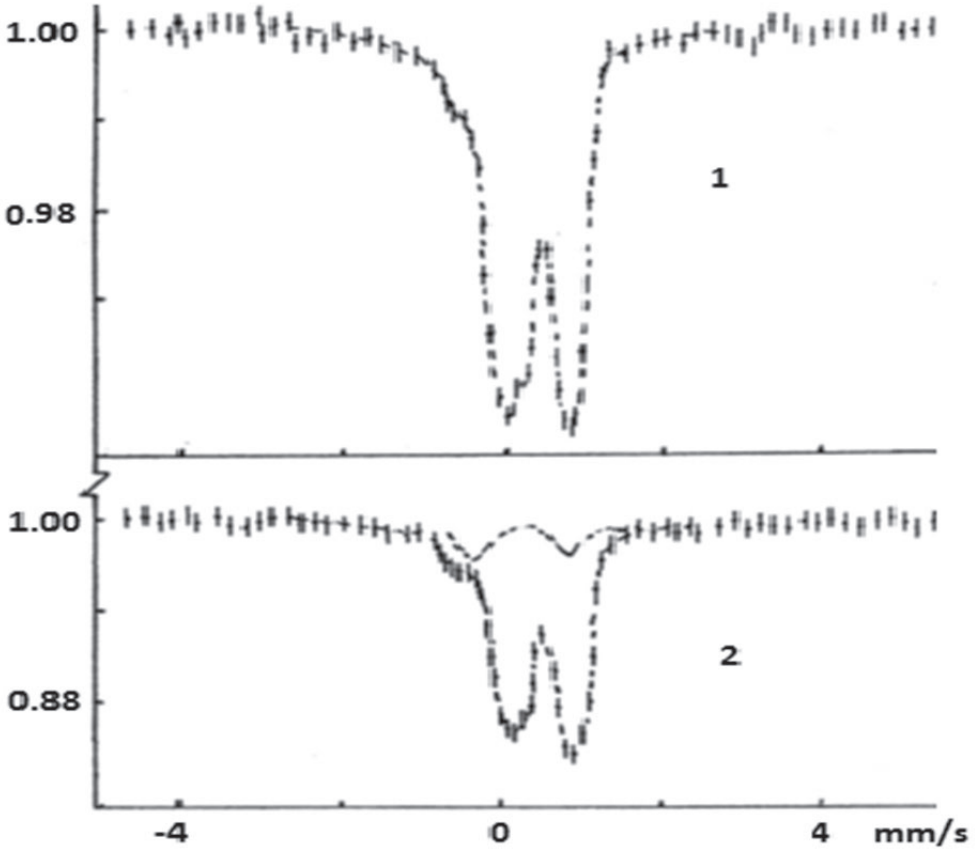

Figure 1-24. Mössbauer spectra at 300 (1) and 80 K (2) of copolymer modified by acrylic acid that has retained Fe^{3+} ions from $Fe_2(SO_4)_3$ solution.

Figure 1-23 shows the Mössbauer spectrum of the copolymer modified by acrylic acid retaining Fe^{3+} cations from $Fe(NO_3)_3$ solution.The parameters of the Mössbauer spectrum of this polymer with the retained amount of iron are listed in Table 1-11. One can see that the shape of the spectrum, the values of the isomer shift, quadrupole splitting and width of the peaks indicate the presence of Fe^{3+} ions in the same electronic state. The iron^{3+} ions have an octahedral environment in this copolymer. It may be concluded that the sorption of Fe^{3+} ions from $Fe(NO_3)_3$ solution occurs by the coordination of the cations with carboxylic groups of the modified copolymer.The Mössbauer spectrum of the same modified copolymer retaining Fe^{3+} ions from $Fe_2(SO_4)_3$ solution (Fig. 1-24) shows a superposition of two doublets. This indicates that the Fe^{3+} cations are in two different electronic states, i.e. they form two kinds of the compounds. The doublet with isomer shift $\boldsymbol{\delta}$ = 0.71 mm/s and quadrupole splitting $\boldsymbol{\Delta E_Q}$ = 0.74 mm/s at 300 K and $\boldsymbol{\delta}$ = 0.78 mm/s and $\boldsymbol{\Delta E_Q}$ = 0.74 mm/s at 80 K (Table 1-11) is due to Fe(III) carboxylic complexes. These parameters differ from those for the copolymer retaining Fe^{+} cations from $Fe(NO_3)_3$ solution. This allows us to assume that the coordination sphere of the iron^{3+} ions consists of carboxylic groups and SO_4^{2-} anions. The doublet with parameters $\boldsymbol{\delta}$ = 0.47 mm/s and $\boldsymbol{\Delta E_Q}$ = 1.14 mm/s at 80 K corresponds to Fe^{3+} ions in the jarosite-type compound.

Table 1-11. Parameters of Mössbauer spectra of Fe(III)-containing copolymers

Copolymer	Solution	T, K	Spectrum forme	Mössbauer parameters, mm/s					mg Fe/g
				$\boldsymbol{\delta}$	$\boldsymbol{\Delta E_Q}$	$\boldsymbol{\Gamma_l}$	$\boldsymbol{\Gamma_r}$	H_{ef}, kOe	
\\ / N–CH_2 –CH_2 –COO^-	$Fe(NO_3)_3$	300	Doublet	0.51	0.67	0.58	0.53	0	15.8
\\ / N–CH_2 –CH_2 –COO^-	$Fe_2(SO_4)_3$	300 80	Doublet Doublet Doublet	0.71 0.78 0.47	0.74 0.70 1.14	0.53 0.44 -	0.44 0.44 -	0 0 0	20.1
\\ / N–CH_2 –CH_2 –COO^- *	$Fe_2(SO_4)_3$	300 80	Doublet Sextet Doublet	0.60 0.88 0.56	0.75 0.08 0.76	0.70 - -	0.60 - -	0 476.6 0	35.3
\\ / N –CH_2 –COO^- *	$Fe_2(SO_4)_3$	300 80	Doublet Sextet Doublet	0.60 0.79 0.73	0.80 0.09 0.84	0.70 - -	0.60 - -	0 476.0 0	38.5

To confirm the formation of the jarosite-type compound in the modified copolymer contacted with $Fe_2(SO_4)_3$ solution, this compound was transformed into FeOOH. It is known [82] that jarosite compounds, when heated in water, are converted to highly dispersed particles of FeOOH in a superparamagnetic state. The Mössbauer spectra of FeOOH in the superparamagnetic state show only one doublet and the modification of FeOOH cannot be found. However, when several sorption– heating cycles in water are conducted, large sized FeOOH particles are obtained. The large FeOOH particles allow identification of its modification using Mössbauer spectroscopy [65].

As can be seen from Figs.1-25 and 1-26, the Mössbauer spectra of the modified copolymer after three ‘‘sorption–boiling in aqueous medium’’ cycles present a doublet at 300 K and a sextet with a doublet in the centre of the spectrum at 80 K. Parameters of the Mössbauer spectra ($H_{ef.}$ =0 at 300 K and $H_{ef.}$ = 476 kOe at 80 K) correspond to massive magnetically ordered particles of β-FeOOH [65].

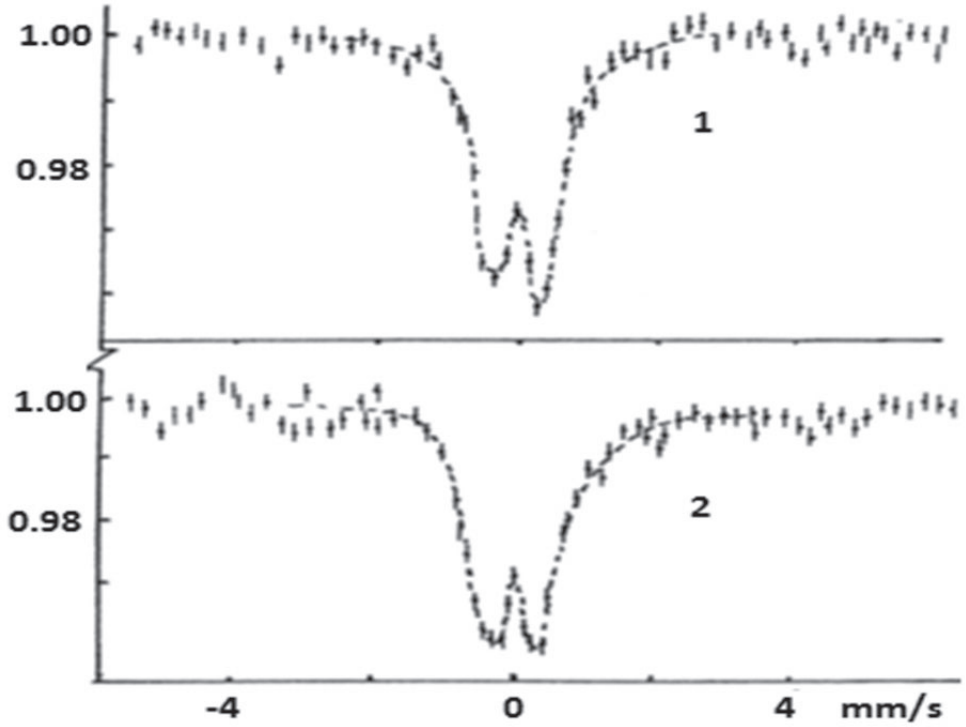

Figure 1-25. Mössbauer spectra at 300 K of copolymer modified by acrylic acid (1) and monochloracetic acid (2) that has retained Fe^{3+} ions from $Fe_2(SO_4)_3$ solution after three “sorption–boiling in aqueous medium” cycles.

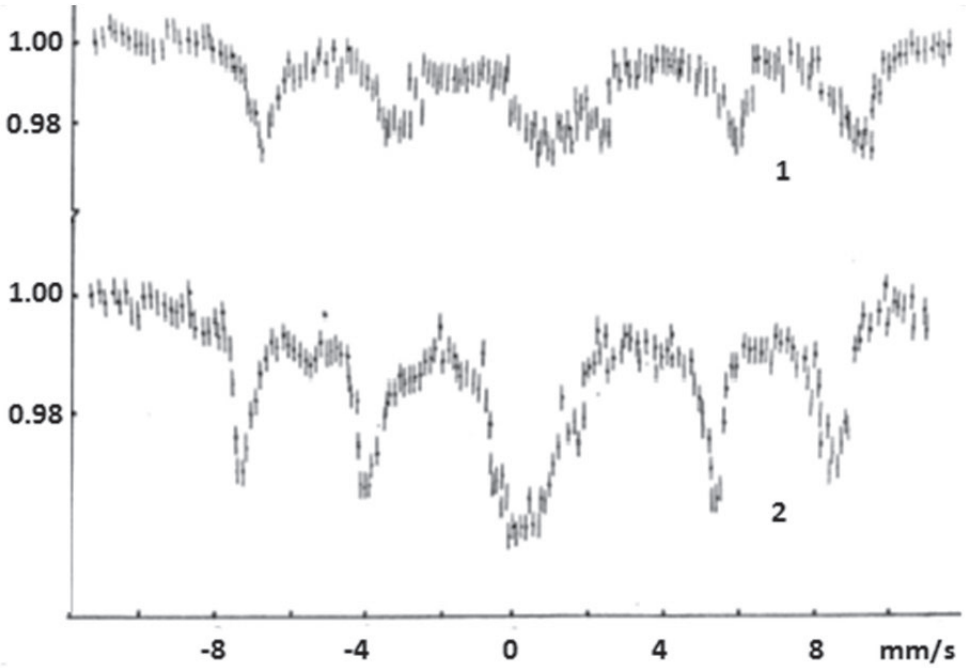

Figure 1-26. Mössbauer spectra at 80 K of copolymer modified by monochloracetic acid (1) and acrylic acid (2) that has retained Fe^{3+} ions from $Fe_2(SO_4)_3$ solution after three “sorption–boiling in aqueous medium” cycles.

The doublet in the centre of the sextet is attributed to higher dispersed β-FeOOH in the superparamagnetic state that remains in the narrow pores of the polymer, and to Fe-carboxylates. Jarosite compounds heated in water are converted into α-FeOOH [82], but in the investigated polymers they are converted into β-FeOOH.

Thus, it has been shown that the jarosite mineral type compounds can also form in the phase of polymers containing strongly basic groups and groups with electrons donor atoms.

II.

CHROMIUM (III) COMPOUNDS IN THE POLYMERS PHASE

2.1. Cr(III)-containing compounds in the strongly basic anion exchangers

In nature there is no mineral Cr-jarosite. We suggested that by contacting a polymer having strong basic groups with a solution of chromium (III) sulfate in the polymer phase, jarosite compounds can form. The obtaining of Cr(III) compounds in the phase of cross-linked ionic polymers with strongly basic groups is of theoretical and practical interest. It is well known that Cr(III) compounds are distinguished by their high chemical stability. Thus, the sorbents and catalysts obtained by modification of polymers with chromium (III) compounds can be used in a more aggressive media than similar sorbents/catalysts containing Fe(III) compounds. On the other hand, Cr(III) and Fe(III) jarosite-type compounds could serve as models with peculiar magnetic properties [83].

The strongly basic commercial anion exchangers AV-17(Cl) (holding $-N(CH_3)_3Cl$ and Varion-AD holding $-N(CH_3)_2C_2H_4OH$ were used. The resins have a polystyrene–divinylbenzene matrix and are of gel type. Their full exchange capacity is 3.5–4.0 mEqv/g [4]. Dried samples (0.2 g) of the polymers were contacted with 100 mL of $KCr(SO_4)_2{*}12H_2O$ solutions. The pH of the solution–sample systems was kept by using either H_2SO_4 or KOH solutions [84]. The samples of polymers stayed connected for 24 h at 30 and 50°C with solutions of various concentrations having an initial pH of 4.35. Sorption isotherms and pH of contacting solutions after sorption are presented in Figures 2-1 and 2-2. As shown in these figures, the sorption processes of Cr(III)-containing cations takes place with a pH decrease of the polymer-solution system. The decrease in pH of the solution contacting with the polymer takes place because of both Cr^{3+} cations hydrolysis and Cr(III)-containing ions sorption. The degree of hydrolysis of Cr^{3+} cations in the polymer phase differs from the one in solution. The Cr(III)-containing cations sorption on strongly basic anion exchangers essentially depends on pH and temperature (Figs. 2-1 and 2-2).

Variation of pH leads to the modification of the solution and the polymer's phase composition. According to Fishtic and Vataman [55] in the solutions of $KCr(SO_4)_2 {*}12H_2O$ used there are some kinds of Cr(III)-containing cations: $[Cr(H_2O)_6]^{3+}$, $[CrOH(H_2O)_5]^{2+}$, $[Cr_2(OH)_2(H_2O)_8]^{4+}$, and $[Cr_3(OH)_4(H_2O)_{10}]^{5+}$. Not all of these cations are able to participate in the formation of Cr(III) compounds in the exchanger's phase. With increasing pH, the concentration of $[Cr(H_2O)_6]^{3+}$ cations in the solution decreases, but sorption of the Cr(III)-containing ions on strongly basic anion exchangers grows. From solutions of pH < 1.5 the sorption of Cr(III)-containing ions is absent. So, $[Cr(H_2O)_6]^{3+}$ cations do not take part in the formation of the Cr(III) compounds in the polymer's phase. It is known[57] that polynuclear cations cannot easily be restructured to form new units. Consequently, during the formation process of the Cr(III) compounds in the polymer's phase it is probable that the $[CrOH(H_2O)_5]^{2+}$ cations participate, the concentration of which increases at pH > 1.5. Since the ionic composition of the $KCr(SO_4)_2{*}12H_2O$ solution depends on temperature, it was expected that the Cr(III)-containing ions sorption on strongly basic anion exchangers will depend on temperature, too. Therefore, in the investigations of Cr(III)-containing ions sorption on such polymers the influence of temperature is of interest.

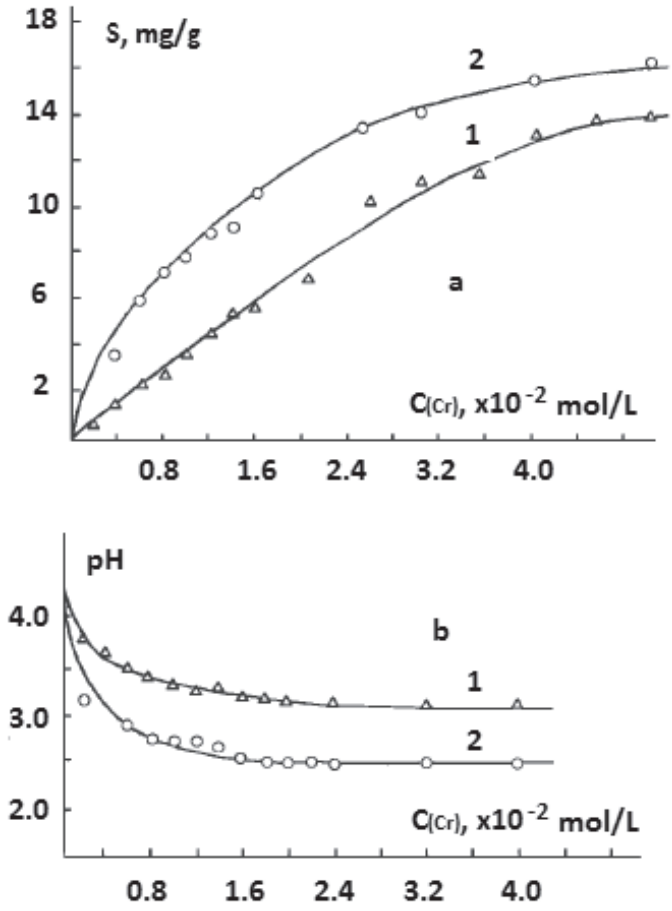

Figure 2-1. Sorption isotherms of Cr(III)-containing cations by polymer AV-17 (a) and equilibrium pH of the solution after sorption (b) at 30 (1) and 50°C (2).

As is shown in Figure 2-3, the sorption of Cr(III)-containing ions from the $KCr(SO_4)_2 * 12H_2O$ solutions with constant pH at 4.0 on exchangers AV-17 and Varion-AD (depending on temperature) passes through a maximum at about 60 °C.

The important conclusion from the pH and temperature dependence of the Cr(III)-containing ions retention on polymers is that the sorption is not a physical but a chemical process. This fact excludes ion exchange as a possible process for the sorption of Cr(III)-containing cations. It also excludes sorption due to the formation of a $Cr(OH)_3$ precipitate in the polymer phase. We suggest that the retention of the Cr(III)-containing cations on the strongly basic anion exchangers is due to the formation of jarosite-type compounds in the polymer's phase, as in the case of Fe(III) containing ions retention on such polymers [33, 53].

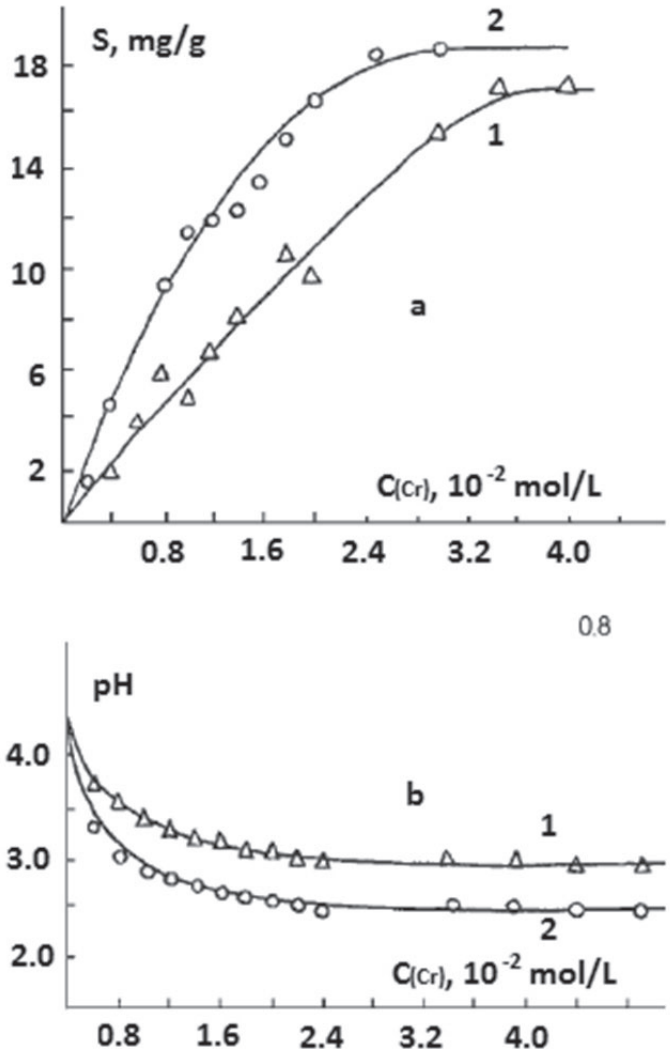

Figure 2-2. Sorption isotherms of Cr(III)-containing cations by polymer Varion-AD (a) and equilibrium pH of solution after sorption (b) at 30 (1) and 50°C (2).

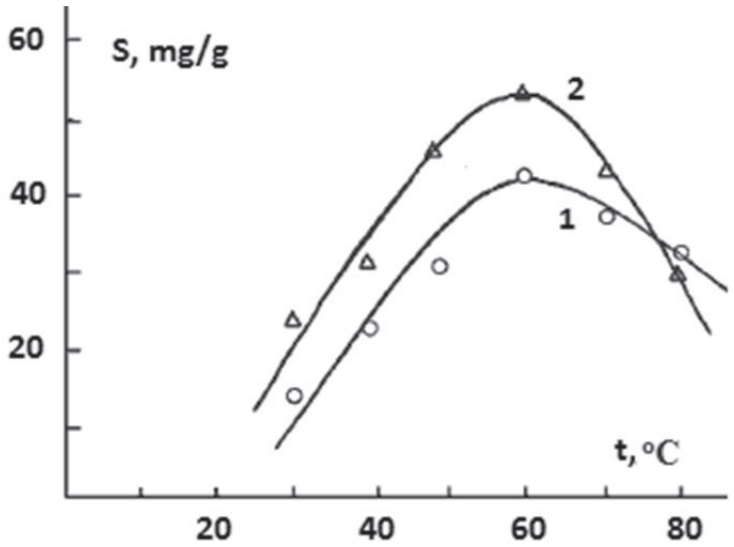

Figure 2-3. Temperature dependence of the Cr(III)-containing cations' sorption on anion exchangers Varion-Ad (1) and AV-17 (2).

The pH and temperature influence on the Cr(III)-containing cations sorption is explained to be due to the modification of $[CrOH(H_2O)_5]^{2+}$ ions concentration in solution contacting with the polymer. During the contact of the polymers in the Cl^- form with $KCr(SO_4)_2 * 12H_2O$ solution the anion exchange processes take place according to Equation (2-1):

$$2R_4NCl + SO_4^{2-} \leftrightarrow (R_4N)_2 SO_4 + 2Cl^- \quad (2\text{-}1)$$

The rate of the process (2-1) is more than that of the Cr(III)- containing ions sorption. In the polymer phase, the concentration of SO_4^{2-} ions is much higher than in the contact solution and the equilibria (2-2) and (2-3) may be established:

$$(R_4N)_2 SO_4 + HOH \leftrightarrow R_4NHSO_4 + R_4NOH \quad (2\text{-}2)$$

$$2R_4NHSO_4 \leftrightarrow (R_4N)_2 SO_4 + 2H^+ + SO_4^{2-} \quad (2\text{-}3)$$

With increasing pH of the contacting polymer solution, the number of R_4NOH groups in the polymer phase increases as well. The R_4NOH groups of polymers take part in the formation of jarosite-type compounds in the polymer's phase. Unfortunately, the particles of the Cr(III) jarosite-type compounds in the polymer phase are too small and have low crystallinity to use the X-ray diffraction method for their identification.

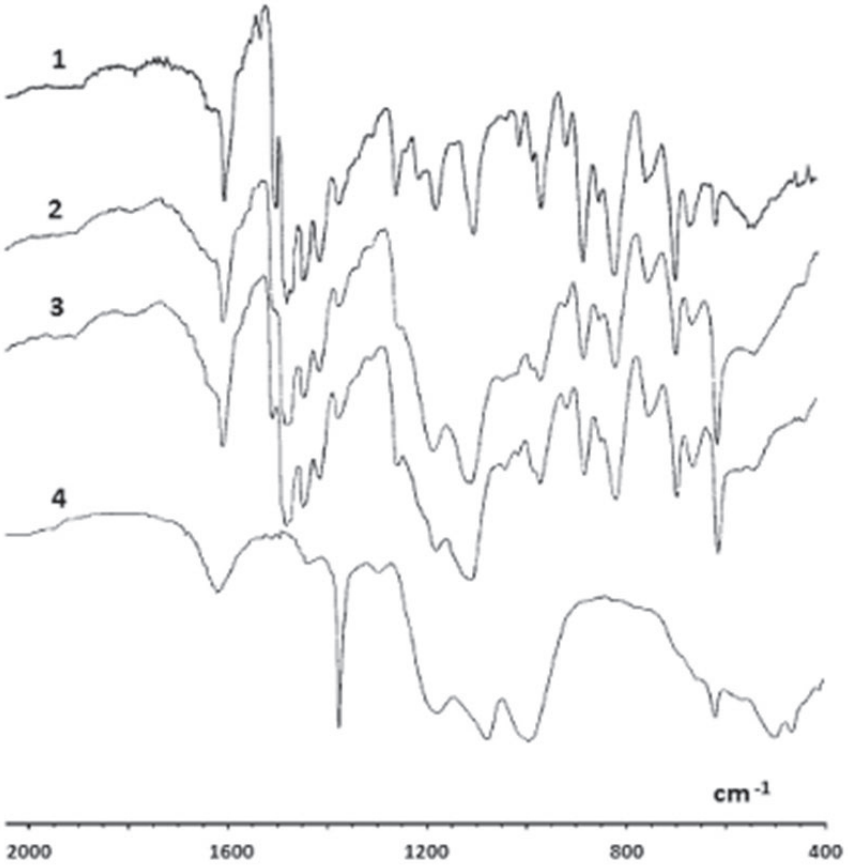

Figure 2-4. IR spectra of the samples: unmodified with metal AV-17(SO_4) polymer (1), AV-17 containing Cr(III) compounds (2), AV-17 containing Fe(III) compounds (3) and $K[Fe_3(OH)_6(SO_4)_2]$ (4).

The low crystallinity is characteristic for synthetic jarosite [58]. According to [30] jarosite particles are in the superparamagnetic state, characteristic of ultrafine particles (with a radius less than 4 nm for Fe_2O_3) [52]. The IR spectra of the Cr(III)-containing polymers are a little informative because they contain a very large absorption band at about 1100 and 620 cm^{-1}. The large absorption band (Fig.2-4) is a superposition of some bands from SO_4^{2-} and HSO_4^- ions (retained electrostatically by the R_4N^+ groups of polymers) and from SO_4^{2-} coordinated with three metallic ions [58].

Since the sorption of Cr(III)-containing cations from the $CrCl_3$ solutions does not take place on the strongly basic anion exchangers, we assume the sorption mechanism from the Cr(III) sulfates solutions to be the same as the Fe(III)-containing ions sorption investigated by the more informative method of Mössbauer spectroscopy [33, 53, 76]. Therefore we suggest that the Cr(III) compounds in the phase of strongly basic anion exchangers are formed according to Equation (2-4):

$$2(R_4N)_2SO_4 + 3R_4NOH + 3CrOH(H_2O)_5^{2+} \leftrightarrow R_4N[Cr_3(OH)_6(SO_4)_2] + 6R_4N^+ + 15H_2O \quad (2\text{-}4)$$

Some of the Cr(III) compounds in the polymer phase may be in the form of $K[Cr_3(OH)_6(SO_4)_2]$ and $H_3O[Cr_3(OH)_6(SO_4)_2]$ as in the cases of jarosite compounds [53].

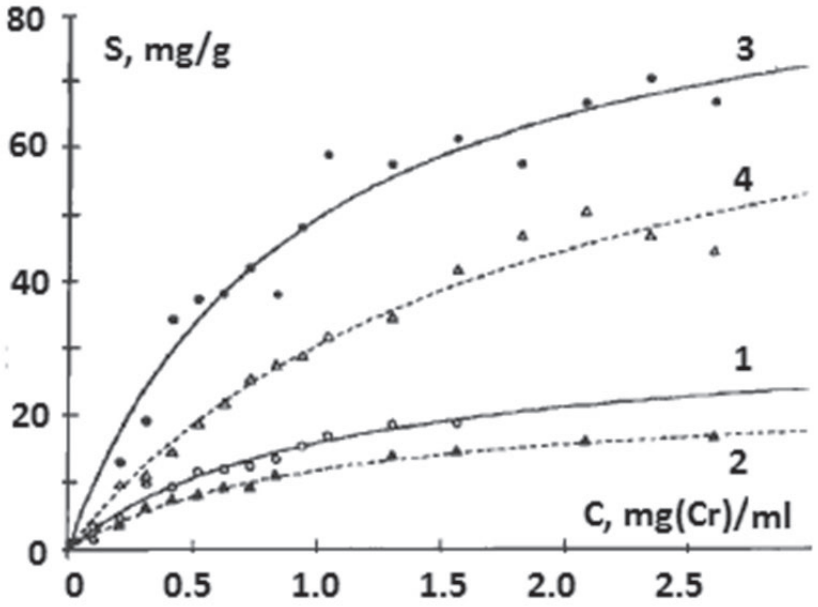

Figure 2-5. Sorption isotherms of Cr(III)-containing cations on Varion-AD (1, 3) and AV-17 (2, 4) polymers at 60°C from the solution with constant pH 4.2 during the sorption process (3, 4) and at 50°C from the solutions with initial pH of only 4.2 (1, 2).

Because the pH and temperature essentially influence the Cr(III)-containing cations sorption on strongly basic anion exchangers, we considered it necessary to obtain sorption isotherms at 50 and 60°C with and without maintaining $KCr(SO_4)_2 * 12H_2O$ solutions' pH constant. In these investigations the polymer samples interacted for 24 h with $KCr(SO_4)_2 * 12H_2O$ solutions having constant pH 4.2 during the sorption process at 60°C, and having an initial pH of only 4.2 at 50°C. As seen in Figure 2-5, the sorption of Cr(III)-containing cations at 60°C from solution with constant pH 4.2 is much more than in the cases of sorption at 50°C from the solutions with decreasing pH from 4.2 to about 2.5 (see Figs. 2-1 and 2-2).

Table 2-1. The values of sorption (S) from solutions of Cr(III)-containing cations by different polymers at 60^0C

No.	Polymer	Place of manufacture	Functional group group	DVB, %	S, mg Cr/g
1.	AV-17(Cl)	Russia	$-N^+(CH_3)_3$	8	71.8
2.	AV-17-2P	Russia	$-N^+(CH_3)_3$	2	66.1
3.	Varion-AD	Hungary	$-N^+(CH_3)_2\,C_2H_4OH$	8	55.9
4.	Purolite A-400	England	$-N^+(CH_3)_3$	8	30.2
5.	Amberlite IRA-410	USA	$-N^+(CH_3)_2\,C_2H_4OH$	8	45.2
6.	4-VP-AN	Romania	$\geq N^+CH_2CH_2CN$	8	78.0
7.	4-VP-AM	Romania	$-N^+(CH_3)_2\,C_2H_4CONH_2$	8	78.6
8.	4-VP-MVC	Romania	$-N^+(CH_3)_2\,C_2H_4CH_3$	8	58.9
9.	KU-2	Ukraine	$-SO_3H$	8-10	88.8
10.	KB-2	Russia	>C-COOH | >C-COOH	2-3	89.5
11.	KB-4	Russia	>CH-COOH	6	45.9
12.	KB-4P-2	Russia	>CH-COOH	2.5	43.1
13.	Amberlite IRC-50	USA	>CH-COOH	8	35.8

The sorption isotherms obtained at 60°C are well described by the Langmuir sorption model for a single type of equivalent active centres (Eq. (1-9)).

The calculated isotherm constants are K_L = 0.667 mL/mg and S_L = 100 mg Cr/g for Varion-AD; K_L = 0.417 mL/mg, and S_L= 100 mg Cr/g for AV-17. (For the sorption isotherm obtained at 50 and 60°C (Fig. 2-5), new portions of polymers were used). The ability of strongly basic anion exchangers to keep metallic cations from solutions is an unusual phenomenon. The chemistry of the metallic cation retention on such kind of polymers completely differs from the one on sulfo- or carboxylic cation exchangers. Therefore it is interesting to compare the capacity of Cr(III)-containing cations sorption of different kinds of exchangers. For the investigation, samples of polymers that interacted

at 60°C for 18 h with 0.038 M $KCr(SO_4)_2 * 12H_2O$ solution having constant pH 4.2. Characteristics of used commercial exchangers are given in Ref. [4].

The obtained sorption capacities of the investigated exchangers are listed in Table 2-1. As seen in Table 2-1, the metallic cations sorption capacity of strongly basic anion exchangers is comparable with the capacity of cation exchangers. The small sorption capacity of the KB-4, KB-4P-2, and Amberlite IRC-50 is due to the low dissociation degree of the carboxylic groups of polymers at pH 4.2, although sorption takes place through the complex formation. The higher sorption capacity of the carboxylic exchanger KB-2 is on account of its ability to form chelate compounds with Cr^{3+} cations.

2.2. Kinetics of Cr(III)-containing cations sorption

The kinetic curves of Cr(III)-containing cations sorption were obtained at 60 °C using $4 \cdot 10^{-2}$M $KCr(SO_4)_2 * 12H_2O$ solutions with constant pH 4.2 (Fig.2-6). Their analysis was performed using different models:

1. Assuming that ions sorption kinetics is limited by external diffusion, Equation (2-5) may be applied [85]:

$$\ln(1-F) = - k \tau \quad (2\text{-}5)$$

where F = S/S∞ , *S* is the sorption at given time *τ* ,*S*∞ is maximal sorption at equilibrium, and *k* is the rate constant. The constant *k* can be calculated using Equation (2-6):

$$k = \frac{3D^l}{r_o l k_d} \quad (2\text{-}6)$$

where D^l is the diffusion constant through the liquid layer around the polymer granule, r_o is the granule radius, *l* is the thickness of the liquid layer around the granule, k_d is the ion distribution constant, expressed by the ratio of ion content in the polymers at equilibrium (mmol/g) and in solution (mmol/mL).

The kinetics of the process limited by external diffusion can also be expressed according to Nernst's theory about the external mass transfer [86]:

$$\ln(1-F) = - \frac{A\beta\tau}{W k_d} \quad (2\text{-}7)$$

where *A* is the surface of the polymer spherical granule, *W* is the granule volume, ß and is the empiric coefficient of mass transfer (mm/s). For spherical particles

$$A/W = 3/r_o \text{ and } \ln(1-F) = \frac{3\beta\tau}{r_o k_d} \quad (2\text{-}8)$$

In this conditions the ratio $- \frac{3\beta\tau}{r_o k_d}$ is a constant, expressed further through *γ*. Thus, Equation (2-8) converts into Equation (2-9):

$$\ln(1-F) = \gamma\tau \quad (2\text{-}9)$$

2. Assuming that the limiting stage is the internal diffusion, the kinetic model could be expressed by Equation (22-10) [85]:

$$F = 1 - \frac{6}{\pi^2} \sum_{n=1}^{\infty} \frac{1}{n^2} \exp\left(-\frac{D^i \pi^2 n^2 \tau}{r_o^2}\right) \quad (2\text{-}10)$$

where D^i is the internal diffusion constant.
Taking $\beta = D^i\pi^2/r_o^2$, Equation (2-9) changes into Equation (2-11):

$$F = 1 - \frac{6}{\pi^2} \sum_{n=1}^{\infty} \frac{1}{n^2} \exp(-\beta n^2 \tau) \quad (2\text{-}11)$$

It is considered that for F < 0.05 [86], only the external layer of the granule contains ions and

$$F = 1.08\sqrt{\beta\tau} \quad (2\text{-}12).$$

Thus, the characteristic element of internal diffusion for low values of τ is the linear dependence $F = f(\sqrt{\beta\tau})$.

3. Assuming that the sorption rate is limited by the chemical process in the polymer phase, the kinetics may be described by Equation (2-13) [86]:

$$\ln(1-F) = -k\tau \quad (2\text{-}13)$$

Formally, Equation (2-13) for the chemical process and Equation (2-5) for the external diffusion are similar, but these kinetic mechanisms can differ, taking into account that the rate of a chemical reaction depends neither on sorbent granules size nor on solution stirring degree but is dependent only on concentration and temperature.

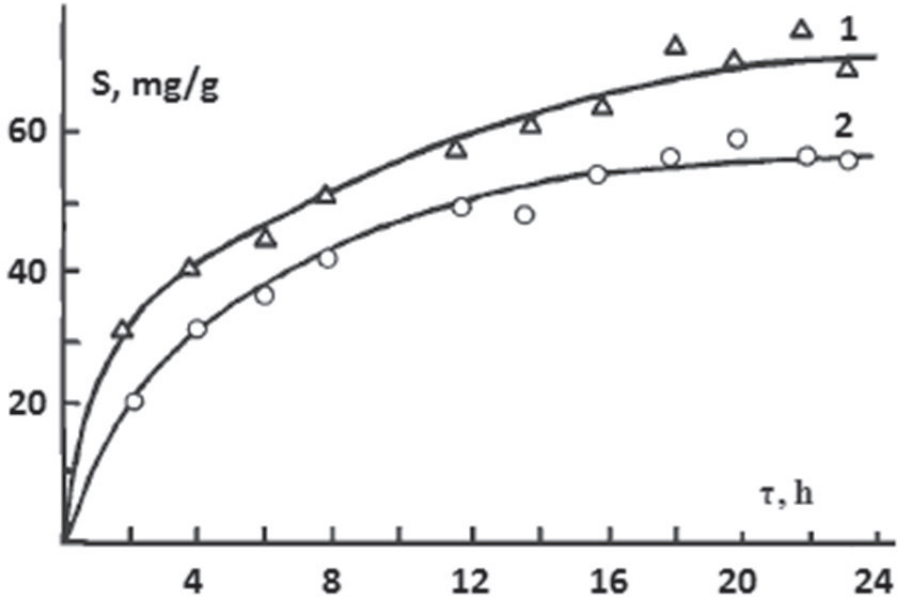

Figure 2-6. Kinetic curves of Cr(III)-containing cations' sorption at 60°C on anion exchangers AV-17 (1) and Varion-AD (2).

The main factors that are considered to determine the sorption rate are k_d and r_o. In certain conditions of temperature and stirring of the solution, the ratio between them determines the value of β constants in Equations (2-5) and (2-6). The sorption rate is limited by the external diffusion if $\beta/k > 1$. As Equations (2-5) and (2-11) are formally identical, the influence of external diffusion of the chemical reaction on sorption speed can be determined using these equations. Thus, the verification of the hypothesis about the influence of the chemical rate could be evaluated by means of Equation (2-13), the hypothesis about the influence of external diffusion using Equation (2-8), and the hypothesis about the internal diffusion is verified applying Equation (2-11). The role of diffusion in sorption kinetics will be checked using the ratio β/k:

$$\beta/k = N \text{ or } \beta = kN \quad (2\text{-}14)$$

where N can have a value higher or lower than 1.

The significance of k in Equation (2-14) results from Equations (2-5) and (2-6), which unfortunately could not be applied in these forms because of the formal identity with Equation (2-13). By combining Equations (2-14) and (2-11) arises the possibility of determining constants k and N. Equations (2-5) and (2-13) can be solved either graphically [85] or by the method of linear regression analysis. which is more efficient. We have applied the method of nonlinear regression analysis which more efficient.

The parameters of kinetic equations, calculated for different kinetic methods of Cr(III) sorption by the AV-17 and Varion-AD polymers are presented in Table 2-2.

Table 2-2. Parameters of kinetics regarding sorption of Cr(III)-containing cations on the polymers AV-17 and Varion-AD

Diffusion through external layer of liquid (Eq. (2-8)).	Exchanger	S_e, mg/g	β, cm/s	R_o, cm	k_d
	AV-17 Varion -AD	60.5 54.7	8.46×10^{-6} 6.0×10^{-6}	0.0164 0.0165	21.6 21.6
Chemical processes in the polymer (Eq. (2-13)).		S_e, mg/g		k, 1/s	
	AV-17 Varion-AD	60.5 54.7		7.63×10^{-5} 5.18×10^{-5}	
Internal diffusion through polymer granules (Eq. (2-11)).		S_e, mg/g		β, 1/s	
	AV-17 Varion-AD	70.5 67.3		2.45×10^{-5} 1.60×10^{-5}	
Internal diffusion through polymer granules (Eqs. (2-11) and (2-14)).		S_e, mg/g	K, 1/s	N	β, 1/s
	AV-17 Varion-AD	65.6 65.4	3.83×10^{-5} 2.21×10^{-5}	0.85 0.72	3.25×10^{-5} 1.60×10^{-5}

The analysis of the obtained data proved that the experimental kinetic curves are most efficiently described by equations of internal diffusion (Eqs. (2-11) and (2-14)). The verification using Equation (2-14) has denoted that the value N is lower than 1, a fact confirming that Cr(III) ions kinetic sorption by the polymers is determined by the internal diffusion (through polymer granules).

The thickness of diffusion layer *l* around the granules can vary in the range of 5×10^{-4} to 5×10^{-3} cm [86]. Equation (2-15) is obtained from Equations (2-6) and (2-8):

$$D^l / l = \beta \quad \text{or} \quad D^l = \beta l \tag{2-15}$$

Table 2-3. Constants of internal diffusion of CR(III)-containing cations through polymer particles

Constant	Anion exchanger	
	AV-17	Varion-AD
D^l, cm^2/s	$4.2 \div 8.5 \times 10^{-9}$	$3 \div 6 \times 10^{-9}$
D^i, cm^2/s	6.7×10^{-10}	4.3×10^{-10}
D^i, cm^2/s (from Eqs. (2-11) and (2-14))	8.8×10^{-10}	4.3×10^{-10}

It has allowed the estimation of range of diffusion values D*l* through the liquid layer around the polymer granule (Tab.2-3). The value of β estimated using Equations (2-11) and (2-14) stands for the relation between D^i and r_o.

As one can see from Table 2-3, the values of the D^l constant are 5–10 times higher than those of the corresponding D^i constant. The ratio between D^l and D^i constants is generally very close to that obtained by Boyd et al. [85], this being a supplementary confirmation of the hypothesis that internal diffusion is the limiting stage of kinetics. The small values of D^i can be explained by the fact that Cr^{3+} hydroxocomplexes have the same electric charge as the polymer matrix. In this case, the cations diffusion takes place through the liquid layer in the polymer phase and not through jumping from one functional group to another, like cations diffusion in the phase of sulfo-cationites [78].

2.3. The behaviour of the AV-17(Cr) sorbent in various media

It is known that chromium compounds are chemically more stable than iron compounds. Therefore, it is expected that polymers containing Cr^{3+}-compounds may present advantageous properties as sorbents or as catalysts. Their potential application needs thorough knowledge about their behaviour in various conditions. The use of sorbents can be in different environments, so it is necessary to know their behaviour in such environments. The behaviour of chromium-containing sorbent AV-17(Cr) in solutions of various mineral acids and upon heat treatment in the presence of air and in an inert atmosphere was investigated.

The process of obtaining the sorbent AV-17(Cr) takes place according to Ref. [87]. A sample of 5 g of dried AV-17(Cl) polymer was placed in contact with 0.5 L of a solution containing 2 g Cr^{3+}/L at 60 ±1°C for 10 h. The pH of $Cr_2(SO_4)_3$ solution was kept at 4.1 ±0.1 using either H_2SO_4 or NaOH solutions. After 8 h of contacting with the chromium sulfate solution, the polymer sample was filtered, washed with distilled water and dried in air. The polymer modified with metallic compounds contains mostly $R_4N[M_3(OH)_6(SO_4)_2]$ compounds and lower amounts of $H_3O[M_3(OH)_6(SO_4)_2]$. The Cr^{3+} content (32.5 mg Cr/g) in the prepared sorbent AV-17(Cr) was determined by photocolorimetry [26] after desorption [88].

The stability of the AV-17(Cr) sorbent in the HNO_3, H_2SO_4 and HCl acid solutions with 1, 2, 3, 4 and respectively 5 N concentrations was investigated. Samples of 0.1 g of the AV-17(Cr) sorbent were placed in contact with 50 ml of each acid solution for 8 h at 19°C. After 8 h of the contact with acid solutions, sorbent samples were filtered and in solution was determined the Cr^{3+} content. The Cr^{3+} desorption degree (Ds, %) served as a measure of sorbent stability [89].

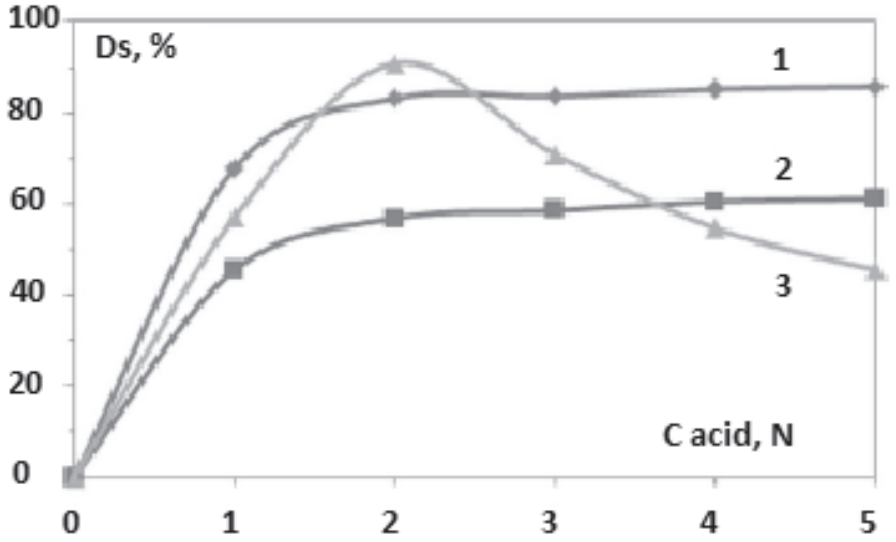

Figure 2-7. Desorption degree (Ds. %) of Cr^{3+} from sorbent AV-17(Cr) in HNO_3 (1), H_2SO_4 (2) and HCl (3) acid solutions.

As shown in Figure 2-7, the nature and concentration of the acid have a drastic influence on the stability of the Cr^{3+}-containing compounds in the polymer phase. While all acid solutions react destructively on the chromium compounds found in the polymer phase, as expected, the extent of their action depends on the acid nature and concentration. Placed under similar conditions, an extensive destruction of the chromium compounds takes place in nitric acid solutions, then in solutions of sulfuric acid. The largest amount of chromium compounds is destroyed when AV-17(Cr) sorbent is in contact with 1–2 N solutions of nitric or sulfuric acid. A further increase in acid concentration does not lead to significant added destruction of the chromium compounds. On the other hand, another behaviour is seen when the AV-17(Cr) sorbent is placed in contact with the hydrochloric acid solutions. As shown in Figure 2-7, the maximum desorption degree (Ds. %) of Cr^{3+} ions found within the AV-17(Cr) sorbent phase occurs at the contact with 2 N HCl solution. Surprisingly, the desorption degree of chromium ions decreases when higher than 2 N concentration hydrochloric acid solutions are used.

All the above considerations lead to the conclusion that the stability of chromium compounds in the sorbent phase depends primarily on the concentration of H^+ ions in the acid solution that is in contact with the polymer. However, the nature and concentration of the acid anions are not indifferent to the compounds' destruction processes. The destruction process of the chromium compounds in the sorbent phase may be described by the following Equation (2-16):

$$2R_4N[Cr(OH)_6(SO_4)_2] + 12H^+ \leftrightarrow (R_4N)_2SO_4 + 2Cr^{3+} + 3SO_4^{2-} + 12H_2O \quad (2\text{-}16)$$

The NO_3^- anions in aqueous solutions have a very low tendency to form complexes with metallic cations. The destruction of chromium compounds goes ahead therefore to a higher extent in nitric acid solutions. The tendency of SO_4^{2-} ions to form complexes is much higher than that characteristic to the NO_3^- ions. This explains why the chromium compounds are less decomposed in sulfuric than in the nitric acid solutions, when the same concentration of both acids is used.

An increase in the sulfuric acid concentration from 2 to 5 N has a negligible effect on the degree of destruction of chromium compounds in the sorbent phase due to the fact that the additional SO_4^{2-} anions present in the system shift the equilibrium (2-16) to the left. In the case of contact with an HCl solution with a concentration of up to 2 N, the process of destruction of chromium compounds in the sorbent phase of AV-17(Cr) continues according to Equation (2-16). Process (2-17) takes place at the same time:

$$(R_4N)_2SO_4 + 2Cl^- \leftrightarrow 2R_4NCl + SO_4^{2-} \quad (2\text{-}17)$$

The accumulation of Cl^- ions in the polymeric phase leads to the completion of processes (2-18) and (2-19):

$$R_4N[Cr_3(OH)_6(SO_4)_2] + 6Cl^- \leftrightarrow R_4N[Cr_3(OH)_6(Cl)_6]^{2-} + 2SO_4^{2-} \quad (2\text{-}18)$$

$$R_4N[Cr_3(OH)_6(Cl)_6]^{2-} + 6Cl^- \leftrightarrow R_4N[Cr_3(Cl)_6(Cl)_6]^{2-} + 6OH^- \quad (2\text{-}19)$$

During the ligands exchange process (2-18), 6 Cl^- ions occupy 6 coordination sites in the axial position of three Cr^{3+} ions belonging to three octahedra. Meanwhile, due to the accumulation of chloride ions in the polymer phase, the process (2-19) of the replacement of OH^- groups in the equatorial plane of the chromium complexes occurs and thus the hydrogen ions cannot destroy the chromium complexes anymore. This process explains why an increase in HCl concentration in solution beyond 2 N leads to a decrease in the desorption degree of Cr^{3+} ions from AV-17(Cr) sorbent (Fig.2-7). According to Equations (2-18) and (2-19) the sorbent AV-17(Cr) becomes able to keep cations from solution after treatment with 5 N HCl solutions.

The substitution of SO_4^{2-} and OH^- groups in the sorbent phase with Cl^- ions has been confirmed by FT IR spectroscopy. In the FT IR spectrum of the AV-17(Cr) sorbent, a large absorption band at about 1100 cm^{-1} and a small band at 620 cm^{-1} from SO_4^{2-} groups were seen.

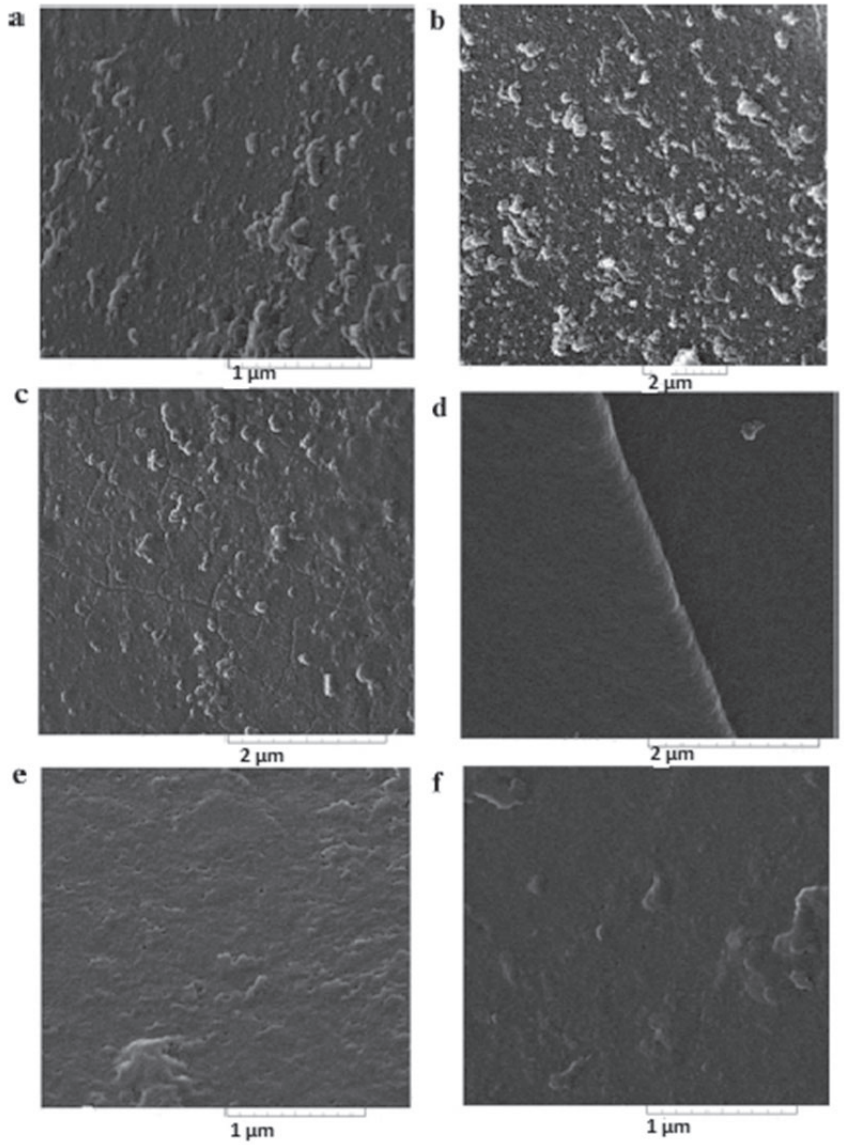

Figure 2-8. SEM images of the Cr^{3+}-containing particles on the surface (a) and in the volume (b) of an AV-17(Cr) sorbent granule. SEM images of the Cr^{3+}-containing particles on the surface (c) and in the volume (d) of an AV-17(Cr) sorbent granule after treating with 5N H_2SO_4 solutions. SEM images of the Cr^{3+}-containing particles on the surface (e) and in the volume (f) of an AV-17(Cr) sorbent granule after treating with 5N HCl solutions.

After treating of the sorbent with 5 N HCl acid solutions these absorption bands were absent from the FT IR spectrum, while new bands appeared at 392 and 396 cm^{-1}. Both show the existence of bonded chloride ions [36] in the sorbent sample: end-bonded ions at 392 cm^{-1} and bridge-bonded ones at 396 cm^{-1}.

A scanning electron microscope (Vega II LSH with an accelerating voltage of 30 kV – Tescan Company) was used to examine the morphology of the compounds on the surface and within the bulk phase. The solid samples were attached to aluminium holders using a silver-based adhesive. Samples conductivity was achieved by sputter coating with a 15 nm layer of gold. The materials investigated by SEM microscopy include samples of AV-17(Cr) sorbent,

freshly prepared and 8 months later, fresh AV-17(Cr) sorbent treated with 5 N H_2SO_4 acid solutions and fresh AV-17(Cr) sorbent treated with 5N HCl acid solutions. The last 2 sorbent samples were prepared according to the method described above.

The SEM spectroscopy investigation was conducted to prove the existence of chromium compounds in the AV-17(Cr) sorbent phase following the treatment with 5 N HCl and respectively H_2SO_4 acid solutions. As shown in Figure.2-8 (a, b), Cr^{3+}-containing compounds exist both on the surface as well as in the volume of the AV-17(Cr) sorbent granule. The powder X-ray diffraction of the AV-17(Cr) sorbent presented the typical spectrum for an amorphous polymer. This spectrum did not show any peaks that are characteristic to the crystalline compounds. After treating of the AV-17(Cr) sorbent with 5 N H_2SO_4 solutions, Cr^{3+}-containing compounds particles were not evidenced within the bulk of the sorbent granule, but some of them were present on the granule surface [Fig. 2-8 (c, d)].

This leads to the conclusion that the Cr^{3+}-containing compounds in the polymer phase are not destroyed completely upon contact with 1–5 N H_2SO_4 acid solutions. This observation is entirely consistent with the data presented in Figure 2-7. In the case of sorbent treatment with 5N HCl solutions, Cr^{3+}-containing compounds were observed both on the surface and within the bulk of the sorbent granule [Fig.2-8 (e, f)]. This confirms that on treating of the sorbent with HCl acid solutions more concentrated than 2N, the degree of destruction of the Cr^{3+}-containing compounds in the polymeric phase decreases.To use the AV-17(Cr) sorbent in processes involving gases, its thermal behaviour needs to be studied. Thermogravimetric (TG) and derivative thermogravimetric (DTG) curves were recorded in the air, at a 20 ml/min outflow, within the 25–900 ◦C temperature range, using a Mettler Toledo TGA-SDTA851^e thermogravimetric analysis device. The test samples mass was between 2.5 and 4.5 mg, and the preferred heating rate was 10^{o}C/min.

The thermal degradation of the ionic polymers was also analysed in an inert (He) atmosphere using a TG/FTIR/MS system, within the 30–600^{o}C temperature range, and at the same 10^{o}C/min heating rate. The system is equipped with an apparatus of simultaneous thermogravimetric FTIR spectrophotometer model Vertex-70 (Bruker, Germany) and a mass spectrometer model QMS 403 C Aëolos (Netzsch, Germany). The test sample on which the experiment was conducted weighed between 10 and 12 mg. The carrier gas of choice was helium flowing at 50 ml/min and 20 ml/min protective purge for thermobalance. Further information on the technical characteristics and operation of the TG/FTIR/MS system is to be found in Ref. [90]. The analysed sorbent samples: AV-17(Cr), AV-17(Cr) heated in a boiling water bath, AV-17(Cr) treated with 5N H_2SO_4 acid solution and AV-17(SO_4) polymer for comparison were investigated by differential thermal analysis method.

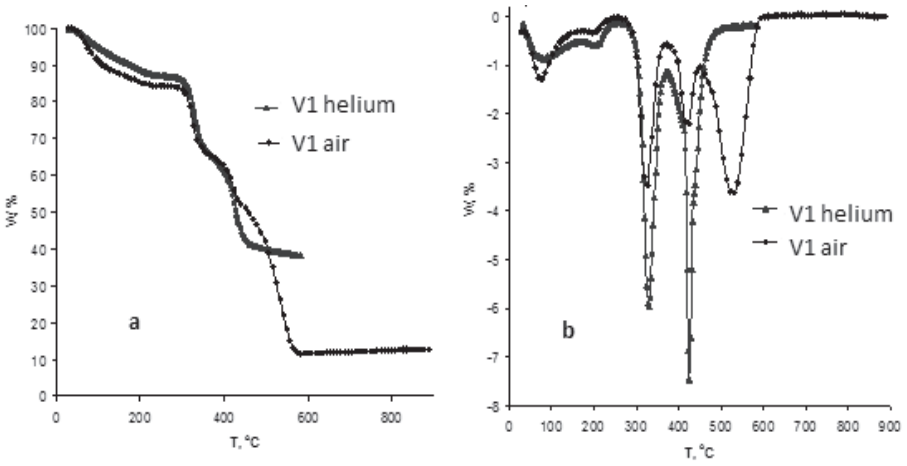

Figure 2-9. Thermogravimetric (a) and derivative thermogravimetric (b) curves for sample V1.

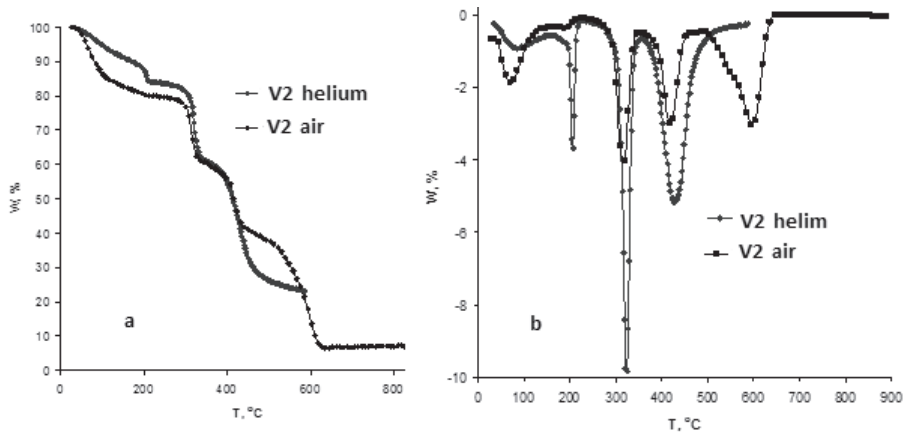

Figure 2-10. Thermogravimetric (a) and derivative thermogravimetric (b) curves for sample V2.

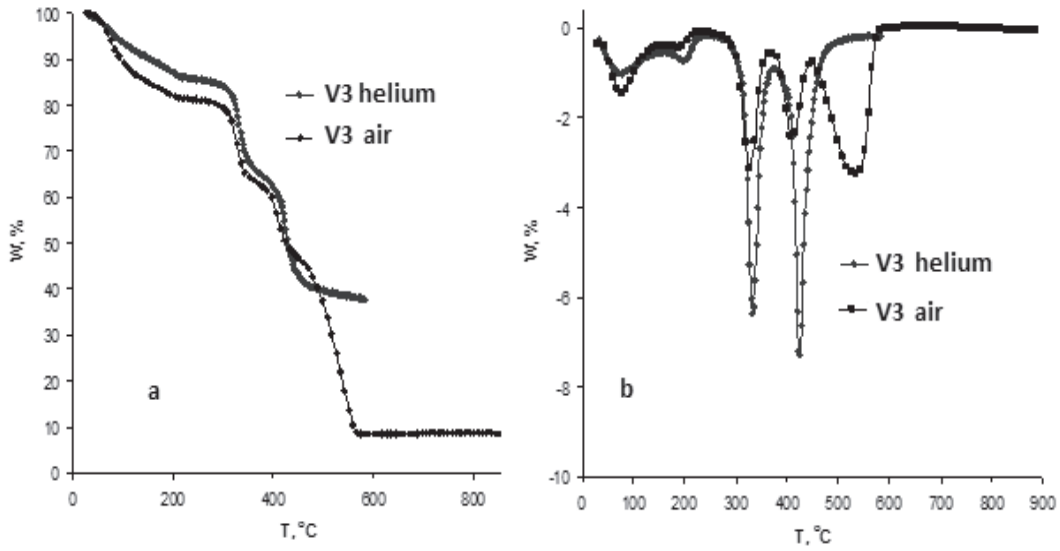

Figure 2-11.Thermogravimetric (a) and derivative thermogravimetric (b) curves for sample V3.

The following samples were analysed: AV-17(Cr), denoted as V2, AV-17(Cr) heated in a boiling water bath as V3, and AV-17(Cr) treated with 5N H_2SO_4 acid solutions as V4. For comparison, the AV-17(SO_4) polymer, denoted as V1, was also investigated.

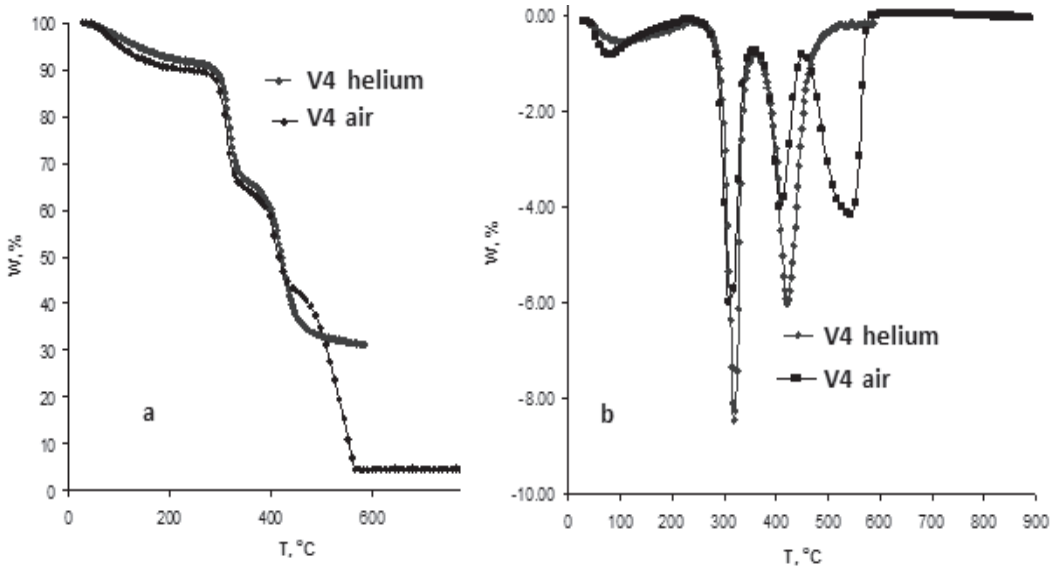

Figure 2-12. Thermogravimetric (a) and derivative thermogravimetric (b) curves for sample V4.

The thermogravimetric (TG) and derivative thermogravimetric (DTG) curves recorded both in inert atmosphere (He) and in the air are shown in Figures 2-9 and 2-12.

The obtained results reveal a complex degradation mechanism that includes from three to five degradation stages, depending on the chemical structure of the compounds, and on the atmosphere in which the degradation process occurs. The degradation process is not complete in all the test samples. The amount of remaining residue in air at 900 ◦C ranges between 4 and 18% of the sample weight. The amount of remaining residue in helium at 600^{o}C is higher and ranging from 23 to 38% of the sample weight.

The main thermogravimetric characteristics are T_{onset}, the temperature at which the thermal degradation starts; T_{peak}, the temperature at which the thermal degradation is maximum; and T_{endset}, the temperature at which the degradation process ends and W % – the percentage weight loss during each stage. Table 2-4 presents comparative data about thermal degradation, the characteristics for the AV-17(SO_4) polymer and the three samples of AV-17(Cr).

Table 2-4. Thermogravimetric characteristics of ionic polymers

Samples thermal degradation stages		Helium				Air			
		T_{onset} (°C)	T_{peak} (°C)	T_{enset} (°C)	W (%)	T_{onset} (°C)	T_{peak} (°C)	T_{enset} (°C)	W (%)
V1	I	36	73	122	7.83	54	72	127	10.97
	II	122	204	250	5.31	127	203	230	4.78
	III	310	327	345	21.38	312	324	342	20.06
	IV	410	436	465	27.24	414	422	441	14.48
	V	-	-	-	-	497	531	570	38.73
	Residue	38.24[a]				10.98[b]			
V2	I	37	87	131	7.51	49	71	100	15.54
	II	196	206	252	8.59	100	189	240	4.70
	III	300	324	344	22.42	302	316	328	20.63
	IV	405	428	481	38.33	405	420	438	20.23
	V	-	-	-	-	532	601	622	32.59
	Residue	23.15[a]				6.31[b]			
V3	I	35	80	137	8.92	53	76	108	12.19
	II	137	200	248	4.92	108	189	247	6.77
	III	315	333	352	22.87	305	327	346	18.12
	IV	407	424	457	25.42	394	408	430	38.53
	Residue	37.87[a]				8.11[b]			
V4	I	39	99	240	7.89	60	72	230	10.06
	II	294	319	344	26.67	296	312	324	25.81
	III	384	430	464	34.34	396	409	432	22.47
	IV	-	-	-	-	477	542	565	37.50
	Residue	31.10[a]				4.16[b]			

a Residue at 600◦C (Netzsch system).
b Residue at 900◦C (Mettler Toledo system).

The results show a similar degradation mechanism for all the analysed sorbent samples in helium and air up to about 460 °C. The temperature at which the degradation is maximum (T_{peak}) for the degradation stage of the raw polymer having polystyrene–divinylbenzene is about 430 °C, a value that is comparable to the temperature obtained by other researchers in similar conditions [91-93]. When the degradation proceeds in the air, these compounds also undergo a thermal oxidation process within the 460–570 °C temperature range, that is characterized by the same percentage of weight loss, due to the $(R_4N)_2SO_4$ groups that are present in all the samples.

The thermogravimetric study reveals a complex degradation mechanism for the V1–V4 samples both in an inert atmosphere and in the air. We continue by discussing the TG-MS-FTIR study, the main goal of which is to find the ionic fragments resulting from the thermal decomposition of these samples, aiming to clarify the degradation mechanism. The results confirm that the first degradation stages consist partly in water removal (both phases of hydration and free water) from the polymer and partly in the following process (2-20):

$$2[RCH_2N(CH_3)_3]_2SO_4 + 2H_2O \rightarrow 2RCH_2OH + [RCH_2NH(CH_3)_2]_2SO_4 + [N(CH_3)_4]_2SO_4 \quad (2\text{-}20)$$

that takes place at temperatures higher than 300 °C, with $[N(CH_3)_4]_2SO_4$ intermediate decomposition (Eq.(2-21)):

$$[N(CH_3)_4]_2SO_4 \rightarrow 2N(CH_3)_3\uparrow + C_2H_6\uparrow + SO_2\uparrow + O_2\uparrow \quad (2\text{-}21)$$

Figure 2-13 shows the ionic current variation for the m/z = 18 (H_2O^+) fragment within the temperature range in which the TG-MS-FTIR curves were recorded. Two peaks were evidenced for the V1–V3 samples and only one peak for the V4 sample within the 30–300 °C temperature range, results that agree with those previously revealed by the thermogravimetric data.

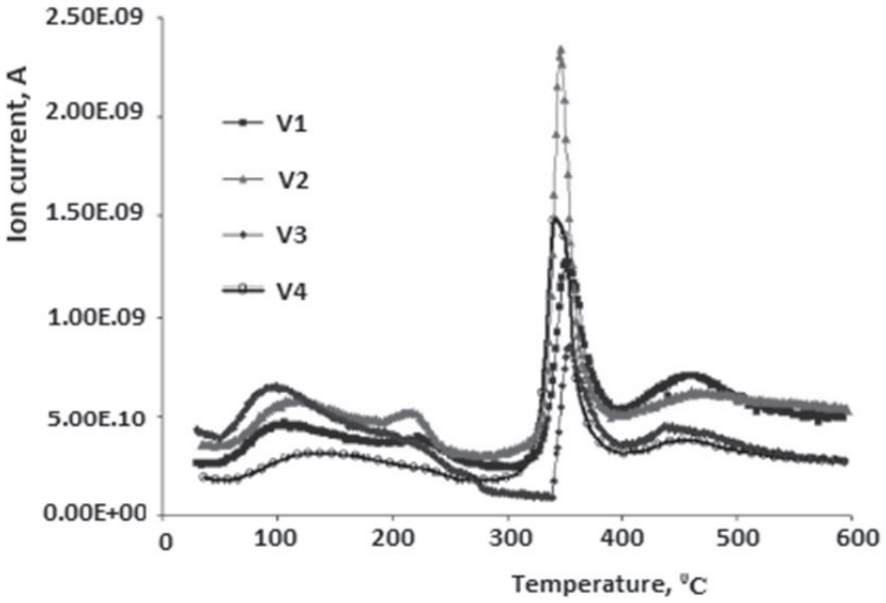

Figure 2-13. Ionic current variation with temperature for the *m/z* = 18 fragment.

Also, higher ionic current intensity values were recorded for the *m/z* = 18 (H_2O^+) fragment, within this temperature interval, in the V3 and V2 test samples, that may also have $R_4N[Cr_3(OH)_6(SO_4)_2]$ and $H_3O[Cr_3(OH)_6(SO_4)_2]$, respectively, the decomposition of which may result in an additional amount of removed water compared to the other two samples:

$$2R_4N[Cr_3(OH)_6(SO_4)_2] \rightarrow [R_4N]_2SO_4 + 2CrSO_4 + 2Cr_2O_3 + SO_2\uparrow + 6H_2O\uparrow + O_2\uparrow \quad (2\text{-}22\ a)$$

$$\text{and } 2R_4N[Cr_3(OH)_6(SO_4)_2] \rightarrow 6CrOOH + (R_4N)_2SO_4 + 3H_2SO_4 \text{ only for V3} \quad (2\text{-}22\ b)$$

$$H_3O[Cr_3(OH)_6(SO_4)_2] \rightarrow H_3O[(Cr_3O_2)(SO_4)_2(OH)_2] + 2H_2O\uparrow \quad (2\text{-}23)$$

$$H_3O[(Cr_3O_2)(SO_4)_2(OH)_2] \rightarrow CrSO_4 + Cr_2O_3 + H_2SO_4 + H_2O\uparrow \quad (2\text{-}24)$$

$$H_2SO_4(10) \rightarrow (10)SO_3(10) + (10)H_2O\uparrow \quad (2\text{-}25)$$

$$SO_3 \rightarrow SO_2\uparrow + 1/2O_2\uparrow \quad (2\text{-}26)$$

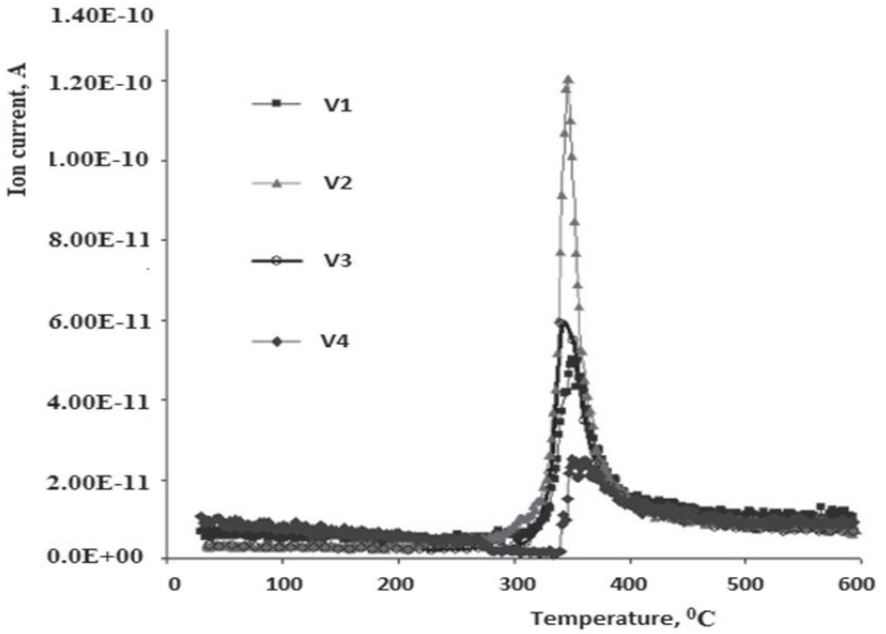

Figure 2-14. Ionic current variation with temperature for the *m/z* = 30 fragment.

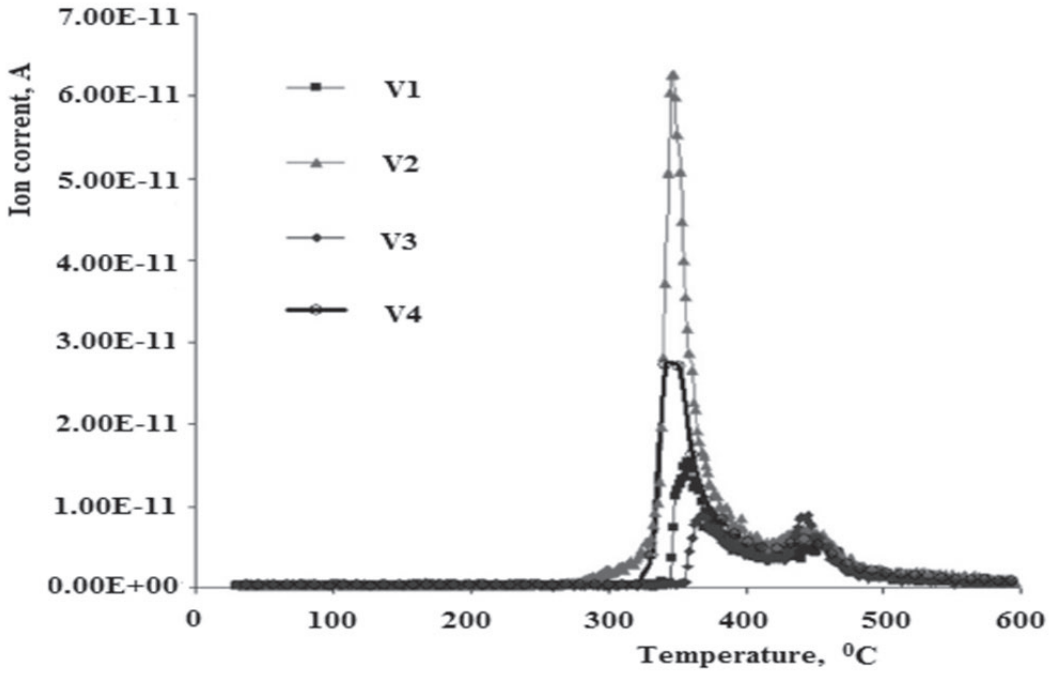

Figure 2-15. Ionic current variation with temperature for the *m/z* = 59 fragment.

The MS spectra presented in Figures 2-14 and 2-17 reveal the presence of the following ionic fragments within the 300–400 ^{o}C temperature interval: *m/z* = 30 ($C_2H_6^+$), *m/z* = 9($N(CH_3)_3^+$), *m/z* = 64(SO_2^+) and *m/z* = 16 (O^+), all confirming the proposed (2-20)–(2-26) processes sequence in the thermal decomposition mechanism. These results agree with the ones obtained by other researchers for compounds with similar structures [70, 94-96].

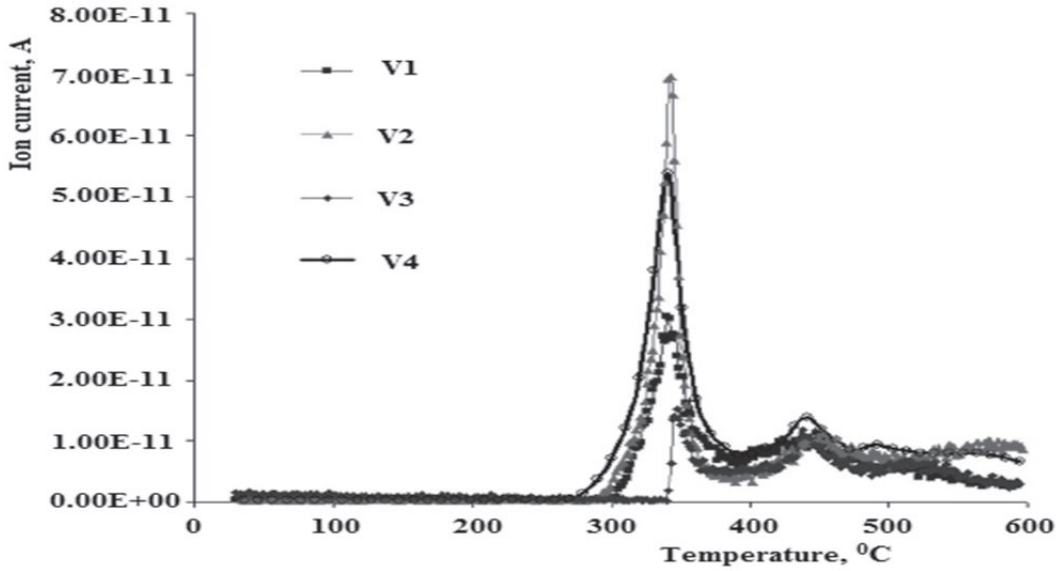

Figure 2-16. Ionic current variation with temperature for the *m/z* = 64 fragment.

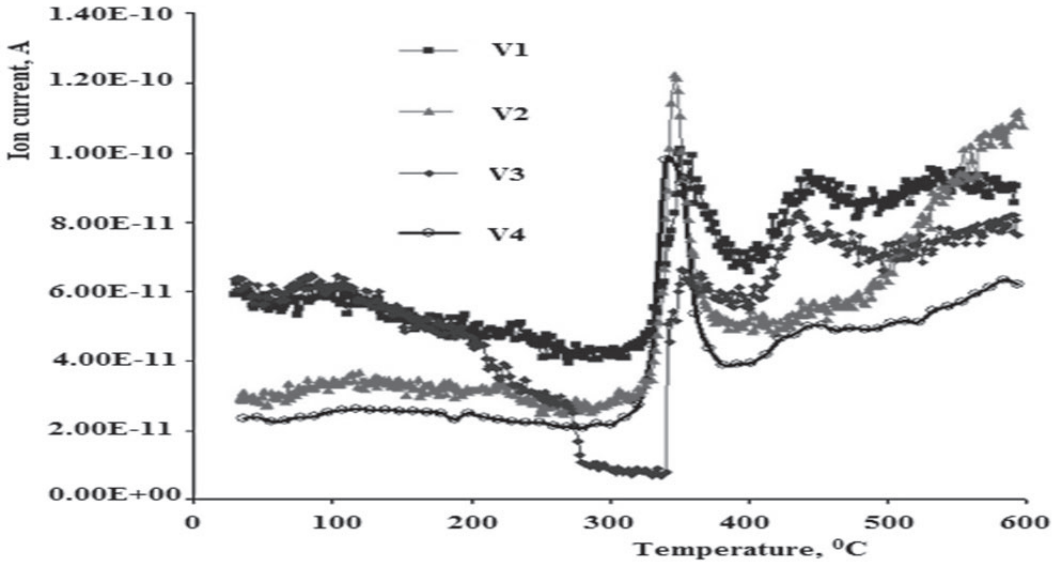

Figure 2-17. Ionic current variation with temperature for the *m/z* = 16 fragment.

The last degradation stage, occurring at temperatures higher than 380°C, corresponds to the thermal decomposition of the raw polymer structure that holds polystyrene–divinylbenzene [13]. We found the *m/z* = 27, 51, 78, 104 ionic fragments specific to the styrene monomer; *m/z* = 118 of α-methyl styrene; *m/z* = 77, 91, 105, 119, 148 of alkylbenzene; *m/z* = 27, 39, 51, 65, 77, 91, 106 of dimethylbenzene, etc. Also, one may note a higher intensity of the band specific to the trophylium (*m/z* = 91) ion, confirming the presence of substituted benzene rings (Fig. 2-18).

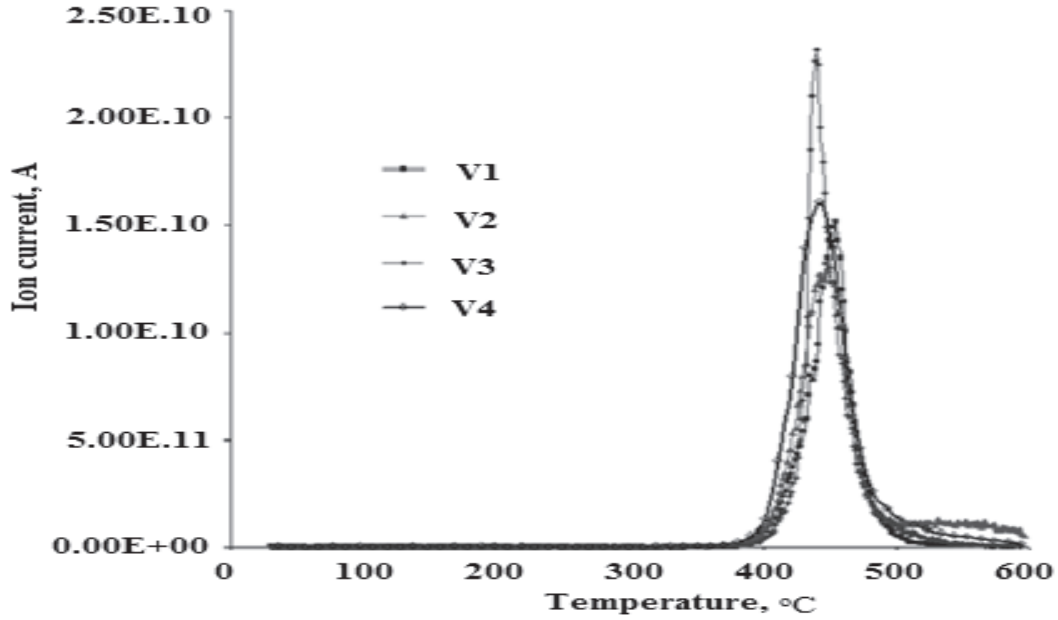

Figure 2-18. Ionic current variation with temperature for the *m/z* = 91 fragment.

The FTIR spectra recorded also support the proposed degradation mechanism. Thus, according to Figure 2-19, for the V2 test sample, for instance, the bands specific to water in the vapour state occur within the 1390–1860 cm^{-1} and 3500–3900 cm^{-1} range, respectively [97,98]. During the first two stages, the intensity of these peaks is weaker and it increases at temperatures higher than 300°C, when we suppose that the dehydroxylation process occurs and an additional amount of water results.

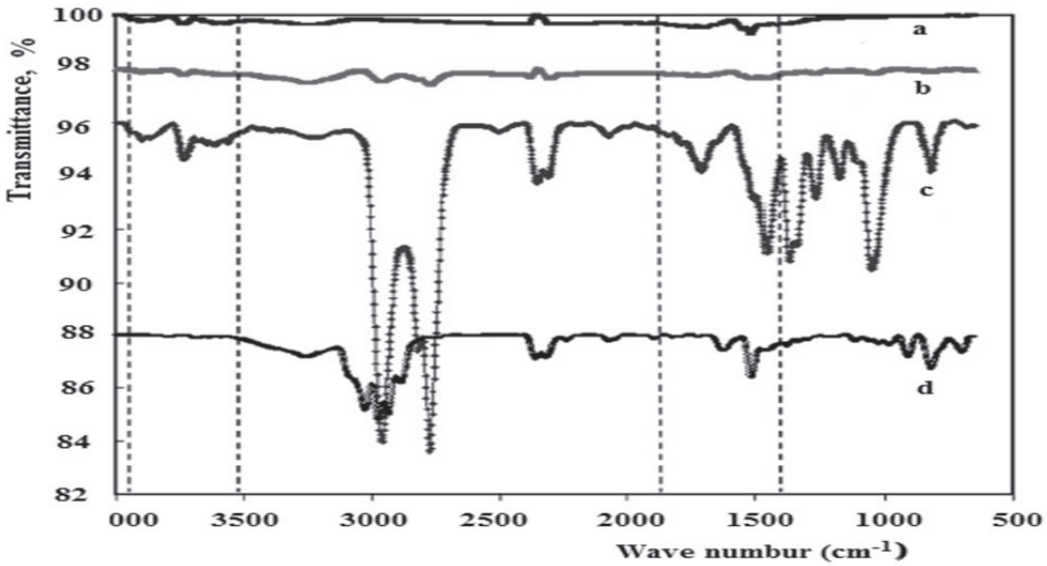

Figure 2-19. FTIR spectra for the V2 sample: (a) 87°C, (b) 206°C, (c) 324°C, and (d) 428°C.

Figure 2-20 includes a comparison of the FTIR spectra for the V1–V4 test samples corresponding to the T_{peak} temperatures within the 300–400 °C temperature range. The FTIR bands found at 1158 and 1274 cm^{-1} may relate to the C–N bond vibration in the *m/z* = 59 ($N(CH_3)_3^+$) fragment. The bands shown at about 1362 and 1375 cm^{-1}, respectively, confirm the SO_2 release [99, 100]. The *m/z* = 30 ($C_2H_6^+$) ionic fragment found in the MS spectra may be associated with the presence of the bands occurring at 1458 and 2970 cm^{-1} [99, 101] in the FTIR spectra.

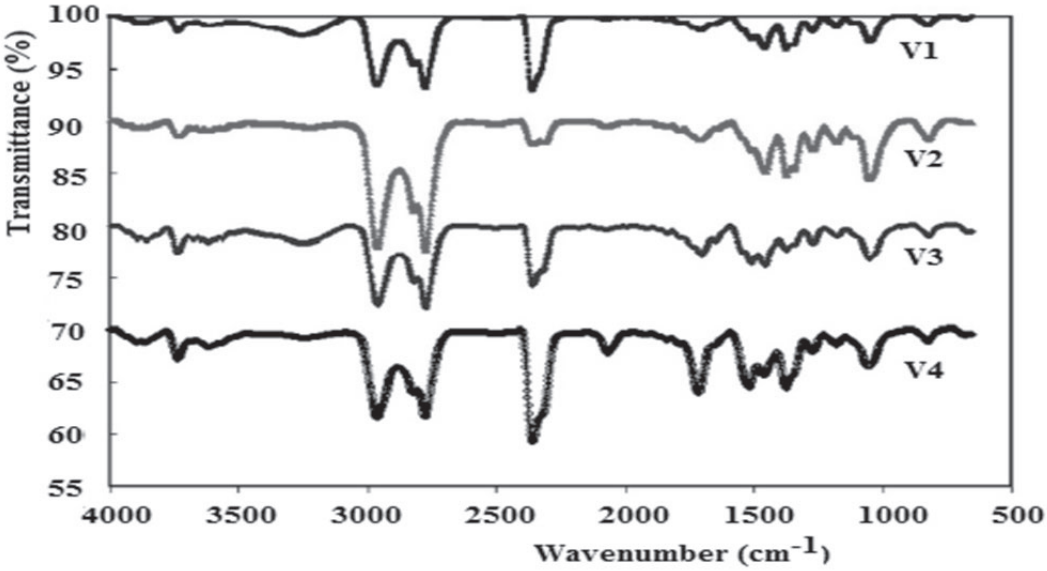

Figure 2-20. FTIR spectra for samples: V1 (T_{peak} = 327°C), V2 (T_{peak} = 324°C), V3(T_{peak} = 333°C) and V4 (T_{peak} = 319°C).

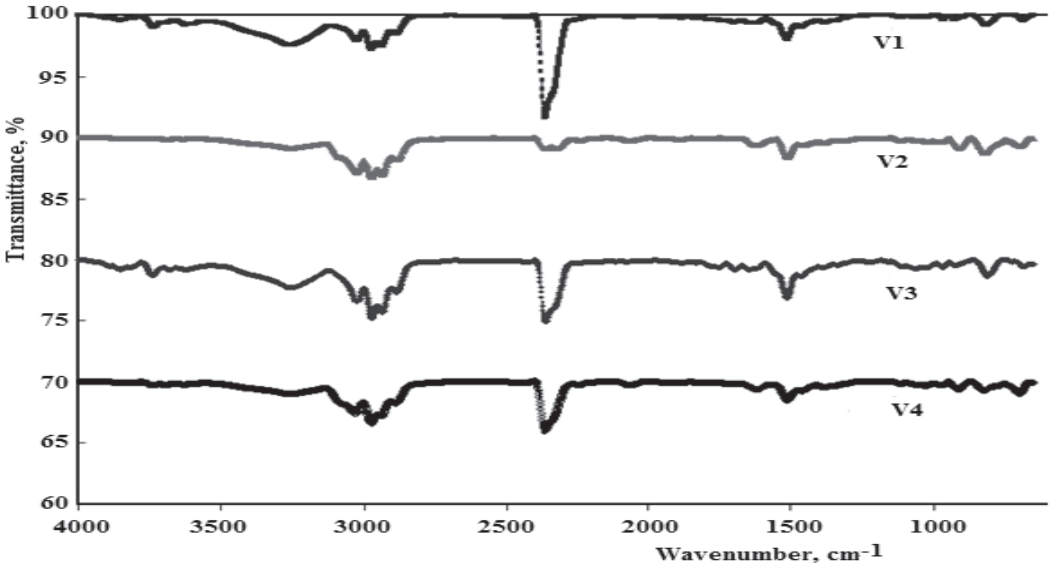

Figure 2-21. FTIR spectra for samples of the raw polymer structure containing polystyrene–divinylbenzene in the last stage.

The FTIR spectra presented in Figure 2-21 confirm the thermal decomposition of the raw polymer structure containing polystyrene–divinylbenzene in the last stage, within the 400–500 ^{o}C temperature range. Thus, for the analysed ionic polymers, we found the bands specific to the vinyl groups at 910, 989 and 1630 cm^{-1}; the bands located at 3078 cm^{-1} specific to the aromatic cycles of the styrene monomer; those specific to the monosubstituted benzene ring at 694, 773, 1726, 1819 and 1940 cm^{-1}; those specific to the methyl groups from α-methyl styrene at 2860 cm^{-1} and cycles of the styrene monomer; those specific to the monosubstituted benzene ring at 694, 773, 1726, 1819 and 1940 cm^{-1}; those specific to the methyl groups from α-methyl styrene at 2860 and 2920 cm^{-1}; the bands specific to aliphatic –CH_2- groups from polystyrene at 3026 cm^{-1} and the bands positioned at 1072, 1186, 1282, 1441, 1491 and 1600 cm^{-1} that may be specific to aromatic polystyrene cycles [102, 103]. Considering that, according to the proposed reaction sequences, oxygen also results at temperatures higher than 300 $^{\circ}$C; one may also identify the bands specific to CO_2 at 672 cm^{-1} and 2352 cm^{-1} in the FTIR spectra [101].

III.

AL(III)-COMPOUNDS IN THE POLYMER PHASE

In nature, there is an alunite mineral $K[Al_3(OH)_6(SO_4)_2]$ which is isostructural with the jarosite $(K,Na)[Fe_3(OH)_6(SO_4)_2]$. Research has shown that alunite can be synthesized in the phase of cross-ionic polymers having strongly basic groups.

The studies were conducted under static conditions using polymers AV-17(Cl) and Varion-AD(Cl) [104]. To determine Al(III)-containing cations sorption as a function of temperature, 0.2 g of polymer samples were contacted with 100 ml of $2*10^{-2}$ M $Al_2(SO_4)_3 \cdot 18H_2O$ solution at pH 3.5 for 24 hours. The Al^{3+} content in the polymer samples was determined by photocolorimetry [26] after desorption using the 2M HCl solution. The results obtained are shown in Figure 3-1. Unexpectedly, when the temperature increases to 90 °C, the sorption of cations containing Al(III) continuously increases and does not pass through a maximum, as in the case of the sorption of Fe(III) or Cr(III)-containing cations. We assume that the formation of metallic compounds in the polymer phase occurs with the participation of hydroxycomplexes of $[AlOH(H_2O)_5]^{2+}$ whose concentration in solution with pH 3.5 is very small. As the temperature increases, the concentration of $[AlOH(H_2O)_5]^{2+}$ in the solution increases too, which leads to an increase in sorption. As is known [55], in solution, depending on pH, Al(III) exists in various ionic forms, which do not all participate in the formation of jarosite mineral type compounds: $[Al(H_2O)_6]^{3+}$, $[AlOH(H_2O)_5]^{2+}$, $[Al(OH)_2(H_2O)_4]^{+}$ and others. Therefore, it was expected that the sorption of cations containing Al(III) by the polymer will depend substantially on the pH of the solution (Fig.3-2). It should be noted that sorption as a function of pH occurred at 90 ^{o}C, and the pH was periodically adjusted to the proper value.

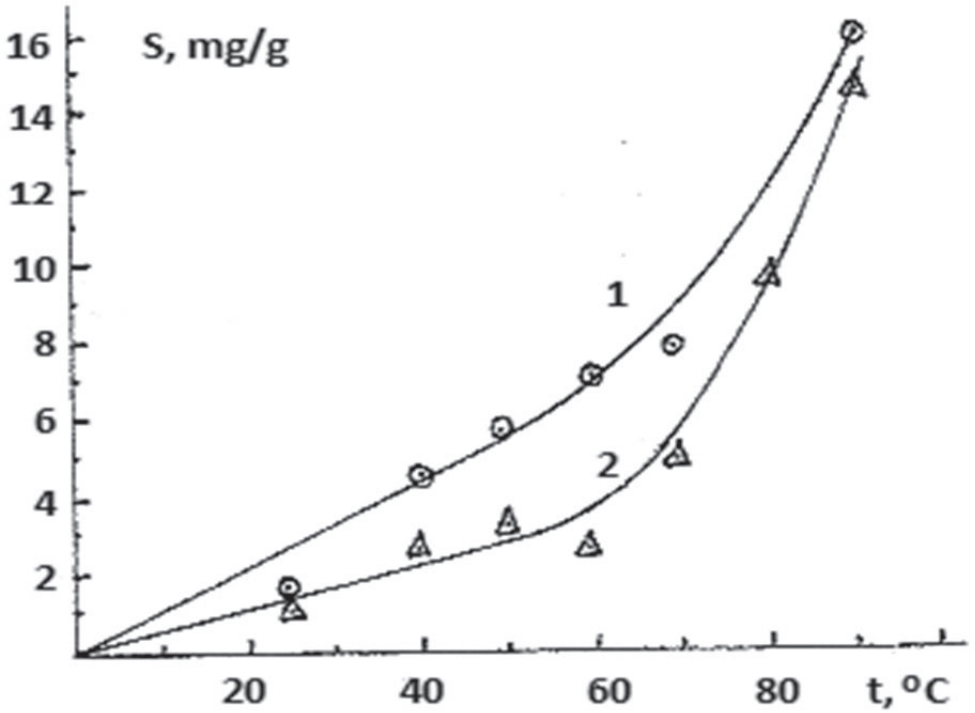

Figure 3-1. Sorption of Al(III)-containing cations on AV-17 (1) and Varion-AD (2) as a function of temperature.

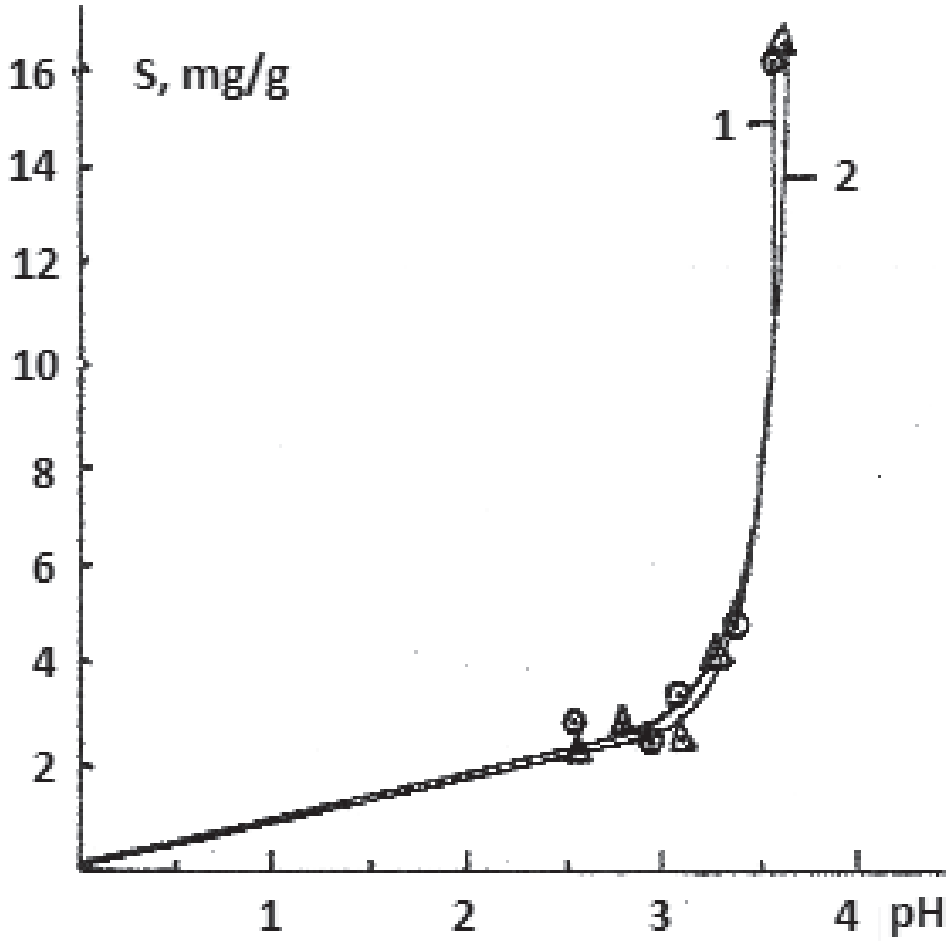

Figure 3-2. Sorption of Al(III)-containing cations on AV-17 (1) and Varion-AD (2) as a function of pH.

Adsorption isotherms, obtained at 87±3 ^{o}C from solution with pH 3.45, appear to be described with the Henry sorption model (Fig.3-3).

As can be seen from the kinetic curves, obtained at 87±3 ^{o}C from solution with pH 3.45 (Fig.3-4), the sorption equilibrium of cations containing Al(III) is reached at 12-14 hours of contact of the solution with the polymer.

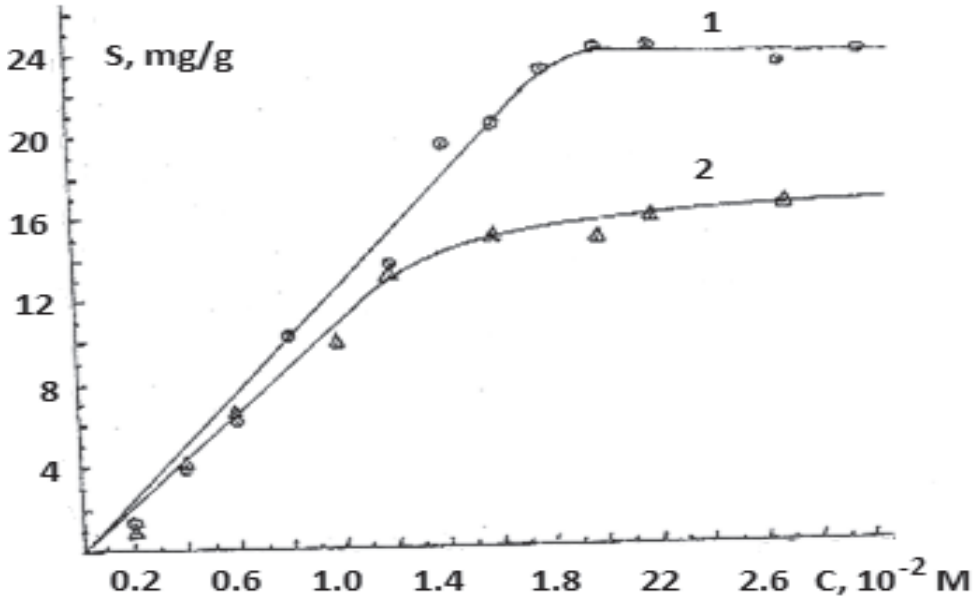

Figure 3-3. Sorption isotherms of Al (III)-containing cations on polymers AV-17 (1) and Varion-AD (2).

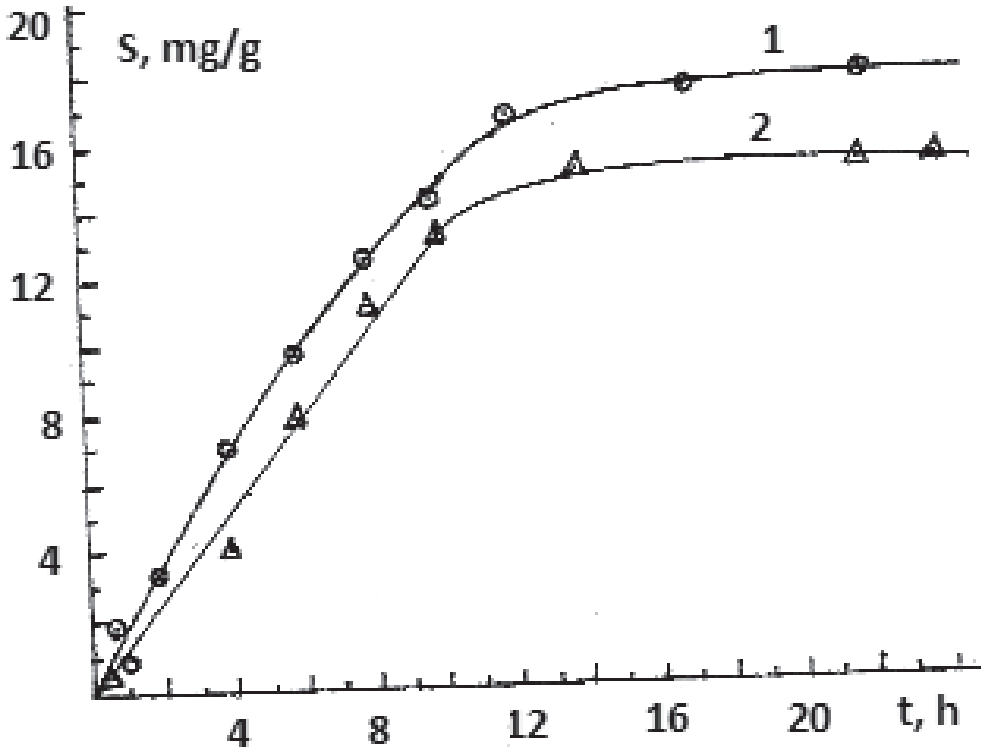

Figure 3-4. Kinetic curves of Al(III)-containing cations' sorption on AV-17(1) and Varion-AD (2).

As a result of the research, a process for obtaining a sorbent containing aluminium compounds was developed [105].

IV.

LANTHANIDES (III) COMPOUNDS IN THE POLYMER PHASE

4.1. Some factors that influence the retention of lanthanide (III) cations on a strongly basic anion exchanger

Lanthanides are used in catalysis [106,107], glass and ceramic industries [108] metallurgy, electronics and even in water treatment [109] and biomedicine [110]. The fluorescent properties of the Lanthanide compounds are of special interest [111]. It is of great interest to immobilize the Lanthanide compounds on a support of the chemically active cross-linked polymers. This allows the use of Lanthanide compounds in processes in which separation of the phases is required. Anion exchangers are widely used in the separation and concentration of Lanthanides (III) [112-114]. Usually, Lanthanides (III) are in the form of anionic complexes and interact electrostatically with anion exchangers. Sorption of anions as a result of anion exchange, practically, is not selective because it is conditioned by Coulomb's electrostatic interactions. But will cations of Lanthanides (III) interact with cross-linked ionic polymers holding strongly basic groups? We have assumed that Lanthanide (III) cations can be kept on such polymers as a result of the formation of ultrafine particles of jarosite-type compounds in their phase.

For investigation strongly basic anion exchanger Purolite A-400, a commercial polymer, has been used [4]. Also, for the investigation, solutions of $La_2(SO_4)_3$, $Nd_2(SO_4)_3$, $Eu_2(SO_4)_3$ and $Er_2(SO_4)_3$ have been used. The 0.1 g polymer samples were contacted with a 50 mL solution of 1 mmol/L concentration. The equilibrium pH of the solutions in the majority of the cases was 6.0. The concentration of Lanthanides (III) cations in the solution was determined by photocolorimetry using Arsenazo III [26]. The formation of metallic compounds in the polymer phase depends on several factors – polymer porosity, concentration, temperature, solution pH, the existence of electrolytes in the system and others. According to [55], in the concentration range 10^{-5}-10^{-1} mol/L at 25°C in Lanthanide (III) solutions, hydrated cations may be presented up to pH 6. In solutions with a pH >6 there may be $LaOH^{2+}$, $La(OH)_2^{+}$, $La(OH)_3$, $La(OH)_4^{-}$ and other particles**.** It must be mentioned that the solution in the pores of the polymer has a different pH than in the liquid phase. So, the degree of hydrolysis of cations in the polymer phase will be different from that in the liquid phase. Since the ionic composition of the solutions depends on temperature, it was expected that the Lanthanide (III) cations sorption on the strongly basic crosslinked polymer will depend on temperature, too. Therefore, in the investigation of Lanthanide (III) cations sorption on the polymer, the influence of temperature is of special interest.

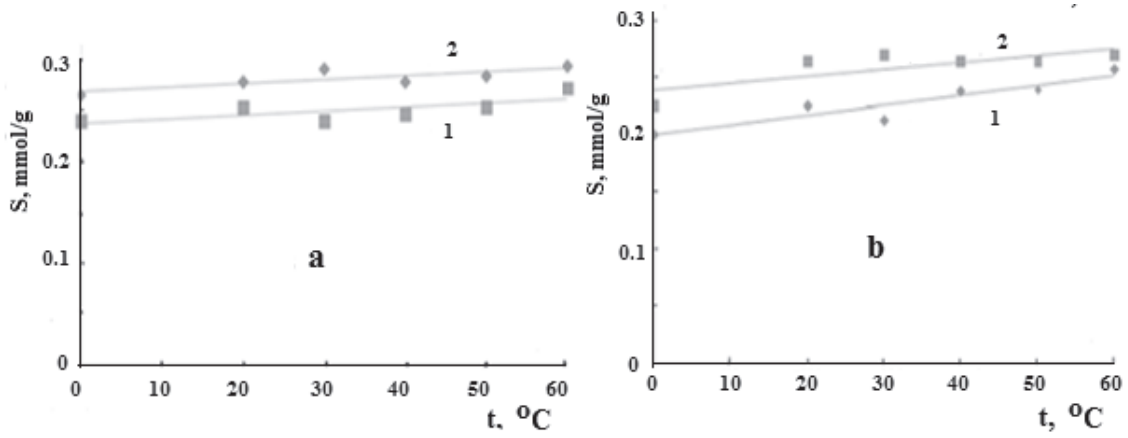

Figure 4-1. **S**orption of Er^{3+} (1) and La^{3+} (2) ions (a) and Nd^{3+} (1) and Eu^{3+} (2) ions (b) as a function of temperature.

As can be seen from Figure 4-1, the sorption of Lanthanide (III) cations on the Purolite A-400 polymer increases slightly with increasing temperature. The sorption of the cations containing Er^{3+}, La^{3+}, Eu^{3+} and Nd^{3+} is respectively 39.72, 36.39, 34.19 and 28.85 mg/g at 0 °C, and 44.28, 40.28, 49.85 and 36.92 mg/g at 60 °C. Generally, the sorption depending on the nature of the cation decreases in the following order: $Er^{3+} > Eu^{3+} \approx La^{3+} > Nd^{3+}$. It is known [115], that the Er^{3+} cations in the aqua complexes have a coordination number of less than 9, while the La^{3+}, Nd^{3+} and Eu^{3+} cations have the coordination number 9. Probably, the interactions of the Er^{3+} cations with the O atoms of the OH^- and SO_4^{2-} groups in the jarosite mineral-type compounds are stronger than those of other investigated cations.

The degree of hydrolysis of cations as a function of the pH of a solution is much higher than in the case of temperature. So, the ratio of the amounts of different particle species in the solution depends on its pH. Under similar conditions, the concentration of OH^- anions in the polymer phase is higher than in the solution. Therefore, the sorption of Lanthanides (III) cations on Purolite A-400 polymer could be expected to depend on the pH of the solution. Indeed, experimental results confirm this.

As shown in Figures 4-2 and 4-3, both at 21°C and 50 °C with the pH increase of the solution, the sorption of the lanthanide (III) cations on the Purolite A-40 polymer increases significantly.Usually, at the same value of pH, sorption at 50 °C is higher than at 21 °C. And in the case of pH influence, as with temperature, the sorption of cations containing Er^{3+} differs slightly from that of the other cations. Increasing the pH, sorption of cations containing Er^{3+} at 50 °C increases more than at 21 °C (Fig.4-3).

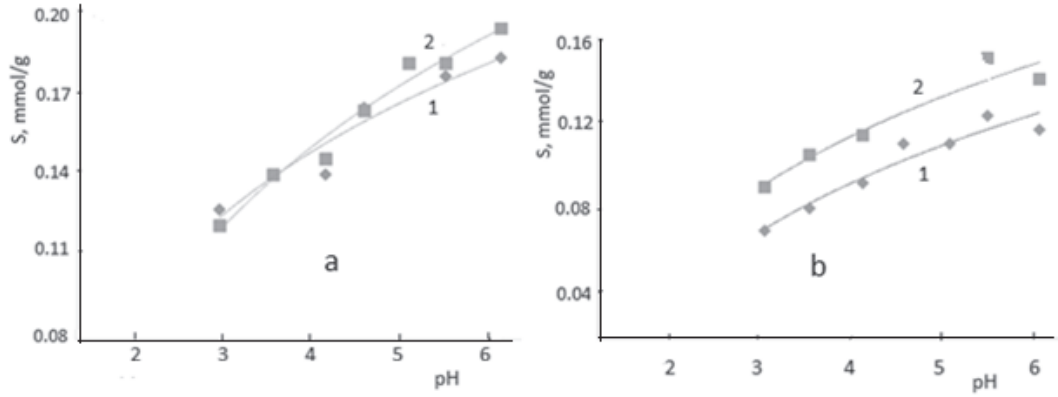

Figure 4-2. Sorption of La^{3+} (a) and Nd^{+3} (b) ions at 21 (1) and 50°C (2) as a function of the solution pH.

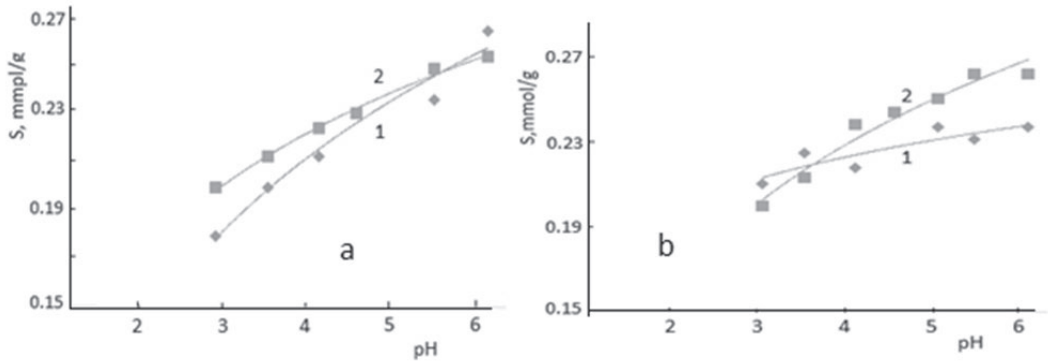

Figure 4-3. Sorption of Eu^{3+} (a) and Er^{+3} (b) ions at 21 (1) and 50°C (2) as a function of the solution pH.

At 50 °C the sorption from the solution with pH 3.0 is 33.45 mg/g, and from the solution with pH 6.0 it is 43.8 mg/g. Only in the case of cations containing Nd^{3+}, does the pH dependence of sorption at 21 °C increases, the same as at 50 °C (Fig.4-2). Usually, the dependence of sorption on the nature of cations and pH at 50 °C decreases in the following order: $Er^{3+} > Eu^{3+} > La^{3+} \approx Nd^{3+}$. It is to be noted that the sorption of cations containing La^{3+} and Nd^{3+} was made from the solution with a concentration of 0.8 mmol/L, while the sorption of other cations was from the solutions containing 1.0 mmol/L.

For the kinetic studies, the amount of the adsorbed Lanthanide (III) cations as a function of the contact time of the sorbent with the solution (*St*, mg cation/g) was calculated by Equation (4-1):

$$St = \frac{(Co - Ct) * V}{m}, \qquad (4\text{-}1)$$

where: *Co* and *Ct* are the Lanthanide (III) cations concentrations in solution respectively before and after contact with the sorbent (mg M^{3+}/mL), *V* is the volume of the solution in contact with the sorbent (mL), and *m* is the mass of the air-dried polymer (g).

To investigate the kinetics mechanism, which controls the sorption process of Lanthanide (III) cations on Purolite A-400 the nonlinear forms of the pseudo-first-order (PFO) and pseudo-second-order (PSO) kinetic models [116, 117] were used.

The nonlinear form of the integrated PFO kinetic model is described by Equation (4-2):

$$St = Se(1 - e^{-k_1 t}), \tag{4-2}$$

where: *St* and *Se* are the quantity of cations adsorbed at a time *t* and at equilibrium (mg cation/g), respectively; k_1 is the rate constant in the PFO kinetic model (min^{-1}).

The value of k_1 was determined using the linear form of the PFO kinetic model which is expressed by Equation (4-3):

$$\ln(Se - St) = \ln\ Se - k_1 t \tag{4-3}$$

The nonlinear form of the PSO kinetic model is expressed by Equation (4-4):

$$St = \frac{k_2 Se^2 t}{1 + k_2\ Se\ t}\ , \tag{4-4}$$

where: *St* and *Se* have the same meaning as in Equation (4-2), and k_2 is the rate constant of the PSO kinetic model (g mg^{-1} min^{-1}).

The values of k_2 and *Se* were determined using the linear form of the PSO kinetic model which is expressed by Equation (4-5):

$$\frac{t}{Se} = \frac{1}{k_2 Se^2} + \frac{1}{Se}t\ , \tag{4-5}$$

In order to determine the sorption limiting step, the graph of Equation (4-6) [118] has been used:

$$-ln(1 - F) = f(t), \tag{4-6}$$

where: $F = St/Se$, and *t* is time (min).

The kinetics of Lanthanides (III) cations sorption on the Purolite A-400 from solutions with pH 6.0 were investigated at 21 and 50 ^{o}C. The calculations have shown that experimentally obtained kinetic curves do not match the PFO kinetic model. In contrast, they are very well described with the PSO kinetic model both at 21 and at 50^{o}C. Table 4-1 shows the kinetic characteristics of Lanthanides (III) cations sorption on Purolite A-400

Table 4-1. The kinetic characteristics of Lanthanide (III) cations' sorption

Ion	t, ^{o}C	Se, mmol/g	Se, mg/g	K_2, $g.mmol^{-1}$ min^{-1}
La^{3+}	21	0.274	38.06	21.382
	50	0.285	39.59	17,606
Nd^{3+}	21	0.225	32.40	9.551
	50	0.240	34,56	8.680
Eu^{3+}	21	0.262	39,81	12.953
	50	0.275	41.79	9.452
Er^{3+}	21	0.250	41.75	8.532
	50	0.273	46,92	5.125

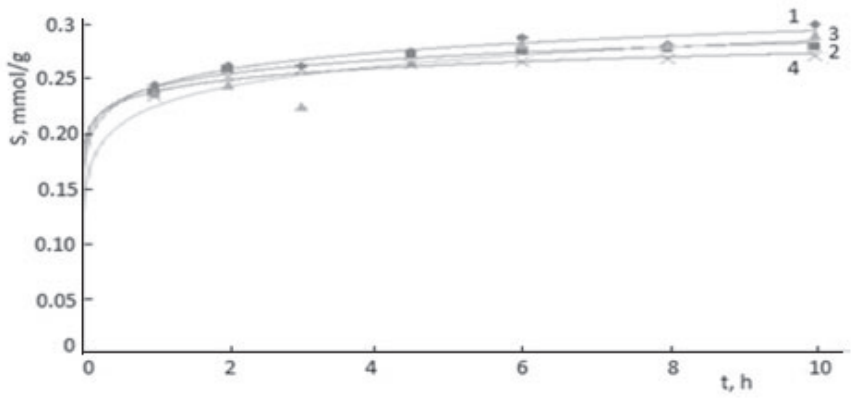

Figure 4-4. The kinetic curve of La^{3+} ion sorption on Purolite A-400, obtained experimentally at 50 (1) and 21^{o}C (2) and calculated with the pseudo-second-order kinetic model at 50 (3) and 21^{o}C (4).

calculated with the PSO kinetic model. The larger is the k_2 value, the slower is the adsorption rate. Thus, the data included in Table 4-1 show that the sorption rate of Lanthanides (III) cations on Purolite A-400 at 50°C is higher than at 21°C. They also show that at 21°C the rate of cations sorption decreases in the order $Er^{3+} > Eu^{3+} > Nd^{3+} > La^{3+}$ and at 50 °C in the order $Er^{3+} \approx Eu^{3+} > Nd^{3+} > La^{3+}$.

The hydration enthalpy of cations (M^{3+}) of Lanthanide (III) decreases in the same order. But the M^{3+}- O distance and diffusion coefficient in water decreases in the series $La^{3+} > Nd^{3+} > Eu^{3+} > Er^{3+}$ [115]. Probably the interactions of the Er^{3+} cations with the O atoms of the OH^- and SO_4^{2-} groups in the jarosite mineral-type compounds are stronger than those of other investigated cations. The kinetic curves of Figures 4-4, 4-5, 4-6 and 4-7, calculated with the PSO model, are close to those obtained experimentally, which confirms that this model adequately describes the kinetics of sorption of Lanthanide (III) cations on the Purolite A-400 polymer.

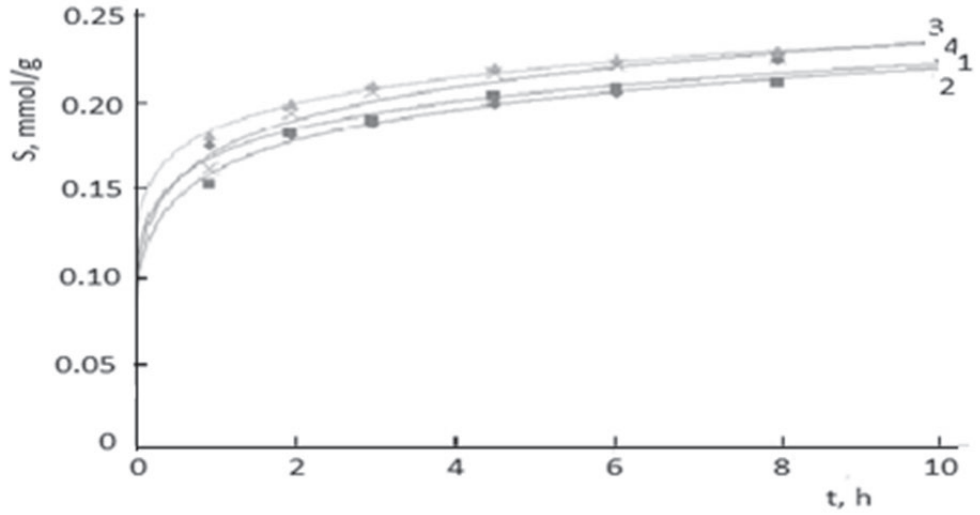

Figure 4-5. The kinetic curve of Nd^{3+} ion sorption on Purolite A-400, obtained experimentally at 50 (3) and 21°C (1) and calculated with the pseudo-second-order kinetic model at 50 (4) and 21°C (2).

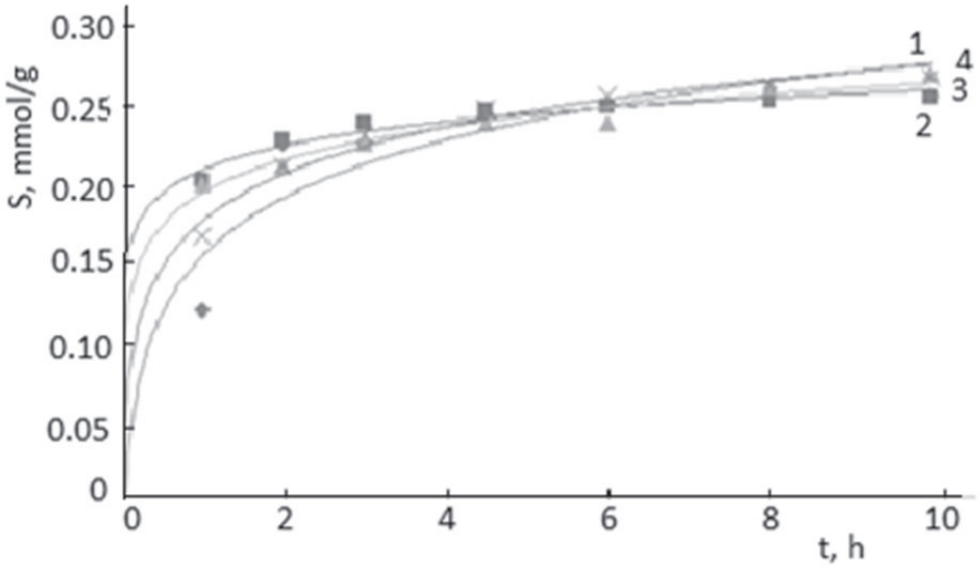

Figure 4-6. The kinetic curve of Eu^{3+} ion sorption on Purolite A-400, obtained experimentally at 50 (4) and 21°C (1) and calculated with the pseudo-second-order kinetic model at 50 (3) and 21°C (2).

To determine the process limiting the rate of sorption of lanthanide (III) cations on Purolite A-400, the dependence of the -ln(1-F) function on t was constructed (Figs.4-8 and 4-9).

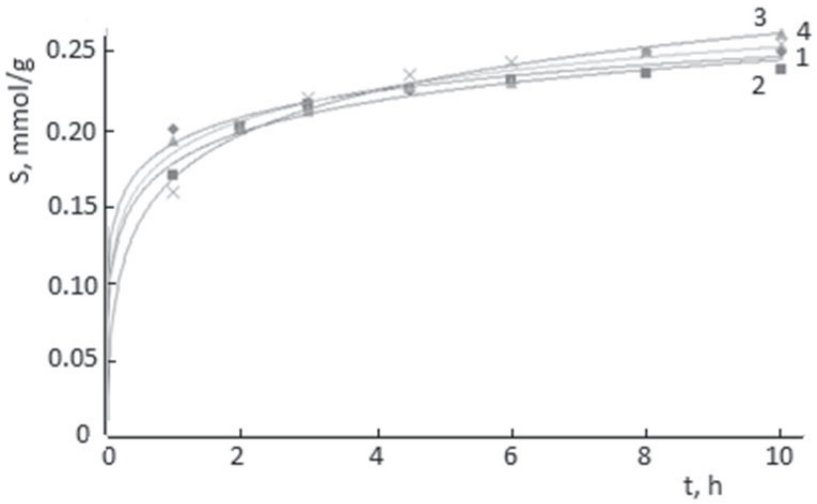

Figure 4-7. The kinetic curve of Er^{3+} ion sorption on Purolite A-400, obtained experimentally at 50 (3) and 21°C (1) and calculated with the pseudo-second-order kinetic model at 50 (4) and 21°C (2)

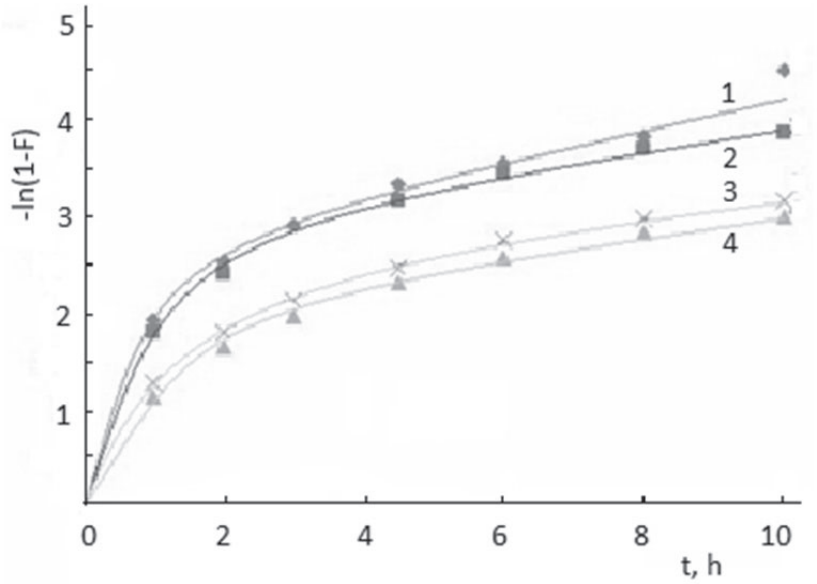

Figure 4-8. Dependence -ln(1-F) = f(t) for the La^{3+} sorption on Purolite A-400 at 21 (1), and 50°C (2) and Nd^{3+} at 21 (3) and 50°C (4).

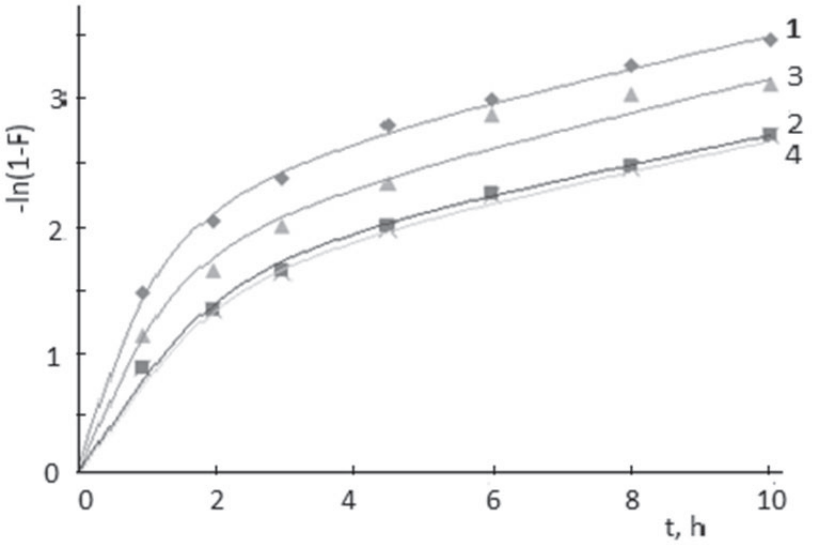

Figure 4-9. Dependence -ln(1-F) = f(t) for the Eu^{3+} sorption on Purolite A-400 at 21 (1), and 50°C (2) and Er^{3+} at 21 (3) and 50°C (4.)

The non-linear dependence of -ln(1-F) = f(t) shows that the sorption rate of cations containing Lanthanides(III) on Purolite A-400 at both 21 and at 50°C is limited by the internal diffusion [118]. In fact, it was expected that the sorption rate-limiting step would be the internal diffusion if taking into consideration that the polymer matrix has positive electric charges like Lanthanide (III) cations.

4.2. Sorption isotherms

Isotherms of the Lanthanides (III)-containing cations sorption on Purolite A-400 polymer were obtained at 21 and 50°C from solutions with pH 6.0. The contact time of the polymer with the solution was 8 hours. The experimentally obtained isotherms were calculated using the Langmuir (Eq1-9) and Freundlich (Eq.1-6) sorption models. As can be seen from Figures 4-10 and 4-11, both sorption models well describe the isotherms obtained experimentally.

Two different error functions were used to determine the validity of kinetic models and isotherms, which were fitted by the non-linear regression method: the coefficient of determination (R^2), and the nonlinear Chi-square (χ^2) test, estimated by Equation (4-7):

$$\chi^2 = \sum \frac{(S_{exp} - S_{calc})^2}{S_{calc}} \tag{4-7}$$

where $S_{exp.}$ and $S_{calc.}$ were obtained experimentally and calculated sorption respectively.

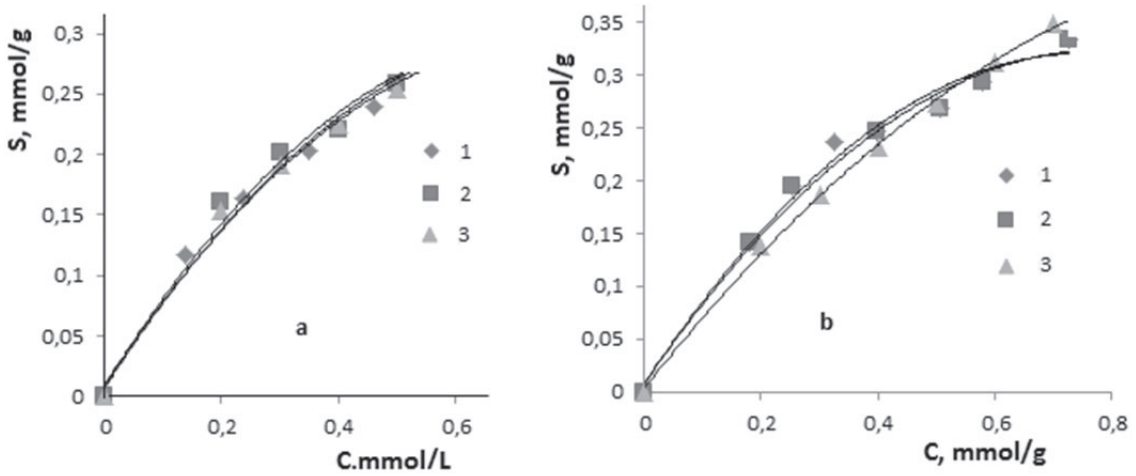

Figure 4-10. Equilibrium sorption isotherms of Lanthanum (III)-containing cations on Purolite A-400 at 21°C (a) and 50°C (b): obtained experimentally (1) and calculated by Langmuir (2) and Freundlich (3) sorption models.

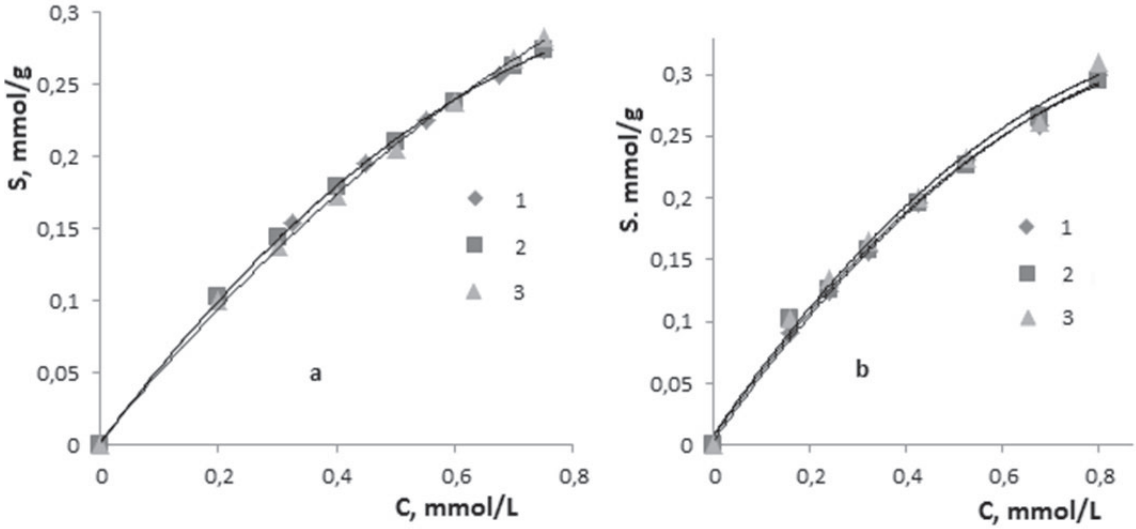

Figure 4-11. Equilibrium sorption isotherms of Neodymium (III)-containing cations on Purolite A-400 at 21°C (a) and 50°C (b): obtained experimentally (1) and calculated by Langmuir (2) and Freundlich (3) sorption models.

The high values of R^2 and the low values of X^2, are the best theoretical approach for describing the sorption data.

The feasibility of adsorption in a certain concentration range can be expressed in terms of the non-dimensional constant R_L (Eq.4-8), called the constant separation factor or equilibrium parameter [119].

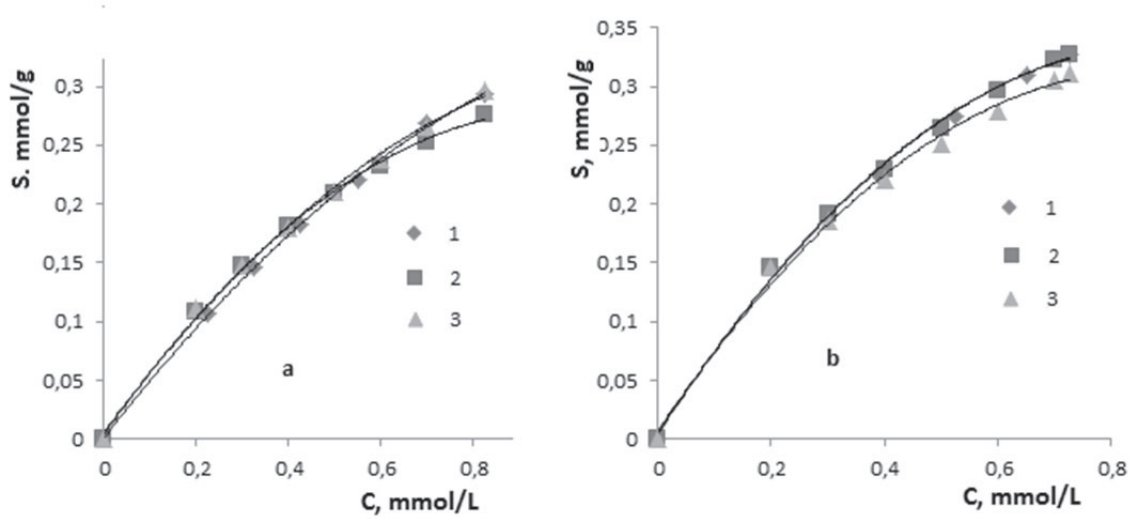

Figure 4-12. Equilibrium sorption isotherms of Europium (III)-containing cations on Purolite A-400 at 21°C (a) and 50°C: obtained experimentally (1) and calculated by Langmuir (2) and Freundlich (3) sorption models.

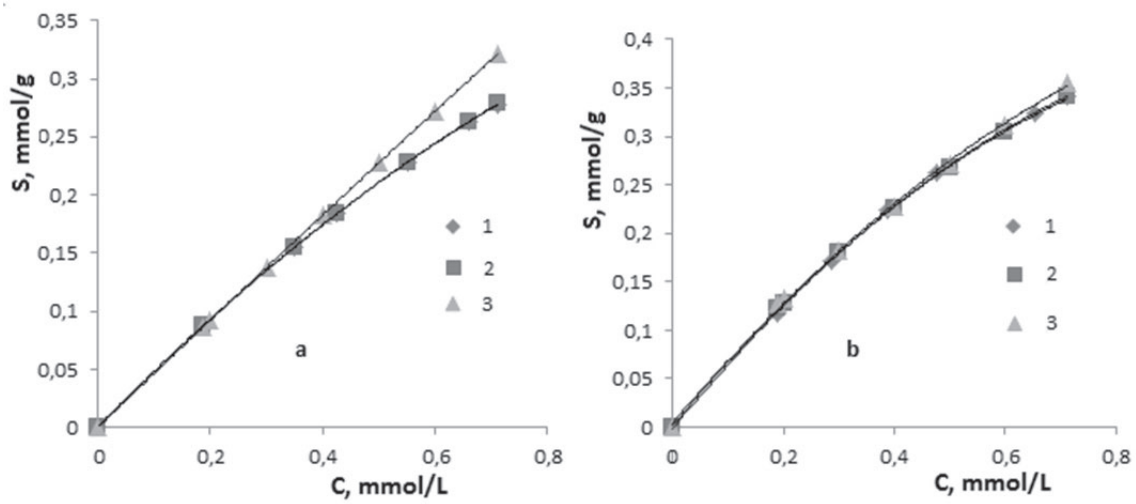

Figure 4-13. Equilibrium sorption isotherms of Erbium (III)-containing cations on Purolite A-400 at 21°C (a) and 50°C (b): obtained experimentally (1) and calculated by the Langmuir (2) and Freundlich (3) sorption models.

$$R_L = \frac{1}{1+K_{LC_i}} \quad , \tag{4-8}$$

where: K_L is the Langmuir sorption constant (L/mg), and Ci is the initial concentration of metal ions (mmol/L).

According to the values of R_L, the sorption is: unfavourable when $R_L > 1$; linear when $R_L = 1$; favourable when $0 < R_L < 1$; and irreversible when $R_L = 0$.

The isotherm parameters that resulted from the nonlinear Langmuir and Freundlich sorption models are presented in Table 4-2.

Table 4-2. Isotherm parameters of Langmuir and Freundlich sorption models for the sorption of Lantanides (III)-containing cations on Purolite A-400

	Langmuir model	Freundlich model	Langmuir model	Freundlich model
	T, 21°C		T, 50°C	
La	S_L = 0.4252 mmol/g S_L = 59.06 mg/g K_L = 1.8292 L/mmol R^2 = 0.9866 R_L = 0.4385 X^2 = 0.0066	K_F = 0.3716 1/n = 0.55 R^2 = 9924 X^2 = 0.006	S_L = 0.5393 mmol/g S_L= 74.91 mg/g K_L = 2.125 L/mmol R^2 = 0.9967 R_L = 0.3936 X^2 = 0.0017	K_F = 0.4535 1/n = 0.453 R^2 = 0.9984 X^2 = 0.0013
Nd	S_L = 0.691 mmol/g S_L = 99.67mg/g K_L = 0.8754 L/mmol R^2 = 0.9996 R_L = 0.6036 X^2 = 0.0017	K_F = 0.3548 1/n = 0.7869 R^2 = 0.9991 X^2 = 0.0018	S_L = 0.7023 mmol/g S_L= 101.3 mg/g K_L = 0.905 L/mmol R^2 = 0.9962 R_L= 0.58 X^2 = 0.0014	K_F = 0.3621 1/n = 0.6914 R^2 = 0.9923 X^2 = 0.0027
Eu	S_L = 0.5415 S_L = 82.29 mg/g K_L = 1.2563 L/mmol R^2 = 0.9985 X^2 =0.0017 R_L= 0.49	K_F = 0.3246 1/n = 0.6393 R^2 = 0.9967 X^2 = 0.0011	S_L = 0.6814 mmol/g S_L= 103.55mg/g K_L= 1.2847 L/mmol R^2 = 0.9971 X^2 = 0.0028 R_L= 0.52	K_F = 0.3753 1/n = 0.5833 R^2 = 0.9941 X^2 = 0.0044
Er	S_L = 1.2195 mmol/g S_L= 203.97 mg/g K_L = 0.4168 L/mmol R^2 = 1.000 R_L= 0.4356 X^2 = 0.0167	K_F = 0.4493 1/n = 0.9825 R^2 = 9948 X^2 = 0.0132	S_L = 0.9633 mmol/g S_L= 161.12 mg/g K_L = 0.7673 L/mmol R^2 = 0.9997 R_L= 0.6465 X^2 = 0.0005	K_F = 0.463 1/n = 0.7765 R^2 = 0.9986 X^2 = 0.0017

Table 4-2 shows that the maximum sorption capacity (S_L) of cations holding Lanthanide (III) is quite large, being greater at 50°C than at 21°C. The maximum sorption capacity (mmol/g) of Amberlite A-400 for cations holding Lanthanide (III) at 21°C but also at 50 °C increases in the order La < Eu < Nd < Er. The sorption capacity of the polymer for cations holding Europium (III) differs from the series of increases in the molecular mass of the elements. This deviation is seen and in the M^{3+}- O distance and diffusion coefficient in water of the Lanthanide (III) aqua complexes [115]. As is known in jarosite-type compounds, metal cations are coordinated with oxygen atoms of hydroxyl and sulfate groups: $NH_4[M_3(OH)_6(SO_4)_2]$.

Table 4-3. Thermodynamic data of the sorption of lanthanide (III) cations on Purolite A-400 at 21 and 50 °C

La	Nd	Eu	Er
ΔG_{294} = -18.36 kJ/mol G_{323} = - 20.57 kJ/mol ΔH = 4.081 kJ/mol ΔS_{294} = 76.33J/mol*.K ΔS_{323} = 76.32 J/mol*K	ΔG_{294} = -16.56 kJ/mol ΔG_{323} = - 18.28kJ/mol ΔH = 0.905 kJ/mol ΔS_{294} = 59.40 J/mol*.K ΔS_{323} = 59.40 J/mol*K	ΔG_{294} = -17.44 kJ/mol ΔG_{323} = - 19.223 kJ/mol ΔH = 0.609 kJ/mol ΔS_{294} = 61.39 J/mol.K ΔS_{323} = 61.40 J/mol.K	ΔG_{294} = -14.75 kJ/mol ΔG_{323} = -17.84 kJ/mol ΔH = 16.61 kJ/mol ΔS_{294} = 106.7 J/mol.K ΔS_{323} = 106.7 J/mol.K

The R_L values, calculated for the entire range of initial concentrations of metal ions, show that the sorption process is favourable.

The data calculated according to the Langmuir sorption model allowed the thermodynamic functions of the sorption process to be calculated.

Variation of Gibbs energy (ΔG) was calculated according to Equation (4-9):

$$\Delta G = - RT \ln K_{L,} \quad (4\text{-}9)$$

where: K_L is the Langmuir sorption constant.

The enthalpy variance, considering it to be constant in the T_1-T_2 temperature range, was calculated with Equation (4-10):

$$\Delta H = \frac{RT_1T_2\, ln\frac{k_2}{k_1}}{T_2 - T_1}, \quad (4\text{-}10)$$

where: k_1 is the Langmuir sorption constant K_L at T_1 and k_2 is K_L at T_2.

The enthalpy variance was calculated with Equation (4-11):

$$\Delta S = \frac{\Delta H - \Delta G}{T} \quad (4\text{-}11)$$

The results of the calculation of thermodynamic functions are presented in Table 4-3.

The values and sign of the free enthalpy (ΔG) confirm that sorption of cations holding Lanthanides (III) is a spontaneous process. For sorption of cations holding Lanthanide (III) - ΔG decreases in the order: La > Eu > Nd > Er. The sorption rate decreases in the same order (Tab.4-1). According to ΔH, it is confirmed that sorption is an endothermic process. Interestingly, ΔS does not depend on temperature. The temperature independence of ΔS can be explained by the assumption that the change in the heat capacity of the formation of metal compounds in the polymer phase is zero (ΔCp = 0).

The data in Table 4-3 prove that the sorption of Lanthanide (III) containing cations on the Purolite A-400 polymer is a complex process that includes the destruction and formation of compounds.

V.

BISMUTH (III) COMPOUNDS IN THE POLYMER PHASE

Theoretically, Bi (III)-containing cations should not be kept on the monofunctional strongly basic anion exchangers containing NH_4^+. In order to form compounds of the jarosite mineral type in the system, there must be sulfate anions, but the Bi(III) sulfate is insoluble in water. On the other hand, the Bi^{3+} cations in water hydrolyse very strongly, at pH approximately 0.5 and more in the system will be sediment. However, to our surprise, we noticed that Bi(III)-containing cations in the $Bi(NO_3)_3$ solution are able to be retained on the strongly basic anion exchangers [120-122]. This led to the need to investigate in more detail the sorption process of cations holding Bi (III) on strongly basic anion exchangers [123].

The commercial strongly basic anion exchangers AV-17 and Purolite A-400 in Cl^- form were used. Both exchangers were gel-type cross-linked polystyrene–divinylbenzene polymers holding $–N^+(CH_3)_3$ functional groups and 8% divinylbenzene.

The sorption of Bi(III)-containing cations took place upon the contact of 0.2 g of dried polymer samples with 100 mL of $Bi(NO_3)_3$ solution at pH of about 0.25. The $Bi(NO_3)_3$ solutions were prepared by dissolving metallic Bi in an HNO_3 solution. The temperature of the polymer–solution systems was a supported constant with an error of ± 1 ^oC. The Bi^{3+} content in the polymer was determined by photocolorimetry with thiourea [26] after desorption [121].

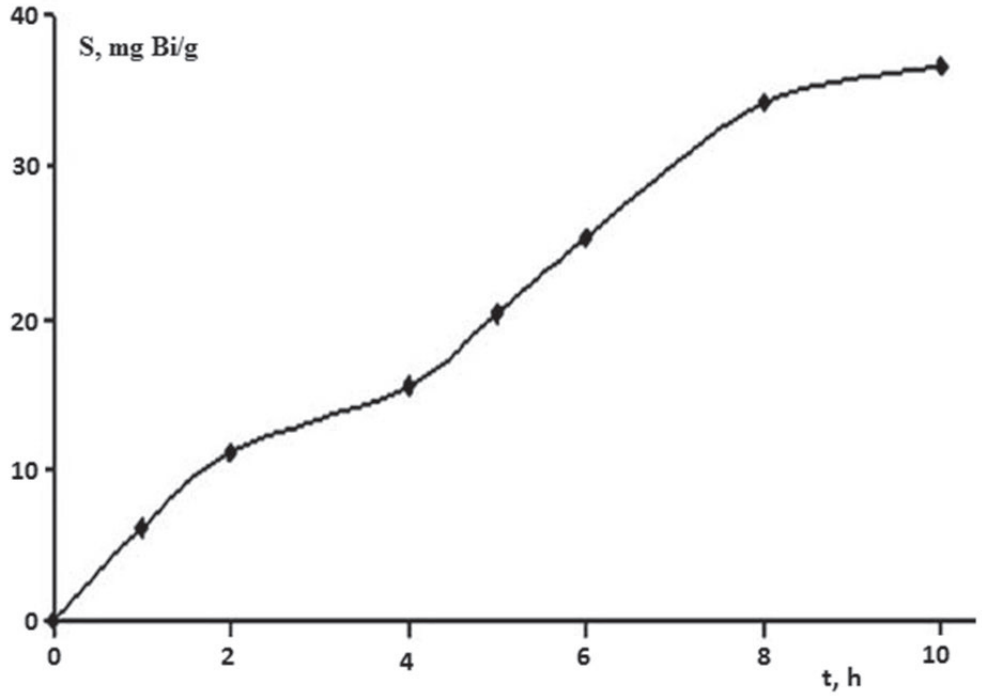

Figure 5-1. Kinetic curve of the Bi(III)-containing cation sorption at 55^{o}C on the AV-17 polymer.

As shown in Figure 5-1, the sorption equilibrium of the Bi(III)-containing cations on the strongly basic anion exchanger AV-17 was established at about 10 h of polymer contact with a 0.015M $Bi(NO_3)_3$ solution at 55^{o}C. In a previous study, it was shown [121] that the sorption of Bi(III)-containing cations on strongly basic anion exchangers depended on the temperature. The low rate of sorption and its strong dependence on the temperature showed that the retention of Bi(III)-containing cations by anion exchangers is a chemical process.

The S-form of Bi(III) sorption isotherms at different temperatures (Fig.5-2) confirmed the chemical nature of the sorption process. It was suggested that when the strongly basic anion exchanger was in contact with the $Bi(NO_3)_3$ solutions, the formation of Bi(III) compound solid particles in the polymer phase took place. The existence of solid particles of the Bi(III) compounds on the surface and in the volume of the polymer granules was confirmed by the SEM EDX investigation. The obtained SEM images are presented in Figure 5-3.

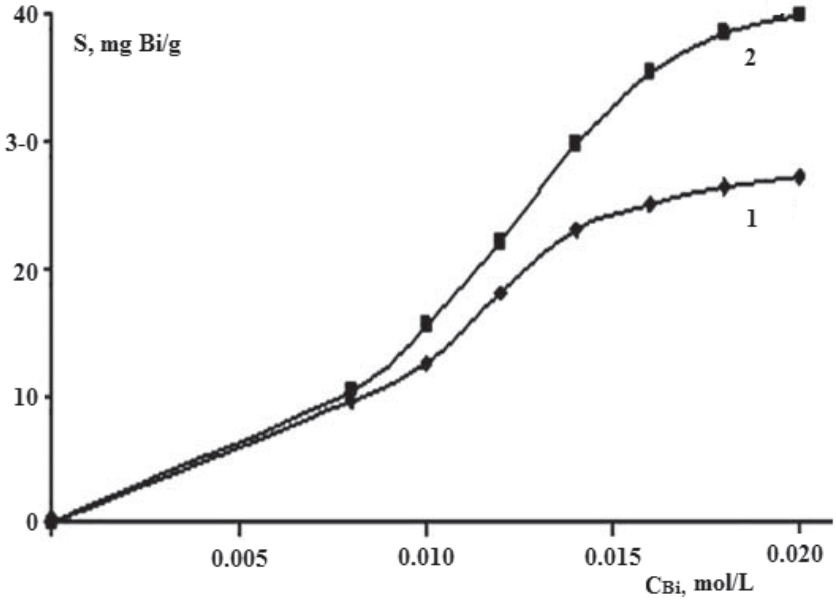

Figure 5-2. Sorption isotherms of the Bi(III)-containing cations on AV-17 at (1) 30 and (2) 50°C.

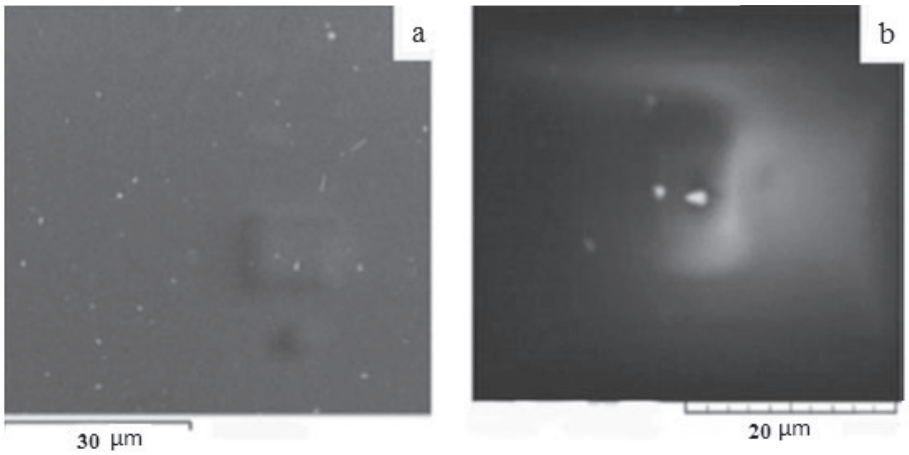

Figure 5-3. SEM images of the (a) surface and (b) volume of the Bi(III)-containing AV-17 granule

Concomitantly, the elemental composition of the Bi(III)-containing structures on the surface and in the polymer granule was determined (Tab.5-1).

Table 5-1. Elemental Composition of the Bi(III)-containing structural units on the surface and in the volume of the AV-17 granule

On the surface of the granule (atom %)				In the volume of the granule (atom %)			
Element	Initial AV-17(Bi)	AV-17(Bi) heated in water	AV-17(Bi) heated in an Na_2SO_4 solution	Initial AV-17(Bi)	AV-17(Bi) heated in water		AV-17(Bi) heated in a Na_2SO_4 solution
					Small particle	Large particle	
C	77.88	82.29	57.71	79.84	87.41	83.90	77.58
N	8.92	-	-	8.52	-	-	-
O	11.69	13.60	32.15	10.22	11.45	9.34	18.80
Cl	1.16	2.47	-	1.06	0.80	3.48	-
Bi	0.37	1.65	10.14	0.35	0.35	3.28	3.62

As shown in Figure 5-3, on the surface and in the polymer granule, there were ultrafine particles of Bi(III) compounds with a particle diameter d < 1 μm. With the data from Table 5-1, the brute formulas of a Bi(III)-containing structural unit were computed and were $Bi_1O_{31.6}Cl_{3.1}N_{24.1}C_{210}$ on the polymer granule surface and $Bi_1O_{29.3}Cl_{3.0}N_{24.3}C_{228}$ in the granule. It was suggested that on the surface and in the polymer granule, really there were BiOCl and $BiONO_3$ particles, and C atoms belonged to the polymer. These particles were situated on the $-CH_2N(CH_3)_3Cl$ and $-CH_2N(CH_3)_3NO_3$ polymer groups. It was also suggested that part of the BiOCl and $BiONO_3$ compounds was in the molecular form. To confirm this, we heated at 87°C the Bi(III)-containing polymer sample in acidulated (with HNO_3 solution) distilled water (pH 3.4) for 3 h. It is known [33], that, upon heating in water in the polymer phase, the fusion of molecular compounds takes place.

The Bi(III)-containing polymer sample obtained after heating in water was investigated with SEM. As shown in Figure 5-4, the fusion of small Bi(III)-containing particles in the polymer phase really took place. On heating in water, the surface of the polymer granule was covered with particles of Bi(III)-containing compounds [Fig.5-4 (a,b)]. On heating in water in the polymer phase, two processes took place: Bi(III)-containing particles became larger, and compounds migrated to the granule surface [Fig.5-4 (c,d)]. Up to the polymer granule surface, Bi(III)-containing particles were greater in number but smaller.

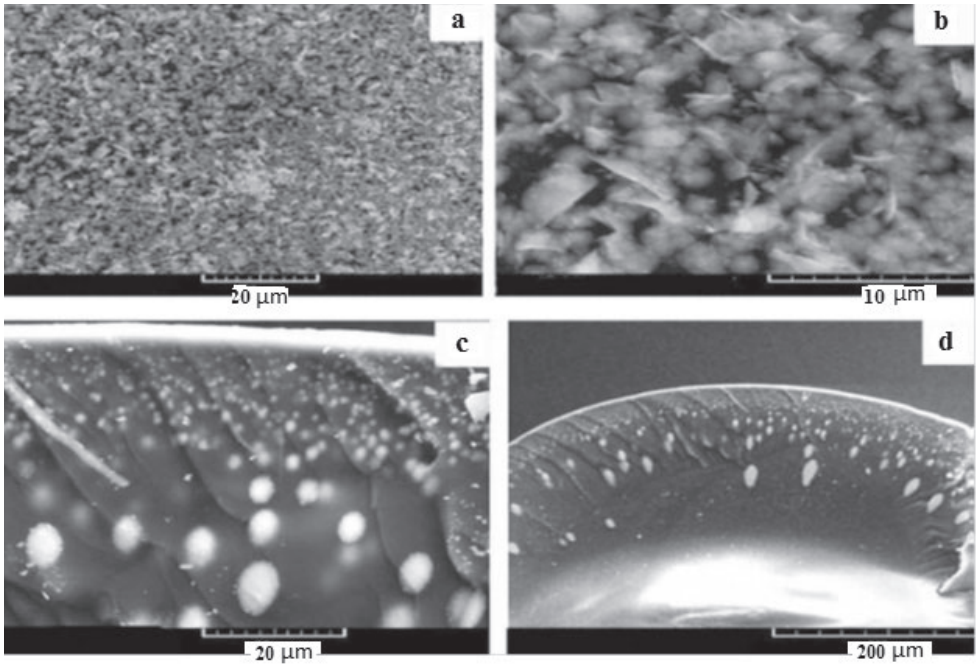

Figure 5-4. SEM images of the (a, b) surface and (c, d) volume of the Bi(III)-containing AV-17 granule after heating in water.

The elemental composition of the Bi(III)-containing structures on the surface and of larger and smaller particles in the polymer granule is presented in Table 5-1. The brute formulas of the Bi(III)-containing structural units on the polymer granule surface and the large and small particles in the polymer granule were $Bi_{1O8.2}Cl_{1.5}C_{49.9}$, $Bi_{1O2.8}Cl_{1.1}C_{25.6}$, and $BiO_{32.7}Cl_{2.3}C_{250}$, respectively.

By comparing the data of Table 5-1, it was determined that after heating in water, N atoms in the Bi(III)-containing structures in the polymer phase were absent. Also, the larger the Bi(III)-containing structures, the lower were the O,

Cl, and C atom contents (Tab.5-1). It was suggested that on the surface and in the polymer' granules heated in water, there were, particularly, BiOCl particles and a small amount of Bi_2O_3 compound. These particles were situated on the $^{-}CH_2^{-}$ and $^{-}CH_3$ groups and O atoms of the $^{-}CH_2N(CH_3)_3NO_3$ polymers groups, and N atoms were not detected. A number of particles containing BiOCl and Bi_2O_3 were situated on the $^{-}CH_2N(CH_3)_3Cl$ groups. Interesting results were obtained on the investigation of the Bi(III)-containing AV-17 after heating in the 0.1M Na_2SO_4 solution (pH 3.4) at 87^{o}C during 3 h (Fig.5-5).

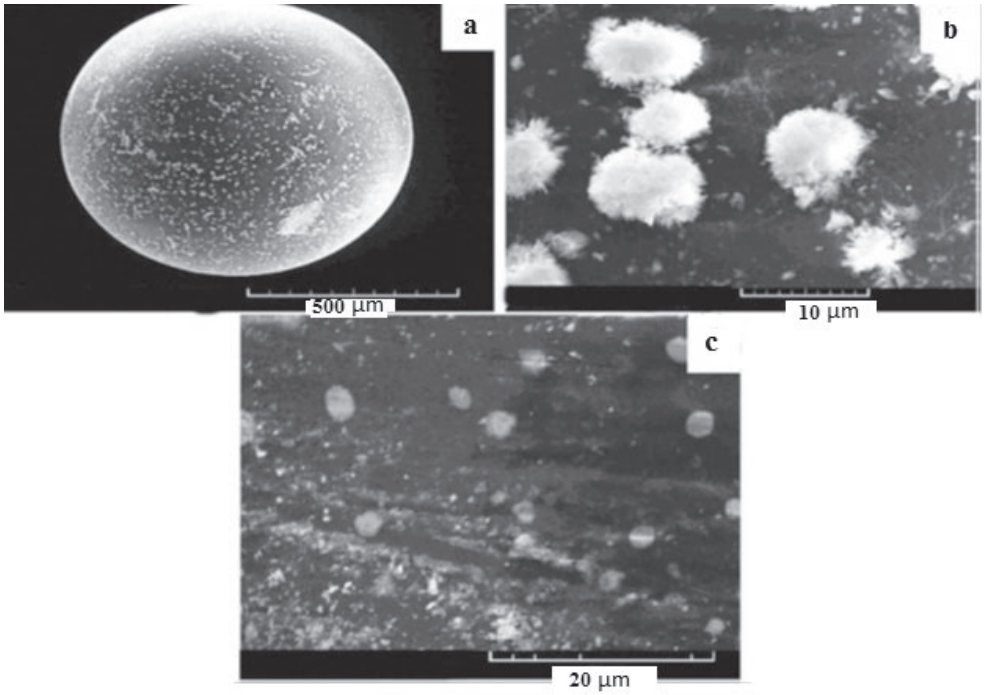

Figure 5-5. SEM images of the (a, b) surface and (c) volume of the Bi(III)-containing AV-17 granule after heating in an Na_2SO_4 solution.

First, it was observed that Bi(III)-containing particles were concentrated on the polymer granule surface. Also, the Bi(III)-containing particles were much larger than before they were heated in the Na_2SO_4 solution. The elemental composition of the Bi(III)-containing structures was different, too (Tab.5-1). The Bi(III)-containing structures in the polymer phase after heating in the Na_2SO_4 solution contained only Bi, O, and C atoms and did not contain N and Cl atoms. The brute formula of the Bi(III)-containing structure on the polymer granule surface was $Bi_1O_{3.2}C_{5.7}$, and that in the polymer granule was $Bi_1O_{5.2}C_{21.4}$. The composition of the Bi(III)-containing structures permitted the conclusion that on the surface and in the polymer granule, there were $Bi(OH)_3$ and Bi_2O_3 particles. These particles were situated on $^{-}CH_2^{-}$, $^{-}CH_3$, and O atoms of $^{-}[CH_2N(CH_3)_3]_2SO_4$ groups. The elemental analysis was focused on Bi_2O_3 particles, but in the polymer phase, there were BiOCl particles, too. This fact was confirmed by powder X-ray diffraction investigation. The X-ray diffractogram (Fig.5-6) of the Bi(III)-containing AV-17 was a typical spectrum of an amorphous polymer with the large broadening of diffraction peaks corresponding to interplanar distances (d's) of 4.7 and 2.5Å . This spectrum did not show any characteristic peaks for bismuth compounds. After the Bi(III)-containing polymer was heated in water at 87 ^{o}C, the crystallized BiOCl appeared, and its sharp diffraction peaks were located on the polymer matrix curve [Fig.5-6 (b)]. When the Bi(III)-containing polymer in the Na_2SO_4 solution was heated, the polycrystals of BiOCl were formed but in smaller quantities (the BiOCl spectrum peaks decreased). In this diffractogram appeared a new peak (d =3.2 Å), which was attributed to the Bi_2O_3 phase [Fig.5-6 (c)].

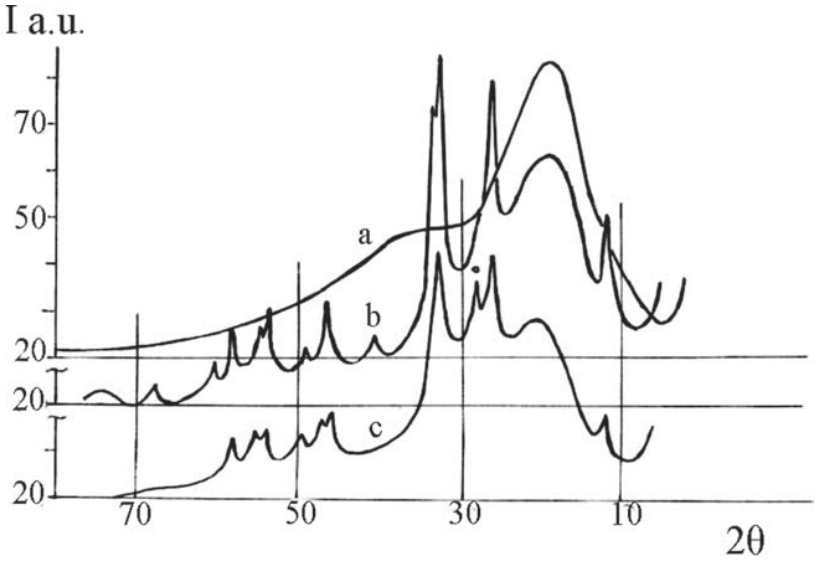

Figure 5-6. X-ray diffraction spectra of the (a) Bi(III)-containing AV-17 and the Bi(III)-containing polymer after heating in (b) water and (c) in 0.1M Na_2SO_4 solution. I, signal intensity, arbitrary units.

To apply Bi(III)-containing polymers to liquid purification, it is necessary to determine their behaviour in different media. In this study, the Bi(III) compounds' destruction in the polymer phase during contact with HCl, HNO_3, and H_2SO_4 solutions of different concentrations (equivalent with solution pH) were studied.

The strongly basic anion exchanger Purolite A-400, having 65.7 mg of Bi/g was used. The Bi(III)- containing polymer was prepared according to Ref.[121]. The Bi(III) compounds in the Purolite A-400 phase were the same as in the AV-17 polymer. The behaviour of the Bi(III) compounds in the Purolite A-400 phase in different acid solutions through the Bi^{3+} desorption (Ds), performed at 20 and 50°C, was investigated.

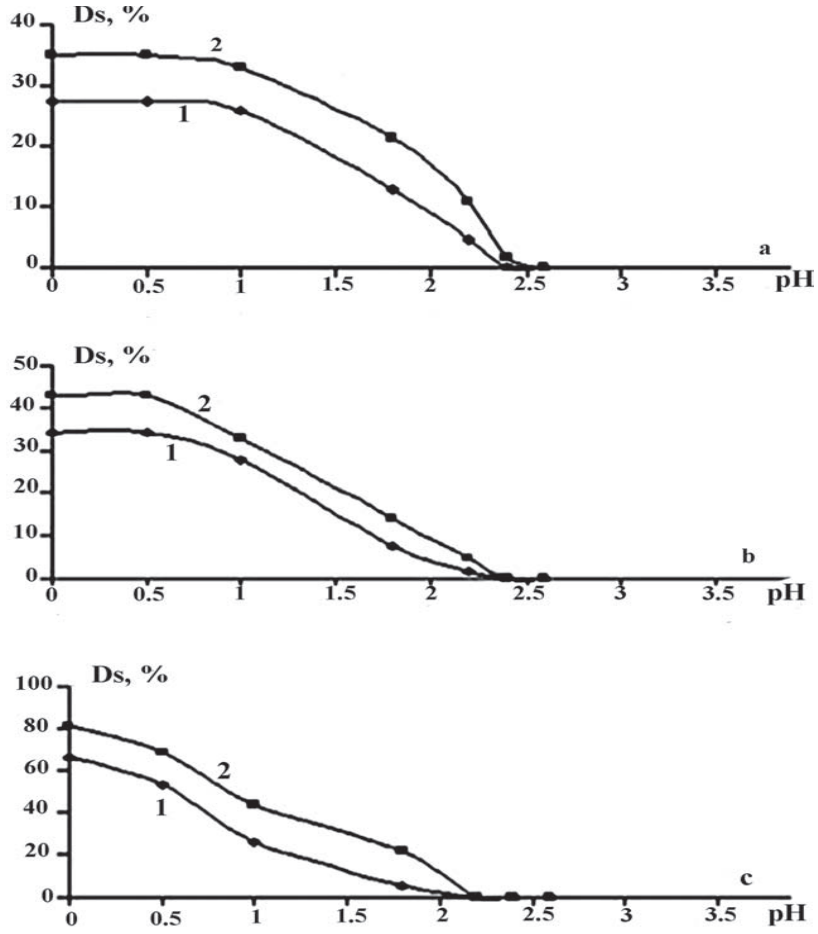

Figure 5-7. Bi^{3+} ion Ds from Purolite A-400 at 20 (1) and 50°C (2) as a function of pH in (a) HCl, (b) H_2SO_4, and (c) HNO_3 solutions.

As shown in Figure 5-7, the Bi(III)-containing compounds in the polymer phase were stable at pH > 2.4 in H_2SO_4 and HCl acid solutions and at pH > 2.2 in HNO_3 acid solution at 20 and 50°C.

The pH dependence of the Bi^{3+} Ds in HNO_3 and H_2SO_4 acid solutions showed that in the polymer phase, there were two kinds of Bi(III) compounds with different solubility. Probably, in the HCl acid solution, all of the Bi(III) compounds were in the form of more stable BiOCl.

Ds of the Bi^{3+} cations from Purolite A-400 in the 1M HNO_3 solution were much greater than in the 1M HCl or 0.5M H_2SO_4 solutions (Fig.5-7). Ds of the Bi^{3+} cations also increased with increasing temperature. The temperature and acid nature influenced the Bi^{3+} ions desorption kinetics (Fig.5-8). The Bi^{3+} ion desorption rate in the 1M HNO_3 acid solution was much greater than in the 1M HCl or 0.5M H_2SO_4 solution. After 10.5 h of

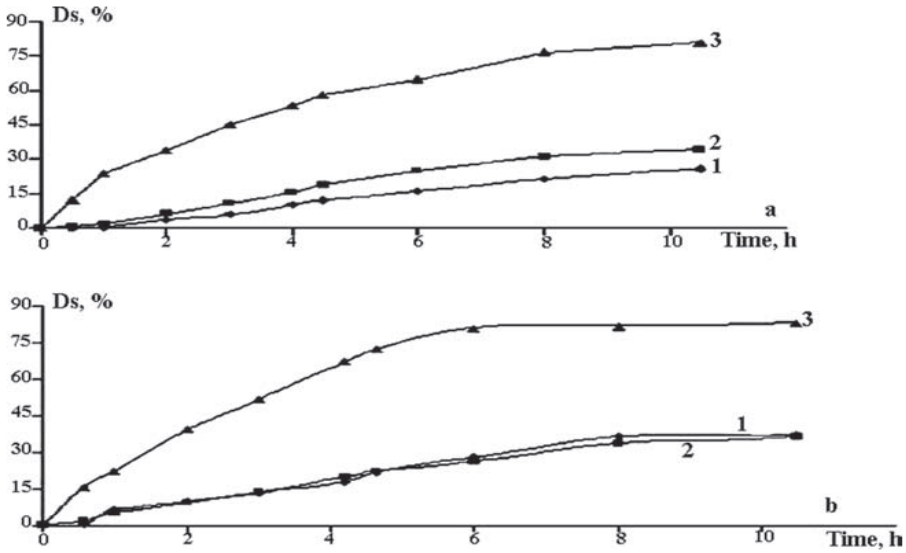

Figure 5-8. Kinetic curves of the Bi^{3+} ion desorption from Purolite A-400 in 1M HCl (1), 0.5M H_2SO_4 (2) and 1M HNO_3 (3) solutions at 20 (a) and 50°C (b).

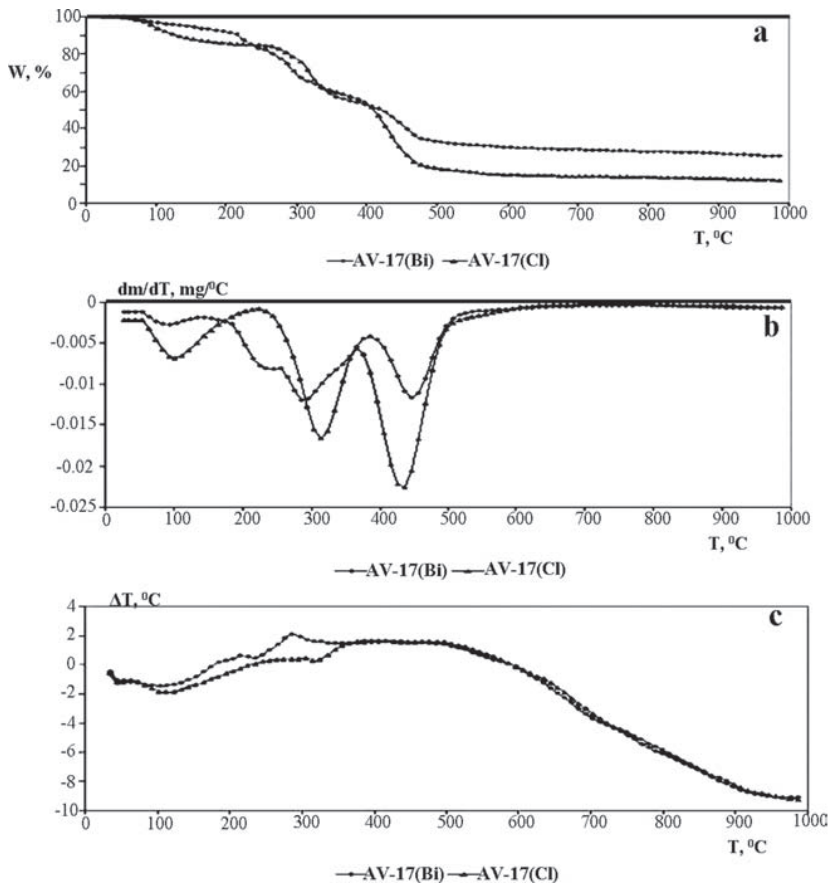

Figure 5-9. TG (a), DTG (b) and DTA (c) curves of the AV-17(Cl) and initial AV-17(Bi).

contact of the Bi(III)-containing polymer with 0.5M H_2SO_4 and 1M HNO_3 acid solutions, the Ds values were about 34 and 36%, respectively, at 20°C and at 50°C, the Ds values were 80.5 and 83%, respectively.

To apply a Bi(III)-containing polymer as a sorbent or a catalyst in processes with gases, it is necessary to determine their thermal behaviour. There was an investigation of the thermal behaviour in an N_2 medium of the Bi(III)-containing AV-17 and, for comparison, that of the AV-17(Cl) under the same conditions.

As shown in Figure 5-9, three stages were distinguished in the thermogravimetry (TG), differential thermogravimetry (DTG), and differential thermal analysis (DTA) curves of the AV-17(Cl). The summary of the important TG characteristics obtained from the thermograms included the initial temperature of thermal degradation (T_{onset}), the temperature corresponding to the maximum degradation rate (T_{peak}), the final temperature at which the degradation process for each stage ended (T_{endset}), mass loss (W; %), and residual weight loss after the end of the decomposition process; these are listed in Table 5-2.

Table 5-2. TG and kinetic data obtained in the investigation of the Bi(III)-containing AV-17(Bi) and AV-17(Cl) samples

Sample	Stage	T_{onset}, °C	T_{peak}, °C	T_{endset}, °C	W (%)	Residue (%)	E_a, kJ/mol	n	Ln A
AV-17 (Bi)	I	64	86	131	6.63	24.37	33.47± 1.07	0.91± 0.002	6.63± 0.38
	II	215	267	243	11.12		54.28 ±3.22	0.12± 0.003	6.78± 0.72
	III	281	333	355	28.83		-	-	-
	IV	417	451	476	29.05		239.9± 1.65	1.42± 0.001	35.87± 0.28
AV-17(Cl)	I	68	99	165	14.47	11.53	56.0± 0.47	2.44 ±0.001	13.68± 0.16
	II	267	316	337	29.14		120.88± 3.66	0.98± 0.005	20.11± 0.79
	III	393	433	470	44.86		194.02± 3.11	1.67± 0.002	28.78± 0.55

In stage I, two processes took place: elimination from the polymer phase of hydration and free water and, partially, the following process [71]:

$$2RCH_2N(CH_3)_3Cl + HOH = RCH_2OH + RCH_2N(CH_3)_2HCl + N(CH_3)_4Cl \quad (5\text{-}1)$$

The process in Equation (5-1) continued at temperatures greater than 265°C. In stage II, the processes of $N(CH_3)_4Cl$ decomposition took place according to Equation (5-2) with the elimination of $N(CH_3)_3$ and CH_3Cl:

$$N(CH_3)_4Cl = N(CH_3)_3 + CH_3Cl \quad (5\text{-}2)$$

In stage III, the complete decomposition of the polymer residue took place.

The TG, DTG, and DTA curves of the Bi(III)-containing AV-17 (Fig.5-9) differed from those of AV-17(Cl). The examination of the TG and DTG curves in Figure 5-9 also reveals the existence of a thermal stability domain in the 120–160 °C temperature interval for the AV-17(Bi) sample. The temperature in the beginning of the second degradation stage was about 215°C. In stages II and III, there was a superposition of some thermal processes. On heating of the Bi(III)-containing AV-17, in addition to the processes in Equations (5-1) and (5-2) and water elimination, the decomposition of the Bi(III) compounds took place. More important was that the Bi(III)-containing polymer could be used as a catalyst or as a sorbent without an irreversible state up to 120–160°C.

The surveys were extended with the kinetic processing of the TG data. The Freemann–Caroll [71] method is based on the calculation of the kinetic parameters (Eqs. (1-16) to (1-18)).

The *n* and *Ea* values (Tab.5-2) indicated that the thermal decomposition of the Bi(III)-containing polymer and AV-17(Cl) was a complicated process. The kinetic parameter value determination for each thermal decomposition stage supplied information on the degradation mechanism. The thermal degradation process consisted of successive reactions, and higher *Ea* values occurred in the last stage at temperatures exceeding 400°C. This stage corresponded to thermal polymer degradation. The almost similar *Ea* values occurring in the last stage suggested similar degradation mechanisms.

The main conclusion is that cross-linked ionic polymers, containing strongly basic groups are able to retain Bi(III)-containing cations (hydroxocations) from $Bi(NO_3)_3$ solutions. However, their retention on such polymers is not due to the formation of jarosite compounds, but to the formation of oxide and bismuthyl chloride.

VI.

SOME METAL COMPOUNDS IN THE POLYMER PHASE – PRECURSORS FOR NEW SORBENTS AND CATALYSTS

In the previous paragraphs, it has been shown that cations containing Fe(III), Cr(III), Al(III) and Lanthanides (III) are retained on cross-linked ionic polymers containing strongly basic groups as a result of the formation in their phase of jarosite mineral type compounds: $R_4N[M_3(OH)_6(SO_4]$.

On the other hand, it was demonstrated that cations containing Bi(III) are retained on this type of polymers as a result of the formation of Bi_2O_3 and BiOCl compounds. There was further investigation of the possibility of the simultaneous formation in the polymer phase of various compounds that would hold one or two metals. This opens supplementary opportunities for obtaining new sorbents and catalysts [124].

First of all, the Bi(III)-containing polymer was prepared according to Ref. 121. The preparation took place upon the contact of 50 g of dried AV-17(Cl) during 6 h with 2 L of 0.015 mol/L $Bi(NO_3)_3$ solution with pH about 0.25 and temperature of 50°C. After that, the AV-17(Bi) polymer sample was filtrated, washed with distilled water, and dried in air. The obtained Bi(III)-containing AV-17 has been used for the preparation of other metal-containing polymer samples as follows:

1. AV-17(Bi,Al)—the sample of the polymer containing Bi(III) and Al(III) compounds. The 5 g of dried AV-17(Bi) sample was 12 h in contact with 500 mL of $Al_2(SO_4)_3 * 12H_2O$ solution holding 2.5 g Al/L and having pH 3.4 and temperature of 87°C [88]. After that, the sample was filtrated, washed with distilled water, and dried at 60°C for 3 h.

2. AV-17(Bi, Fe)—the sample of the polymer containing Bi(III) and Fe(III) compounds. The 6 g of dried AV-17(Bi) sample was 8 h [72] in contact with 500 mL of the solution containing 7 g $Fe_2(SO_4)_3$/L and having pH 1.95 and temperature of 50 °C. After that, the sample was filtrated, washed with distilled water, and dried at 60°C for 3 h.

3. AV-17(Bi, FeOOH)—the sample of the polymer containing Bi(III) compounds and β-FeOOH.

The 4 g of the AV-17(Bi, Fe) sample was introduced in the 400 mL distilled water and heated for 5 h in the boiling water bath [33, 64]. Then the polymer was filtrated and dried in air.

4. AV-17(Bi, Cr)—the sample of the polymer containing Bi(III) and Cr(III) compounds. The 7 g of dried AV-17(Bi) sample was 12 h in contact with 1 L of $KCr(SO_4)_2 * 12H_2O$ solution containing 2 g Cr^{3+}/L and having pH 4.1 and temperature of 60°C. The pH of the solution which had contact with AV-17(Bi) was periodically adjusted to 4.1 using NaOH solution [87]. Then the polymer was filtrated, washed with distilled water and dried at 60°C during 1 h.

5. AV-17(Bi, Fe, Cr)—the sample of the polymer containing Bi(III), Fe(III), and Cr(III) compounds. The 2 g of the AV-17(Bi, Fe) sample was in contact with 200 mL of $KCr(SO_4)_2 * 12H_2O$ solution containing 2 g Cr^{3+} /L in the conditions of the AV-17(Bi,Cr) sample preparation (Sample 4).

6. AV-17(Bi, FeOOH, Cr)—the sample of the polymer containing Bi(III), β-FeOOH and Cr(III) compounds. The 2 g of the AV-17(Bi, FeOOH) sample was in contact with 200 mL of $KCr(SO_4)_2 * 12H_2O$ solution in the conditions of the AV-17(Bi,Cr) sample preparation.

The content of metals in the polymer phase was determined after desorption with 3M HNO_3 solution at 60°C. The Bi^{3+} cations were determined by photocolorimetry with thiourea, and Fe^{3+}, Al^{3+}, and Cr^{3+} ions by atomic absorption spectroscopy. Scanning electron microscopy images were obtained using the Tescan SEM-EDX microscope. Powder X-ray diffraction was carried out using the DRON-UM1 diffractometer (Cu Ka radiation, Ni filtered, θ/2θ method).

The thermal behaviour of the polymer samples containing metallic compounds was investigated under an N_2 atmosphere with the Mettler Toledo TGA-SDTA 851 derivatograph in the range 20-1000 °C. The N_2 gas flow rate was 20 mL/min and the heating rate was 20 °C/min. The FT-IR spectra were recorded over the interval 400–4000 cm^{-1} on a Bruker Vertex 70 spectrometer. The samples were run as KBr disks (composition 1/200).

The metal content in the modified AV-17 polymer samples is shown in Table 6-1.

When jarosite holding polymer (AV-17(Fe) sample) was heated for 5 h in the boiled water bath, the AV-17(β-FeOOH) sample was obtained [33, 64], according to Equations (6-1) and (6-2):

$$2R_4N[Fe_3(OH)_6(SO_4)_2] = 6((\beta\text{-FeOOH}) + (R_4N)_2SO_4 + 3H_2SO_4 \quad (6\text{-}1)$$

$$H_3O[Fe_3(OH)_6(SO_4)_2] = 3((\beta\text{-FeOOH}) + 2H_2SO_4 + H_2O \quad (6\text{-}2)$$

The processes (6-1) and (6-2) are accompanied by passing a part of the metallic cations from the polymer to the liquid phase [125]. But, as seen in Table 6-1,the obtaining of the AV-17(Bi, FeOOH) sample on heating in water medium of the AV-17(Bi, Fe) sample is not accompanied with the iron ions lost.

The processes of obtaining AV-17(Bi, Fe, Cr) from the AV-17(Bi, Fe) sample and AV-17(Bi, FeOOH, Cr) from the AV-17(Bi, FeOOH) sample are accompanied with the considerable loss of iron ions. Obviously, when the AV-17(Bi, Fe) samples were in contact with $KCr(SO_4)_2 * 12H_2O$ solution to obtain AV-17(Bi, Fe, Cr) and AV-17(Bi, FeOOH, Cr), replacement of the Fe^{3+} cations in the jarosite type compounds by the Cr^{3+} ions took place according to the processes (6-3) and (6-4):

$$R_4N[Fe_3(OH)_6(SO_4)_2] + Cr^{3+} \leftrightarrow R_4N[Cr_3(OH)_6(SO_4)_2] + Fe^{3+} \quad (6\text{-}3)$$

$$H_3O[Fe_3(OH)_6(SO_4)_2] + Cr^{3+} \leftrightarrow H_3O[Cr_3(OH)_6(SO_4)_2] + Fe^{3+} \quad (6\text{-}4)$$

Process (6-5) could also take place:

$$H_3O[Fe_3(OH)_6(SO_4)_2] + Cr^{3+} + K^{+} \leftrightarrow K[Cr_3(OH)_6(SO_4)_2] + Fe^{3+} + H_3O^{+} \quad (6\text{-}5)$$

The Fe^{3+} cations were replaced by Cr^{3+} ions in the FeOOH too. In fact, at pH 4.1 and temperature of 60 ^oC, there were no $[Cr(H_2O)_6]^{3+}$ cations in the $KCr(SO_4)_2 * 12H2O$ solution [55], but hydroxocomplexes which were destroyed in the processes (6-3) to (6-5).

The sorbent samples shown above were investigated using SEM, X-ray diffraction, FT-IR spectroscopy and thermogravimetric methods.

The AV-17(Bi, Al) sample. As seen in Figure 6-1(a,b), the surface of the polymer granule is covered with metallic compounds in the crystalline state. In the volume of the polymer granule [Fig. 6-1(c)], compounds particles are in the pseudo-spherical form with a diameter of about 5 μm. The morphology of the metal-containing compounds particles on the surface and in the volume of the polymer granule is quite different. It is known that the particles sizes and the morphology of Bi(III) compounds on

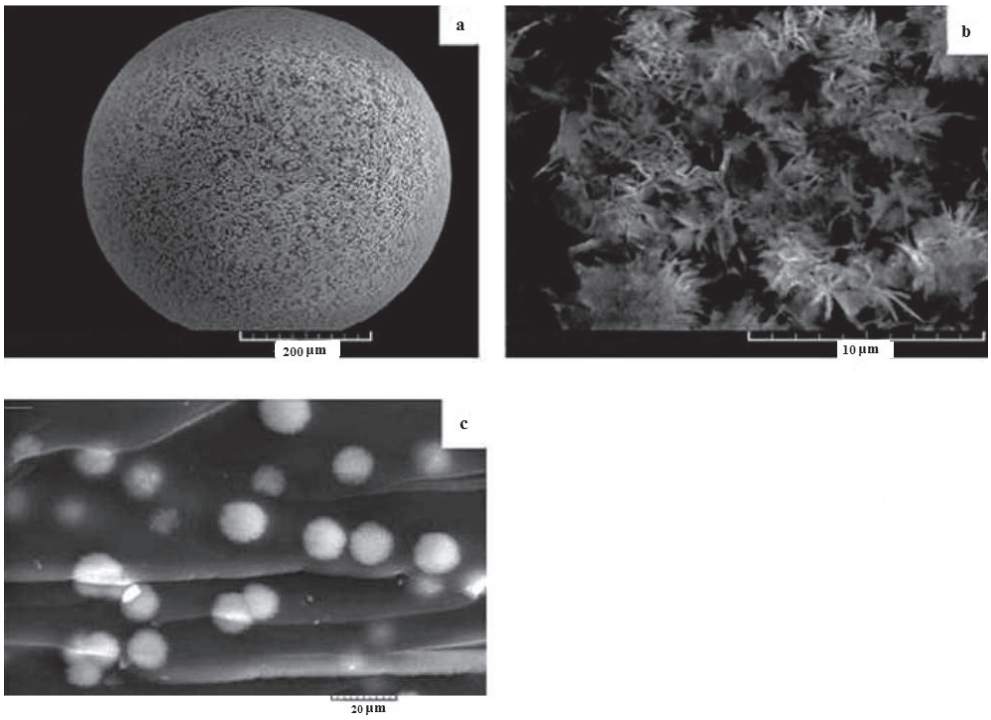

Figure 6-1. SEM images of the metal-containing compounds on the surface (a, b) and in the volume (c) of the AV-17(Bi, Al) polymer granule.

the AV-17 granule surface depend on the temperature and the existence of SO_4^{2-} anions in the system upon sample preparation [122]. The obtaining of the AV-17(Bi, Al) sample was carried out at a temperature of 80^oC in the solution of $KAl(SO_4)_2 * 12H_2O$, but the morphology of the metallic compounds on the polymer granule surface differs from that observed in the Ref.[123]. Therefore we can conclude that the existence of the Al(III) hydroxocomplexes in the polymer solution system influenced the morphology of metallic compounds on the AV-17(Bi, Al) granule surface.

Table 6-1. Elemental composition (atoms, %) of metal containing structural units on the surface of polymer granule

AV-17(Bi, Al)			AV-17 (Bi, Fe)	AV-17 (Bi, FeOOH)	AV-17 (Bi, Cr)	Av-17 (Bi, Fe, Cr)	AV-17 (Bi, FeOOH, Cr)
Element	Small particles	Large particles					
Bi	-	13.51	20.52	6.36	0.44	14.73	19.19
Al	0.28	0.30	-	-	-	-	-
Fe	-	-	1.07	19.83	-	-	-
Cr	-	-	-	-	4.37	1.94	1.88
Cl	-	11.41	19.06	6.24	-	15.54	19.8
S	2.52	-	-	4.89	6.30	-	-
O	16.48	24.66	30.21	36.59	15.44	23.52	28.90
C	80.73	50.13	29.13	26.09	73.44	44.28	30.32

The elemental composition of metal-containing structural units is listed in Table 6-2. The metal content in the investigated samples is shown in Table 6-1. Following from the data of Tables 6-2 and 6-3, the Bi(III)-containing compounds are concentrated in the large particles on the surface and in the volume of the polymer granule.

Table 6-2. The metal content in the polymer samples

Samples	Metal content, mg/g		
	Bi	Fe	Cr (Al)
AV-17 (Bi, Al)	52.4	-	(53.0)
AV-17 (Bi, Fe)	60.5	51.0	-
AV-17 (Bi, FeOOH)	59.7	52.0	-
Av-17 (Bi, Cr)	50.0	-	97.0
AV-17 (Bi, Fe, Cr)	40.2	10.0	60.0
AV-17 [(Bi, FeOOH), Cr]	42.2	12.0	30.0

Using the data from Tables 6-2 and 6-3, the brut formula of the metal-containing structural units was computed. The brut formula of the structural units on the surface of the polymer granule is $Al_1O_{58.8}S_9C_{288}$ for small particles and $Bi_1Al_{0.02}O_{1.8}C_{l0.8}C_{3.7}$ for large particles. In the volume of the polymer granule, the brut formula of the structural units is $Al_1O_{78.8}S_{10.8}C_{409}$ for small particles and $Bi_1Al_{0.07}O_{7.9}C_{25.9}$ for large particles. The small particles on the surface and in the volume of the polymer granule do not contain Bi(III) and Cl^- ions. The large particles on the polymer granule surface do not contain sulfur atoms and those in the granule volume do not contain sulfur and chlorine atoms. Therefore, the composition of the small and large metal-containing particles, on the surface and in the volume of the polymer granule is different.

Table 6-3. Elemental composition (atoms, %) of metal-containing structural units in the volume of a polymer granule

AV-17(Bi, Al)			AV-17 (Bi, Fe)		AV-17 (Bi, FeOOH)	Av-17 (Bi, Fe, Cr)	AV-17 (Bi, FeOOH, Cr)
Element	Small particles	Large particles	Small particles	Large particles			
Bi	-	2.73	-	8.69	3.06	1.54	0.16
Al	0.20	0.20	-	-	-	-	-
Fe	-	-	0.96	1.85	0.83	0.12	0.19
Cr	-	-	-	-	-	0.81	0.93
Cl	-	-	0.45	-	3.07	1.48	0.41
S	2.15	-	2.74	-	2.83	2.39	4.03
O	15.74	21.74	9.09	17.80	8.34	11.59	7.00
C	81.91	71.31	86.72	71.66	81.86	82.06	82.26

As seen in the the data of Tables 6-2 and 6-3 and in the brut formula, the metal-containing structural units have many carbon atoms. The metal-containing compounds cannot have atoms of carbon; therefore, they belong to the AV-17 polymer chain and its functional groups.

The X-ray diffractogram [Fig. 6-2 (a)] of the AV-17(Bi, Al) sample is a typical spectrum of an amorphous polymer with the large broadening diffraction peaks corresponding to interplanar distances with d = 4.7 and 2.5 Å. Sharp diffraction peaks found on the polymer matrix curve correspond to the crystalline phase of the BiOCl. Therefore, a part of Bi(III)-containing compounds represents a crystalline BiOCl which is only in the large particles on the polymer granule surface. According to the brut formula of the large particles situated on the surface of the polymer granule,

there are more Bi atoms than Cl^- ions. Therefore, we conclude that in the polymer phase there are and other compounds of Bi(III) then BiOCl. It is likely that these compounds are BiOOH because the colour of the sample is the same (yellow) as BiOOH. The Al(III) compounds are probably of an alunite-jarosite type. The content of the oxygen atoms in the composition of the metal-containing structural units is much more than is necessary to form BiOCl, BiOOH, $Al(OH)_3$, and jarosite type compounds, especially in the smaller particles. The AV-17 polymer matrix does not have oxygen atoms. We propose that metal-containing particles are situated on functional groups and chains of AV-17 polymer, the oxygen and carbon atoms of the $[-N(CH_3)_3]_2SO_4$ groups being included in the structural units.

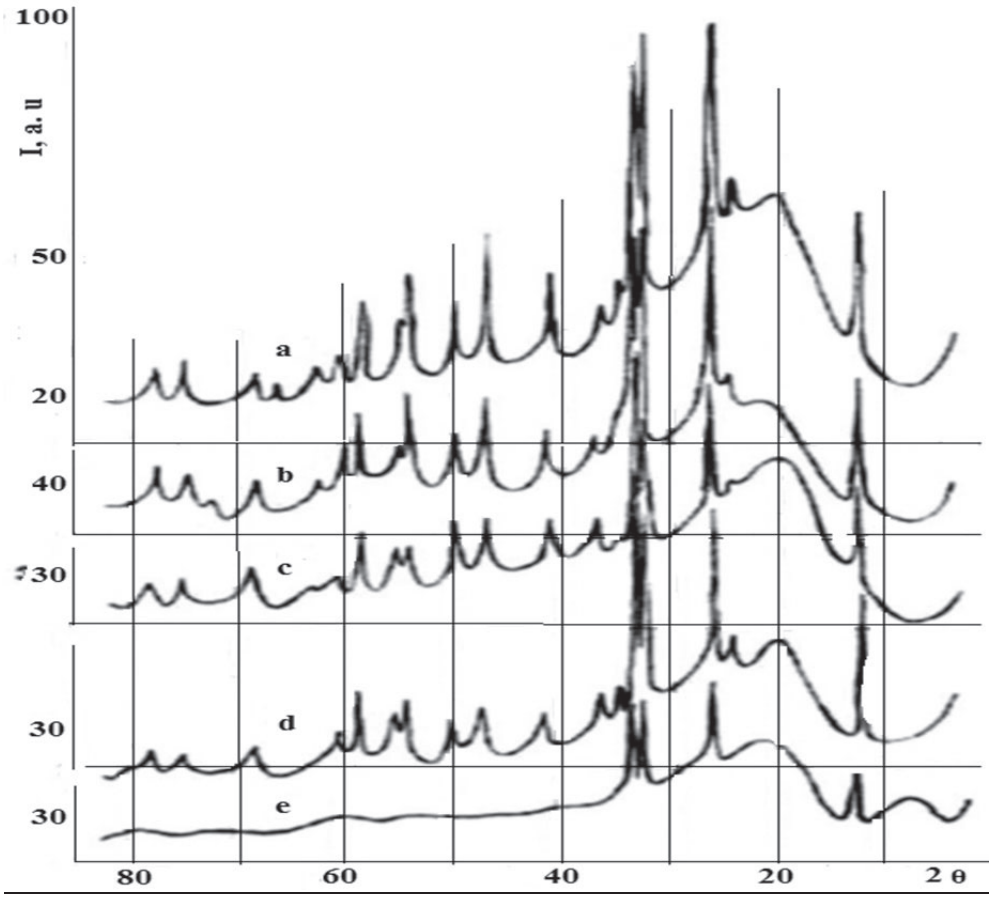

Figure 6-2. X-ray diffraction spectra of AV-17(Bi, Al) (a), AV-17(Bi, Fe) (b), AV-17(Bi, FeOOH) (c), AV-17(Bi, Cr) (d) and AV-17(Bi, Fe, Cr) (e) samples.

Under the preparation of metal-containing polymer samples, the AV-17(Cl) was in contact with $Bi(NO_3)_3$ and then with Al(III), Fe(III), or Cr(III) sulfate solutions. Therefore, besides the formation of metallic compounds, in the polymer phase processes (6-6) and (6-7) took place:

$$R_4NCl + NO_3^- \leftrightarrow R_4N\,NO_3 + Cl^- \quad (6\text{-}6)$$

$$2R_4N\,NO_3 + SO_4^{2-} \leftrightarrow (R_4N)_2SO_4 + 2NO_3^- \quad (6\text{-}7)$$

The FT-IR spectra of all metal-containing polymer samples investigated in this article, contain intensive peaks at 1110 and 616 cm^{-1} which belong to SO_4^{2-} ions and at 1384 and 1352 cm^{-1} – they are attributed to NO_3^- ions [36] (Fig.6-3).

As seen in Tables 6-2 and 6-3, the composition of the metal-containing structural units in the AV-17(Bi, Al) sample does not have N atoms. The sulfur atoms have only small particles. The data confirm that metal-containing particles are situated on the $[-N(CH_3)_3]_2SO_4$ and $-N(CH_3)_3NO_3$ polymer groups and oxygen and carbon atoms of these groups are included in the composition of the structural units. As seen in Tables 6-2 and 6-3, the large particles have more oxygen and fever carbon atoms than the small particles.

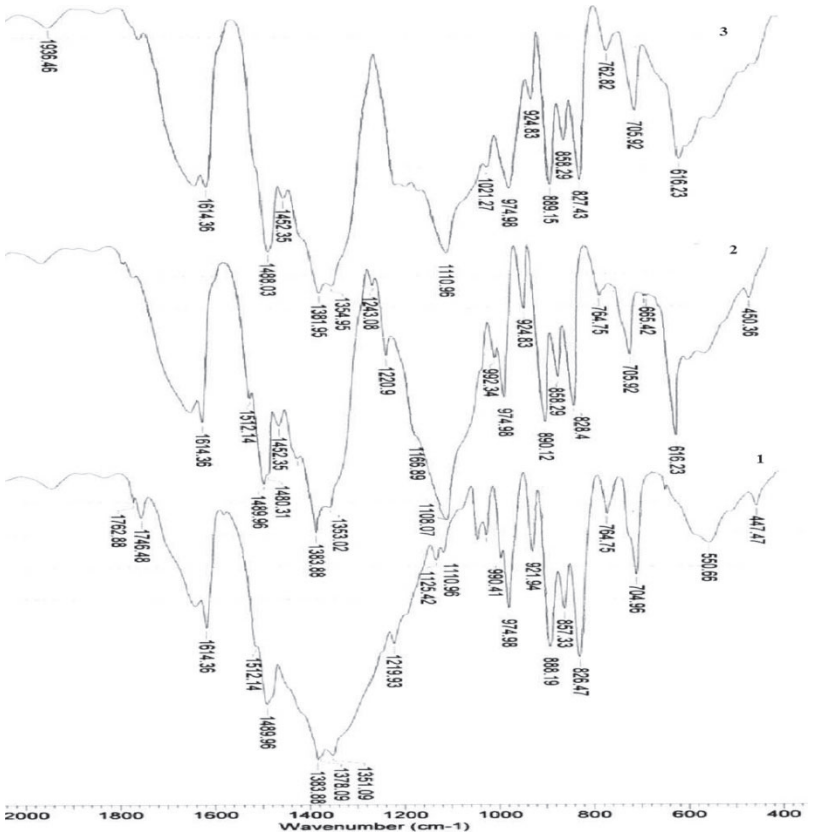

Figure 6-3. FT-IR spectra of the AV(Bi) (1), AV (Bi, Al) (2) and AV (Bi, Fe) (3).

The AV-17(Bi, Fe) sample. The SEM images of the AV-17(Bi, Fe) polymer granule are presented in Figure 6-4. As seen in Figure 6-4(a, b), the polymer granule surface is covered with amorphous metallic compounds. In the volume of the polymer granule, there are two kinds of particles [Fig. 6-4 (c)]. The biggest particles have a pseudo spherical form with a 4–5 μm diameter. Table 6-2 data show that Bi(III) containing compounds are concentrated on the surface of the polymer granule. In the volume of the polymer granule, the small particles do not hold Bi and the large particles do not contain chlorine and sulfur atoms.

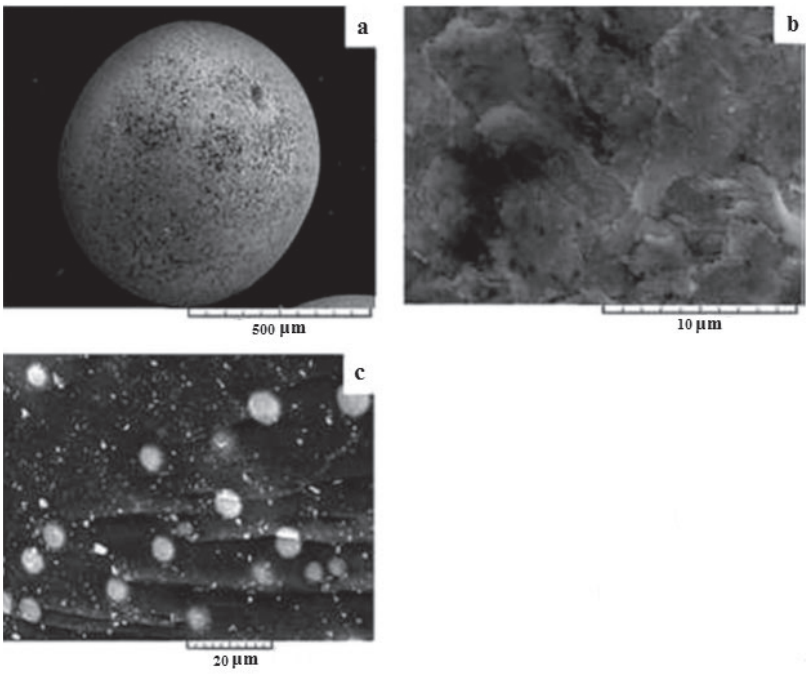

Figure 6-4. SEM images of the metal-containing compounds on the surface (a, b) and in the volume (c) of the AV-17(Bi, Fe) polymer granule.

The brut formula of the metal-containing structural unit on the polymer granule surface is $Bi_1Fe_{0.05}O_{1.47}Cl_{0.93}C_{1.42}$. The brut formula of the structural unit of the small particles in the volume of the polymer granule is $Fe_1O_{9.47}Cl_{0.47}C_{90.3}$ and of the large particles is $Bi_1Fe_{2.1}O_{2.05}C_{8.25}$. According to Figure 6-2 (b), the content of the crystalline phase of BiOCl in the AV-17(Bi, Fe) is less than in the AV-17(Bi, Al) sample. Because the AV-17(Bi, Fe) sample was prepared at lower temperature than AV-17(Bi, Al), in the first sample a large part of the BiOCl remained in an amorphous state. Only small particles in the volume of the polymer granule have jarosite type compounds. The Fe-containing compounds on the polymer granule surface and in the large particles in the polymer granule volume are, probably, FeOOH. The metal-containing particles are situated on functional groups of the polymer, and a part of the C and O atoms are involved in the composition of the structural units.

The AV-17(Bi, FeOOH) sample. The AV-17(Bi, FeOOH) was obtained from the AV-17(Bi,Fe) sample by heating in water medium in a boiling water bath. The morphology of the metal-containing particles in the AV-17(Bi, Fe) and AV-17(Bi, FeOOH) samples differs very much. As seen in Figure 6-5, (a,b), the surface of the polymer granule is covered with metal-containing particles, most of which are in an amorphous state. The pseudo spherical particles in the volume of the polymer granule represent clews of nanometre fibres [Fig.6-5, (c,d)].

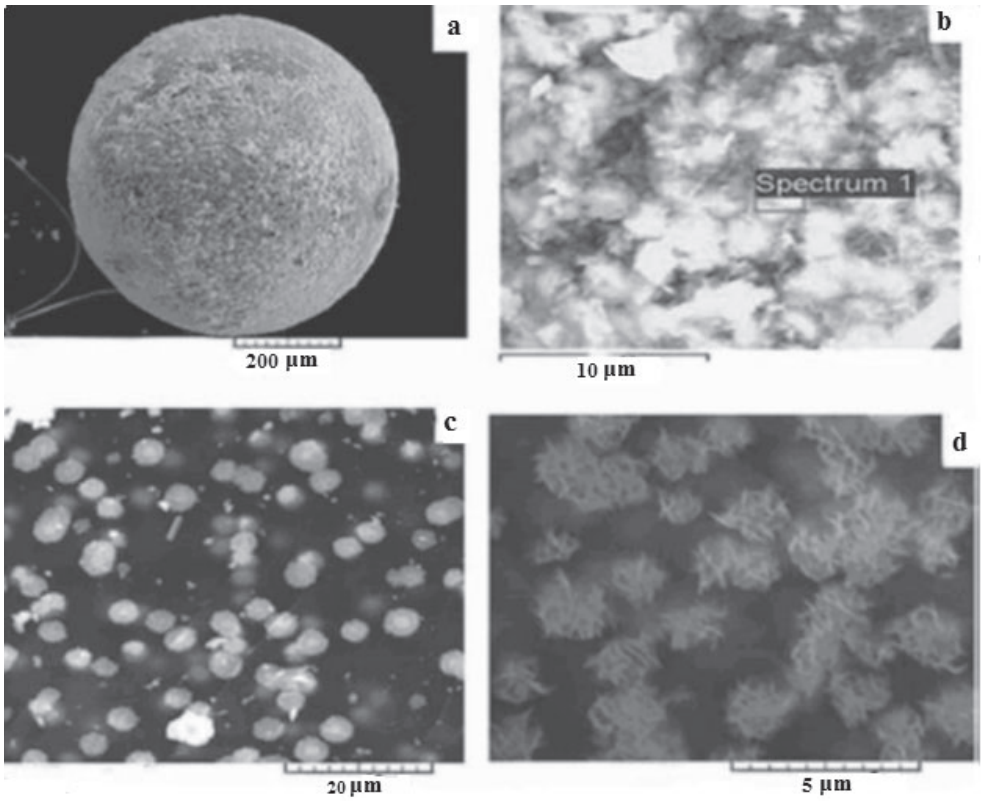

Figure 6-5. SEM images of the metal-containing compounds on the surface (a, b) and in the volume (c, d) of the AV-17(Bi, FeOOH) polymer granule.

The elemental composition of the metal-containing structural units on the surface and in the volume of the AV-17(Bi, FeOOH) granule is shown in Tables 6-2 and 6-3. The data in the table permitted us to calculate the brut formula of the structural units which is $Bi_1Fe_{0.27}O_{2.72}Cl_{1.0}\ S_{0.92}C_{26.71}$ in the volume and $Bi_1Fe_{3.12}O_{5.75}Cl_{1.0}\ S_{0.98}C_{4.1}$ on the surface of the polymer granule. The data provided in Tables 6-2 and 6-3 show that on heating AV-17(Bi, Fe) in water medium in a boiling water bath, besides the transformation of compounds, the migration of the Fe(III)-containing compounds to the polymer granule surface takes place. On the polymer granule surface, there is some crystalline BiOCl [Fig, 6-2, (c)] and much FeOOH. In the polymer granule volume, there is a compound containing both Bi(III) and Fe(III) ions. The compounds in the form of clew may be BixFe(1–x)OOH which contains some Cl^- ions. It is known [46,48] that the ß-FeOOH forming process takes place in the presence of Cl^- (or F^-) ions which entered the β-FeOOH structure [50, 51]. If taking into consideration a large content of carbon, oxygen, and sulfur atoms in the composition of metal-containing structural units, we can suggest that metallic compounds particles are situated on the polymer functional groups, especially on the $[-N(CH_3)_3]_2SO_4$ groups.

The AV-17(Bi, Cr) sample. The SEM images of the AV-17(Bi, Cr) polymer granule are shown in Figure 6-6. As seen in Figure 6-6, practically all metal-containing compounds are on the surface of the polymer granule. The polymer granule surface is covered with a dense layer of amorphous and crystalline compounds (Fig. 6-6).

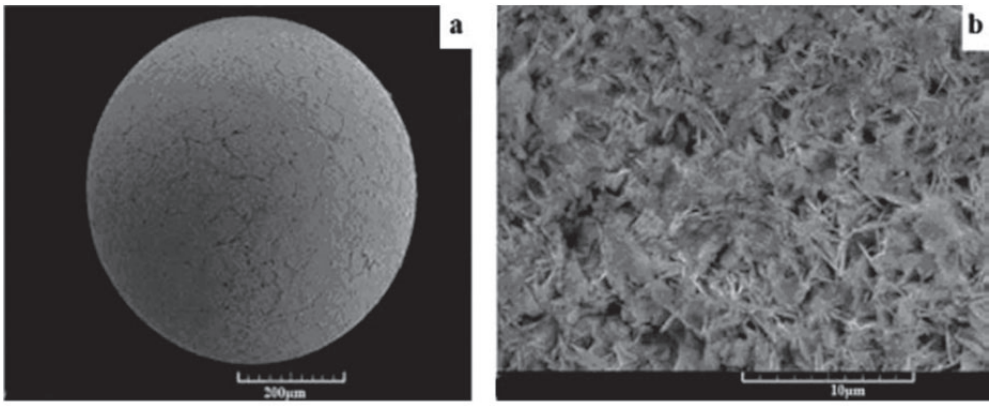

Figure 6-6. SEM images of the metal-containing compounds on the surface (a, b) of the AV-17(Bi, Cr) polymer granule.

This layer of compounds on the polymer surface may influence considerably the sorption and catalytic kinetics on AV-17(Bi, Cr). The elemental composition of the metal-containing structural unit on the polymer granule surface is shown in Table 6-2. The brut formula of the structural unit is $Bi_1Cr_{9.93}O_{35.09}S_{14.32}C_{166.9}$. As seen in the brut formula of the structural unit, there are no chlorine atoms, in its composition, although some crystalline BiOCl in the AV-17(Bi, Cr) phase was detected [Fig. 6-2, (d)]. Perhaps BiOCl crystals are in the volume of the polymer granule. The Cr(III) compounds in the polymer granule volume are likely of jarosite type. The metallic compounds particles are situated on the $[-N(CH_3)_3]_2SO_4$ polymer functional groups.

The AV-17(Bi, Fe, Cr) sample. The SEM images of the AV-17(Bi, Fe, Cr) polymer granule are shown in Figure 6-7. In Figure 6-7 (a, b), it is seen that the polymer granule surface is covered with amorphous and crystalline metallic compounds. These compounds contain only Bi(III) and Cr(III) metallic cations. They do not contain Fe(III) cations and SO_4^{2-} ions (Tab. 6-2). It means that upon the AV-17(Bi, Fe, Cr) sample preparing from AV-17(Bi, Fe), the Fe^{3+} cations are replaced Cr^{3+} cations and passed in the liquid phase (in $KCr(SO_4)_2 * 12H_2O$ solution).

The elemental composition of the metal-containing structural unit on the surface of the polymer granule is $Bi_1Cr_{0.13}O_{1.6}Cl_{1.05}C_3$ and in the volume $Bi_1Fe_{0.08}Cr_{0.53}O_{7.53}Cl_{0.96}S_{1.6}C_{53.3}$.

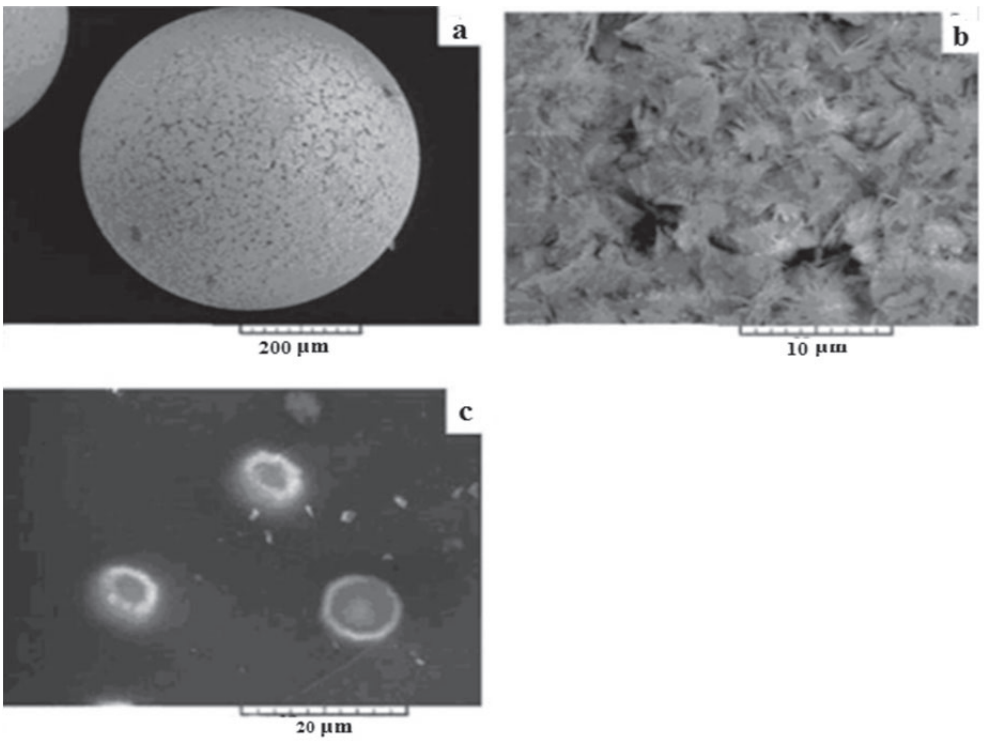

Figure 6-7. SEM images of the metal-containing compounds on the surface (a, b) and in the volume (c) of the AV-17(Bi, Fe, Cr) polymer granule.

The Fe(III) containing compounds are only in the volume of the polymer granule. The passing of Fe(III) ions from the polymer granule to $KCr(SO_4)_2 * 12H_2O$ solution, on AV-17(Bi,Fe,Cr) preparation using AV-17(Bi, Fe), is confirmed by the small content of Fe (III) in the polymer phase (Tab. 6-1). Taking into consideration the content of sulfur and oxygen atoms in the structural units in the volume of the polymer granule, it may be suggested that there are

compounds of jarosite type. In the AV-17(Bi,Fe,Cr) sample, there is some crystalline BiOCl, but less than in the precedent examined samples of the metal-containing polymer [Fig. 6-2 (e)]. A new interesting fact was seen on investigation of the AV-17(Bi, Fe, Cr) sample. In a diffractogram of this sample [Fig. 6-2 (e)], in the spectrum of the amorphous phase of the AV-17 polymer, in a low range of 2θ angles, a new maximum appeared. After desorption of metals, this maximum despaired. It means that a part of the AV-17 polymer chains, including functional groups, is involved in metal-containing structural units.

The AV-17(Bi, FeOOH, Cr) sample. The surface of the polymer granule of this sample is covered with metal-containing compounds in a crystalline and amorphous state [Fig. 6-8(a, b)]. The morphology of the metal-containing compounds particles on the polymer granule surface looks like the case of the AV-17(Bi, Fe, Cr) sample [Fig. 6-7, (a, b)].

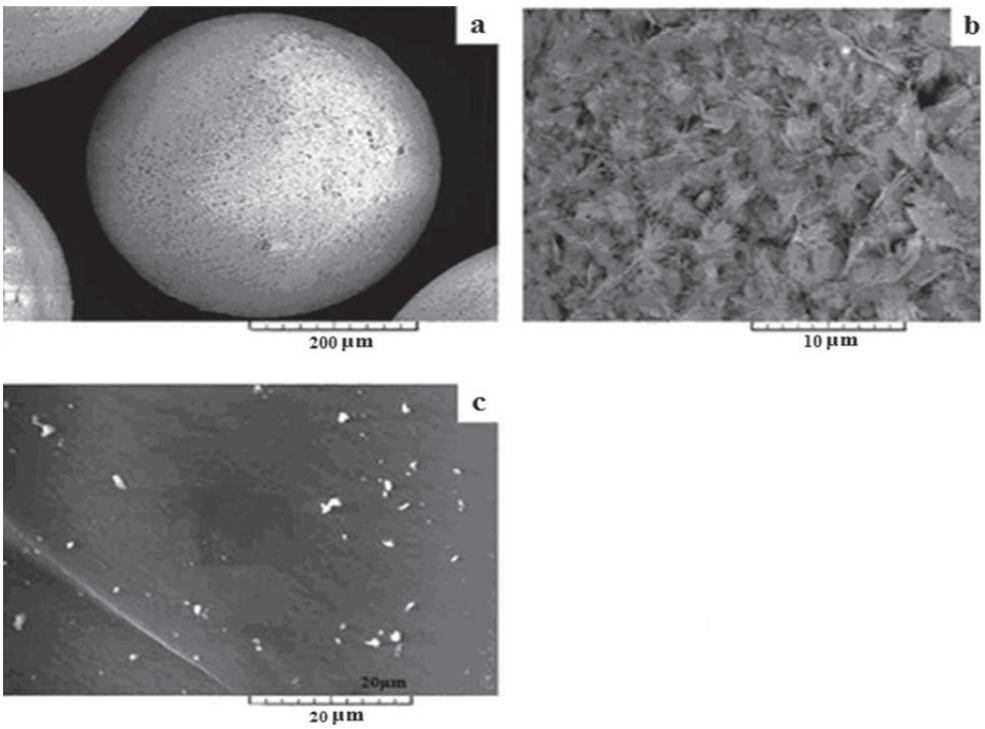

Figure 6-8. SEM images of the metal-containing compounds on the surface (a, b) and in the volume (c) of the AV-17(Bi, FeOOH, Cr) polymer granule.

The morphology of the particles in the volume of the polymer granule of AV-17(Bi, FeOOH, Cr) [Fig. 6-8 (c)] and AV-17(Bi, Fe, Cr) [Fig. 6-7, (c)] is quite different. From Tables 6-2 and 6-3 data, it is seen that metal-containing compounds are accumulated on the polymer granule surface of AV-17(Bi, FeOOH, Cr). The brut formula of the metal-containing structural unite on the polymer granule surface is $Bi_1Cr_{0.1}O_{1.5}Cl_{0.99}C_{1.57}$ and in the granule volume it is $Bi_1Fe_{1.19}Cr_{5.81}O_{36.8}Cl_{2.16}S_{25.2}C_{459}$. In the composition of the metal-containing compounds on the polymer granule surface, there are no Fe^{3+} and SO_4^{2-} ions (Tables 6-2 and 6-3), and therefore, jarosite type compounds are absent. There is some BiOCl in the crystalline state and that could be BixCr(1–x)OOH. In the volume of the polymer granule, there are Cr(III)-jarosite type compounds and β-FeOOH.

The thermal behaviour of the metal-containing polymer samples was evaluated by dynamic thermogravimetry in nitrogen gas, at a heating rate of 20°C/min. The TG, derivative TG (DTG) and differential thermal analyses (DTA) curves, recorded under the same experimental conditions, are presented in Figure 6-9.

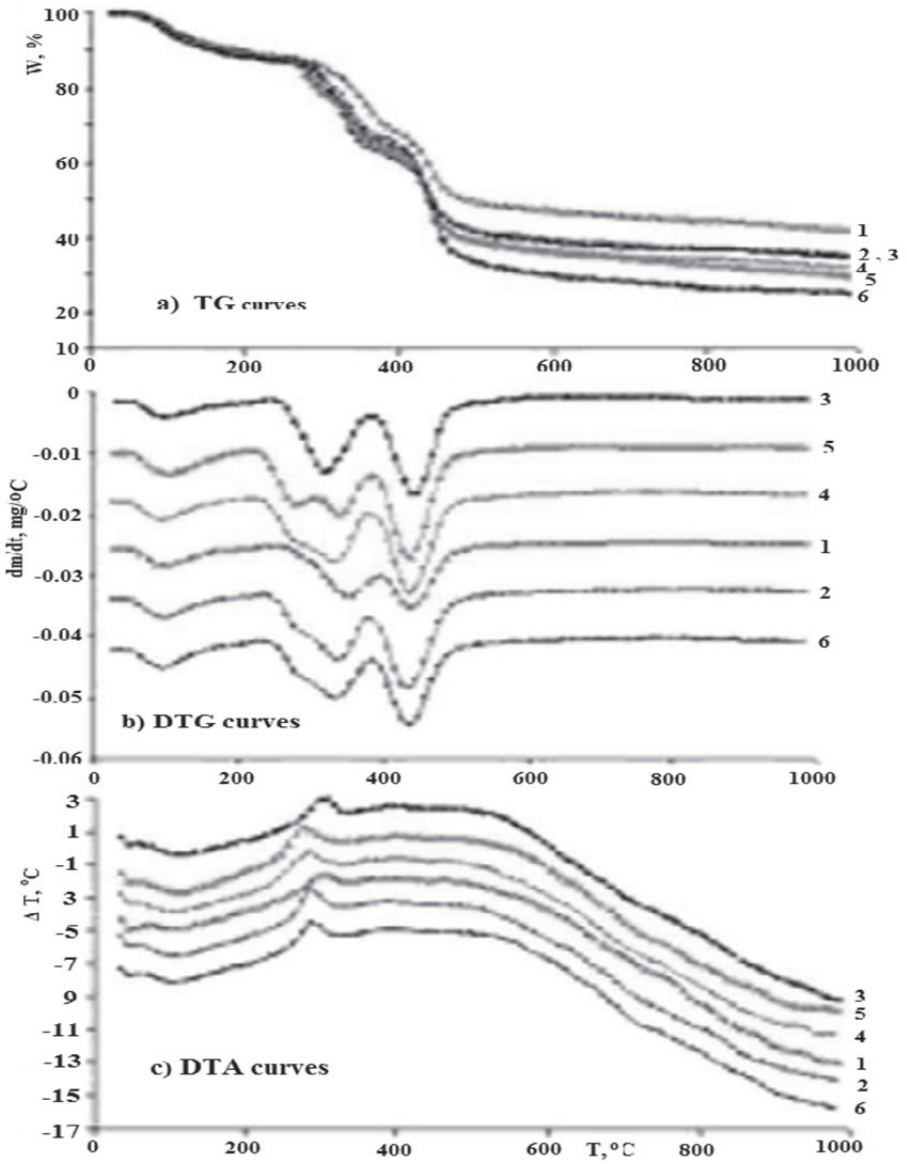

Figure 6-9. TG, DTG and DTA curves of AV-17(Bi, Al) (3), AV-17(Bi, Fe) (5), AV-17(Bi, FeOOH) (4), AV-17(Bi, Cr) (1), AV-17(Bi, Fe, Cr) (2), and AV-17(Bi, FeOOH, Cr) (6), samples.

The summary of the important TG characteristics of the sample obtained from the thermograms is listed in Table 6-4. For every sample, the degradation processes are not complete, for each case a residue is left. Table 6-4 reveals TGA data such as T_i- the initial temperature thermal degradation, T_m- the temperature corresponding to the maximum degradation rate, T_f- the final temperature at which the degradation process for each step ends, and mass loss (W %), corresponding for each step.

Table 6-4. Thermogravimetrical and kinetic data obtained, for the sorbents samples

Samle	Step	T_i, °C	T_m, °C	T_f, °C	W, %	Resi-due, %	E, kJ/mol	n	Ln A
AV-17	I	66	95	175	13.44	-	18.11±0.29	1.7±0.07	1.7±0.04
(Bi,Al)	II	289	319	346	24.66	25.00	58.91±1.23	0.88±0.002	7.05±0.15
	III	418	442	464	36.90	-	447.98±5.74	2.95±0.004	72.20±1.00
AV-17	I	67	97	150	11.43	-	35,06±0.27	2.20±0.003	6.42±0.27
(Bi,Fe)	II	263	272	291	11.41	28.81	281.48±2.98	2.31±0.002	58.16±0.67
	III	310	344	365	14.88	-	299.84±4.34	2.84±0.004	56.03±0.89
	IV	407	436	467	33.47	-	374.67±2.79	2.55±0.002	60.17±0.49
AV-17 (Bi,	I	65	88	156	10.95		40.96±1.33	2.72±0.006	8.74±0.46
FeOOH)	II	259	277	295	11.59	31.28	205.90±2.32	1.16±0.002	40.67±0.52
	III	320	342	354	14.75	-	469.22±2.21	2.61±0.001	90.43±0.45
	IV	416	438	465	31.43	-	391.37±1.99	2.33±0.001	62.81±0.35
AV-17	I	68	85	215	12.40	-	31.78±0.93	2.50±0.010	27.01±0.17
(Bi,Cr)	II	291	349	380	21.43	41.01	161.80±2.54	1.63±0.003	27.01±0.17
	III	405	440	477	25.16	-	424.39±6.12	3.17±0.004	68.37±1.06
AV-17 (Bi,	I	71	91	170	11.95	-	41.36±0.96	2.81±0.001	8.82±0.91
Fe,Cr)	II	272	287	305	8.78	-	352.6±1.74	1.62±0.008	72.35±0.38
	III	323	345	351	13.18	34.10	437.99±2.40	2.27±0.001	85.13±0.48
	IV	409	435	470	31.99	-	364.26±1.59	2.73±0.005	58.34±1.32
AV-17 (Bi,	I	66	89	141	12.98	-	53.88±0.81	2.22±0.002	13.30±0.28
FeOOH,Cr)	II	276	295	310	9.41	33.70	289.90±0.93	1.17±0.006	58.55±0.20
	III	321	342	350	13.36	-	338.31±1.70	1.76±0.008	63.35±0.34
	IV	418	437	466	30.55	-	373.10±1.20	2.55±0.006	59.93±2.10

Table 6-4 data indicate that the thermal degradation mechanism of investigated samples is complex and occurs in several steps. The samples AV-17(Bi, Al) and AV-17(Bi, Cr) exhibited three steps of degradation having the maximum decomposition temperature in the range 85–95 °C, 319–349°C, and 440–442°C, respectively. The further samples exhibited four steps of degradation having the maximum decomposition temperature in the range 88–97°C, 272–295°C, 342–345°C, and 434–438°C, respectively. The char yields of 1000°C were in the range 25–41%.

The first step (65–175°C) for all samples is assignable to the loss of water from their structures.

The thermal degradation in the nitrogen atmosphere of the samples AV-17(Bi, Al) and AV-7(Bi, Cr) shows one exothermic peak at 307°C and, for the further metal-containing polymer samples, at 287°C. The most important mass loss for all samples has been recorded in the last stage of the thermal degradation, at temperatures onset over about 410°C. Comparing the DTG curve in Figure 6-9, it can be found that the degradation curves of the six samples are close to each other in shape in the last stage, the temperature corresponding to the maximum degradation rate is about 438°C.

The surveys were extended with the kinetic processing of the TG data. The Freemann–Caroll [71] method is based on the calculation of the kinetic parameters (Eqs. (1-16) to (1-18)).The reaction order (n) and activation energy (E) values (Table 6-4), indicate that the thermal decomposition of the metal-containing polymer samples is a complicated process.

The small difference in the Tm values (436, 438, 435, and 437°C) and that in the values of the activation energies (375, 391, 363, and 373 kJ/mol), suggest the same degradation mechanism in the last stage of thermal degradation for the samples AV-17(Bi, Fe), AV-17(Bi, FeOOH), AV-17(Bi, Fe, Cr), and AV-17(Bi, FeOOH, Cr).

PART II.

APPLIED RESEARCH

VII.

THE USE OF COMPOSITES IN THE APPLIED RESEARCH

7.1. Some perspectives

As is known in nature there are minerals jarosite and alunite: **(Na,K)[$Fe_3(OH)_6${SO_4]** and **(Na,K)[$Al_3(OH)_6${SO_4]**. According to Ref. [58], jarosite materials are formed as layers of three or six octahedral cycles. The SO_4^{2-} groups are in the axial position, each of the coordinating three metal ions belonging to three octahedral and OH–groups is positioned in the equatorial plane, forming a bridge between two metal cations. Between the jarosite polymer layers, there are mobile cations kept by Coulomb's electrostatic interactions.

The generalized formula of compounds of the jarosite mineral type is **$A[M_3(OH)_6(XO_4)_2]$,** where **A** is a cation, **M**- a three charged cation, and **XO_4** - a two charged tetrahedral anion. In this formula **A** may be different cations such as H_3O^+, Na^+, K^+, Pb^{2+} and others [26, 126].

Cations **"A"** in the jarosite type compounds are retained by Coulomb's electrostatic interactions. Thus, the compounds of the jarosite type possess cation exchange properties. However, in the polymer phase, the cationic exchange properties of $R_4N[M_3(OH)_6(XO_4)_2]$ compounds are less pronounced. This is explained by the fact that the R_4N^+ group is fixed to the polymer chain and cannot diffuse into the liquid phase. But in the case of $H_3O[M_3(OH)_6(XO_4)_2]$ which can form in an acidic medium, the exchange of cations is not restrained. The **M** in the generalized formula may be Fe^{3+}, Al^{3+}, Cr^{3+}, V^{3+} and other three charged cation.

Dutrizac and co-authors [127-130] synthesized many of the jarosite mineral type compounds in which Fe^{3+} is replaced by cations of other metals. The jarosite mineral type compounds of different metals were obtained and in the phase of cross-linked polymers having strongly basic groups. But the most interesting processes with an application character are those involving the XO_4 groups. The XO_4 groups may be substituted with different tetrahedral anions such as CrO^{2-}, PO_4^{3-}, AsO_4^{3-}, MoO_4^{2-}, VO_4^{2-} and others. Moreover, the XO_4 groups can be substituted with an ion or molecule having electron donor atoms. Thus, polymers containing compounds of the jarosite type become selective sorbents and catalysts with excellent hydro- and aerodynamic properties. And if the substituent of the XO_4 group is a polydentate ligand, then various ion-molecular compositions can be constructed in the polymer phase. So, polymers that contain such ion-molecular constructions become sorbents and catalysts with several active centres.

7.2. Cr(VI)-containing anion sorption on polymer modified with Cr(III) compounds

It is well known that cross-linked ionic polymers bearing R_4N^+ functional groups are widely used in industry and science. Their main applications in the field of water purification and wastewater treatment usually involve the strongly basic anion exchanger property:

$R_4NA+B^- \leftrightarrow R_4NB+A^-$. These polymers are nonselective toward sorption of inorganic anions and often it is considered that they are able to participate only in anion exchange processes. The controlled processes of metallic compounds formation within polymeric support change considerably the polymer properties and may expand the possible applications of ion-exchange materials by producing selective sorbents and catalysts.

It is known that chromium (III) compounds are chemically more stable than iron compounds. Using Cr(III) compounds to modify polymeric matrices may, therefore, offer the advantage of obtaining elective sorbents and catalysts. In order to apply Cr(III)-containing polymers in catalysis, liquids, or gases purification, it is necessary to evaluate their thermal behaviour in various media. In the paper [89] there has been investigation of the chemical and thermal stability of a strongly basic anion exchanger modified with compounds of Cr(III). It was shown that the nature of acid solution (HCl, HNO_3, and H_2SO_4) has influenced the chemical and thermal stability of the sorbent obtained by modification of the polymer with compounds of Cr(III).

Modifying commercial cross-linked ionic polymers bearing strongly basic functional (R_4N^+) groups with Cr(III) compounds and subsequently using them as adsorbents for CrO_4^{2-} and $Cr_2O_7^{2-}$ ions is an issue of particular practical interest due to the fact that Cr(VI) is highly toxic and often contaminates technological waters in galvanic sections. In order to apply Cr(III)-containing polymers in water purification, it is necessary to evaluate their sorption properties toward CrO_4^{2-} and $Cr_2O_7^{2-}$ ions and their thermal behaviour in various media [131]. This study aims to provide an answer to the above-mentioned problems.

The process of obtaining AV-17 modified with Cr(III)-containing compounds (AV-17(Cr)) has been conducted according to Ref. [87]. The Cr^{3+} content in the polymeric phase was 32.5 mg Cr/g). To obtain sorption isotherms of Cr(VI)-containing anions, AV-17(Cr) sorbent samples (0.2 g) were placed in contact with 100 mL aliquots of K_2CrO_4 solutions with pH 3.0 or, respectively, 8.0 at temperatures of 19 and, respectively, 60 ^oC for 8 hr. For comparison, the

Cr(VI)-containing anions sorption was also investigated in the same conditions and on the starting material AV-17(Cl). The concentration of chromium (VI) ions was determined by the photocolorimetry method.

The AV-17(Cl) polymer contains only one type of functional groups R_4N^+ that is energetically equivalent. It was therefore expected that the sorption isotherms of Cr(VI)-containing anions would fit the Langmuir model. This was not the case since the data regarding the sorption process of Cr(VI)-containing anions on the AV-17(Cl) exchanger from solutions with pH 3 do not fit the Langmuir model, as shown in Figure 7-1, (a). In aqueous solutions with pH 3 and a Cr(VI) concentration of 10^{-1} mol/L, chromium (VI) ions are known to exist both as $HCrO_4^{2-}$ and as $Cr_2O_7^{2-}$ species, with the latter being preponderant. When the ion concentration reaches 10^{-5} mol/L, at pH 3, all Cr(VI) ions are in the form of $HCrO_4^-$ anions [55].

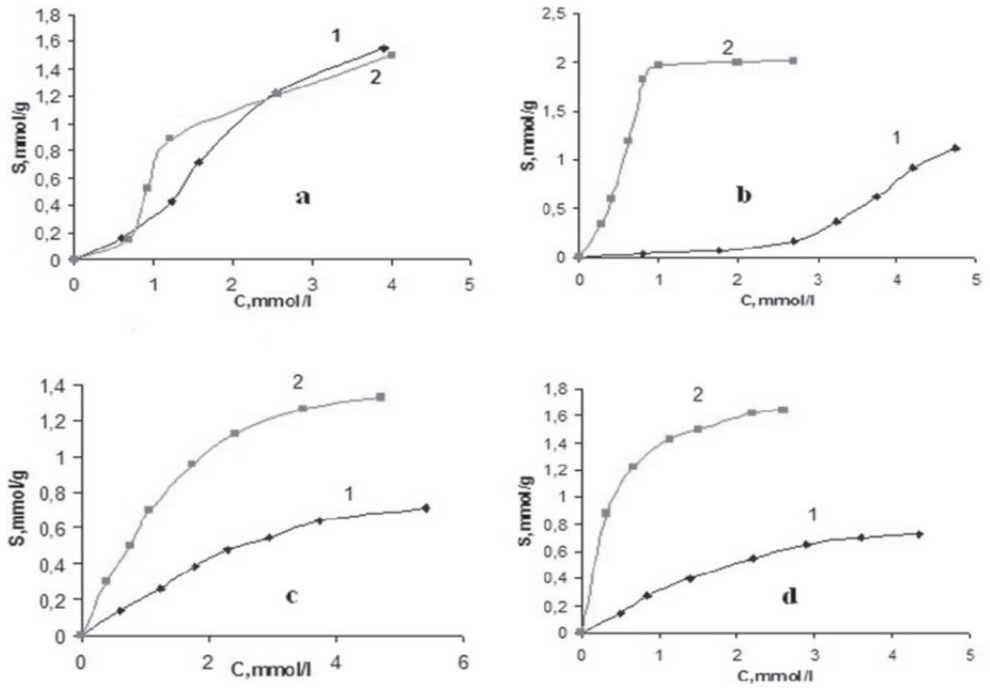

Figure 7-1. (a) Sorption isotherms of Cr(VI)-containing anions from K_2CrO_4 solutions with pH 3 and temperature of 19 (1) and 60°C (2) on the exchanger AV-17(Cl); (b) Sorption isotherms of Cr(VI)-containing anions from K_2CrO_4 solutions with pH 3 and temperature of 19 (1) and 60°C (2) on the sorbent AV-17(Cr); (c) Sorption isotherms of Cr(VI)-containing anions from K_2CrO_4 solutions with pH 8 and temperature of 19 (1) and 60°C (2) on the exchanger AV-17(Cl); and (d) Sorption isotherms of Cr(VI)-containing anions from K_2CrO_4 solutions with pH 8 and temperature of 19 (1) and 60°C (2) on the sorbent AV-17(Cr).

The shape of the isotherms presented in Figure 7-1, (a) indicates the presence of interactions between the two Cr(VI) anion species and may be explained by the fact that in the polymeric phase the $HCrO_4^- \leftrightarrow Cr_2O_7^{2-}$ equilibrium is shifted toward the formation of $Cr_2O_7^{2-}$ ions. The temperature increase also influences the equilibrium. It is well known that the sorption value of inorganic ions, conditioned by ion exchange processes, practically is not dependent on temperature. The temperature can influence only the sorption kinetics.

The sorption isotherms on the AV-17(Cr) support [Fig. 7-1(b)] are different from those previously discussed. First of all, it is noticeable that the sorption of Cr(VI)-containing anions at 19°C on AV-17(Cr) is much lower than on AV-17(Cl) and begins at Cr(VI) concentrations that are higher than 2 mol/L [Fig. 7-1(b), curve 1]. On the other hand, sorption from solutions with a temperature of 60°C is higher on the AV-17(Cr) sorbent than on the AV-17(Cl) exchanger [Fig. 7-1(b), curve 2]. The shape of the isotherms in Figure 7-1(a, b) and their dependence on temperature show that the sorption mechanism of ions containing Cr(VI), on sorbent AV-17(Cr) is different than on the AV-17(Cl) exchanger. On the AV-17(Cl) exchanger the sorption process may be expressed by Equations (7-1) and (7-2): modifying commercial cross-linked ionic polymers bearing strongly basic functional groups

$$2R_4NCl + Cr_2O_7^{2-} \leftrightarrow (R_4N)_2Cr_2O_7 + 2Cl^- \quad (7\text{-}1)$$

$$R_4NCl + HCrO_4^- \leftrightarrow R_4N\,HCrO_4 + Cl^- \quad (7\text{-}2)$$

The sorption on the AV-17(Cr) sorbent is a chemical process that may be expressed by Equations (7-3) and (7-4):

$$R_4N[Cr_3(OH)_6(SO_4)_2] + 2Cr_2O_7^{2-} \leftrightarrow R_4N[Cr_3(OH)_6Cr_2O_7)_2] + 2SO_4^{2-} \quad (7\text{-}3)$$

$$R_4N[Cr_3(OH)_6(SO_4)_2] + 2HCrO_4^- \leftrightarrow R_4N[Cr_3(OH)_6(HCrO_4^-)_2]^{2+} + 2SO_4^{2-} \quad (7\text{-}4)$$

It is known that ligands in Cr(III) complexes are no labile. That is why the sorption of Cr(VI) from diluted solutions with the temperature of 19°C is low [Fig. 7-1(b), curve 1]. Moreover, in the outcome of process (7-4), the SO_4^{2-} anions partially remain in the external sphere of the $R_4N[Cr_3(OH)_6(HCrO_4)_2]SO_4$ complex, thus contributing to the equilibrium (7-4) shift to the right. In the sorption from solution with a temperature of 60°C, process (7-3) prevails. That is why the sorption from these solutions is higher and takes place in diluted solutions [Fig.7-1(b), curve 2]. In the solution of K_2CrO_4 with pH 8, Cr(VI) ions exist only as CrO_4^{2-} species [55]. The sorption of CrO_4^{2-} anions on the AV-17(Cl) exchanger takes places because of the anion exchange process described by Equation (7-5):

$$2R_4NCl + CrO_4^{2-} \leftrightarrow (R_4N)_2CrO_4 + 2Cl^- \quad (7\text{-}5)$$

It is surprising that sorption of the CrO_4^{2-} ions on the AV-17(Cl) exchanger is strongly influenced by temperature [Fig. 83(c)], although it is known that the ion exchange process is almost independent of temperature. Obviously, at 19°C process (7-5) takes place. Although at 60°C, the Cr(VI) ions present in solution exist only in CrO_4^{2-} species, within the polymeric phase they partially reside as $HCrO_4^-$ ions and the sorption process takes place according to Equation (7-2).

In solutions with pH 8, the sorption isotherms of CrO_4^{2-} ions on the AV-17(Cr) sorbent [Fig.7-1(d)] are similar to those obtained on the AV-17(Cl) support [Fig. 83(c)]. The sorption isotherm obtained at 19°C [Fig. 83 (d), curve 1] proceeds according to process (7-6), while that obtained at 60°C [Fig. 7-1(d), curve 2] is characterized by processes (7-6) and (7-7):

$$R_4N[Cr_3(OH)_6(SO_4)_2]+2CrO_4^{2-}+2HOH \leftrightarrow R_4N[Cr_3(OH)_6(HCrO_4^-)_2]SO_4 + SO_4^{2-}+2OH^- \quad (7\text{-}6)$$

$$R_4N[Cr_3(OH)_6(HCrO_4^-)_2]SO_4 +2HCrO_4^{2-} \leftrightarrow R_4N[Cr_3(OH)_6Cr_2O_7)_2] + SO_4^{2-} + 2HOH \quad (7\text{-}7)$$

In solutions with pH 8 and temperature of 60°C sorption of Cr(VI)-containing anions on the AV-17(Cr) material is slightly higher than on the AV-17(Cl). However, this is not an essential difference. The important feature is that sorption on AV-17(Cr) is a chemical process, and therefore, the sorption is selective. The sorbent AV-17(Cr) is able to retain selectively only the anions with a tetrahedral configuration from solution.

The isotherms in Figure 7-1 (c, d) may be described by the Langmuir adsorption model: $S = S_L K_L C/1+K_L C$, where S is sorption (mmol Cr(VI)/ g), C is the equilibrium concentration of Cr(VI) (mmol/L), and S_L and K are isotherm constants. The isotherm constants values are presented in Table 7-1. The data in Table 7-1 show that the value of the constant S_L of Cr(VI) sorption isotherms on the AV-17(Cl) exchanger is the same at 19 and at 60°C. This means that at the limit each active centre (R_4N^+) retains a single particle of Cr(VI) (see Eqs. (7-1), (7-2) and (7-5)). The constant S_L of Cr(VI) sorption isotherms on the AV-17(Cr) sorbent is higher, especially at 60°C. The chemical affinity (K_L) of Cr(VI)-containing anions for the AV-17(Cr) sorbent, especially at 60°C, is much higher than the one for the AV-17(Cl) exchanger (Tab. 7-1).

Table 7-1. The values of isotherm constants and thermodynamic functions

Sorbent	T, °C	S_L, mmg/g	K_L, L/mol	ΔG, kJ/mol	ΔH, kJ/mol	ΔS, J/mol
AV-17(Cl)	19	1.39	21.6	-13.05	25.4	131.65
AV-17(Cl)	60	1.40	78.3	-18.45		131.66
Av-17(Cr)	19	1.44	26.9	-13.52	52.5	226.05
Av-17(Cr)	60	1.83	37.68	-22.80		226.07

For the sorption of the Cr(VI)-containing anions in solutions of K_2CrO_4 with pH 8, the thermodynamic functions, namely the variation of Gibbs energy (ΔG), enthalpy (ΔH), and entropy (ΔS) were calculated using the formulas (4-9) to (4-11). The values of these functions are shown in Table 7-1. As shown in this table, ΔG depends on temperature, having a higher value at 60°C. Moreover, ΔS does not depend on temperature but depends on the sorbent nature, showing a much higher value for the sorption on the AV-17(Cr) sorbent than on the AV-17(Cl) exchanger. The sorption processes are usually exothermic. The calculated values of ΔH indicate that the sorption process is endoterm and in the sorbent phase the Cr(VI)-containing anions undergo significant changes.

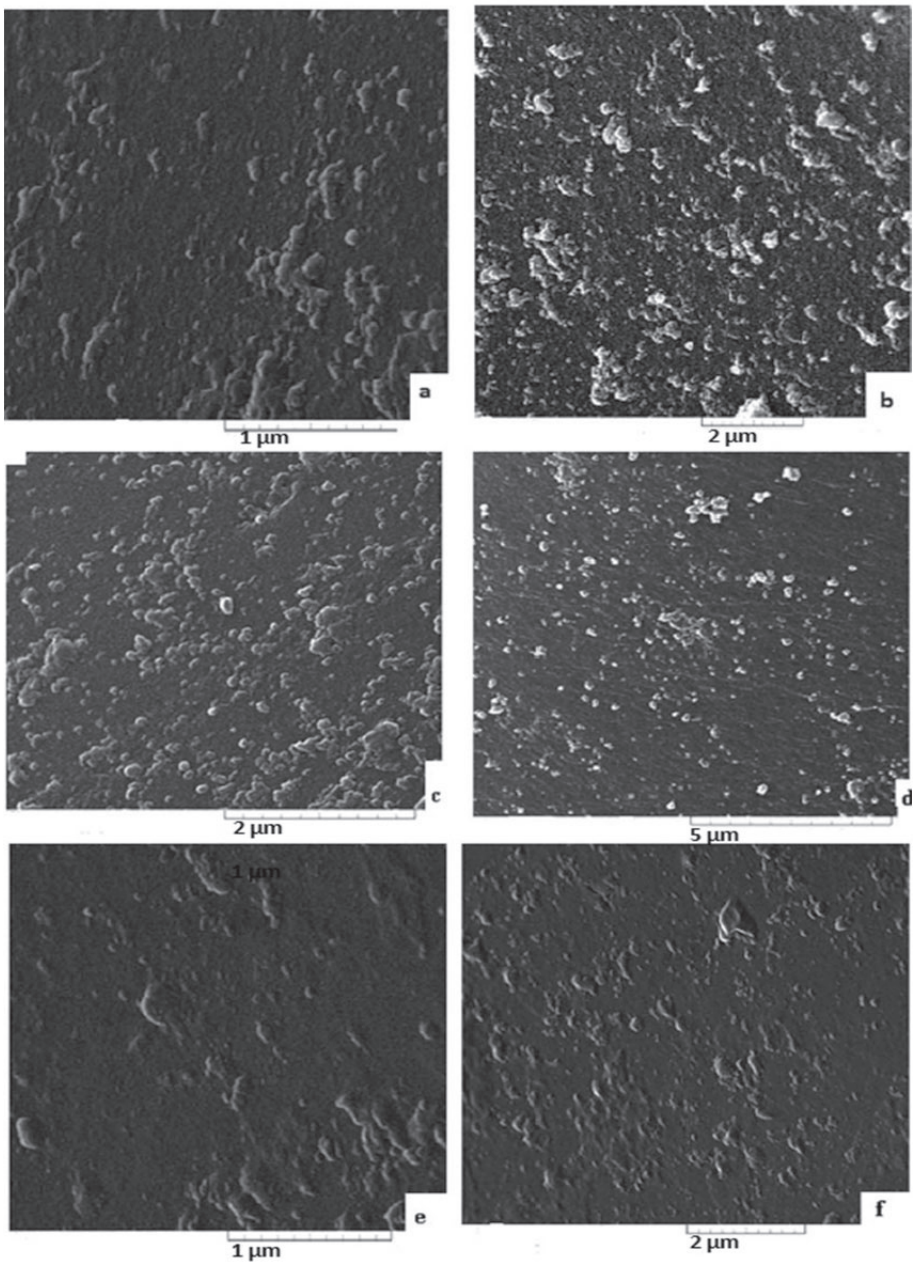

Figure 7-2. SEM images: of chromium (III) compounds on the surface (a) and in the volume (b) of an AV-17(Cr) sorbent granule; of chromium (III) compounds on the surface (c) and in the volume (d) of an AV-17(Cr) sorbent granule after sorption of CrO_4^{2-} ions from solution with temperature of 19°C and pH 8; of chromium (III) compounds on the surface (e) and in the volume (f) of an AV-17(Cr) sorbent granule after sorption of Cr(VI)-containing anions from solution with temperature of 19°C and pH 3.

A scanning electron microscope (Vega II LSH with accelerating voltage of 30 kV—Tescan Company) was used to examine the size and morphology of Cr(III) compound particles on the surface and within the volume of the polymeric granule. The samples were attached to aluminium holders using a silver-based adhesive. Samples conductivity was achieved by sputter coating with a 15 nm layer of gold [89].

The SEM images of samples of AV-17(Cr) sorbent confirmed that Cr(III) compounds in the polymer phase are in the form of ultrafine particles [Fig. 7-2(a, b)]. The existence of chromium compounds particles within the phase of the AV-17(Cr) sorbent and their morphology are the same before and after sorption of Cr(VI)-containing ions [Fig. 7-2(c-f)]. The particles of chromium compounds are distributed chaotically both on the surface and within the volume of sorbent granules. The prior testing of the AV-17(Cr) sorbent samples by using X-ray powder diffraction spectroscopy showed that in the sorbent phase there are no crystalline phases. The SEM images of samples of the AV-17(Cr) sorbent confirm that chromium compounds are amorphous both on the surface and within the volume of sorbent granules.

The thermogravimetric (TG) and derivative thermogravimetric (DTG) curves are recorded in air, at a 20 mL/min out flow, within the 25–900°C temperature range, using a Mettler Toledo TGA-SDTA851^e thermogravimetric analysis device. The test samples weighed between 2.5 and 4.5 mg, and the preferred rate of heating was 10°C/min. To calculate the apparent activation energy, thermogravimetric curves were also recorded at the following heating rates:

7, 13, and 16°C/min. The derivatograph employed has a temperature measuring accuracy of ±0.25°C and a reproducibility of ± 0.15°C, whereas the resolution provided by the balance for measuring the sample quantity is 1 μg. The device was temperature and sensitivity calibrated based on the standard melting points of metals such as In, Al, Zn, and Au. Samples of AV-17(Cr) sorbent treated with CrO_4^{2-} solutions were investigated by comparison with the raw ion exchanger AV-17(Cl).

The thermal degradation processes conducted both on the sorbent and the exchanger were also analysed in an inert atmosphere (He) using a TG/FTIR/MS system, within the 30–600 °C temperature range, at the same heating rate of 10 °C /min. The system is equipped with an apparatus of the simultaneous thermogravimetric spectrophotometer FTIR model Vertex-70 (Bruker-Germany) and the mass spectrometer model QMS 403C Aëolos (Netzsch-Germany). The experiments used samples between 10 and 12 mg. Helium with a flow rate of 50 mL/min was used as a carrier and as a protective purge for the thermobalance at 20 mL/min. The thermogravimetric analyser was calibrated for temperature and sensitivity using the melting points of the standard metals (Hg, In, Sn, Bi, and Zn). Further information on the technical characteristics and operation of the TG/FTIR/MS system is detailed in Ref. [90].

Table 7-2. Thermogravimetric characteristics of the sorbent samples

Sample	Stage	Helium				Air			
		T_{onset}, °C	$T_{peak.}$, °C	T_{endset}, °C	W, %	T_{onset}, °C	T_{peak}, °C	T_{endset}, °C	W, %
Av-17(Cr) (So)	I	37	87	131	7.51	49	71	100	15.54
	II	196	206	252	8.59	100	189	240	4.70
	III	300	324	344	22.42	302	316	328	20.63
	IV	405	428	481	38.33	405	420	438	20.23
	V	-	-	-	-	532	601	622	32.59
	Residue				23.15[a]				6.31[b]
AV-17(Cr)+Cr_2O_7)	I	38	102	154	4.12	54	75	115	13.93
(1)	II	172	240	330	14.28	218	236	286	9.73
	III	380	417	424	17.78	286	377	416	10.09
	IV	424	432	437	11.29	416	424	428	14.26
	V	437	442	482	16.82	453	464	546	33.76
	Residue				35.71[a]				18.23[b]
AV-17(Cr)+Cr_2O_7)	I	38	102	157	5.48	57	75	115	12.29
(2)	II	287	345	380	17.12	326	370	390	16.94
	III	380	417	425	2765	416	423	429	11.00
	IV	425	432	452	21.18	429	461	551	41.89
	Residue				28.57[a]				17.88[b]

a) Residue at 600°C (Netzsch system)
b) Residue at 900°C (Mettler Toledo system).

As far as the sorbents are concerned: raw AV-17(Cr) (Sample So), treated with K_2CrO_4 solution at 19°C and pH 3 (sample 1) and sorbent treated with K_2CrO_4 solution at 19°C and pH 8 (sample 2), the degradation mechanism is influenced by the atmosphere in which the thermal degradation process occurs. Therefore, at temperatures higher than 300°C, the thermal decomposition processes affecting samples 1 and 2 are separated differently in helium compared to air. Kannan, P. [132] pointed out that the working environment influences the thermal degradation mechanism of polystyrene. Thermogravimetric characteristics of the sorbent samples are shown in Table 7-2 at a heating rate of 10°C/min. He achieved activation energies that were higher when the degradation occurred in helium (about 190 kJ/mol) than when it occurred in the air (only 120 kJ/mol). This is the case with samples 1 and 2; considering the steeper TG curve slope in helium than in air (Figs. 7-3, 7-4 and 7-5), the activation energy values are higher in an inert atmosphere and the degradation mechanism is different in the two working atmospheres.

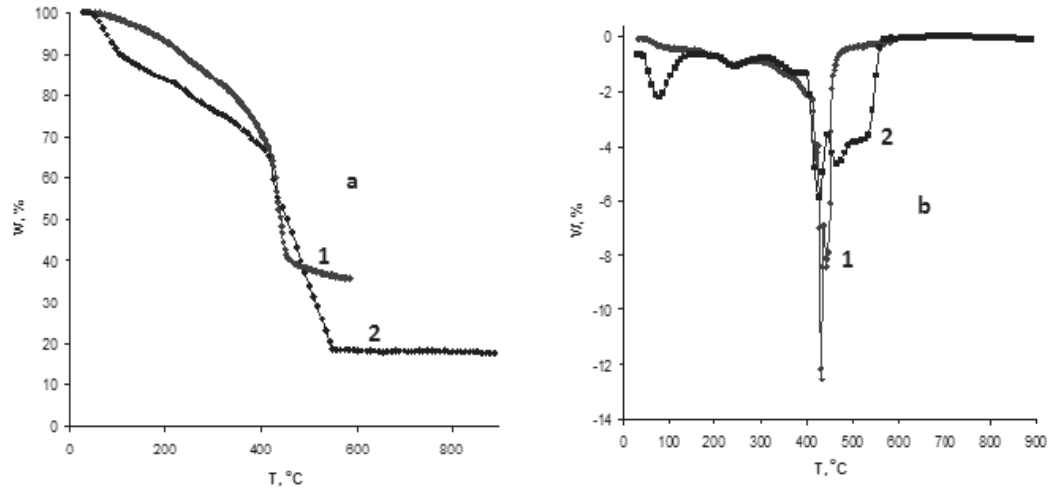

Figure 7-3. Thermogravimetric (a) and derivative thermogravimetric (b) curves obtained in He (1) and in air (2) for the sorbent AV-17(Cr) after sorption of Cr(VI)-containing anions from solution with temperature of 19°C and pH 3 – sample **1** at heating rate 10°C/min.

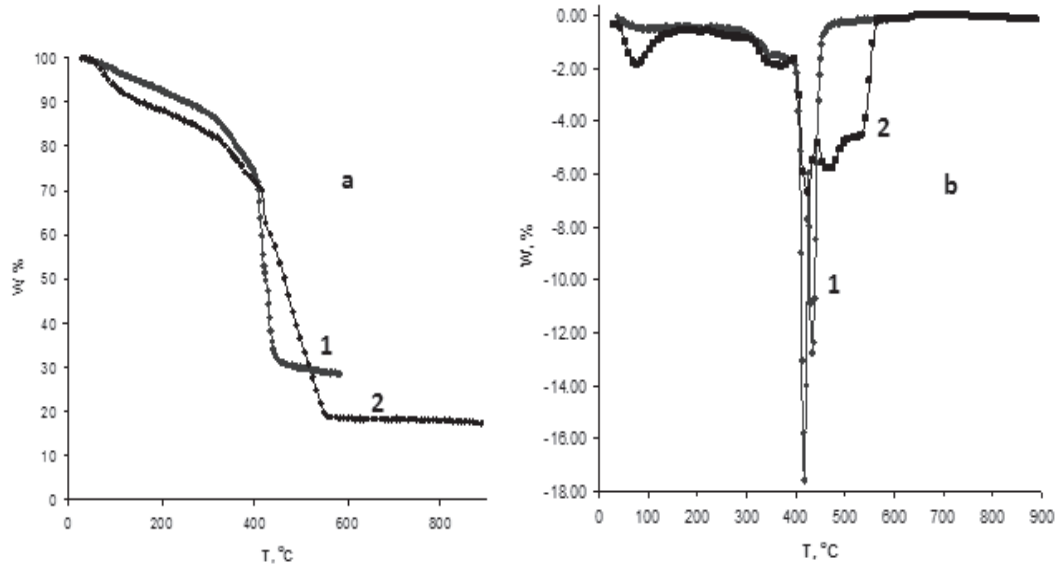

Figure 7-4. Thermogravimetric (a) and derivative thermogravimetric (b) curves obtained in He (1) and in air (2) for the sorbent AV-17(Cr) after sorption of CrO_4^{2-} ions from solution with temperature of 19°C and pH 8 – sample **2** at heating rate 10°C/min.

Variation of activation energy with conversion degree was determined by the Friedman [133] method, using thermogravimetric curves recorded in air and helium at the following heating rates: β =7, 10, 13, and 16°C/min. This differential method suggested by Friedman does not use any type of approximations. Hence, it is thought to be more exact than integral iso-conversional methods [134].

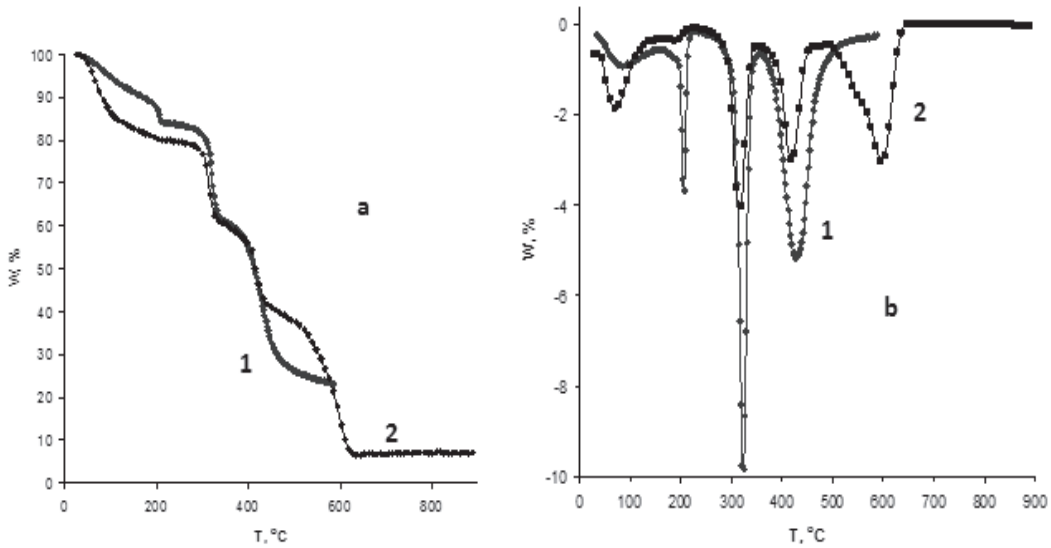

Figure 7-5. Thermogravimetric (a) and derivative thermogravimetric (b) curves obtained in He (1) and in air (2) for the sorbent AV-17(Cr) – sample **S0** at heating rate 10^{O}C/min.

The Friedman method is a generally applicable method allowing apparent activation energy determination by means of the following Equation (7-8):

$$\ln[\beta\,(\frac{d\alpha}{dT})] = \ln[F(\alpha)\,A] - \frac{E_\alpha}{RT_\alpha}\,, \qquad (7\text{-}8)$$

where α is constant, the graphical application of the $\ln[\beta\,(\frac{d\alpha}{dT})] = f(\frac{1}{T_\alpha})$ values (pairs of values read at the following four heating rates: β =7, 10, 13, and 16°C/min) results into a line the inclination of which provides the apparent activation energy value E_α. The correlation coefficients read in samples 1 and 2 on the graphical representation of the $\ln[\beta\,(\frac{d\alpha}{dT})] = f(\frac{1}{T_\alpha})$ lines for various conversion degree values were higher than 0.9. The apparent activation energy variation calculated by the Friedman method depending on the conversion degree is shown in Figure 7-4(*a*) for sample 1 and Figure 7-4(*b*) for sample 2. Our results support both the complexity of the degradation mechanism and the fact that it is influenced by the environment where the thermal degradation process occurs.

We also noted that at conversion degrees higher than 0.7 and at temperatures exceeding 380°C the apparent activation energy values are higher in an inert atmosphere than in the air. This finding agrees with the results of other researchers [132] considering that the degradation of the basic polymer containing polystyrene– divinylbenzene occurs at temperatures higher than 380°C (according to the TG-MS-FTIR study described hereunder). Samples 1 and 2 have a degradation mechanism slightly different from the sample of the AV-17(Cr) sorbent (Fig. 7-5). Sample 1 contains mostly $(R_4N)_2Cr_2O_7$ and $R_4N[Cr_3(OH)_6(Cr_2O_7)_2]$, whereas sample 2 contains $(R_4N)_2CrO_4$ and $R_4N[Cr_3(OH)_6(CrO_4)_2]$. The first stages consist partly of sorbent water removal (phase of hydration and free water) and partly of the following process for sample 1 (Eq. (7-9)):

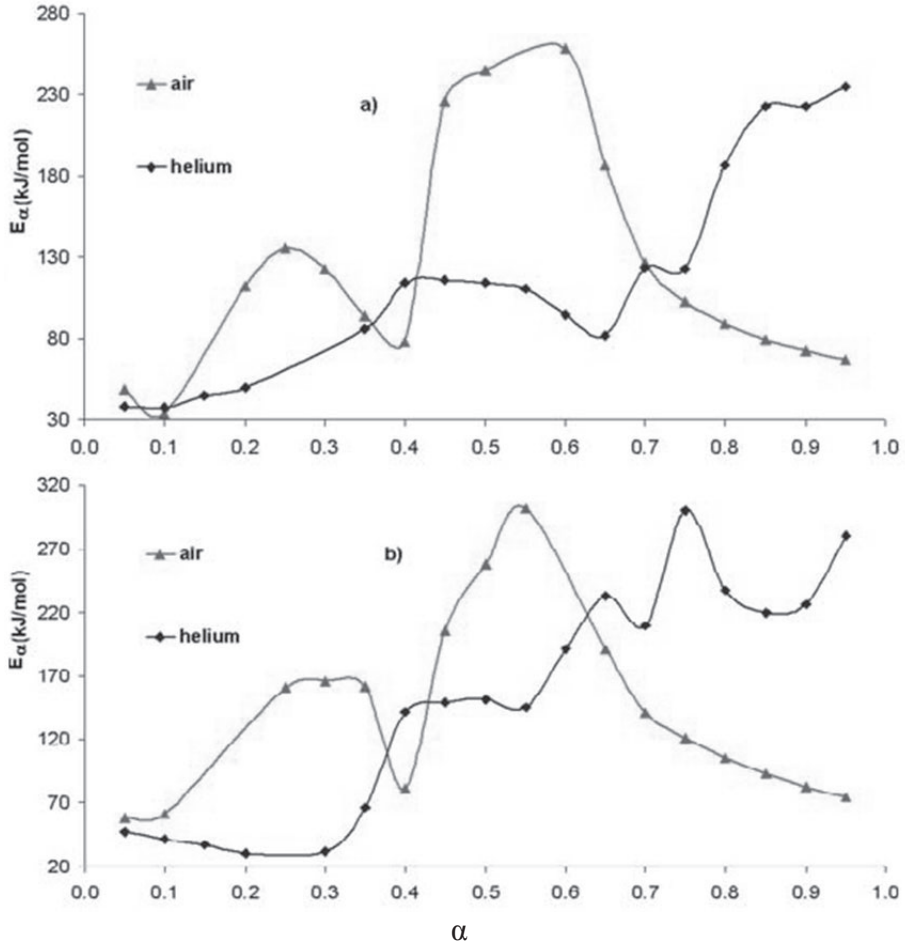

Figure 7-6. Activation energy variation with the conversion degree for sample 1 (a) and sample 2 (b).

$$2[RCH_2N(CH_3)_3]_2Cr_2O_7 + 2H_2O \rightarrow 2RCH_2OH + [RCH_2N(CH_3)_2]_2Cr_2O_7 + [N(CH_3)_4]_2Cr_2O_7 \quad (7\text{-}9)$$

which continues at temperatures higher than 170 ^oC with $[N(CH_3)_4]_2Cr_2O_7$ intermediate decomposition (Eq.(7-10)):

$$[N(CH_3)_4]_2Cr_2O_7 \rightarrow 2N(CH_3)_3\uparrow + C_2H_6\uparrow + Cr_2O_3 + 2O_2\uparrow \quad (7\text{-}10)$$

The process that may occur in sample 2 when water is present, is shown in the following (Eq.(7-11)):

$$2[RCH_2N(CH_3)_3]_2CrO_4 + 2H_2O \rightarrow 2RCH_2OH + [RCH_2NH(CH_3)_2]_2CrO_4 + [N(CH_3)_4]_2CrO_4, \quad (7\text{-}11)$$

which continues at temperatures higher than 200^oC with $[N(CH_3)_4]_2CrO_4$ intermediate decomposition (Eq.(7-12)):

$$2[N(CH_3)_4]_2CrO_4 \rightarrow 4N(CH_3)_3\uparrow + 2C_2H_6\uparrow + Cr_2O_3 + 5/2O_2\uparrow \quad (7\text{-}12)$$

According to the following reaction sequences, an additional amount of water also results for these samples, at temperatures higher than 300^oC, due to the dehydroxylation process (7-13) and (7-14):

$$2R_4N[Cr_3(OH)_6(Cr_2O_7)_2] \rightarrow (R_4N)_2Cr_2O_7 + 6Cr_2O_3 + 6H_2O\uparrow + 9/2O_2\uparrow, \quad (7\text{-}13)$$

$$2R_4N[Cr_3(OH)_6(CrO_4)_2] \rightarrow (R_4N)_2CrO_4 + 9/2Cr_2O_3 + 6H_2O\uparrow + 9/4O_2\uparrow \quad (7\text{-}14)$$

The MS spectra recorded for these two test samples (1 and 2) support the proposed mechanism. Therefore, Figure 7-7 shows the ionic current variation for the m/z =18 (H_2O^+) fragment, Figure 7-8 for the m/z =16 (O^+) fragment, Figure 7-9 for the m/z =30 ($C_2H_6^+$) fragment, and Figure 7-10 for m/z =59 ($N(CH_3)_3^+$).

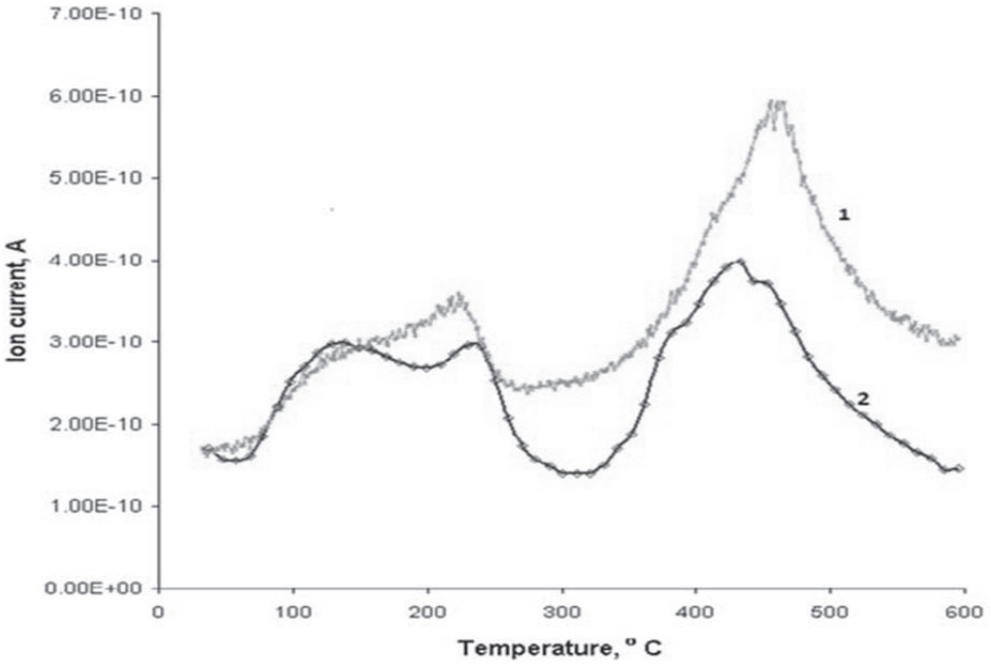

Figure 7-7. Ionic current variation with temperature for the sorbent AV-17(Cr) containing $Cr_2O_7^{2-}$ (1) and sorbent AV-17(Cr) containing $Cr_2O_4^{2-}$ (2) for the m/z-18 fragment.

The thermal decomposition processes of the basic structure of the polymer containing polystyrene–divinylbenzene occur at temperatures higher than 380°C [93]. Ionic fragments

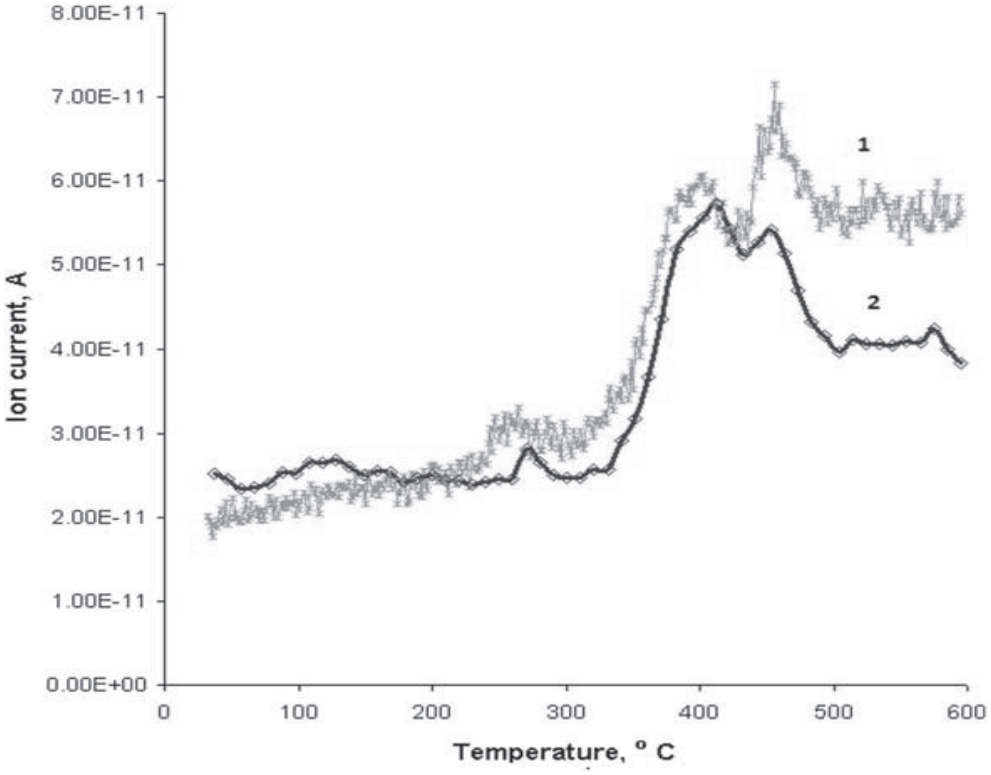

Figure 7-8. Ionic current variation with temperature for the sorbent AV-17(Cr) containing $Cr_2O_7^{2-}$ (1) and sorbent AV-17(Cr) containing CrO_4^{2-} (2) for the m/z-16 fragment.

specific to the styrene monomer, to α-methyl styrene, to dimethylbenzene or to alkylbenzene, etc. are also identified for these polymers. As far as samples 1 and 2 are concerned, we also noted a separation tendency of several degradation processes within the 380–480°C temperature range (represented by two or three peaks in the DTG curves, compared to only one peak in the sorbent raw AV-17(Cr)-sample ***So*** (see Figs.7-3, 7-4 and 7-5). They probably occur due to the different rate at which the random split processes occur, as a result of which there are various fragments of alkylbenzene. Figures 7-11, 7-12 and 7-13 show the MS spectra for the m/z =91 ($C_7H_7^+$), m/z =105 ($C_8H_9^+$), and m/z

=120 ($C_9H_{12}^+$) ionic fragments that illustrate the separation of several processes within the above mentioned temperature range.

The FTIR spectra recorded for test samples 1 and 2 also support the proposed degradation mechanism. According to Figures 7-14 and 7-15, the bands specific to water in the vapour state occur within the 1390–1860 cm^{-1} and 3500–3900 cm^{-1} ranges, respectively [97, 98]. The FTIR bands from 1158 to 1274 cm^{-1} that occurs at 240°C for test sample 1 and at 345°C for test sample 2 may be connected to C-N bond vibration. The presence of the bands located at 1458 and 2970

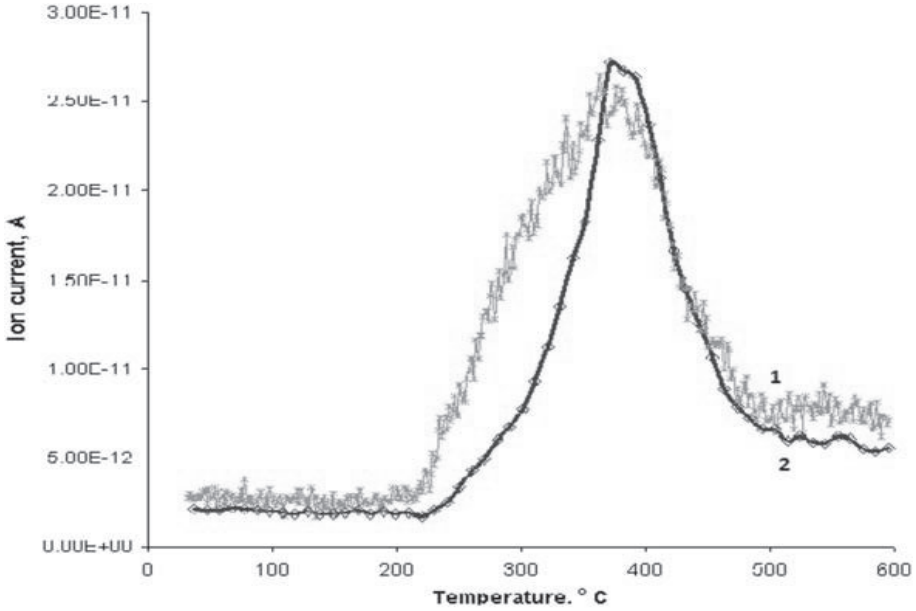

Figure 7-9. Ionic current variation with temperature for the sorbent AV-17(Cr) containing $Cr_2O_7^{2-}$ (1) and sorbent AV-17(Cr) containing CrO_4^{2-} (2) for the m/z-30 fragment.

cm^{-1} in the FTIR spectrum [99, 101] may be connected to the m/z =30 (C_2H6^+) ionic fragment identified in the MS spectrum.

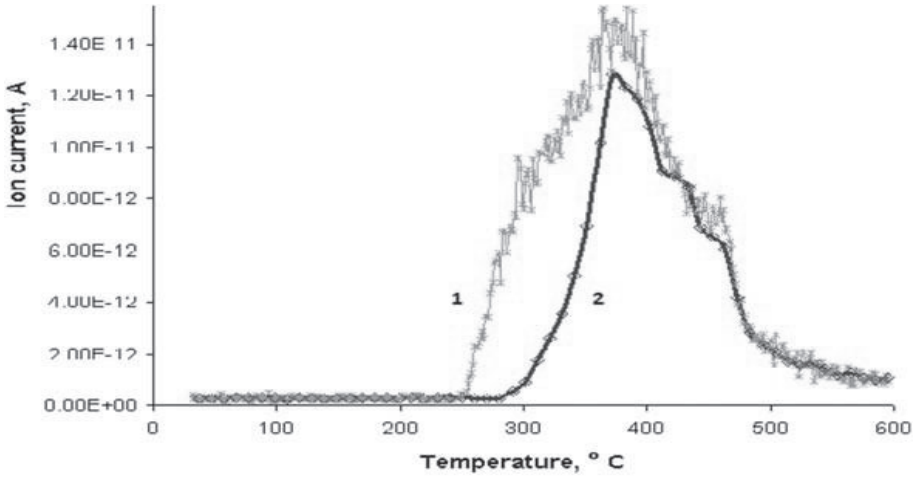

Figure 7-10. Ionic current variation with temperature for the sorbent AV-17(Cr) containing $Cr_2O_7^{2-}$ (1) and sorbent AV-17(Cr) containing CrO_4^{2-} (2) for the m/z-59 fragment.

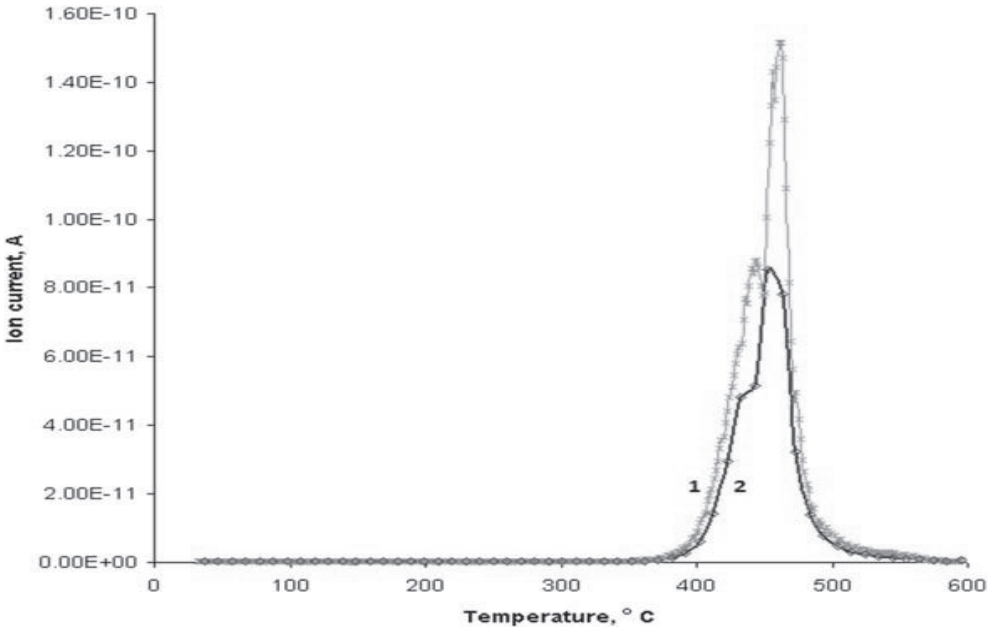

Figure 7-11. Ionic current variation with temperature for the sorbent AV-17(Cr) containing $Cr_2O_7^{2-}$ (1) and sorbent AV-17(Cr) containing CrO_4^{2-} (2) for the m/z-91 fragment.

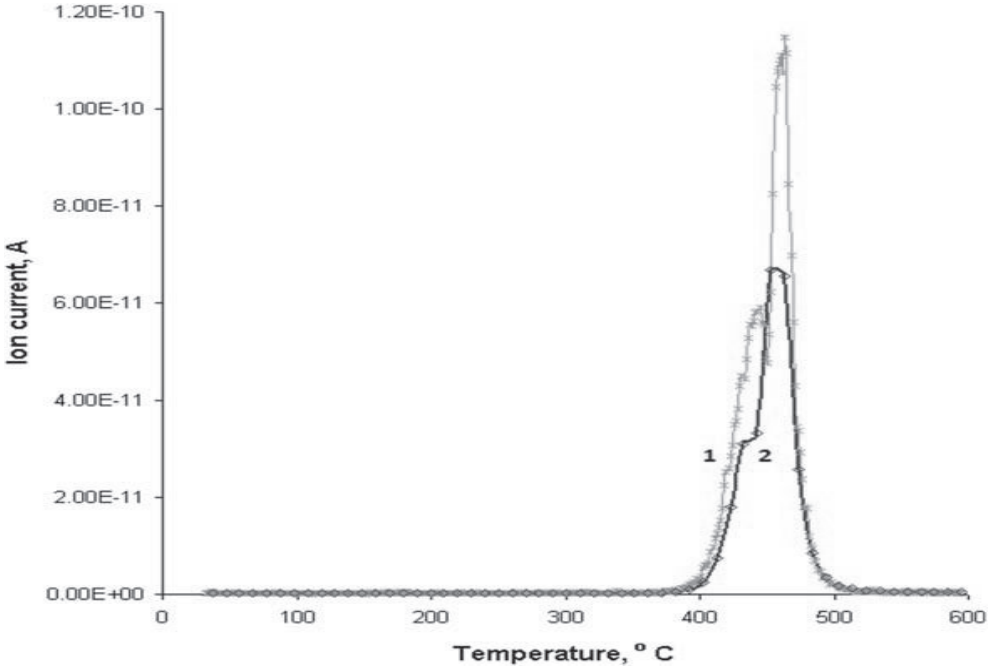

Figure 7-12. Ionic current variation with temperature for the sorbent AV-17(Cr) containing $Cr_2O_7^{2-}$ (1) and sorbent AV-17(Cr) containing CrO_4^{2-} (2) for the m/z-105 fragment.

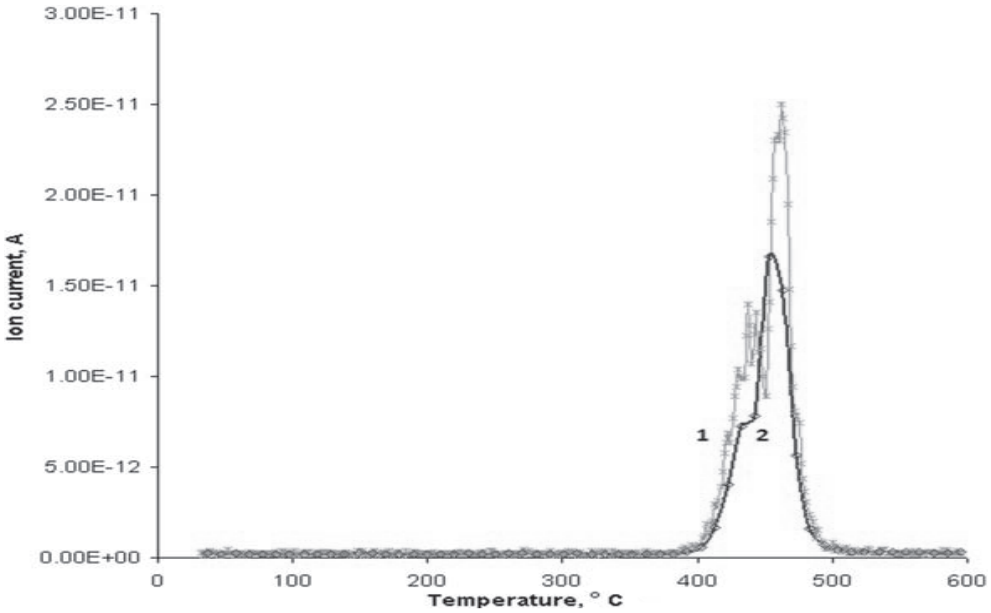

Figure 7-13. Ionic current variation with temperature for the sorbent AV-17(Cr) containing $Cr_2O_7^{2-}$ (1) and sorbent AV-17(Cr) containing CrO_4^{2-} (2) for the m/z-120 fragment.

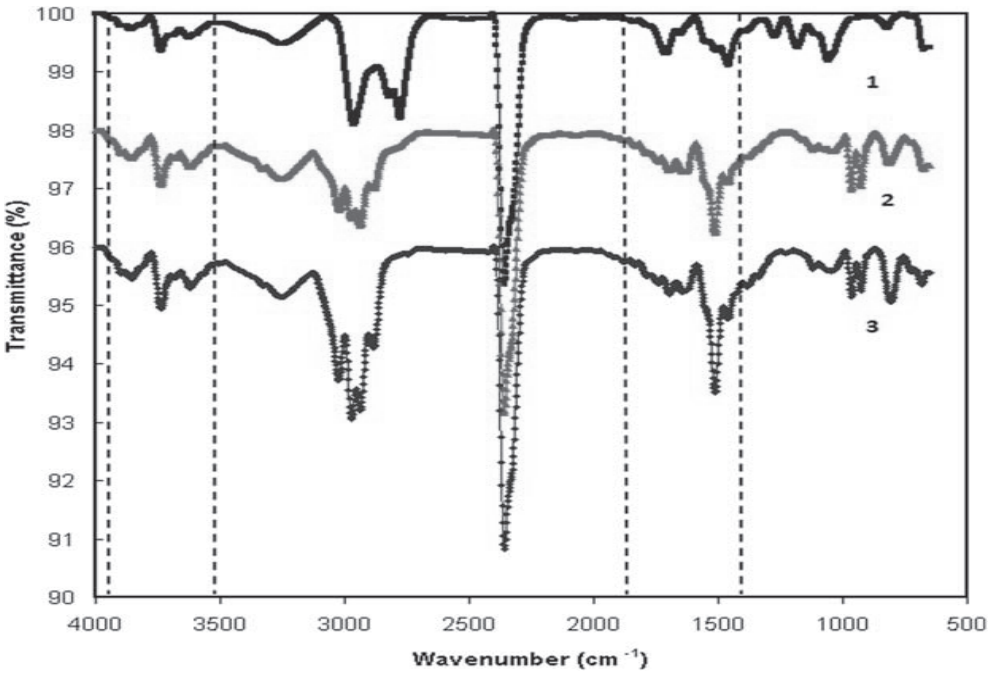

Figure 7-14. FTIR for the sorbent AV-17(Cr) containing $Cr_2O_7^{2-}$ at 240 (1), 417 (2), and 442°C (3).

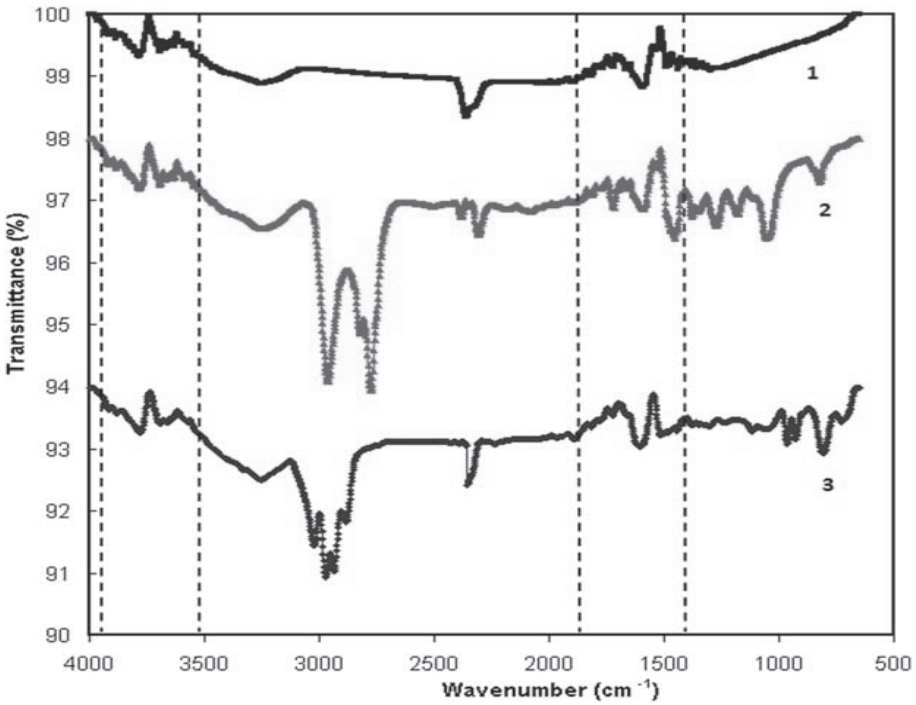

Figure 7-15. FTIR for the sorbent AV-17(Cr) containing $Cr_2O_7^{2-}$ at 102 (1), 345 (2), and 432°C (3)

The FTIR spectra in Figure 7-14 (spectra 2 and 3) and in Figure 7-15 (spectrum 3) support the thermal decomposition theory of the basic structure of polymers containing polystyrene–divinylbenzene, at temperatures higher than 380°C. Noted, for instance, are the bands from 3078 cm^{-1} which are characteristic of the aromatic cycles of the styrene monomer; those from 2860 and 2920 cm^{-1} in connection to the methyl groups belonging to a methyl styrene; the bands specific to aliphatic $–CH_2$ groups from polystyrene at 3026 cm^{-1} [102, 103]. As far as samples 1 and 2 are concerned, we also identified in the FTIR spectra the bands specific to CO_2 at 672 and 2352 cm^{-1} at temperatures higher than 200°C [101]. They have a higher intensity for the 1 polymer, the thermal degradation of which results in a higher amount of oxygen that may lead to CO_2 formation.

7.3. Nitrate and nitrite sorption on polymer modified with Cr(III) compounds

7.3.1. Nitrite ions sorption

Water pollution with nitrite ions is a severe problem for many countries, especially those with a developed agro-industrial sphere. An excess of these ions in water and in food is dangerous for the health of human and animal species. Removal of NO_2^- ions from liquids is a rather an actual problem.

The application of anion exchangers for the removal of nitrite ions, especially strongly basic exchangers, is not reasonable. Sorption of anions, including NO_2^-, as a result of anion exchange, practically, is not selective because it is conditioned by Coulomb's (electrostatic) interactions and the modern technologies of purification of various categories of fluids and gases, and concentration and separation of substances requiring new selective sorbents. Some publications [135, 136] contain data on the sorption of nitrite ion by anion exchangers containing secondary amine groups. In fact, the removal of NO_2^- ions was done not because of anion exchange which is a physical process, but as the result of a chemical process, which most likely is decomposition of anions in the polymer phase ($R_2NH_2^+ \leftrightarrow R_2NH + H^+$; $H^+ + NO_2^- \leftrightarrow$…).

The process of decomposition of NO_2^- ions in the polymer phase may be confirmed with sorption. The polymer containing secondary amine groups cannot have a sorption capacity of 3.1 g NO_2^-/g, as shown in the article [136]. In neutral and alkaline environments, the degree of protonation of amine groups decreases and tends to zero. Because of this, the ion exchange capacity of the polymer decreases and tends to zero.

Being modified with metallic compounds, strongly basic anion exchangers became selective sorbents for some anions and molecules in the function of the metal nature. So, modified with Fe(III)-containing compounds ($R_4N[Fe_3(OH)_6SO_4)_2]$), strongly basic anion exchangers become selective sorbents for CN^-, NCS^-, and NCO^- ions [74].

The jarosite mineral type compounds in the polymers phase change essentially their physical-chemical properties. The R_4N^+ and H_3O^+ ions from jarosite type compounds can be exchanged with different cations and the anions SO_4^{2-}- with different anions or molecules capable of forming coordinate bonds with the central metal ions. Thus, selective sorption of ions or molecules on jarosite containing exchangers is due to the ligand-ligand exchange process.

This section discusses the results of the research of the sorption of NO_2^- ions on the sorbent Purolite A-400(Cr) [137]. The choice of the Cr(III) compounds containing polymer as a sorbent is determined by the high stability of the

metallic compounds in the polymer phase. For comparison, NO_2^- ions sorption has been studied on Purolite A-400(Cl) as well. For investigation Purolite A-400 was used containing 40 mg Cr/g. Solutions of nitrite ions were prepared using $NaNO_2$. The concentration of NO_2^- ions in solutions was determined by photocolorimetry using the Griess reagent [138]. In all experiences, samples of 0.2 g of polymer were in contact with 100 ml of solution. In the case of the sorption isotherms obtained and sorption of NO_2^- as a function of solution pH, polymer samples contacted with a solution at room temperature during 24 h.

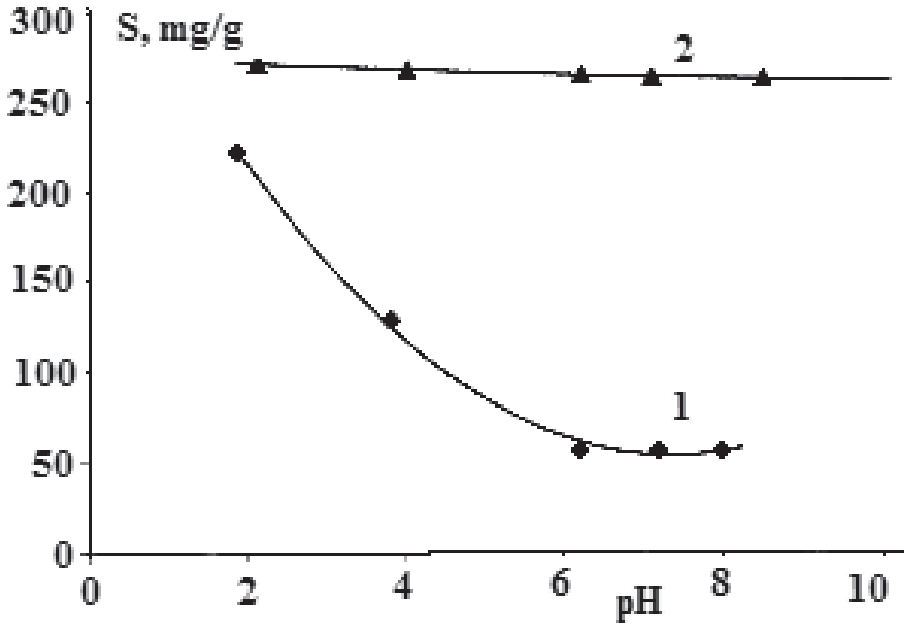

Figure 7-16. Sorption of the NO_2^- ions on Purolite A-400 (Cl) (1) and on Purolite A-400 (Cr) (2) as a function of pH of the $NaNO_2$ solution.

As seen in Figure 7-16, sorption of NO_2^- ions on Purolite A-400 (Cl) from $NaNO_2$ solution having 0.555 mg NO_2^- /mL (initial concentration) at room temperature hardly depends on solution pH, increasing considerably at pH<5. At pH 1.85 the apparent sorption capacity of the polymer is higher than its theoretical exchange capacity.

Sorption of NO_2^- ions on Purolite A-400(Cl) from solutions with pH>4 takes place mainly due to the ion exchange process (7-15):

$$R_4NCl + NO_2^- \leftrightarrow R_4NNO_2 + Cl^- \quad (7\text{-}15)$$

The apparent high sorption of NO_2^- ions from solutions with pH<5 may be explained through the NO_2^- decomposition processes (7-16) and (7-17) that takes place in solution and in the polymer phase, in which nitrite ions concentration is higher [139]:

$$2NO_2^- \xrightarrow{H^+} 2HONO \leftrightarrow N_2O_3 + H_2O \quad (7\text{-}16)$$

$$N_2O_3 \leftrightarrow NO^{\bullet} + NO_2^{\bullet} \xrightarrow{O_2} 2NO_2 \quad (7\text{-}17)$$

The IR spectra of the Purolite A-400 (Cl) treated with 0.01 M $NaNO_2$ solution at a different pH confirmed the existence of the above-mentioned processes. As seen in Figure 7-17, in an IR spectrum of the polymer treated with $NaNO_2$ solution at pH 6 appears a large absorption band at 1220 cm^{-1} which belongs to NO_2^- ions. In the IR spectrum of the polymer treated with $NaNO_2$ solutions at pH 3, this absorption band is almost absent.

In the Purolite A-400 (Cr) – $NaNO_2$ solution system at the corresponding pH, processes (7-16), (7-17) and (7-19) take place. On the preparation of Purolite A-400(Cr), some of the R_4N^+ polymer's groups are in the jarosite type compounds but most of them remain able for anion

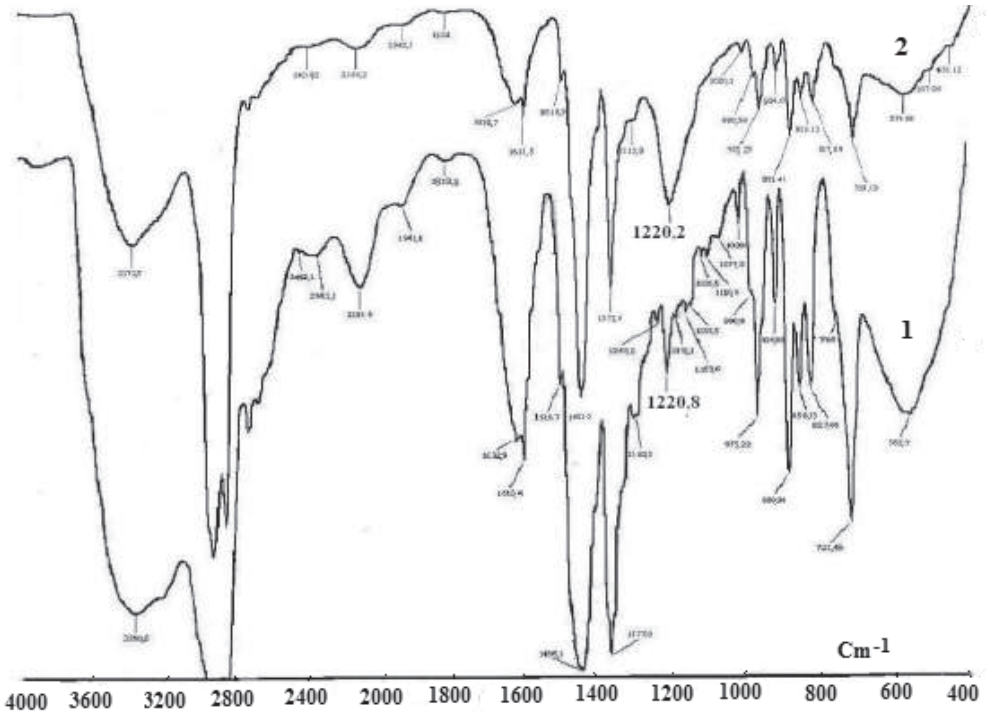

Figure 7-17. IR spectra of Purolite A-400(Cl) treated with 0.01M $NaNO_2$ solution with pH 3 (1) and pH 6 (2).

exchange process according to Equation (7-18) and the polymer contain not only jarosite type compounds, but also SO_4^{2-} ions:

$$2R_4NCl + SO_4^{2-} \leftrightarrow (R_4N)_2SO_4 + 2Cl^- \quad (7\text{-}18)$$

Being in contact with $NaNO_2$ solution, on Purolite A-400(Cr) takes place process (7-19):

$$(R_4N)_2SO_4 + 2NO_2^- \leftrightarrow 2R_4NNO_2 + SO_4^{2-} \quad (7\text{-}19)$$

Besides these processes in the system, sorption of NO_2^- ions also takes place through the ligand-ligand exchange. On treating of the Purolite A-400 (Cr) with 0.01 M $NaNO_2$ solution at pH 3, in the polymer phase, there are many SO_4^{2-} ions (bands at 1095 and at about 610 cm^{-1}) and some NO_2^- ions (Fig. 7-18). With the increasing of the system pH (up to 6 and more), the NO_2^- ions content in the polymer phase increases and SO_4^{2-}decreases (Fig. 7-18).

Considering that NO_2^- ions coordinate monodentate with Cr^{3+}, the ligand-ligand exchange process takes place according to Equation (7-20):

$$R_4N[Cr_3(OH)_6(SO_4)_2] + 6NO_2^- \leftrightarrow R_4N[Cr_3(OH)_6(NO_2)_6]^{2-} + 2SO_4^{2-} \quad (7\text{-}20)$$

On treating the Purolite A-400(Cr) with 0.1 M $NaNO_2$ solution at pH 6, all SO_4^{2-} ions in the polymer phase are replaced by NO_2^- ions (Fig. 7-18). Besides the absorption band at 1220 cm^{-1} a new band appears at 1560 cm^{-1}. It means that in the polymer phase a part of the NO_2^- ions coordinate with Cr^{3+} forming a bridge between metal ions [36]. Taking into consideration that in

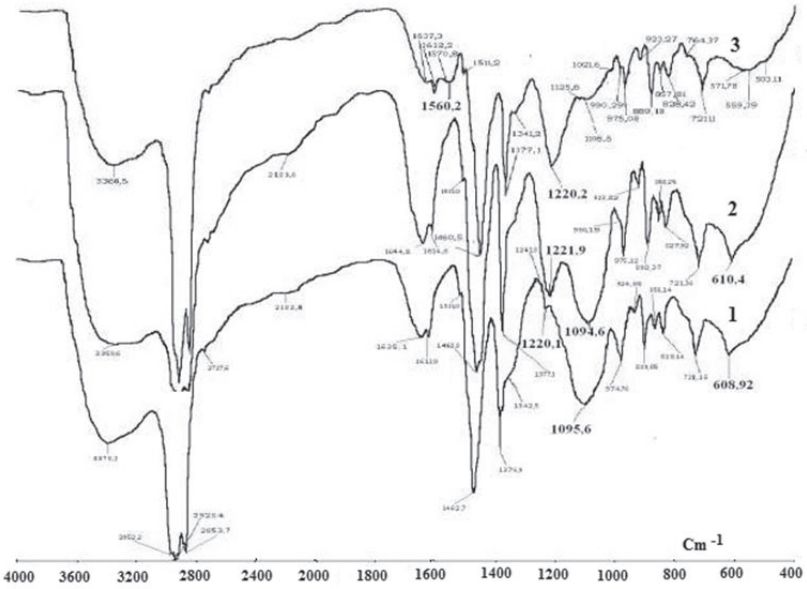

Figure 7-18. IR spectra of the Purolite A-400(Cr) treated with 0.01M $NaNO_2$ solution with pH 3 (1) and pH 6 (2) and with 0.1M $NaNO_2$ solution with pH 6 (3).

the region of 600 – 400 cm^{-1} there is a large absorption band (Fig. 7-18) due to M-O and M-N vibrations, we can conclude that in the polymer phase Cr^{3+} coordinates through the O and N atoms of NO_2^- ions, forming the following coordination centres:

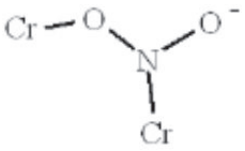

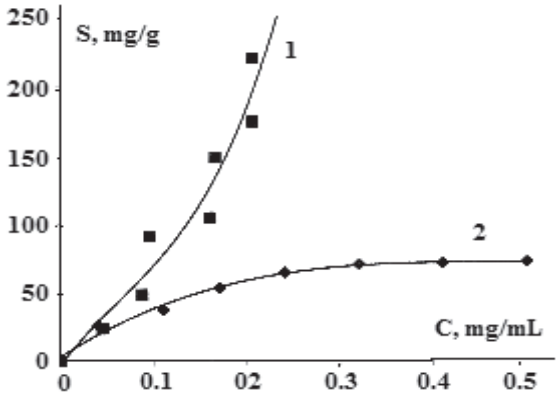

Figure 7-19. The NO_2^- ions sorption isotherms on Purolite A-400(Cr) (1) and on Purolite A-400 (Cl) (2).

This process can be described by Equation (7-21):

$$R_4N[Cr_3(OH)_6(SO_4)_2] + 3NO_2^- \leftrightarrow R_4N[Cr_3(OH)_6(NO_2)_3]^+ + 2SO_4^{2-} \quad (7\text{-}21)$$

The sorption isotherms of NO_2^- ions on Purolite A-400(Cl) and on Purolite A-400(Cr) were obtained at 17°C (Fig. 7-19). Polymer samples were in contact with solutions with pH=6.2 during 24 h, and that was enough for sorption equilibrium to establish. Sorption isotherm on Purolite A-400(Cl) may be described by the Langmuir sorption model (Eq. 7-22):

$$S = S_L K_L C/1 + K_L C, \quad (7\text{-}22)$$

where S_L = 123 mg NO_2^-/g and K_L = 4.28 mL/mg.

On Purolite A-400(Cr), the sorption isotherm apparently may be approximated with the type III isotherms of the BET classification.

To evaluate the influence of numerous factors (concentration of $NaNO_2$, KCl and K_2SO_4, pH and temperature of the solution, duration of the polymer contacting with solution) on NO_2^- ions sorption (Tab. 7-3), the method of statistical mathematics was used [24, 25]. The experiences were conducted according to a matrix of Fractional Factorial Experiment plan type FFE 2^{7-4} (Tab.7-4). The following responses of the system were measured and calculated as a mean of two parallel experiences: Y_1 – sorption of NO_2^- ions (mg NO_2^-/g) and Y_2 – solution pH at sorption equilibrium. The significance criterion b_{sig} was calculated at a level of significance of 5 % and a degree of freedom f =7.

Table 7-3. Examined factors and their code and levels of variation

Code	Factor	Lower level (-)	Upper level (+)
X_1	NO_2^- concentration, mg NO_2^-/mL	0.5	0.8
X_2	Temperature	19.5	50
X_3	pH	4.0	5.0
X_4	KCl concentration, N	0.01	0.05
X_5	K_2SO_4 concentration, N	0.01	0.05
X_6	Time of contact, h	6.0	8.8
X_2X_3	-	-	-

The obtained results (Tab.7-4) were used for the calculation of the coefficients of the regression Equations (7-23) and (7-24):

$$Y_1=98.85+1.58X_1+17.26X_2-18.36X_3-5.46X_4+6.37X_5+17.29X_6-1.49X_2X_3, \quad b_{sign}=1.19 \tag{7-23}$$

$$Y_2=4.44+0.24X_1+0.19X_2+0.11X_3+0.02X_4-0.19X_5-0.02X_6+0.21X_2X_3, \quad b_{sign}=0.03 \tag{7-24}$$

Table 7-4. The matrix of the Fractional Factorial Experiment plan type FFE 2^{7-4} and the obtained results

N_0 of experiment	X_1	X_2	X_3	X_4	X_5	X_6	X_2X_3	Y_1	Y_2
1	+	+	+	+	+	+	+	116.05	5.00
2	-	+	+	-	-	-	+	76.50	4.90
3	+	-	+	-	+	-	-	60.85	4.20
4	-	-	+	+	-	+	-	68.60	4.10
5	+	+	-	+	-	-	-	108.40	4.80
6	-	+	-	-	+	+	-	163.50	3.83
7	+	-	-	-	-	+	+	116.50	4.75
8	-	-	-	+	+	-	+	80.50	3.95

All the studied factors, the temperature (X_2) and the duration of the polymer contacting with a solution (X_6) (Eq. (7-23)) being increased have the strongest positive effect on NO_2^- ions sorption. Such a strong influence of temperature and contact duration of the polymer with a solution, confirm once again that NO_2^- ions sorption is determined by the chemical process. As seen in Equation (7-23), increasing the solution pH has a strongly negative effect on NO_2^- ions sorption. This fact and that of the strongest positive effect on the NO_2^- ions sorption concentration (more than the initial pH influence (X_3) on the final pH) on the solution pH (X_1 in Equation (7-23)) indicates that in the polymer-solution system processes (7-16) and (7-17) take place. It means that the NO_2^- ion sorption value is apparent because a part of NO_2^- ions is not retained by the polymer but is removed from the system in the form of NO_2. It is in accordance with the form of the sorption isotherm of NO_2^- ions on Purolite A-400(Cr) (Fig. 7-19).

The low value of the coefficient at X_4 (Eq. (7-23)) also indicates that anion exchange involving NO_2^- ions is not a prevalent process in NO_2^- ions sorption. The negative influence of increasing Cl^- ions concentrations on NO_2^- ions sorption is clear from Equation (7-15). The influence of SO_4^{2-} anions (X_5, Eq. (7-23)) on NO_2^- sorption is unexpected. It is known that anion exchangers retain SO_4^{2-} stronger than Cl^- ions, and the SO_4^{2-} influence on NO_2^- sorption must be negative. Moreover, increasing SO_4^{2-} ions concentration in solution will shift the equilibrium (7-19) and (7-20) to the left and the coefficient at X_5 in the Equation (7-23) must be negative. The positive influence of the SO_4^{2-} ions concentration on NO_2^- ions sorption and the negative effect on solution pH show that SO_4^{2-} ions are not only involved in the anion exchange process. Maybe in the polymer phase, where the concentration of SO_4^{2-} is high, the formation of HSO_4^- ions takes place, and HSO_4^- served as a source of protons in the process (7-16). The obtained results permit us

to consider that the removal of NO_2^- ions from solution using the Cr(III)-containing polymer takes place through the processes (7-16), (7-17), and (7-19) to (7-21).

The obtained regression equations provide a means for optimizing responses. We optimized only the removal of the NO_2^- ions from solution using the Cr(III)-containing polymer.

Table 7-5. Nitrite ions' sorption on Purolite A-400(Cr) optimizing

No of experiment	X_1	X_2	X_3	X_5	X_6	Y_1
1	0.85	25	3.5	0.23	9	245.3
2	0.95	20	3	0.33	10	279.7
3	1.05	20	3	0.43	10	314.1
4	1.15	20	3	0.53	10	348.5
5	1.25	20	3	0.63	10	382.5

In the optimizing experiments, KCl was excluded from the system and pH, temperature and contact duration of the polymer with solution were limited corresponding to 3, 20°C and 10 h. The steepest-ascent steps were 0.1 mg NO_2^-/g, 0.1N K_2SO_4 and 1.0 h. The obtained results are presented in Table 7-5. As shown in Table 7-5, with the increasing of NO_2^- and SO_4^{2-} ions concentration, the removal of nitrite ions from solution rises considerably, but in the limit of these experiments do not reach the maximum. The obtained results showed that the experiment plan is true and the regression equation described adequately the NO_2^- removal process. Continuously increasing NO_2^- removal in the optimizing experiments confirms that in the polymer-solution system processes (7-16) and (7-17) take place.

7.3.2. Nitrate ions removal from solution

Pollution with nitrate/nitrite ions is a serious problem for many countries, especially those with a developed agro-industrial complex. Excess of these ions in water and food is dangerous for the health of human and animal species. Removal of nitrate/nitrite ions from liquids is a very actual problem.

It is known that now nitrate ions are removed either by physicochemical or biological methods. There was investigation [140] of the application of catalysts in the removal of nitrate and nitrite ions from drinking water. The nitrate and nitrite ions were reduced with hydrogen on catalysts (noble metal palladium or palladium activated with copper). The products of the reaction are gaseous nitrogen and dissolved ammonia, which is undesirable in drinking water.

The application of the anion exchangers, especially strongly basic anion exchangers, for nitrate and nitrite ions removal was also investigated [135, 136, 141]. Sorption of anions, including NO_3^- or NO_2^-, on strongly basic anion exchangers is not selective because it is conditioned by Coulomb's (electrostatic) interactions and the modern technologies of purification of various categories of fluids and gases, concentration and separation of substances which required new selective sorbents. As selective sorbents can be strongly basic anion exchangers modified with metallic compounds.

In the earlier section it was shown that a strongly basic anion exchanger modified with Cr-jarosite type compounds is able to provide selective sorption of nitrite ions from solution. In this section is investigated the nitrate/nitrite ions removal by a Cr-jarosite containing strongly basic anion exchanger AV-17 142]. For the investigation polymer AV-17 containing 35.46 mg Cr/g was used. Solutions of nitrate ions were prepared using $NaNO_3$. The concentration of nitrate ions was determined by photocolorimetry using Griess reactive after their converting into nitrite ions [138]. Continuous flow adsorption studies were conducted in a column made of Pyrex glass tube having an inner diameter of 1.2 cm and 25 cm height. The column held 3 layers - the first layer (upper layer) consisted of granulated metallic Cd, the second layer consisted of Cr-jarosite containing AV-17 and the third layer consisted of carboxylic cation exchanger (Purolite C-104) in Na-form. In the first layer the transformation of nitrate ions into nitrite takes place. In the second layer nitrite ions were selectively turned by Cr-jarosite containing AV- 17. The carboxylic exchanger was used for the selective sorption of Cd^{2+} (and Cr^{3+} ions that could possibly come out of the polymer phase) cations. As is known, carboxylic exchangers are capable of selective sorption of cations of *d, f*-elements as a result of coordination processes.

The investigation was carried out using the response surface methodology (the G.E.P.Box and K.B.Wilson method) [25]. Removal of nitrate ions was carried out at 20 °C using modelling solutions similar in composition to natural waters. Influencing factors were the concentration of NO_3^- ions, $NaHCO_3$, KCl, Na_2SO_4, solution pH and the flow rate of solution through a column. In all the experiments the Cr(III)-containing AV-17 mass was 2.5g, the Purolite C-400 mass was 1.5 g and that of granulated Cd was 2 g. The mass of the latest two components was arbitrary. From the experimental data were built breakthrough curves for adsorption of nitrate/nitrite ions and calculated sorption process parameters. Removal of nitrate/nitrite ions by Cr(III)-containing AV-17 takes place according to Equations (7-25) and (7-26):

$$NO_3^- + Cd + H_2O \rightarrow NO_2^- + Cd^{2+} + 2OH^- \quad (7\text{-}25)$$

$$R_4N[Cr_3(OH)_6(SO_4)_2] + 6NO_2^- \leftrightarrow R_4N[Cr_3(OH)_6(NO_2)_6]^{2-} + 2SO_4^{2-} \quad (7\text{-}26)$$

Not all of the R_4N^+ groups of the polymer are in the jarosite composition. A part of them is in the form of $(R_4N)_2SO_4$ because the preparation of the Cr(III)- containing polymer occurred in the solution of $Cr_2(SO_4)_3$. They can participate in the anion exchange processes (7-27) where An^{n-} is an anion.

$$n(R_4N)_2SO_4 + 2An^{n-} \leftrightarrow 2(R_4N)nAn + nSO_4^{2-} \quad (7\text{-}27)$$

If there are Cr^{3+} or Cd^{2+} cations in the system, they are selectively retained by the carboxylic cation exchanger, according to Equations (7-28) and (7-29):

$$Cd^{2+} + 2RCOONa \leftrightarrow (RCOO)_2Cd + 2Na^+ \quad (7\text{-}28)$$

$$Cr^{3+} + 3RCOONa \leftrightarrow (RCOO)_3Cr + 3Na^+ \quad (7\text{-}29)$$

In the case of nitrate/nitrite ions removal from food liquids it is reasonable to use the carboxylic exchanger in K^+ form.

The sorption of nitrate/nitrite ions on Cr(III)- containing AV-17 is influenced by many factors. The influencing factors and their codes are shown in Table 7-6.

Table 7-6. Examined factors and their code and levels of variation

Code	Factor	Lower level (-)	Upper level (+)
X_1	NO_3^- concentration, mg NO_3^-/L	50	70
X_2	pH	6.0	7.0
X_3	$NaHCO_3$ concentration, meq/L	2	3
X_4 (X_1X_2)	KCl concentration, meq/L	2	3
X_5 (X_1X_3)	K_2SO_4 concentration, meq/L	2	3
X_6 ($X_1X_2X_3$)	Filtration speed, mL/min	1.0	1.8
X_2X_3	-	-	-

The following responses of the system were measured and calculated:

Y_1- dynamic sorption capacity (DSC-the value of sorption until the appearance of the nitrate/nitrite ions into the filtrate), mg NO_3^-/ g

Y_2 - total dynamic sorption capacity (TDSC-sorption value when sorbent was saturated), mg NO_3^-/ g.

Y_3- relative rate of sorption (W = ((DSC/TDSC) 100), %.

The experiments were carried out according to the matrix of a Fractional Factorial Design (Tab. 7-7). The values of Y_1, Y_2 and Y_3 were determined from the breakthrough curves for adsorption of nitrate/nitrite ions (Figs. 7-20 and 7-21).

The results (Tab. 7-7) are the averages of two independent experiments. The obtained results were used for calculation of the coefficients of the regression Equations (7-30) and (7-31):

$$Y_1 = 11.23 + 0.705X_1 - 0.255X_5 - 0.82X_6 + 0.855X_2X_3, \ b_{sig.} = 0.210 \quad (7\text{-}30)$$

$$Y_2 = 18.32 + 1.848X_1 + 0.434X_4 - 0.432X_5 - 0.886X_6, \ b_{sig.} = 0.399 \quad (7\text{-}31)$$

As seen in Equation (7-30), increasing of the NO_3^- ions concentration (X_1) in the solution has a positive effect on DSC. Increasing of the Na_2SO_4 concentration (X_5) and filtration speed (X_6) negatively influences DSC. Concentration of the $NaHCO_3$, KCl and pH (X_3, X_4 and X_2) practically does not influence the value of DSC, though the common effect of pH and $NaHCO_3$ (X_2X_3) is positive and considerable.

Table 7-7. The matrix of the Fractional Factorial Design and the obtained results

N_0 of experiment	X_1	X_2	X_3	X_4	X_5	X_6	X_2X_3	Y_1	Y_2	Y_3
1	+	+	+	+	+	+	+	11.9	19.53	60.92
2	-	+	+	-	-	-	+	12.4	17.60	70.45
3	+	-	+	-	+	-	-	11.2	19.58	57.23
4	-	-	+	+	-	+	-	8.9	15.84	56.40
5	+	+	-	+	-	-	-	12.6	22.25	56.63
6	-	+	-	-	+	+	-	8.8	15.05	58.49
7	+	-	-	-	-	+	+	12.0	19.32	62.41
8	-	-	-	+	+	-	+	12.0	17.40	68.96

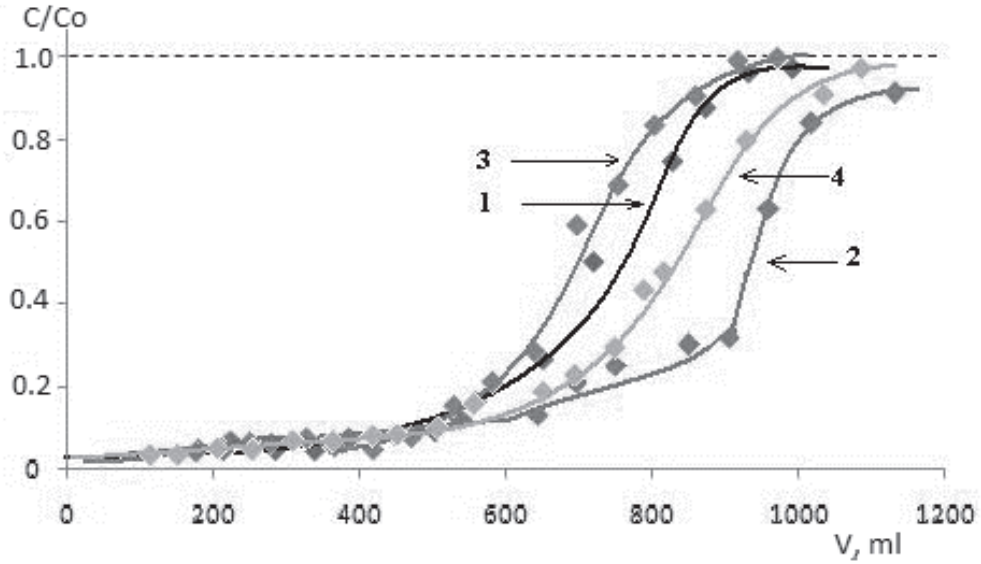

Figure 7-20. Breakthrough curves for adsorption of nitrate/nitrite ions in experiments 1-4 of Table 7-7.

As expected, the increase of $NaNO_3$ concentration, influences positively, but increasing the Na_2SO_4 concentration and the speed of filtration has a negative effect on total sorption capacity (TDSC) of the Cr(III)- containing AV-17 (Eq.(7-31)). The negative influence of the Na_2SO_4 is explained by the shifting of equilibrium (7-26) to the left. Unexpectedly there is a positive and significant influence of KCl concentration (X_4) on the value of the TDSC (Eq.(7-31)).The influence of KCl, probably, is indirect, through the process (7-27). The higher the Cl^- concentration in solution, the higher is the content of Cl^- in the Cr(III)- containing polymer phase and the lower is the content of SO_4^{2-} ions. The existence of $NaHCO_3$ in solution and the value of pH in the examined range of variation (Table 7-6), does not influence the value of the TDSC. But, as you will see below, these factors influence the filtrate pH, which varies between 7.7 and 8.3 in the experiments 1-8 (Tab. 7-7).

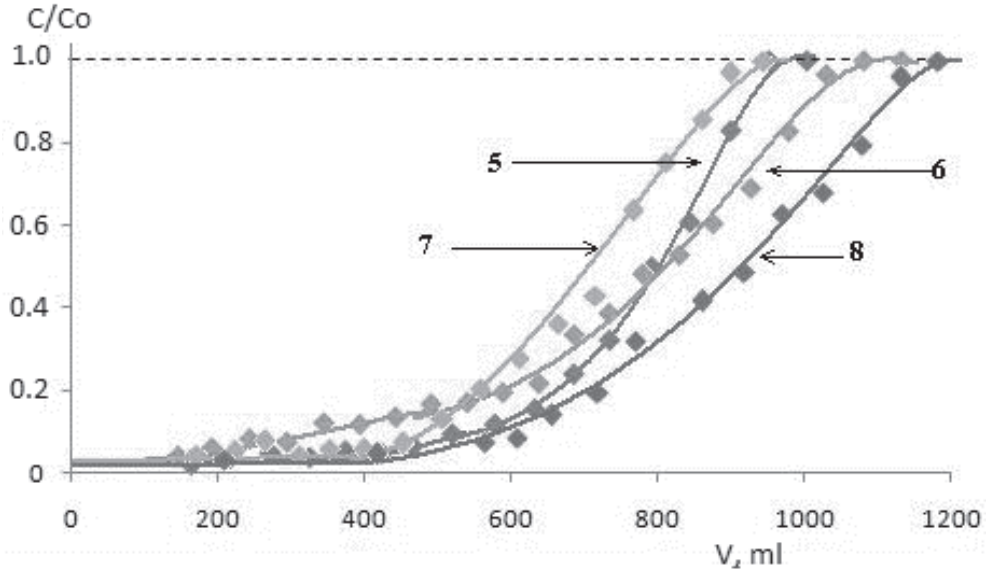

Figure 7-21. Breakthrough curves for adsorption of nitrate/nitrite ions in experiments 5-8 of Table 7-7.

All investigated factors in part do not influence the relative speed of sorption, but $NaHCO_3$ and pH in common (X_2X_3), positively influences (Eq. 7-32).

$$Y_3=61.454 + 4.232X_2X_3, \quad b_{sig} .= 2.163 \tag{7-32}$$

Equations (7-30) and (7-31) enable the planning of the optimization of the parameters DSC and TDSC. We have optimized DSC using equation (7-30). In the optimizing experiments the temperature was 20°C, the mass of Cr(III)-containing AV-17 was 2.5 g, and the pH of the solution was 6.5. In the $NaNO_3$ solution was not added KCl and $NaHCO_3$.

Table 7-8. Nitrate ions removal optimizing

No of Experiment	X_1	X_5	X_6	Y_1	Y_2	Y_3
Step	+5	-0.25	0			
9	65	1.25	1	-	-	-
10	70	1.0	1	-	-	-
11	75	0.75	1	22.80	35.90	63.51
12	80	0.5	1	-	-	-
13	85	0.25	1	28.20	43.20	65.28
14	90.	0	1	-	-	
15	95	0	1	34.96	56.42	61.96

The experiments were performed by the moving on the gradient method [25] in the conditions indicated in Table 7-8. The obtained breakthrough curves 11, 13 and 15 (Fig. 7-22)

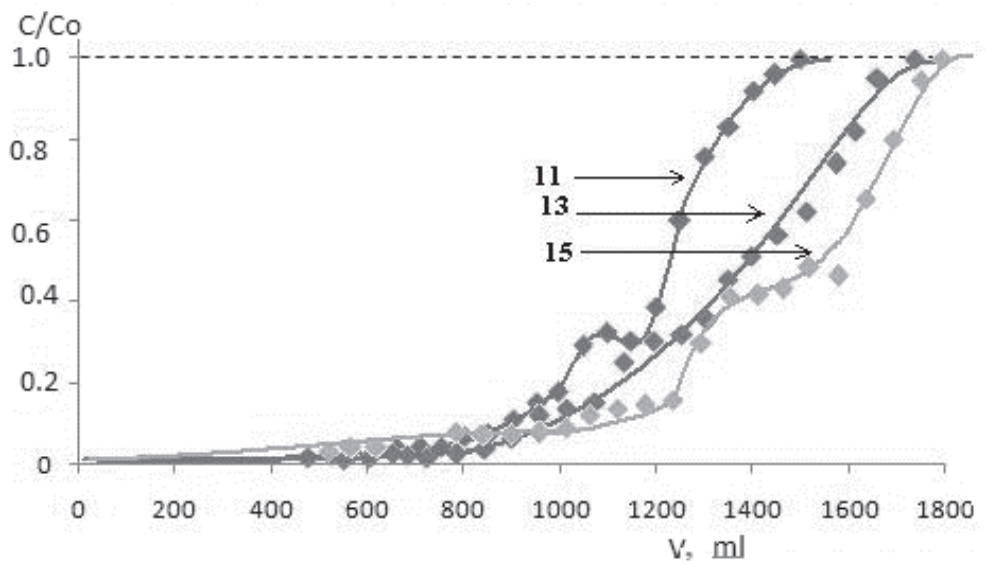

Figure 7-22. Breakthrough curves for adsorption of nitrate/nitrite ions in experiments 11, 13 and 15 of Table 7-8.

for adsorption of nitrate/nitrite ions were obtained according to the conditions corresponding to the experiment number (Tab. 7-8). The calculated sorption parameters are shown in Table 7-8. From the data in Table 7-8 it can be seen that the maximum value of DSC was not reached.

This occurred because the growth of the NO_3^- ions concentration was limited at 95 mg/l. However, the results obtained in the optimization are much higher than those obtained in the first phase of the study (Tab. 4-7). These results confirm that the planning of the experiment is entirely correct. It should be noted that in the experiments of optimization the pH of the filtrate has increased gradually to 9. Increasing pH of the filtrate is due to the process (7-25) and the absence of $NaHCO_3$ in the system. The results obtained in this section have enabled the development of technology for the removal of nitrate and nitrite ions from water [143].

7.4. Phosphate sorption on polymer modified with Cr(III) compounds

Although phosphates in household use are prohibited in some countries, they are still widely used in other countries. But phosphorus compounds are used in many other areas of science and technology. The removal of phosphate excess from various categories of waters using sorption methods requires obtaining selective sorbents and investigation of sorbent-sorbate interactions.

It is known that intensive farming requires the use of different mineral fertilizers. A special role belongs to phosphate fertilizer. The application of phosphorus-containing fertilizers caused significant water eutrophication problems that present a danger to human and environmental health. Unlike other types of fertilizers, fertilizers containing phosphate ions in soil form a different complex chemical equilibrium. In soil a part of the phosphate ions is in solution, another part is labile bonded with soil and the third part of phosphate ions is non-labile bonded with soil:

$P_{solution} \leftrightarrow P_{labile} \leftrightarrow P_{non\text{-}labile}$. Even in the solution, there is a balance of various species of particles containing P(V): $H_3PO4 \leftrightarrow H_2PO_4^- \leftrightarrow HPO_4^{2-} \leftrightarrow PO_4^{3-}$. These equilibria depend on many factors, but mostly they are dependent on the phosphate concentration, pH of the solution and nature of the soil (sorbent). There are many research papers dedicated to the interaction of the phosphate ions with soil as a sorbent. Most of them take into account the particularities of soil in different geographical areas. Usually, the interaction of phosphate ions with the soil is investigated by means of sorption. Here are some works of this kind. Sorption and desorption of phosphate ions on different Philippines soil samples have been investigated [144]. It was shown that the soil with vermiculite and halloysite as the dominant clay minerals had the higher sorption capacity of phosphate ions. In another article [145] it was shown that the total sorbed and exchangeable P on Portuguese soils was described by the modified Freundlich sorption model while the non-exchangeable P was described by the Temkin model. The Langmuir sorption model is also provided to fit the data for non-exchangeable P. The amount of the total sorbed P required to obtain 0.2 mg P/L in solution range from 5.3 to 819 mg P/kg. At this concentration exchangeable and non-exchangeable P values varied from 62.4 to 536.6 and from 0.4 to 322.1 mg P/kg respectively. As expected, phosphorus sorption isotherms varied from soils which varied in mineralogy, texture, and past history of phosphate fertilization [146]. Phosphate sorption isotherms were obtained for three acid highly weathered soils of Sierra Leone, by equilibrating air-dry samples for 24 h with 0.01 M KH_2PO_4 solution at 25 °C [147]. The Langmuir and Temkin equations were used to evaluate the sorption capacities for phosphate. Phosphate sorption maxima of 2439, 2137 and 1429 mg/kg soil were calculated. There was investigation of the effect of citrate and tartrate on phosphate adsorption by amorphous ferric hydroxide [148]. It appeared as though tartrate at 10^{-4} mol/L has no effect on P adsorption up to 750 mg P/g ferric hydroxide adsorbed.

It is important to realize that excessive use of phosphate fertilizers could lead to increased phosphorus concentrations in surface waters. And consequently - the increased abuse of flora in water. Many water sources are polluted with wastewater containing phosphorus compounds. An excess of phosphorus (P) is the most common cause of eutrophication of freshwater resources. Thus, it is very important to reduce the concentration of P to prevent harmful algal blooms. The development of the technology of water purification from phosphate is an actual problem. The sorption methods of water purification from phosphate are quite promising. There was investigation of the effects of contact time of iron-zirconium sorbent, the initial concentration of phosphate solution, temperature, pH of the solution, and ionic strength on the efficiency of phosphate removal [149]. It was shown that the adsorption data are fitted well to the Langmuir model with the maximum P adsorption capacity estimated to 24.9 mg P/g at pH 8.5 and 33.4 mg P/g at pH 5.5. The removal and recovery of phosphate from water using a hybrid nanocomposite containing aluminium nanoparticles (HPN) have been investigated [150]. The HPN-Pr removes 0.80±0.01 mg P/g in a pH interval between 2.0 and 6.5. The sorption mechanism was described by the Freundlich sorption model. Three composite adsorbents, sulfate-coated zeolite, hydrotalcite, and activated alumina were characterized and employed for the removal of phosphate from aqueous solution using equilibrium and kinetic batch experiments [151]. The SEM, FT-IR spectroscopy, and X-ray diffraction spectrum were used to study the surface characteristics of the coated layer. The adsorption of phosphate followed both Langmuir and Freundlich isotherms. The sulfate-coated zeolite was better for phosphate removal compared to hydrotalcite and activated alumina. The adsorption of phosphate was considered to take place mainly by ion exchange. The kinetic data followed a pseudo-second-order kinetic model [151].

In this section there is discussion of the results of the phosphate ions sorption investigation on the Cr(III)-containing strongly basic cross-linked ionic commercial polymer AV-17. Sorption of anions as a result of anion exchange is practically not selective. Sorbent AV-17 (Cr) is capable of sorbing selective phosphate ions. The selectivity of the composite is due to the substitution of SO_4^{2-} ions by molecules or ions that are able to coordinate with metal cations. The choice of the Cr (III) -polymer composite as a sorbent is due to the high kinetic stability of the metallic compounds in the polymer phase. For comparison, phosphate ions sorption has been studied on AV-17(Cl) as well. These sorbents have good hydrodynamic properties, possess selective sorption of phosphate ions and are able to be used cyclically after regeneration. On the other hand, the investigated systems may serve, to some extent, as a model of the behaviour of the phosphate ions in different types of soil as a sorbent. Before the investigation of sorption, the polymer was modified with Cr(III)-containing compounds according to .reference [87] using $KCr(SO_4)_2{*}12H_2O$. For investigation [152], AV-17(Cr) containing 35 mg Cr/g there was used in the form of ultrafine particles of jarosite type compounds $R_4N[Cr_3(OH)_6(SO_4)_2]$ [152]. There were prepared solutions of phosphate using $Na_3PO_4{*}12H_2O$. The concentration of P(V) in the solution was determined by photocolorimetry [26] using NH_4VO_3 and $(NH_4)_6Mo_7O_{24}{*}4H_2O$. In order to adjust the pH of the solutions H_2SO_4 and NaOH were used. All the reagents were of analytical grade.

As shown in Figure 7-23, the phosphate sorption on AV- 17(Cl) depends much on the pH of the solution. In weak acid solutions the phosphate sorption on AV-17(Cl) takes place according to Equation (7-33):

$$R_4NCl + H_2PO_4^- \leftrightarrow R_4NH_2PO_4 + Cl^- \quad (7\text{-}33)$$

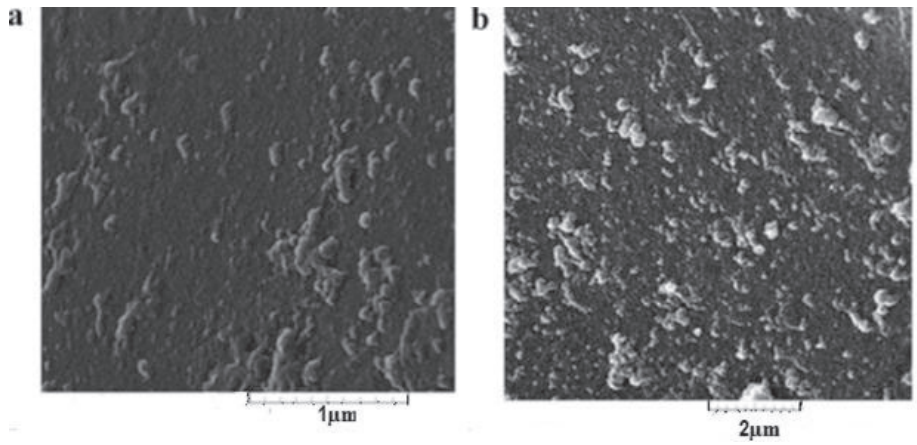

Figure 7-23. SEM images of the Cr (III)-containing particles on the surface (a) and in the volume (b) of an AV-17(Cr) composite granule.

In weakly alkaline solutions, the phosphate sorption on AV-17(Cl) is much lower and takes place specifically in accordance with Equation (7-34):

$$2R_4NCl + HPO_4^{2-} \leftrightarrow (R_4N)_2HPO_4 + 2Cl^- \quad (7\text{-}34)$$

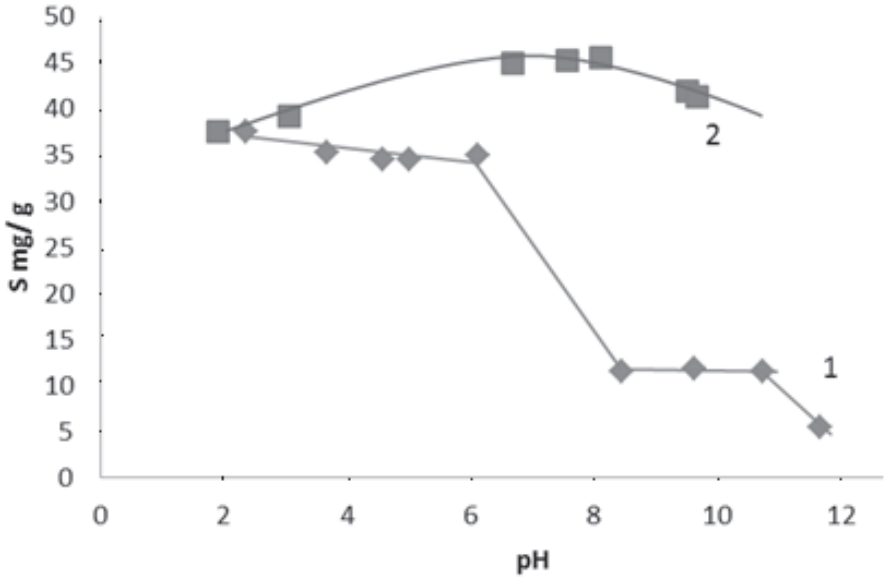

Figure 7-24. Phosphate sorption depending on pH solution on sorbent: 1 – AV-17(Cl), and 2 – AV-17(Cr).

The dependence on the pH of the sorption of phosphate looks quite different in the case of composite AV-17(Cr) (Fig. 7-24). In the pH range 2-10 of solutions, phosphate sorption on composite AV-17(Cr) does not decrease, but on the contrary, increases slightly. This demonstrates that the mechanism of phosphate sorption on the composite AV-17(Cr) differs from that on the AV-17(Cl).

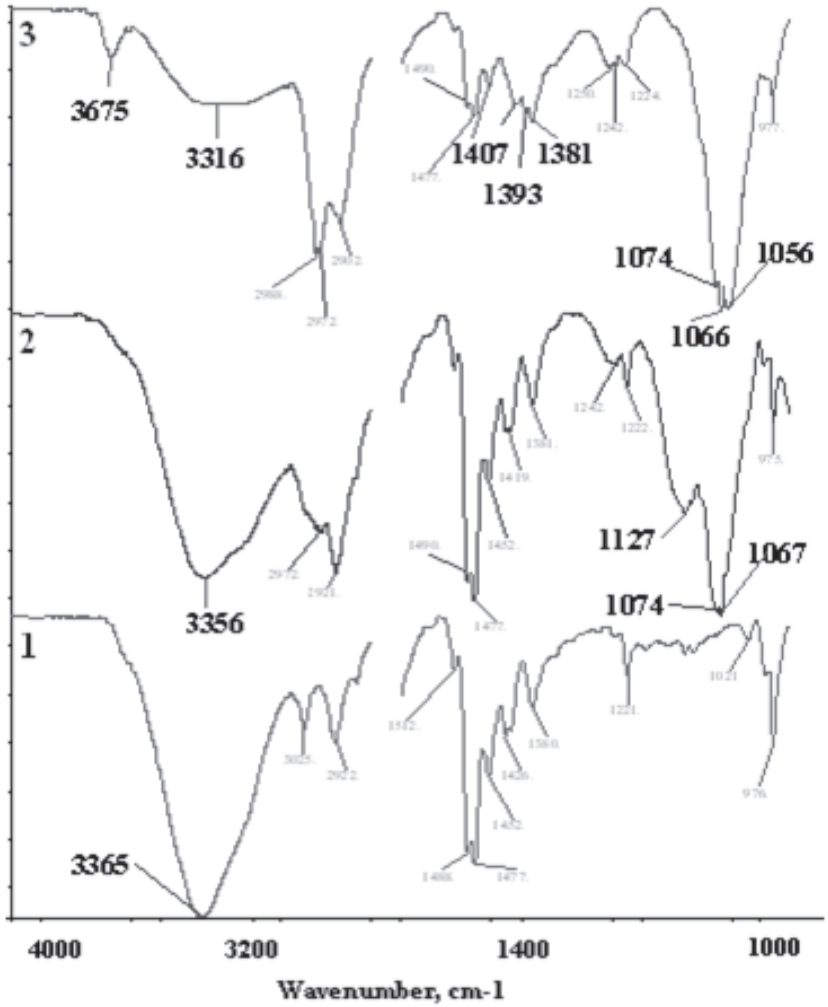

Figure 7-25. FTIR spectra of the sorbent: 1 – AV-17(Cl), 2 – AV-17(Cl) after phosphate sorption in solution with pH 4.6, and 3 – after phosphate sorption in solution with pH 10.

Valuable information about the interaction of the phosphate ions with the sorbent AB-17(Cl) and the composite AV-17(Cr) gives FT-IR spectra (Figs.7-25 and 7-26). In the FTIR spectrum of the sorbent AV-17(Cl), which was in contact with the phosphate solution at pH 4.6, appear two close spectral lines at 1074 and 1067 cm^{-1} and a line at 1127 cm^{-1} (Fig.7-25). In the spectrum of the sorbent AV-17(Cl), which was in contact with the phosphate solution at pH 10, appear three close lines at 1074, 1067 and 156 cm^{-1} and a line at 3675 cm^{-1} (Fig.7-25). In this spectrum a line at 1259 cm^{-1} also appears. According to the references [153, 154], the absorption spectral lines at 1074 and 1067 cm^{-1} in the FT-IR spectrum of the sorbent AV-17(Cl), which absorb phosphate from solution with pH 4.6, belong to $H_2PO_4^-$ but may correspond to the HPO_4^{2-} ions. The state, at least, of a part of phosphate ions in the sorbent phase AV-17(Cl), which was in contact with the solution with pH 10, differs from that with pH 4.6. In the phase of AV-17(Cl), which was in contact with solution with pH 10, there are HPO_4^{2-} ions in which the P=O group does not form H-bonds (line at 1250 cm^{-1}). Also, in this sorbent, the OH group of HPO_4^{2-} ion occupies a special position (line at 3675 cm^{-1}) unlike the OH groups of $H_2PO_4^-$ ions. It is possible to form in the sorbent phase a not too large amount of the phosphate oligomers.

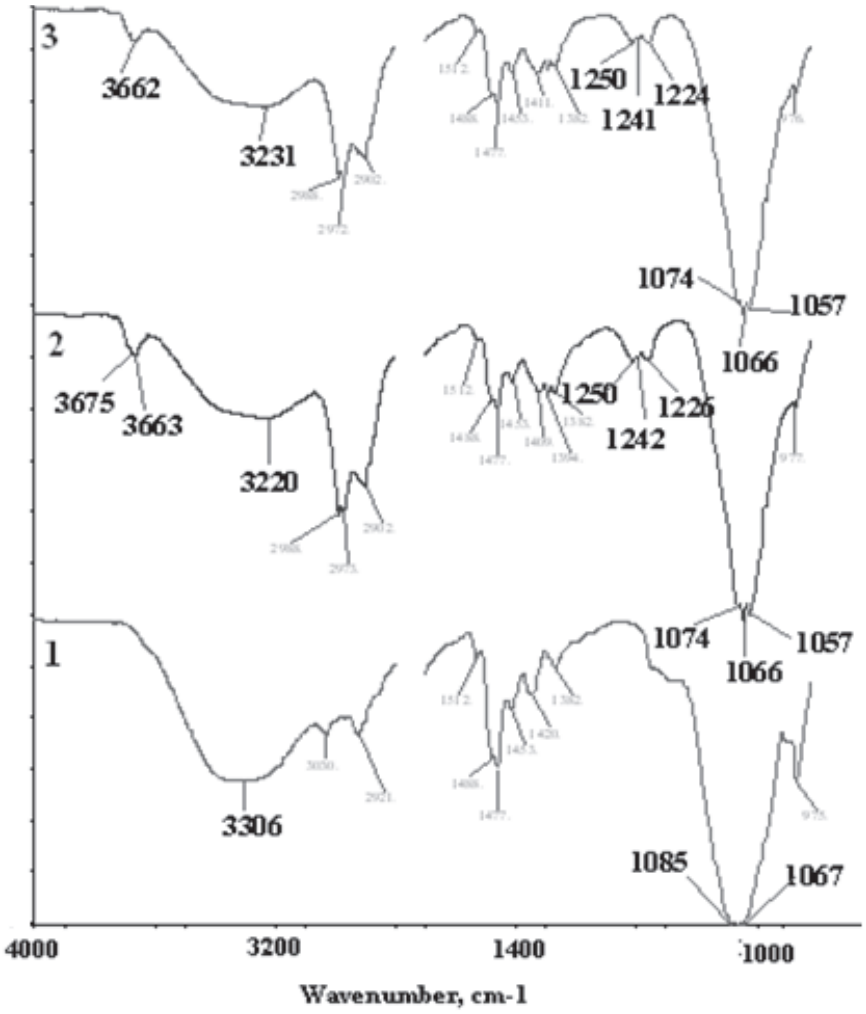

Figure 7-26. FTIR spectra of the composite: 1 – AV-17(Cr), 2 – AV-17(Cr) after phosphate sorption in solution with pH 4.7, and 3 – after phosphate sorption in solution with pH 8.5.

The FTIR spectra of the composite AV-17(Cr) which has been in contact with phosphate solutions with pH 4.7 and pH 8.5 (Fig.7-26), are similar to the spectrum of sorbent AV-17 (Cl), which contacted with the solution with pH 10. Absorption bands around 1000 cm^{-1} of the composite AV-17(Cr), containing phosphate are similar to those of the composite that does not contain phosphate. However, as these bands are in the spectrum of the sorbent AV-17 (Cl), which retained the phosphate from the solution with pH 10, in which there are no SO_4^{2-} ions, the result is that they belong to HPO_4^{2-} ions and maybe to phosphate oligomers. From data of FTIR spectra we can do the main conclusion that whatever the solution pH, the state of the phosphates in the AV-17(Cr) phase is similar. This explains the phosphate sorption on AV- 17(Cr) depending on pH (Fig.7-24). Thus, processes of sorption of phosphates on the composite AV-17(Cr) occur (Fig.7-24). Thus, processes of sorption of phosphates on the composite AV-17(Cr) occur predominantly according to the mechanism, expressed by Equations (7-35) and (7-36):

$$R_4N[Cr_3(OH)_6(SO_4)_2] + 2H_2PO_4^- = R_4N[Cr_3(OH)_6(HPO_4)_2] + 2SO_4^{2-} + 2H^+ \quad (7\text{-}35)$$

$$R_4N[Cr_3(OH)_6(SO_4)_2] + 2HPO_4^{2-} = R_4N[Cr_3(OH)_6(HPO_4)_2] + 2SO_4^{2-} \quad (7\text{-}36)$$

As it can be seen from Equations (7-35) and (7-36), in the phase of the composite, the dihydrogenophosphate ions are destroyed, and the solution becomes acidulated. Indeed, when the sorbent AV(Cr) was in contact with the phosphate solution, the pH decreased. In Equations (7-35) and (7-36) we can also see that regardless of the pH of the solution, the mechanism of interaction of the phosphate ions with the chromium compounds in the polymer phase is the same.

As not all groups of R_4N^+ of the polymer are in the composition of the jarosite mineral type compounds, the remaining R_4NCl groups take part in the processes which are expressed by Equations (7-37) and (7-38):

$$(R_4N)_2SO_4 + 2H_2PO_4^- \leftrightarrow 2R_4NH_2PO_4 + SO_4^{2-} \quad (7\text{-}37)$$

$$(R_4N)_2SO_4 + HPO_4^{2-} \leftrightarrow (R_4N)_2HPO_4 + SO_4^{2-} \quad (7\text{-}38)$$

This conditioned the passage of the phosphate sorption on composite AV-17(Cr) through a weak maximum in the function of the pH of the solution.

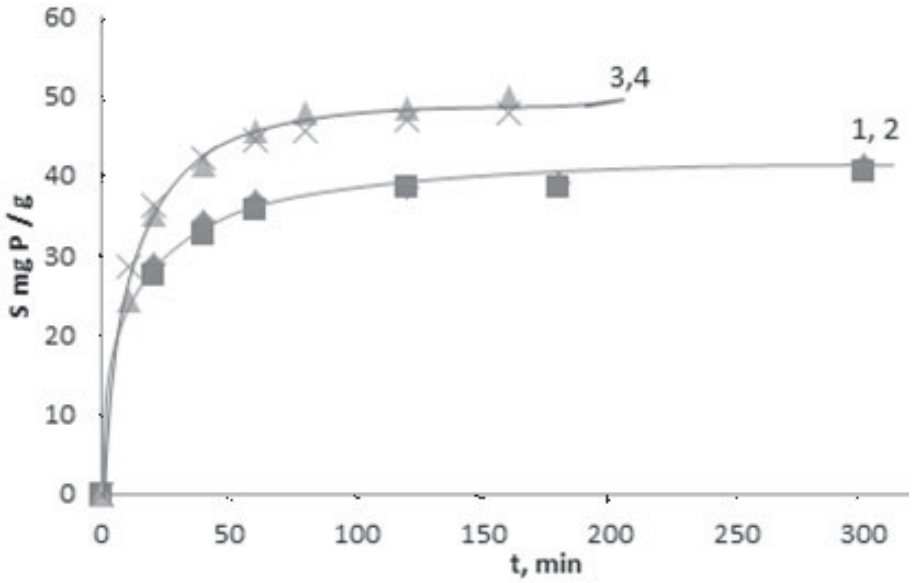

Figure 7-27. Integral kinetic curves of phosphate sorption on AV-17(Cl) at 20°C: 1 – experimentally obtained, 2 – calculated with the PSO kinetic model; and at 54°C: 3 – experimentally obtained and 4 – calculated with the PSO kinetic model.

The integral kinetic curves of phosphate sorption on AV-17(Cl) at 20 and 54°C and on composite AV-17(Cr) at 16 and 60°C are shown in Figures 7-27 and 7-28. After a visual analysis of the curves of these figures, one can at once make 2 conclusions:

1. Sorption of phosphate on composite AV-17(Cr) is much more dependent on temperature than on AV- 17(Cl). This shows that the sorption on AV-17(Cr) predominantly takes place due to the complex formation and not due to the ion exchange, a process that is little affected by temperature.

2. In 300 minutes of the sorbent contact with the solution, the phosphate sorption on the composite AB-17(Cr) does not reach equilibrium. This proves again that sorption on the composite occurs, mainly, due to a chemical process. As it is known, the ligands exchange in the chromium (III) complexes is a slow process.

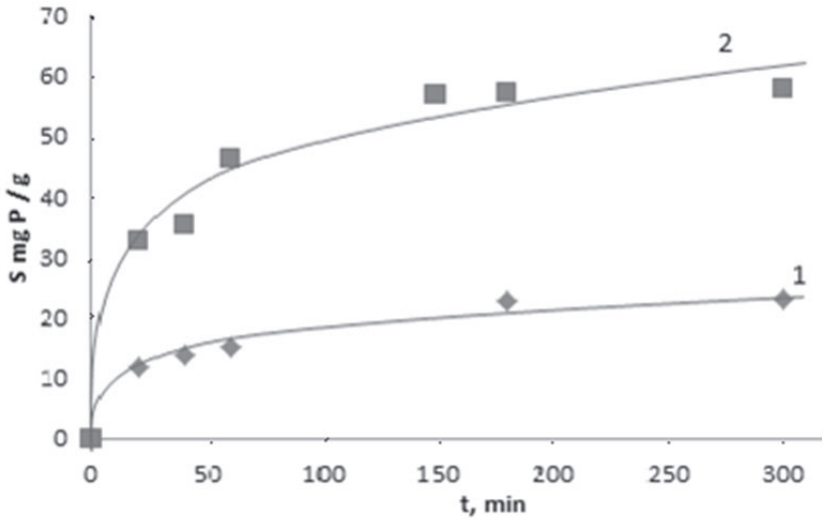

Figure 7-28. Experimentally obtained integral kinetic curves of phosphate sorption on AV-17(Cr) obtained at 15°C (1) and 60°C (2).

In order to investigate the kinetics mechanism, that controls the sorption process of phosphate on AV-17(Cl) and composite AV-17(Cr), the nonlinear forms of the pseudo-first-order (PFO) kinetic model and the pseudo-second-order (PSO) kinetic model [116, 117] were used to fit the experimental data. The nonlinear form of the integrated PFO kinetic model is described by Equation (4-1). The value of k_1 was determined using the linear form of the PFO kinetic model which is expressed by Equation (4-2). The nonlinear form of the PSO kinetic model is expressed by Equation (4--3). The linear form of the PSO kinetic model is expressed by Equation (4-4). The rate constant k_1 (min^{-1}) and *Se* - the amount of phosphate adsorbed at equilibrium (mg P/g), in the PFO kinetic model were determined using Equation (4-2). The rate constant k_2 ($g*mg^{-1}min^{-1}$) and *Se* in the PSO kinetic model were detrmined using Equation (4-4).

To explain the diffusion mechanism of the sorption process, the intraparticle diffusion model [155], expressed by Equation (7-39), was used:

$$S_t = k_{id}.t^{0.5} + C_i \tag{7-39}$$

where k_{id} is the intraparticle diffusion rate constant ($g.mg^{-1}.min^{-0.5}$), S_t is the amount of phosphate adsorbed at a time t (mg P/g) and C_i is a constant that gives an idea about the effect of boundary layer thickness, which means the larger the intercept, the greater is the contribution of the film diffusion in the rate-limiting step.

On the other hand, to determine the sorption limiting step, we have the graph Equation (7-40) [118]:

$$-ln(1 - F) = f(t), \tag{7-40}$$

where $F = S_t / S_e$ (S_t and S_e are the amounts of phosphate adsorbed at a time t and at equilibrium (mg P/g), respectively), t is time (min).

It is known [118], that, the dependency, expressed by Equation (7-40) for the external diffusion processes, should be linear.

Besides the correlation coefficient of determination (R^2), the statistical analysis of errors was performed by the non-linear Chi-square test ($\chi 2$) using Equation (4-7).

The experimental data, regardless of temperature, are well described by the PSO kinetic model for phosphate sorption on AV-17(Cl) only: k_2 =0.00267 $g.mg^{-1}$ min^{-1}, *Se* = 50 mg P/g, at 54°C, and k_2 =0.00228 $g.mg^{-1}$ min^{-1}, *Se* = 41.84 mg P/g, at 20°C. The kinetics of the phosphate sorption on composite AV-17(Cr) at the temperatures 16 and 60°C, is not satisfactorily described either by the PFO kinetic model no by the PSO model. The sorption of a solute, involves three main stages: (i) film diffusion, which is the diffusion of the sorbate particles through the liquid layer to the sorbent surface; (ii) transport of the sorbate particles from the surface to the interior of the sorbent granules, called intraparticle diffusion, or inner diffusion; and (iii) sorption onto the active centres of the sorbent. Usually, the absorption rate is controlled by the first two steps, the last one being very fast, in the case of physical sorption. In the case of chemisorption, the rate-limiting step could be the rate of chemical reaction.

For phosphate sorption at 20 and 54°C on sorbent AV- 17(Cl) the *St* dependence on $t^{0.5}$ is not a straight line which passes through the origin (Fig.7-29). This shows that inter-particle diffusion is not the only rate-controlling step, the boundary layer diffusion having a contribution. Likewise, the dependence -ln(1-F) = f (t) confirms this. As shown in Figure 7-30, the dependence - ln(1-F) = f (t) for the sorption onto AV-17 (Cl) at 20 and 54°C at the beginning is linear, then becomes non-linear. So, in the beginning, phosphate sorption rate is determined by external diffusion, and then by mixed diffusion.

The situation is completely different in the case of phosphate sorption on the composite AV-17(Cr). At a temperature of 16°C the *St* dependency on $t^{0.5}$ is a straight line (Fig.7-29) and is described by Equation $St = 0.9375\ t^{0.5} + 8$. This shows that inter-particle diffusion is the rate-controlling step. The dependence - ln(1-F) = f (t) also confirms this conclusion (Fig.7-30).

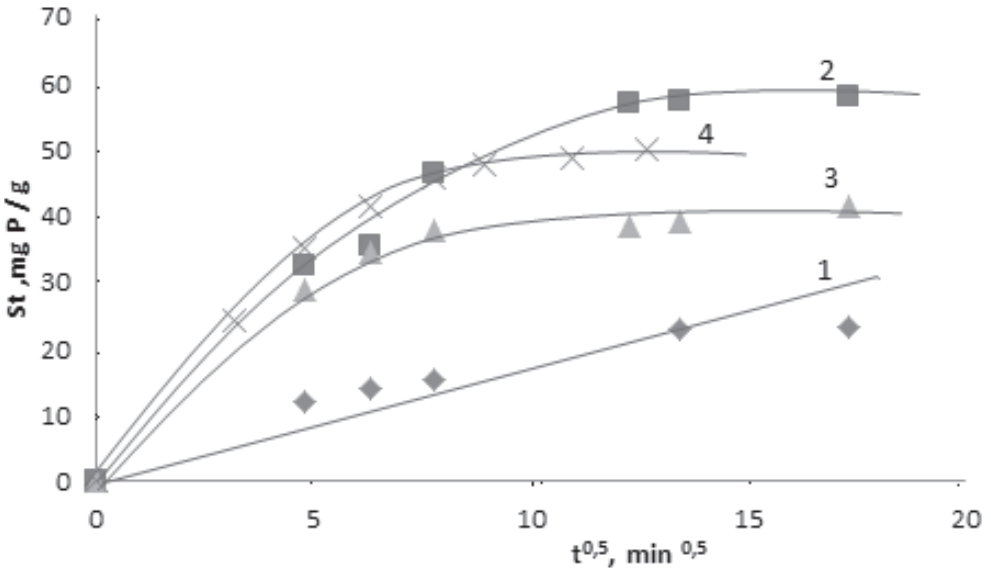

Figure 7-29. Dependence S = f ($t^{0.5}$) for the phosphate sorption on AV-17(Cr) at 16°C (1), 60°C (2), and on the AV-17(Cl) at 20°C (3) and 54°C (4).

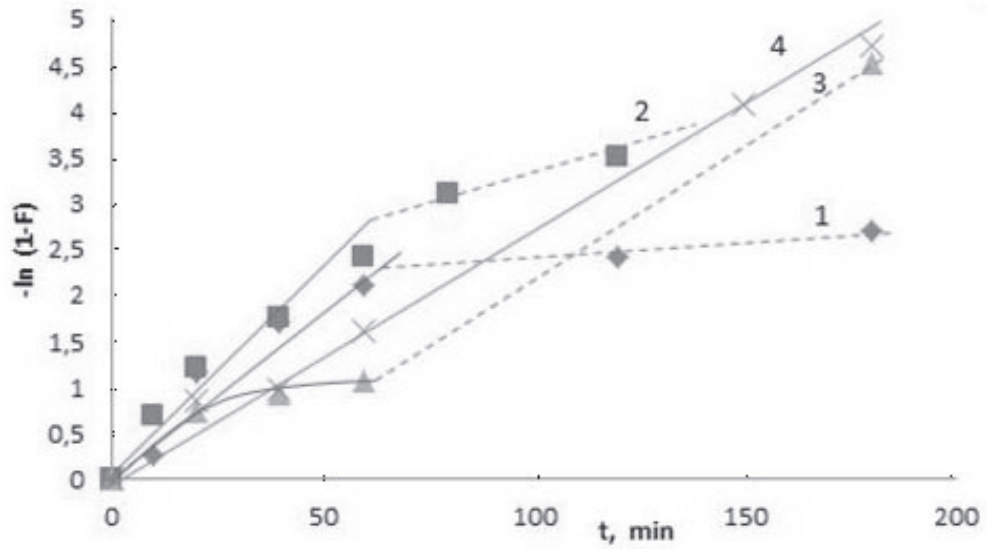

Figure 7-30. Dependence -ln(1-F) = f(t) for the phosphate sorption on AV-17(Cl) at 20°C (1), 54°C (2) and on the AV-17(Cr) at 16°C (3) and 60°C (4).

It sounds strange, but at the temperature of 60°C the situation is reversed. The *St* dependency on $t^{0.5}$ is not a straight line (Fig.7-29), but -ln(1-F) = f (t) is a straight line (Fig.7-30). The rate-controlling step of sorption is the boundary layer diffusion i.e. the external diffusion. This can be explained only if we admit that the phosphate sorption on composite AV - 17(Cr) is a chemical process. At a temperature of 16 °C, the rate of the phosphate-sulfate ligands exchange in the jarosite mineral type compounds is less than the diffusion in the liquid layer surrounding the sorbent bead. With the increasing temperature, the reaction rate of exchange of the ligands grows faster than the rate of diffusion and at 60°C it becomes larger than the external diffusion rate.

Sorption isotherms of phosphate were obtained from solutions on the composite AV-17(Cr) at 16°C. For comparison, the sorption isotherm of phosphate on the sorbent AV-17(Cl) at 20°C has also been obtained. The isotherms were calculated according to different sorption models; Langmuir (Eqs. (1-9) and (1- 10)), Freundlich (Eqs. (1-6) and (1-7)), Sips (Eqs. (7-41) and (7-42)), Dubinin-Radushkevich (Eqs. (7-43) and (7-45)) and BET (Eqs. 7-46 and 7-47).

The Sips isotherm is a combination of the Langmuir and Freundlich sorption models [156, 157]. At a low concentration of sorbate, it corresponds to a Freundlich sorption model, while at a high sorbate concentration; it predicts a monolayer adsorption capacity characteristic of the Langmuir sorption model. The nonlinear form of the Sips isotherm is expressed by Equation (7-41):

$$S = \frac{S_S K_S C_e^{1/n}}{1 + K_S C_e^{1/n}} \tag{7-41}$$

where: S and C_e are the phosphate sorption at the equilibrium (mg P/g) and the phosphate concentrations in solution at the sorption equilibrium (mg P/mL), respectively; K_s is the Sips constant related to the energy of sorption; and S_S is the monolayer sorption capacity (mg P/g).

The constants S and Ks were calculated by the graph of the linear Sips isotherm, Equation (7-42):

$$\frac{C^{1/n}}{S} = \frac{1}{S_S K_S} + \frac{C^{1/n}}{S_s} \tag{7-42}$$

The Dubinin-Radushkevich nonlinear isotherm [156, 157] is expressed by Equation (7-43):

$$S = S_{D\text{-}R} * \exp.\{-K_{D\text{-}R}\,[RT * \ln(1+1/C_e)]^2\} \tag{7-43}$$

where S is the amount of adsorbed phosphate (mg P/g), $S_{D\text{-}R}$ is the maximum adsorption capacity of the ions (mg/g), $K_{D\text{-}R}$ is the Dubinin-Radushkevich isotherm constant (mol^2/kJ^2), Ce is the equilibrium concentration of phosphate (mg P/mL), R is the constant (8.314 J/mol.K), and T is the absolute temperature (K). The Dubinin- Radushkevich isotherm constant, $K_{D\text{-}R}$, is related to the mean free energy of adsorption, E (kJ/mol), defined as the free energy when one mol of cations is transferred from infinity in solution to the surface of solid sorbent and computed using Equation (7-44):

$$E = \frac{1}{(2K_{D-R})^2} \tag{7-44}$$

The value of E is used to estimate the type of adsorption. When E is 1-8 kJ/mol, the sorption is determined by physical forces. The values of E between 9 and 16 kJ/mol are characteristic for ion exchange processes, and more than 16 kJ/mol-for chemisorption.

The constants $S_{D\text{-}R}$ and $K_{D\text{-}R}$ were calculated by the graph of the linear Dubinin-Radushkevich isotherm, Equation (7-45):

$$\ln S = \ln S_{D\text{-}R} - K_{D\text{-}R}\,[RT * \ln(1+1/C)]^2 \tag{7-45}$$

The BET sorption model is based on the idea of multilayer adsorption theory [158]. Although the BET sorption model, just like the Langmuir model, was developed for sorption in the gas phase, it can be used for sorption in the liquid phase [159, 160]. Only in this case, in the equation of the isotherm, instead the saturated vapour pressure is used the concentration of the saturated solution of sorbate (Eq.7-46):

$$S = \frac{S_{BET}\, K_{BET}\, C_e\, S_e}{(C_{s-}\, C_e)[C_s + (K_{BET}-1)C_e]} \tag{7-46}$$

The constants S_{BET} and K_{BET} were calculated by the graph of the linear BET isotherm, Equation (7-47):

$$\frac{C_e}{S(C_s - C_e)} = \frac{1}{S_{BET}K_{BET}} + \frac{(K_{BET}-1)C_e}{S_{BET}K_{BET}C_s} \tag{7-47}$$

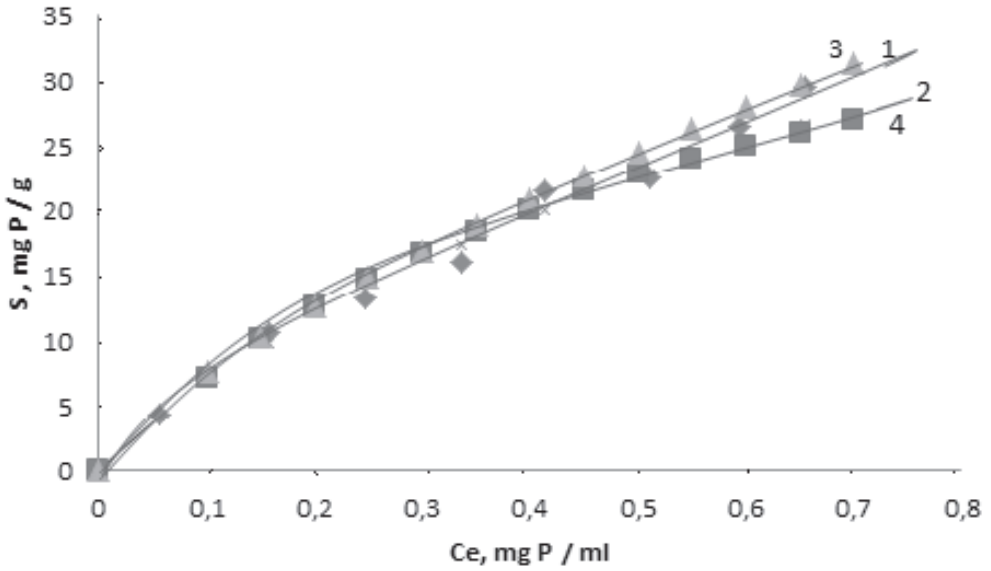

Figure 7-31. Equilibrium sorption isotherms of phosphate on AV-17(Cl): obtained experimentally (1) and calculated by the Langmuir (2), Freundlich (3), and Dubinin-Radushkevich (4) sorption models.

The experimental isotherm of phosphate sorption on AV-17(Cl), obtained at the contact of the sorbent with the solution for 24 hours at 20 ^{o}C, is shown in Figure 7-31 (curve 1). The isotherm was constructed and calculated with the Langmuir, Freundlich, Sips and Dubinin- Radushkevich sorption models (Fig. 7-31, curve 2-4).

The isotherm's parameters and the value of R^2 and $\chi 2$ are listed in Table 7-9. These parameters show that the isotherm of phosphate sorption onto sorbent AV-17(Cl) is best described by the Langmuir sorption model. This was expected, since the active centres (R_4N^+) of the sorbent AV-17(Cl) energetically, are equivalent. The Freundlich and Dubinin-Radushkevich sorption models satisfactorily describe the sorption isotherm of phosphate on AV-17(Cl), but the Sips model cannot describe the isotherm. The value of E = 16.13 kJ/mol (calculated with Eq.(7-44)), demonstrates that sorption of phosphate on AV-17(Cl) occurs, mainly, through the ion-exchange mechanism.

Table 7-9. Isotherm parameters of the Langmuir, Freundlich, Dubinin-Radushkevich and BET sorption models for the sorption of phosphate

Sorbent	T, ^{o}C	Sorption model	Isotherm parameters	R^2	X^2
AV-17(Cl)	20	Langmuir	S_L = 50 mg P/g K_L = 1.667 L/mg	0.9907	0.136
	20	Freundlich	K_F = 40.447 1/n = 0.725	0.9955	1.030
	20	Dubinin-Radushkevich	S_{D-R} = 63.437 mg/g K_{D-R} = 0.00193	0.9797	0.772
AV-17 (Cr)	16	BET	S_{BET} = 18.11 mg P/g K_{BET} = 4424.78 g/mg	0.9440	0.848

As seen from Figure 7-32, the sorption isotherm of phosphate on the sorbent AV-17(Cr) differs from that of sorption on the sorbent AV-17(Cl). The shape of this isotherm is characteristic for the BET sorption model. The isotherm parameters, calculated according to the BET model, are shown in Table 7-9.

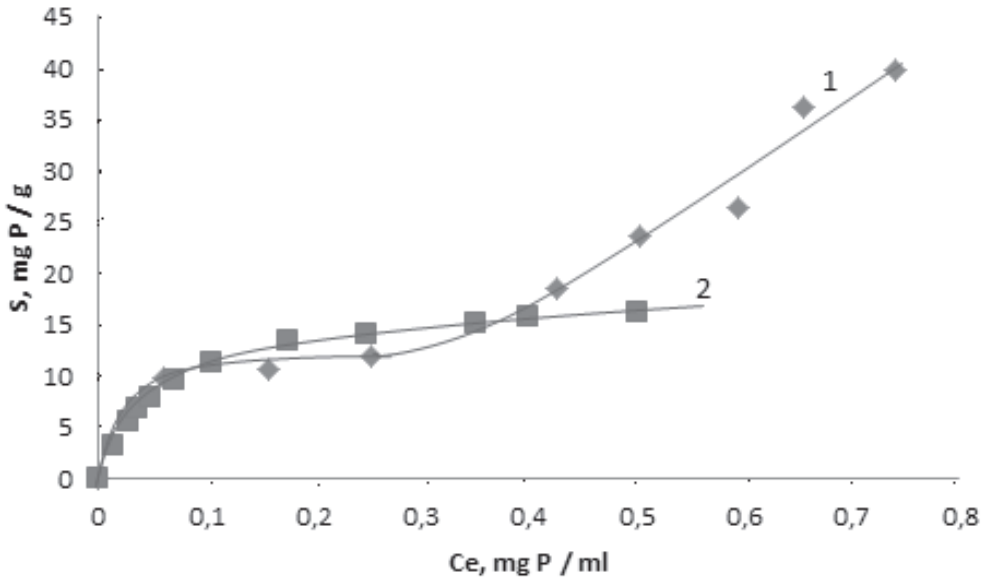

Figure 7-32. Equilibrium sorption isotherm of phosphate on AV-17(Cr): obtained experimentally (1) and calculated by the BET (2) sorption model.

The BET adsorption model describes adequately only a part of the isotherm. This, and, also, the isotherm shape, again proves that the phosphate sorption on the composite AV-17(Cr) is a complex process that includes the exchange of ligands (Eqs. (7-35) and (7-36)), and, to a minor extent, the polyphosphate formation and anions exchange.

To perform optimization of the phosphate sorption on composite AV-17(Cr), first of all, it is necessary to assess the degree of influence of various factors on the process. To evaluate the influence of different factors (concentration of phosphate, Na_2SO_4, KCl, $NaNO_3$, temperature and pH of solution and duration of the polymer contact with solution) the response surface methodology (the G.E.P.Box and K.B.Wilson method) was used [24, 25]. The investigated factors and their levels of variation are shown in Table 7-10. The experiments were conducted according to the matrix of the Fractional Factorial Experiment plan. The influence degree of factors on the studied processes was expressed by the regression equations which were calculated according to [25].

Table 7-10. The factors, their codes and variation levels

Code	Factor	Low level (-)	High level (+)
X_1	Concentration of P, g/L	0.4	0.8
X_2	Temperature, ^{O}C	20	40
X_3	pH	7	8
X_4 (X_1 X_2)	Contact duration of AV-17(Cr) with a solution, h	1	2
X_5 (X_1 X_3)	KCl concentration, mequiv/L	4	8
X_6 (X_2 X_3)	$NaNO_3$ concentration, mequiv/L	4	8
X_4 (X_1 X_2 X_3)	Na_2SO_4 concentration, mequiv/L	4	8

The following responses of the systems, as the results of the averages of two independent experiments, were measured and calculated:

$$Y_1 = 21.966 + 3.351\ X_1 + 3.343\ X_2 + 2.844\ X_4, \qquad b_{sig.} = 1.7542 \qquad (7\text{-}48)$$

where: Y_1 is the sorption of phosphate, (mg P/g);

$$Y_2 = 7.275 - 0.270\ X_2 + 0.440\ X_3 - 0.109\ X_6, \qquad bsig. = 0.0859 \qquad (7\text{-}49)$$

where: Y_2 is the solution pH

From the data of Equation (7-48), it follows that only the phosphate concentration (X_1), temperature (X_2) and duration of contacting of the composite AV-17(Cr) with phosphate solution (X_4), essentially and positively influences the sorption. In the indicated concentration range of Na_2SO_4, $NaNO_3$ and KCl, the coefficients of X_1, X_2, X_5 in the regression equation are insignificant. This shows that the phosphate sorption on composite AV- 17(Cr) is a selective process, which is important for the application of AV-17(Cr) in water purification. On the other hand, the insignificant influence of SO_4^{2-}, NO_3^- and Cl^- ions, the strong influence of temperature and low speed of sorption, strongly

demonstrates that phosphate sorption on the composite AV-17(Cr) is, in fact, a chemical process. The insignificant influence of solution pH (X_3, Eq.(111)) on phosphate sorption confirms the data in Figure 7-24.

The negative influence of temperature on solution pH (X_2 in Equation (7-49)), confirms that during sorption, the dihydrogen phosphate ions are converted into hydrogen phosphate according to Equation (7-35). Equations (7-48) and (7-49) enable planning the optimization of the parameters Y_1 and Y_2. We optimized parameter Y_1. The experiments were performed by moving on the gradient method [25] in the conditions indicated in Table 7-11.

Table 7-11. Phosphate sorption optimizing

Experiment No and step	X_1	X_2	X_3	X_4	X_5	X_6	X_7	Y_1, mg P/g
Step	+ 0.1	+ 5	0	+ 12	0	0	0	-
1	0.7	35	7.5	112	6	6	6	-
2	0.8	40	7.5	124	6	6	6	31.9
3	0.9	45	7.5	136	6	6	6	-
4	1.0	50	7.5	148	6	6	6	36.88
5	1.1	55	7.5	160	6	6	6	-
6	1.2	60	7.5	172	6	6	6	54.9
7	1.3	65	7.5	184	6	6	6	-
8	1.4	70	7.5	196	6	6	6	84.4
9	1.5	75	7.5	208	6	6	6	90.75
10	1.6	75	7.5	232	6	6	6	93.5
11	1.7	75	7.5	244	6	6	6	97.75
12	1.8	75	7.5	256	6	6	6	102.38

During the experiment, the pH of solutions was set at 7.5 and the concentration of the anions SO_4^{2-}, NO_3^- and Cl^- was fixed at 6 mEq./L. The increased level of variables was reasonably stopped. The obtained results are presented in Table 7-11. These data show, that modifying the factors resulted in a considerable increase of phosphate sorption (up to 102,38 mg P/g) by the composite AV-17(Cr). This confirms the validity of the designed experiment and the interpretation of the results obtained previously.

7.5. Ammonium ions sorption on polymer modified with Cr(III) compounds

A prevalent form of pollution of surface waters with nitrogen compounds is their content of ammonium ions. An increased content of ammonium ions in drinking water shows the presence of bacterial contamination and gives the water an unpleasant odour and taste. The constant use of water holding excess ammonium ions leads to a disturbance of the acid-base balance in the body. For this reason, the content of ammonium ions in drinking water is strictly regulated by the hygienic-sanitary state organs. The sources of contamination of surface waters are well known: intensive farming with excessive use of nitrogenous fertilizers, waste from the maintenance of animals, sewage, waters and waste from the meat and marine products processing industry and the decomposition of organic materials that contain nitrogen compounds and waste from the chemical industry.

Ammonium ions in aqueous solutions are in equilibrium with ammonia (Eq.(7-50)):

$$NH_4^+ + H_2O \leftrightarrow NH_3 + H_3O^+ \quad (7\text{-}50)$$

Depending on concentration, pH and temperature, the balance (7-50) may move to the right until the emission of ammonia into the atmosphere takes place [161]. And as we know, ammonia is very toxic. The ammonium ions are hazardous to fish and other creatures of the lakes and rivers, for the ecosystems. Discharges of wastewater that is insufficiently treated by nitrogen compounds are the cause of eutrophication. Considering the above, it is clear that the removal of ammonium is necesary from municipal and industrial wastewater prior to discharge. Various methods for the removal of ammonium ions in water are known. One such method is the chemical oxidation of ammonium nitrogen. The chemistry of oxidation by hypochlorite can be expressed by the following Equations (7-51) and (7-52) [162, 163]:

$$2NH_4^+ + 3NaClO + 2OH^- = N_2 + 3NaCl + 5H_2O \quad (7\text{-}51)$$

$$4NH_4^+ + 3Ca(ClO)_2 + 4OH^- = 2N_2 + 3CaCl_2 + 10H_2O \quad (7\text{-}52)$$

Anaerobic ammonium oxidation (anammox bacterium named *Candidatus Brocadia Anammoxidans*), is an effective ammonium removal process. Anammox oxidize ammonium to nitrogen gas [164, 165]. There are many

investigations in anaerobic oxidation of ammonium ions in water with nitrite ions to form molecular nitrogen by the following overall Equation (7-53):

$$NH_4^+ + NO_2^- = N_2 + 2H_2O. \quad (7\text{-}53)$$

Here are some of them [166-169]. Most of the investigations devoted to eliminating ammonium ions from various categories of water use sorption methods. Methods of eliminating ammonium ions from water using natural and synthetic inorganic sorbents are proposed. It was shown that maximum sorption capacity of the Transcarpathian clinoptilolite toward ammonium evaluated under dynamic conditions varies in the interval 13.56–21.52 mg/g, being significantly higher than determined under static conditions [170]. In another paper [171], it is shown that Transcarpathian clinoptilolite for the removal of ions from aqueous solution attained at an initial ion concentration of 1000 mg/L was 11.6 mg/g. The effectiveness of ion sorption by the clinoptilolite samples decreased somewhat as the fraction size of the solid particles increased from 0.1–0.16 to 1.0–2.0 mm. The Langmuir isotherm gave a more adequate value for the correlation coefficient compared to that for the Freundlich isotherm. The ammonium ions sorption on the natural zeolite, clinoptilolite from Croatia, decreases with an increasing particle size in the range of 1-10 mm [172]. Kinetic studies suggest that ammonium sorption on zeolite could be described more favourably by the pseudo-second-order kinetic model than by the pseudo-first order. The Langmuir sorption model fitted well with the experimental data. The sorption isotherms of the ammonium ions on natural sorbents such as zeolite, glauconite and palygorskite (Ukraine) are best of all described by the Langmuir sorption model [173]. But the sorption isotherm of ammonium on Chinese natural zeolite is better described by the Freundlich sorption model [174]. In the work [175] the optimizing of absorption of ammonium ions from wastewater on natural zeolites was performed. Many articles devoted to the ammonium ions sorption on natural and synthetic inorganic sorbents are reviewed in the Ref.[176]. The sorption of ammonium ions from solutions by natural or synthetic inorganic sorbents is conditioned mainly by the ion exchange process according to Equation (7-54):

$$R\text{-}M^{n+} + nNH_4^+ = R\text{-}nNH_4^+ + M^{n+} \quad (7\text{-}54)$$

The advantages of methods to eliminate ammonium ions from solutions using inorganic sorbent are that many of them are not expensive and the equilibrium sorption process can be established relatively quickly. Disadvantages of these methods are that the ion exchange is a less selective process, usually, sorbents are not stable in an alkaline medium, the phases separation is often difficult, and the sorbent is not rational to be regenerated. This section explores the peculiarities of ammonium ions sorption from solution on a new sorbent [88].

The commercial strongly basic cross-linked ionic polymer (AV-17(Cl)) containing Cr-jarosite type compounds (AV-17(Cr)) has been used. The composite AV-17(Cr) consists of polymer AV-17 in the phase of which, the jarosite mineral type compound was synthesized:

$R_4N[Cr_3(OH)_6(SO_4)_2]$, where **R_4N^+** is a functional group of the polymer. As shown in Figure 7-33, the metal compounds in the phase of sorbent are in the form of ultra-dispersed particles with a very low crystallinity that was confirmed by X-ray diffraction analysis as well. The Cr^{3+} content in the AV-17(Cr) was 32 mg/g. The content of NH_4^+ ions was also determined by photocolorimetry using Nessler reactive and $NaKC_4H_4O_6 .4H_2O$ [26], after contacting of 0.2 g of the sorbent with 100 mL of solution.

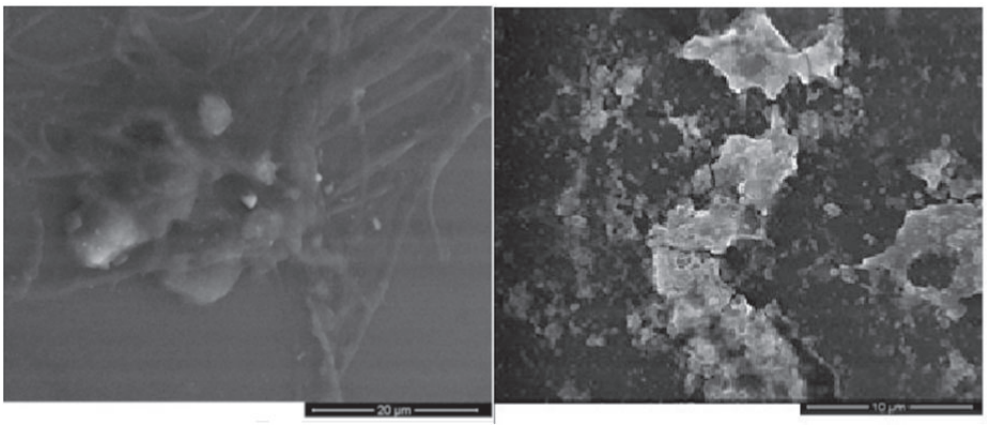

Figure 7-33. SEM images of the Cr(III)-containing sorbent AV-17(Cr).

The absorbent AV-17(Cr) has selective sorption properties towards some anions and molecules due to the coordination process. We propose that sorbent AV-17(Cr) may retain NH_4^+ ions as a result of coordination of $Cr^{3+}$with NH_3 molecules, destroying NH_4^+ cations.

Since the composition of a solution containing an ammonium salt is changing depending on pH, it is obvious that pH will significantly influence the ammonium sorption. Indeed, as shown in Figure 7-34, the sorption of ammonium

ions by sorbent AV-17Cr) depends considerably on the pH of the solution, passing through a maximum and a minimum.

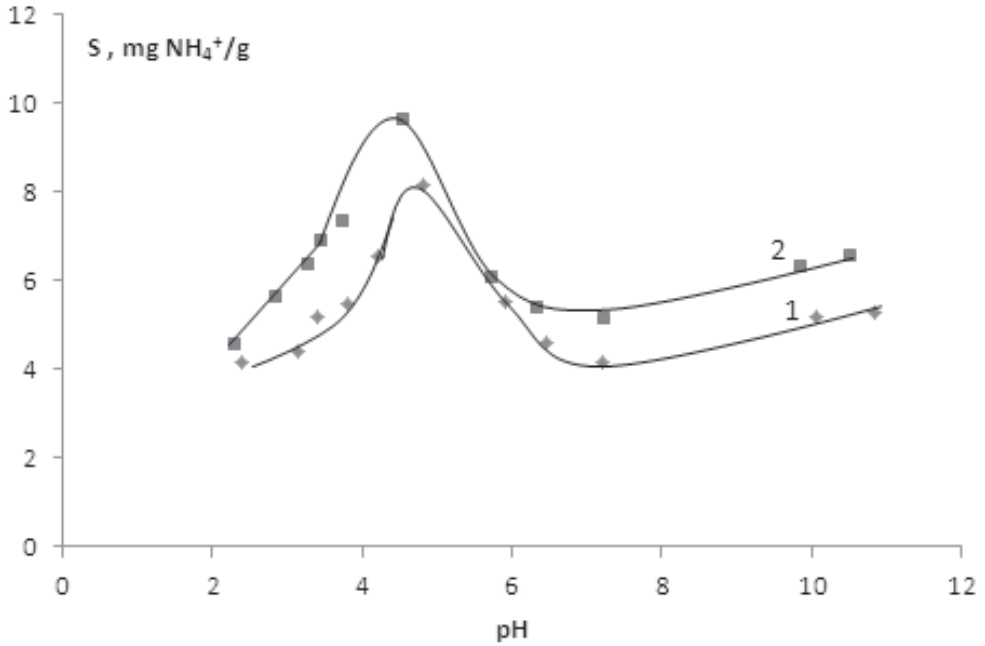

Figure 7-34. Ammonium ions' sorption on AV-17(Cr) as a function of the solution pH at 22 (1) and 50°C (2).

In the article [175], it is mentioned that ammonium ions adsorption on zeolites depends pointedly on the pH of the solution. The sorption of ammonium ions on Egyptian kaolinites depending on the pH passes through the pronounced maximum at pH 7 [177]. But in another article [178] it seems that sorption of ammonium ions on zeolites passes through two maximums (one of the maximums is at pH 8 and a minimum at pH 7) depending on the pH of the solution. In several papers, it is deemed that the sorption of ammonium ions on mineral sorbents (Z-Na+) takes place according to the mechanism of ion exchange (Eq.(7-55)):

$$Z\text{-}Na^+ + NH_4^+ \leftrightarrow Z\text{-}NH_4^+ + Na^+ \quad (7\text{-}55)$$

And the effect of pH on the ammonium ions sorption is conditioned by processes (7-56) and (7-57):

$$Z\text{-}Na^+ + H^+ \leftrightarrow Z\text{-}H^+ + Na^+ \quad (7\text{-}56)$$

$$NH_4^+ + OH^- \leftrightarrow NH_3 + H_2O \quad (7\text{-}57)$$

Probably the absorption of ammonium ions on mineral sorbents is a more complicated process, although the ion exchange is predominant. According to the processes (7-55) to (7-57), sorption of ammonium ions should decrease monotonically with increasing pH of the solution. The changing of solution pH (by adding an acid or hydroxide solution, such as NaOH for example) does not exclude the effect of process (7-56) but only leads to the displacement of it in one side or another.

In investigated systems, we believe that the ammonium ions retention takes place according to some processes. In the polymer phase, we have a part of $R_4N[Cr_3(OH)_6(SO_4)_2]$ and a small part of $H_3O[Cr_3(OH)_6(SO_4)_2]$ compounds. These compounds may take part in the process (7-58):

$$(R_4N, H_3O)[Cr_3(OH)_6(SO_4)_2] + NH_4^+ \leftrightarrow NH_4[Cr_3(OH)_6(SO_4)_2] + (R_4N, H_3O)^+ \quad (7\text{-}58)$$

Adding NaOH solution to change the pH of the system, OH^- ions penetrate faster than Na^+ ions the polymer phase because the polymer matrix contains positive charges (R_4N^+). The OH- ions combining with the H_3O^+, favours the retention of the ammonium by the sorbent AV-17Cr). In solution, depending on pH, the balance (7-59) exists:

$$NH_4^+ + OH^- \leftrightarrow NH_4OH \leftrightarrow NH_3 + H_2O \quad (7\text{-}59)$$

So, with increasing pH, the ammonium ions sorption on the sorbent AV-17(Cr) increases. But at the pH at which takes place the formation of $NH_3 \cdot H_2O$, ammonium (NH_4^+) sorption begins to decrease. From this moment begins the NH_3 complex forming with Cr^{3+} ions of jarosite type compounds (Eq. (7-60)):

$$R_4N[Cr_3(OH)_6(SO_4)_2] + 6NH_4OH \leftrightarrow R_4N[Cr_3(OH)_6(NH_3)_6]^{4+} + 2SO_4^{2-} + 6HOH \quad (7\text{-}60)$$

Since the exchange of ligands in Cr^{3+} compounds is quite slow, the NH_3 sorption rate is also slow. As a result, ammonium NH_4^+ (NH_3) sorption passes through a minimum in a function of the solution pH.

From Figure 7-35(1) it is seen that a part of SO_4^{2-} ions are tridentate bound with Cr^{3+} ions from sorbent (1185, 1099, 1048 cm^{-1}) [36]. But not all R_4N^+ groups of the polymer are part of the composition of the jarosite type compounds. The majority of the sulfate ions are related to the groups forming $(R_4N)_2SO_4$, (Fig.7-35, band at about 1100 cm^{-1}). In the FTIR spectra of the sorbent samples, which retained ammonium from solutions with pH 5-10, adsorption band 1185 cm^{-1} disappeared and band 1048 cm^{-1} is shifted to 1070 cm^{-1}. This shows that a part of ammonium is absorbed in the result of the process (7-60).

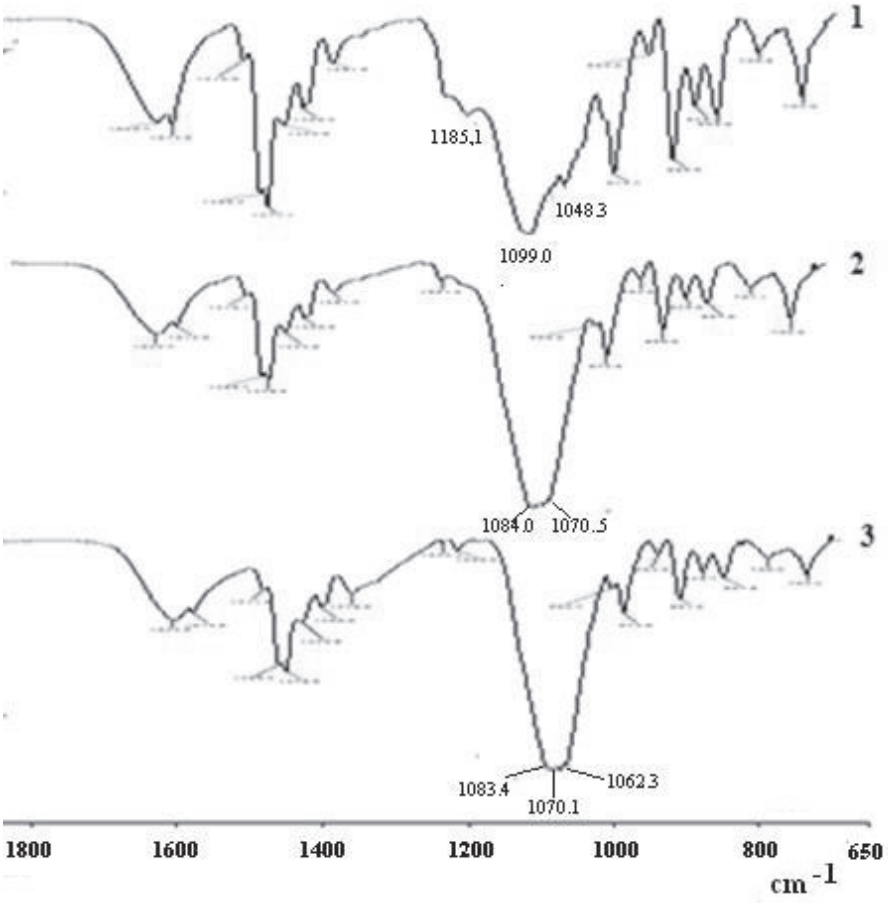

Figure 7-35. FTIR spectra of the AV-17(Cr) after sorption of ammonium ions from solution with pH 2.0 (1), pH 5.0 (2) and pH 10.0 (3).

Sorption kinetics. The integral kinetic curves of ammonium sorption on sorbent AV-17(Cr) at 22^{o}C are shown in Figure 7-36. After a visual analysis of the curves of Figure 7-36, we can make 2 conclusions: 1. Regardless of the pH of the solution, sorption of ammonium on the sorbent AV-17(Cr) is a fairly slow process and equilibrium is not achieved even after 20 hours, and - 2. Kinetic curves confirm that the maximum of ammonia sorption is at the solution pH near 5. FT-IR spectra show that in the solution of pH 5 to 10 some of the sulfate ions in the phase of the composite are substituted by molecules of ammonia. So at least some of the ammonium ions are retained in the composite because of NH_3 coordination with Cr^{3+} ions.

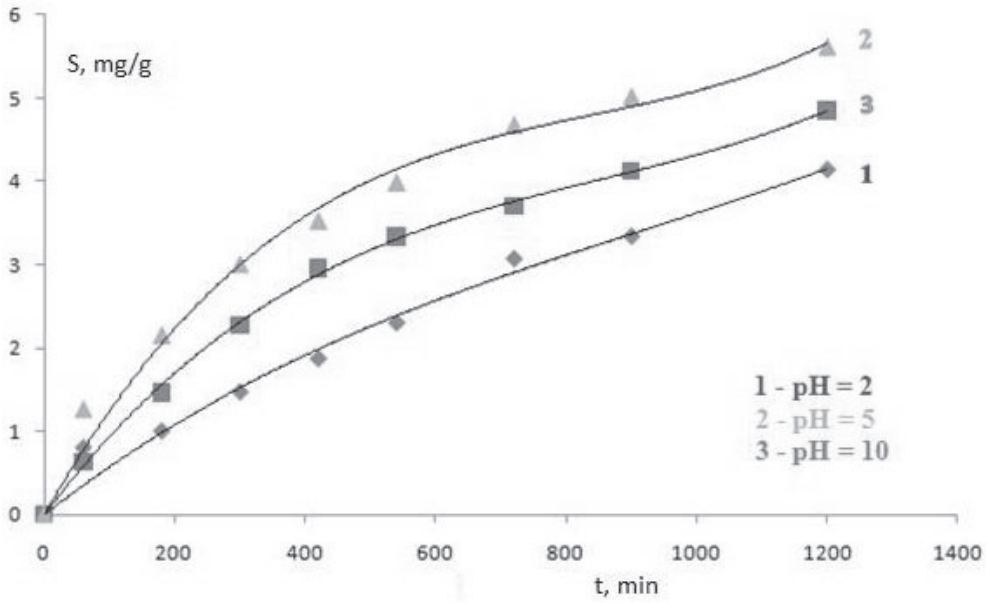

Figure 7-36. Integral kinetic curves of ammonium sorption at 22°C on AV-17(Cr) from a solution with different pH values.

The ammonium sorption balance on mineral sorbents is achieved in different time intervals of the contact of the sorbent with the solution-from 2 hours to 1-2 days [177, 178]. And to be sure of reaching equilibrium, the sorbent was contacted with the solution even at eight days [173]. Although ion exchange is a quick process, and we assume that in the acidic solution sorption of NH_4^+ on sorbent AV-17(Cr) occurs as a result of cation exchange, as shown in Figure 7-36, sorption from solution with pH 2 is slow. This is explained by the fact that the matrix of the organic polymer contains groups with positive charges (R_4N^+).

In order to investigate the kinetic mechanism, which controls the sorption process of ammonium on sorbent AV-17(Cr), the nonlinear forms of the pseudo-first-order (PFO) kinetic model and the pseudo-second-order (PSO) kinetic model [116, 117] were used to fit the experimental data. The nonlinear form of the integrated PFO kinetic model is described by Equation (4-2) and the linear (to calculate the rate constant k_1) form by Equation (4-3). The nonlinear form of the PSO kinetic model is expressed by Equation (4-4) and the linear form by Equation (4-5). The calculated data of the kinetic parameters are shown in Table 7-12.The data in Table 7-12 demonstrates that sorption kinetics of ammonium ions by composite AV-17 (Cr) is described very well by the PFO kinetic model rather than the PSO model. This is well seen in Figures 7-37, 7-38 and 7-39.

Table 7-12. Kinetic parameters of the sorption of ammonium on the sorbent AV-17(Cr)

pH	PFO kinetic model			PSO Kinetic model	
	S_e, mg NH_4^+/g	k_1, min^{-1}	R^2	S_e, mg NH_4^+/g	k_2, g/mg·min
2	5.4	0.0011	0.9765	8.5	$8.01 \cdot 10^{-4}$
5	5.4	0.0028	0.9445	9.35	$1.57 \cdot 10^{-3}$
10	5.4	0.0015	0.9476	6.98	$1.63 \cdot 10^{-3}$

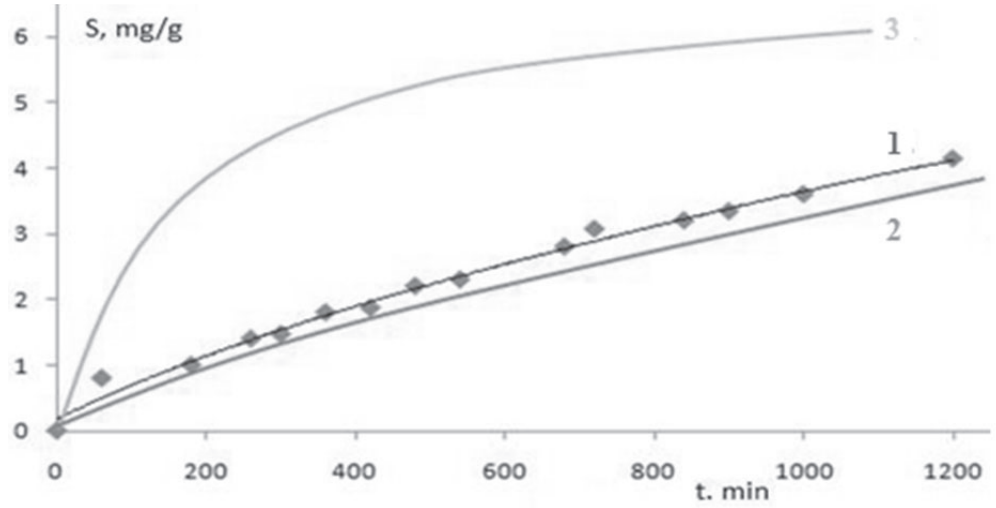

Figure 7-37. Kinetic curves of ammonium sorption by AV-17(Cr) from solutions with pH 2: obtained experimentally (1), calculated with the kinetic model PFO (2) and the kinetic model PSO (3).

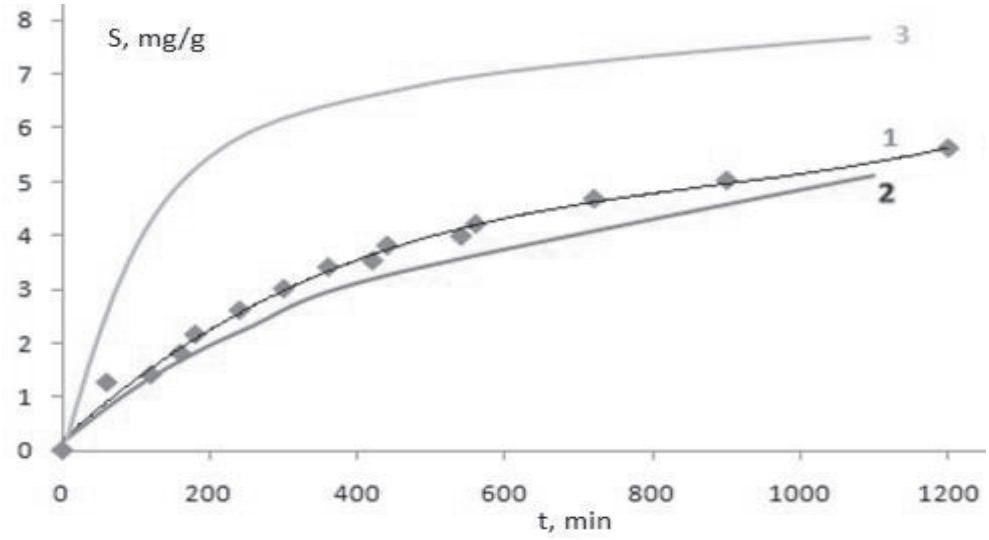

Figure 7-38. Kinetic curves of ammonium sorption by AV-17(Cr) from solutions with pH 5: obtained experimentally (1), calculated with the kinetic model PFO (2) and the kinetic model PSO (3).

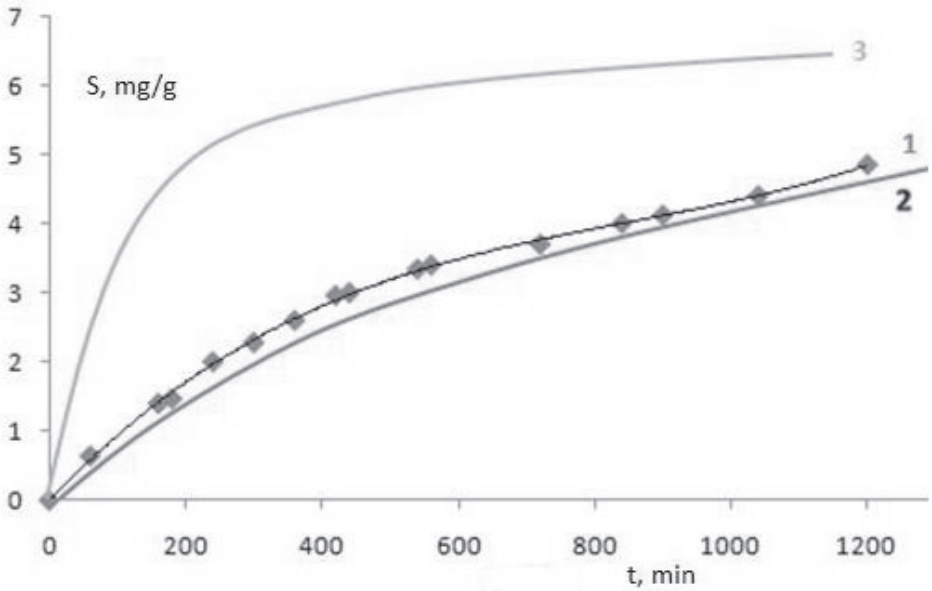

Figure 7-39. Kinetic curves of the ammonium sorption by AV-17(Cr) from solutions with pH 10.0: obtained experimentally (1), calculated with the kinetic model PFO (2) and the kinetic model PSO (3).

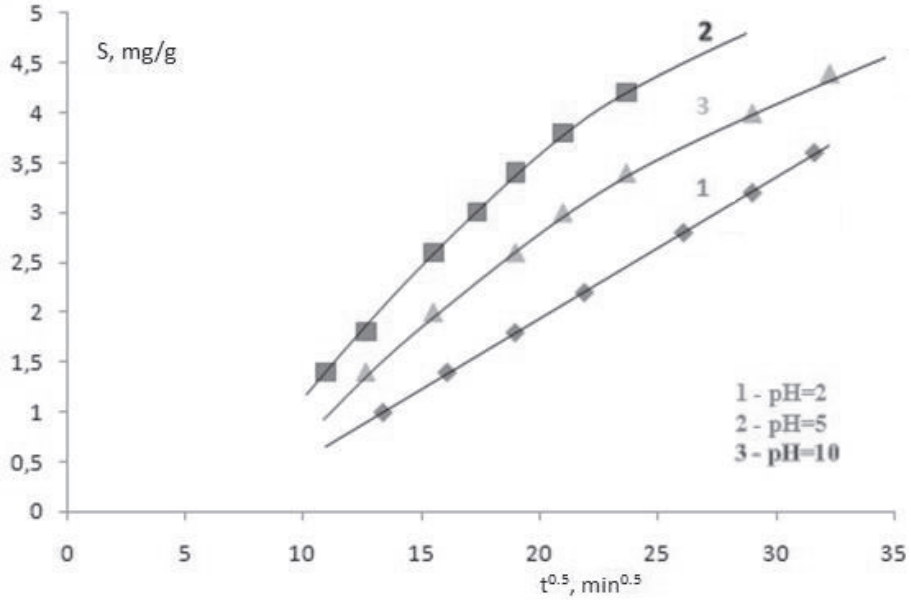

Figure 7-40. Dependence S = f ($t^{0.5}$) for the ammonium sorption on AV-17(Cr) from a solution with different pH.

It is known that the sorption of a solute, involves three main stages: (i) film diffusion, which is the diffusion of the sorbate particles through the liquid layer to the sorbent surface; (ii) transport of the sorbate particles from the surface to the interior of the sorbent granules, called intra-particle diffusion, or inner diffusion; and (iii) sorption onto the active centres of the sorbent. Usually, the absorption rate is mainly controlled by the first two steps, the last one being very fast, in the case of physical sorption. In the case of chemisorption (ligands exchange), the rate-limiting step could be the rate of chemical reaction. To explain the diffusion mechanism of the sorption process, the intra-particle diffusion model [115], expressed by Equation (7-39), was used. On the other hand, in order to determine the sorption limiting step, we have the graph Equation (7-40) [118]. The S = f($t^{0.5}$) dependence on ammonium sorption in solution with pH 2 is a straight line (Fig.7-40).

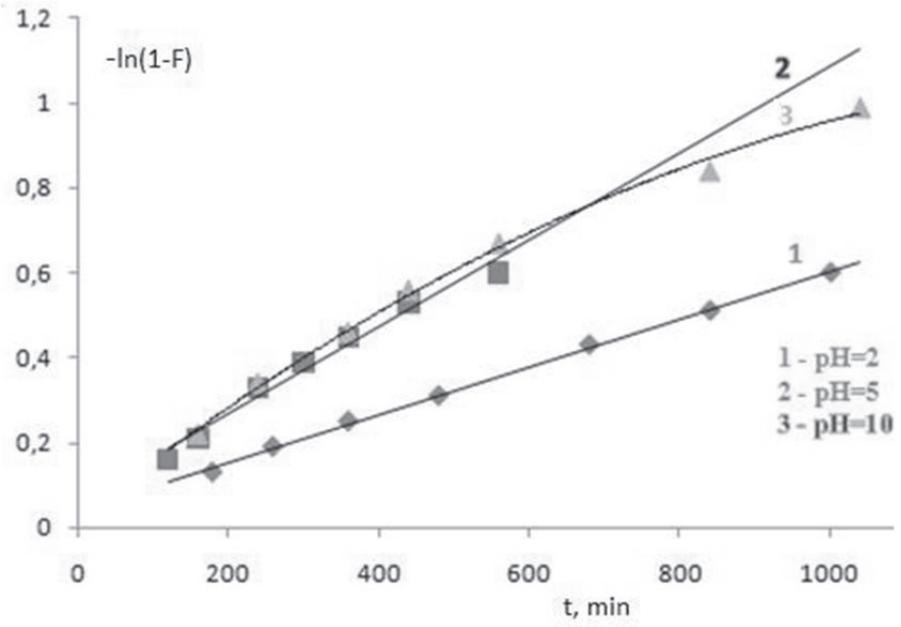

Figure 7-41. Dependence -ln(1-F) = f (t) for the ammonium sorption on AV-17(Cr) from a solution with different pH.

For ammonium sorption in solution with pH 2 dependence –ln(1-F) = f (t) also is linearly (Fig.7-41). This indicates that intra-particle diffusion is the rate-controlling step. For sorption from solution with pH 5 and 10 the St =f($t^{0.5}$) and -ln(1-F) = f (t)are not straight lines.

Table 7-13. Diffusion data for the ammonium sorption process

pH	External diffusion		Internal diffusion		
	K, min^{-1}	R^2	K_{id}, $mg.g^{-1}.min^{-1}$	C	R^2
2	$6 \cdot 10^{-4}$	0.9985	0.1417	-1	0.9999
5	$1 \cdot 10^{-3}$	0.9760	0.2264	-1	0.9900
10	$8 \cdot 10^{-4}$	0.9783	0.1507	-0.3	0.9840

This indicates that inter-particles diffusion is not the only rate controlling step, the boundary layer diffusion having a contribution. The calculated diffusion mechanism data for the sorption process are shown in Table 7-13. The data in Table 7-13 confirm that the limiting step of the kinetic process (intraparticle and interparticle diffusion) of ammonium sorption of composite AV-17(Cr) depends on the pH of the solution.

The dependency of the diffusion mechanism on the pH of the solution can be explained by the fact that the report NH_4^+/NH_3 changes with pH. The NH_3 particles more easily penetrate the polymer phase than NH_4^+, because the polymer matrix contains atoms with positive charges.

Sorption isotherms. Sorption isotherms of ammonium were obtained from solutions on the composite AV-17(Cr) at 22 and 40 ^oC. The isotherms were calculated according to different sorption models: Langmuir (Eqs. (1-9) and (1-10)), Freundlich (Eqs. (1-6) and (1-7)), Sips (Eqs. (7-41) and (7-42)) and Dubinin-Radushkevich (Eqs. (7-43) to (7-45)). Besides the correlation coefficient of determination (R^2), the statistical analysis of errors was performed by the nonlinear Chi-square test (χ^2) using Equation (4-7).

The experimental isotherms of ammonium sorption on composite AV-17(Cr), obtained at the contact of the sorbent with the solution for 24 hours at 22 and 40^oC, are shown in Figures 7-42 and 7-43 curve 1. The isotherms were constructed and calculated with the Langmuir, Freundlich, Sips and Dubinin-Radushkevich sorption models (Figs.7-42 and 7-43, curves 2-5).

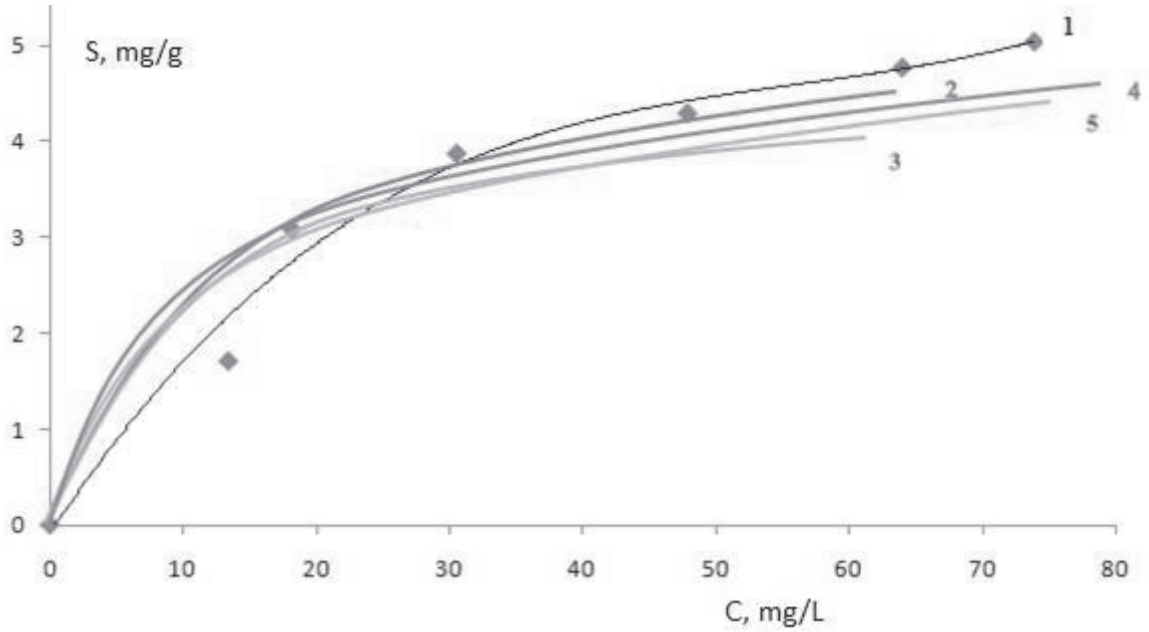

Figure 7-42. Equilibrium sorption isotherms of ammonium ions on AV-17(Cr) at 22^oC, obtained experimentally (1), and calculated by the Langmuir (2), Freundlich (3), Sips (4) and Dubinin-Radushkevich (5) sorption models.

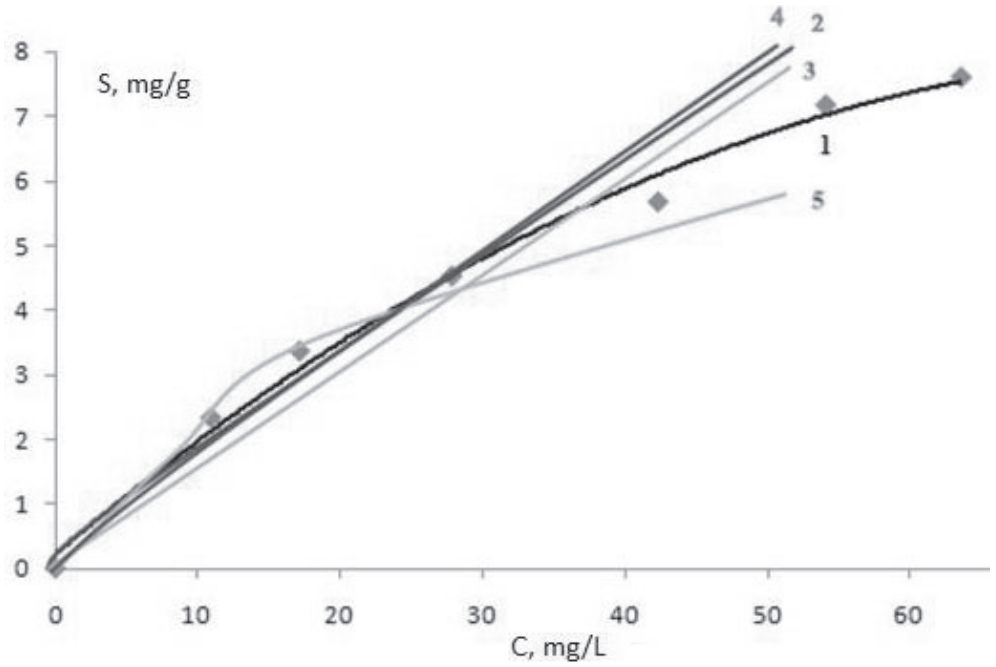

Figure 7-43. Equilibrium sorption isotherms of ammonium ions on AV-17(Cr) at 40°C, obtained experimentally (1), and calculated by the Langmuir (2), Freundlich (3), Sips (4) and Dubinin-Radushkevich (5) sorption models.

The isotherms parameters and the value of R^2 and χ^2 are listed in Tables 7-14 and 7-15. These parameters show that isotherms of ammonium sorption onto sorbent AV-17(Cr) are best described by the Langmuir sorption model both at 22 and 40 °C.

Table 7-14. Parameters of sorption isotherm at t = 22˚C, calculated by the Langmuir, Freundlich, Sips and Dubinin-Radushkevich sorption models

Langmuir model	**S_L, mg/g**	**K_L, L/mg**		**R^2**	**X^2**
	5.4	0.077		0.8258	0.024
Freundlich model	**K_F**	**1/n**		**R^2**	**X^2**
	1.27	0.301		0.8295	0.093
Sips model	**S_S**	**K_S**	**1/h**	**R^2**	**X^2**
	174.44	$7.6 \cdot 10^{-3}$	0.301	0.8253	0.051
Dubinin-Radushkevich model	**S_{D-R}**	**K_{D-R}**	**E, kJ/mol**	**R^2**	**X^2**
	4.22	$2 \cdot 10^{-5}$	15.81	0.8059	0.034

The data in Table 7-14 shows that 3 sorption models (Langmuir, Sips and Dubinin-Radushkevich) describe well enough the experimental sorption isotherm obtained at 22 °C. However, the Langmuir sorption model more adequately describes the experimental isotherm. The obtained isotherm at 22 °C is worst of all described by the Freundlich sorption model. This is seen in Figure 7-42.

Table 7-15. Parameters of sorption isotherm at t = 40˚C, calculated by the Langmuir, Freundlich, Sips and Dubinin-Radushkevich sorption models

Langmuir model	**S_L, mg/g**	**K_L, L/mg**		**R^2**	**X^2**
	18.25	0.012		0.9779	0.096
Freundlich model	**K_F**	**1/n**		**R^2**	**X^2**
	0.27	0.8354		0.9459	0.054
Sips model	**S_S**	**K_S**	**1/h**	**R^2**	**X^2**
	10000	$2.86 \cdot 10^{-5}$	0.8354	0.9479	0.003
Dubinin-Radushkevich model	**S_{D-R}**	**K_{D-R}**	**E, kJ/mol**	**R^2**	**X^2**
	4.39	$1 \cdot 10^{-5}$	22.36	0.8259	0.318

The experimental isotherm, obtained at 40 °C may be described sufficiently well by almost all sorption models, but only at concentrations up to 40 mg NH_4^+/L. This is clearly seen in Figure 7-43. The data in Table 7-15 shows, that we can consider the Langmuir and Sips models most appropriate.

Thermodynamic functions. The fact that the experimental isotherms of ammonia absorption are described well with the Langmuir model, allows us to calculate the thermodynamic functions of sorption. The thermodynamic functions ΔG, ΔH and ΔS of the sorption process were calculated (Eqs 4-9 to 4-11) using the Langmuir isotherm constant K_L. Since the thermodynamic functions are relative to one mole, the K_L constants at 22 and 40°C were calculated based on the data S_L and Ce (Eq.(1-9)) respectively expressed by mol/g and mol/L.

The ΔG value equals to -20.52 kJ/mol at 22 °C and -16.8 kJ/mol at 40°C was obtained.

The value of ΔH, equal to 81.52 kJ/mol, in the assumption that in the range of temperature 22-40°C is constant, was calculated with Equation (4-10), where K_1 is K_L at 22°C and K_2 is K_L at 40°C. At 22°C the ΔS = 221.8 J/mol·K and at 40°C the ΔS = 206.8 J/mol·K.

The values of the thermodynamic functions confirm that ammonium absorption by the composite AV-17(Cr) is a complex and exothermic process which occurs spontaneously.

7.6. Thiosemicarbazone immobilized on polymers holding metal compounds

It is known that thiosemicarbazone and its derivatives exhibit biological activity. Thiosemicarbazones are chemical compounds which have anti - tuberculosis properties [179, 180] and are part of a group of tuberculostatic drugs. The thiosemicarbazone derivatives possess a variety of antimicrobial (*Staphylococcus epidermidis, Bacillus cereus, Moraxella cattarhalis, Staph, Saprophyticus Staphylococcus aureus, Enterococcus faecalis, Cryptococcus*) and antifungal (*Candida albicans, Aspergillus flavans, Paracoccidioides brasiliensis*) activity [181, 182]. An enhanced biological activity has complex combinations of thiosemicarbazones with metals. Antimicrobial activity possesses the complexes of Cu (II), Ni (II), Co (II) with thiosemicarbazone derivatives [183-187] Some metal complexes with thiosemicarbazone derivatives possess not only antibacterial but also anti-cancer and anti-HIV properties [188-190]. Only a few of the articles devoted to biological properties of thiosemicarbazones and their complexes with metals have been cited here. In these articles, the biological activity of thiosemicarbazones and their complex compounds has been investigated under single-phase systems. But when local action of the drugs is required, it is necessary that thiosemicarbazone compounds are immobilized on an inert substrate. In this case, the biological activity occurs slower than in single-phase systems. Upon using the Disc Diffusion Susceptibility Methods it seems that the drug is immobilized on the support [191], but the act of biological activity takes place in a single phase, i.e. in solution.

It is of interest to research the immobilization of thiosemicarbazone and its compounds with metals on the support which would not allow their diffusion in the liquid phase. In this section the processes of immobilization of thiosemicarbazone are studied on cross-linked ionic polymers, on the polymer containing metallic compounds and the coordination of metallic cations with immobilized thiosemicarbazone on the polymer [192].

The commercial strongly basic AV-17(Cl) and weak acid Amberlite IRC-50(H) gel-type cross-linked polymers have been used. The AV-17(Cl), containing R_4N^+ functional groups, had full exchange capacity of 3.5-4.2 mEq/g, and Amberlite IRC-50, containing >CH–COOH functional groups, had exchange capacity of 10.0 mEq./g [4]. Also, the AV-17(Cr) composite has been used. The composite AV-17(Cr) was obtained according to Ref.[84, 87]. The Cr^{3+} content in the polymer was 9.06 mg Cr/g. Thiosemicarbazone 5-NO_2-salicylic aldehyde was immobilized on polymers. Thiosemicarbazone 5-NO_2-salicylic aldehyde was dissolved in 96% (vol) ethanol. The content of Fe^{2+}, Fe^{3+}, Cr^{3+} ions and thiosemicarbazone 5-NO_2-salicylic aldehyde was determined by photocolorimetry [26]. The content of other cations was determined by titrimetry [193].

Kinetics of thiosemicarbazone sorption on AV-17(Cl) and AV-17(Cr). The thiosemicarbazone 5-NO_2-salicylic aldehyde with the formula

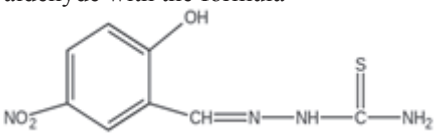

will be noted with HL. On the AV-17(Cl) polymer, HL may be retained predominantly as a result of dispersion (London) interactions, but on the AV-17(Cr) sorbent, and as a result of coordinate bonds with the metal, replacing the SO_4^{2-} groups in the jarosite type compounds $R_4N[Cr_3(OH)_2(SO_4)_2]$. The kinetic curve of HL absorption on AV-17 (Cl) or AV-17(Cr) was obtained at 20.5 °C. For this, 0.2 g of polymer was contacted with 50 ml of HL solution with the concentration of $17 \cdot 10^{-3}$ mmol/L for 24 h.

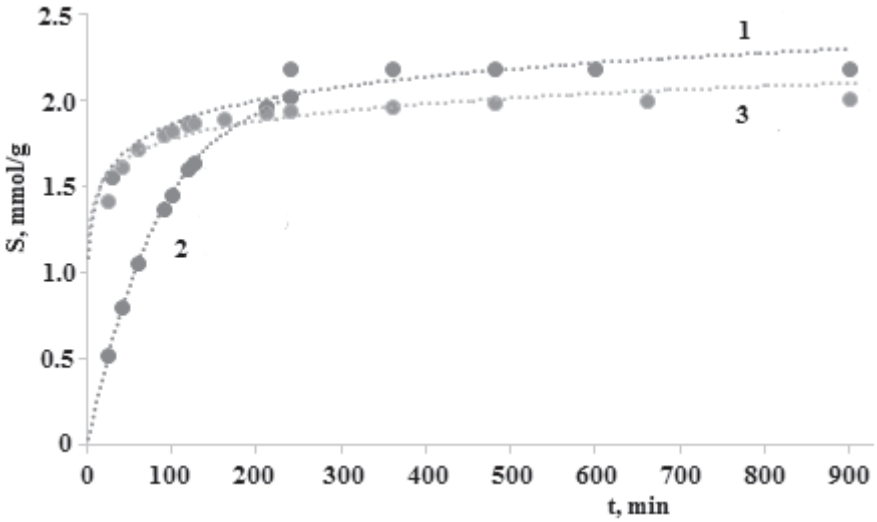

Figure 7-44. The kinetic curves of the thiosemicarbazone sorption on AV-17(Cl): obtained experimentally (1), calculated with PFO (2), and PSO (3) kinetic models.

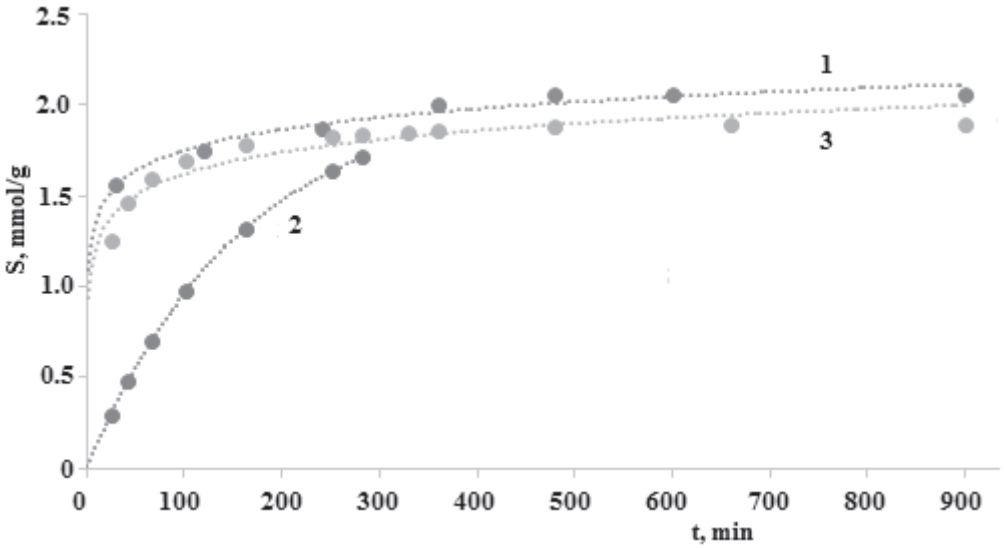

Figure 7-45. The kinetic curves of the thiosemicarbazone sorption on AV-17(Cr): obtained experimentally (1), calculated with PFO (2), and PSO (3) kinetic models.

The kinetic curve of HL sorption on AV-17(Cl) is shown in Figure 7-44 and on AV-17(Cr) in Figure 7-45. From Figures 7-44 and 7-45, it is seen that the sorption equilibrium takes place quite slowly. This occurs because in the ethanol solution of HL the degree of swelling of the polymer is much lower than in water [1] and the diffusion of the thiosemicarbazone molecules in the polymer phase is slow.

To investigate the kinetics mechanism, which controls the sorption process of HL on AV-17(Cl) the nonlinear forms of the pseudo-first-order (PFO) and the pseudo-second-order (PSO) kinetic models [116, 117] were used. The nonlinear form of the integrated PFO kinetic model is described by Equation (4-2) and the linear (to calculate the rate constant k_1) form by Equation (4-3). The nonlinear form of the PSO kinetic model is expressed by Equation (4-4) and the linear form by Equation (4-5). Two different error functions were used to determine the validity of kinetic models and isotherms, which were fitted by the non-linear regression method: the coefficient of determination (R^2), and the nonlinear Chi-square ($\chi 2$) test, estimated by Equation (4-7).

Table 7-16. Values of parameters obtained by the non-linear regression method for sorption of 5-NO_2-salicylic aldehyde thiosemicarbazone

Kinetic model		AV-17(Cl)	AV-17(Cr)
PFO	Se (calculated), $mmol^{-1}$	2.19	2.06
	k_1, min^{-1}	0.011	0.0063
	R^2	0.8742	0.9623
	X^2	2.8800	8.1053
PSO	Se (calculated), $mmol^{-1}$	2.03	1.93
	k_2, g $mmol^{-1}$ min^{-1}	46.0	38.5
	R^2	0.8742	0.9623
	X^2	0.0016	0.0220

Considering the k_1 and k_2 values in Table 7-16, the kinetic curves of HL sorption on the AV-17(Cl) and AV-17 (Cr) sorbents were calculated according to the PFO and PSO kinetic models (Figs. 7-44 and 7-45). The data of Table 7-16 and the curves of Figures 7-44 and 7-45 clearly demonstrate that the kinetics of HL sorption on AV-17 (Cl) and AV-17 (Cr) corresponds to the PSO kinetic model which is more consistent with the experimental data.

It is known [118], that the linear dependence of $-(1-F)= f(t)$ (Eq.(7-40)) denotes that the sorption rate is limited by the external diffusion (through the liquid film on the sorbent granule), and the nonlinear dependence on the internal diffusion (in the sorbent granule). As can be seen from Figure 7-46, the dependence $-ln(1-F) = f(t)$ is non-linear. Therefore, we can consider that the rate of HL sorption to AV-17 (CI) and AV-17 (Cr) is limited by intra-particle diffusion. The fact that the rate of HL sorption on AV-17 (Cl) and AV-17 (Cr) is limited by internal diffusion is more convincingly demonstrated by the linear dependence of $S_t= f(t^{0.5})$, (Eq.(7-39)) [155].

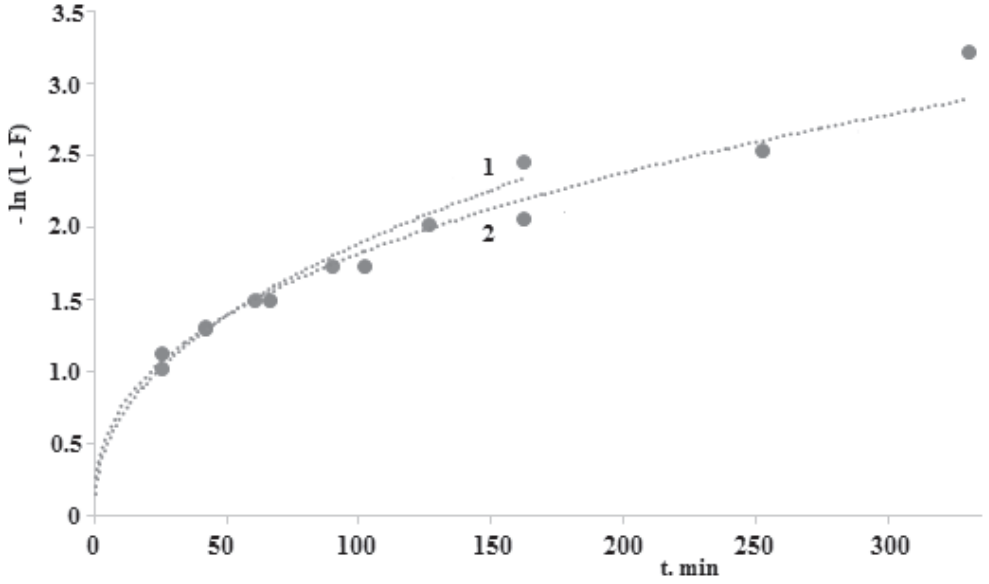

Figure 7-46. The graph $-(1-F) = f(t)$ for the sorption of 5-NO_2-salicylic aldehyde thiosemicarbazone on AV-17(Cl) (1), and AV-17(Cr) (2).

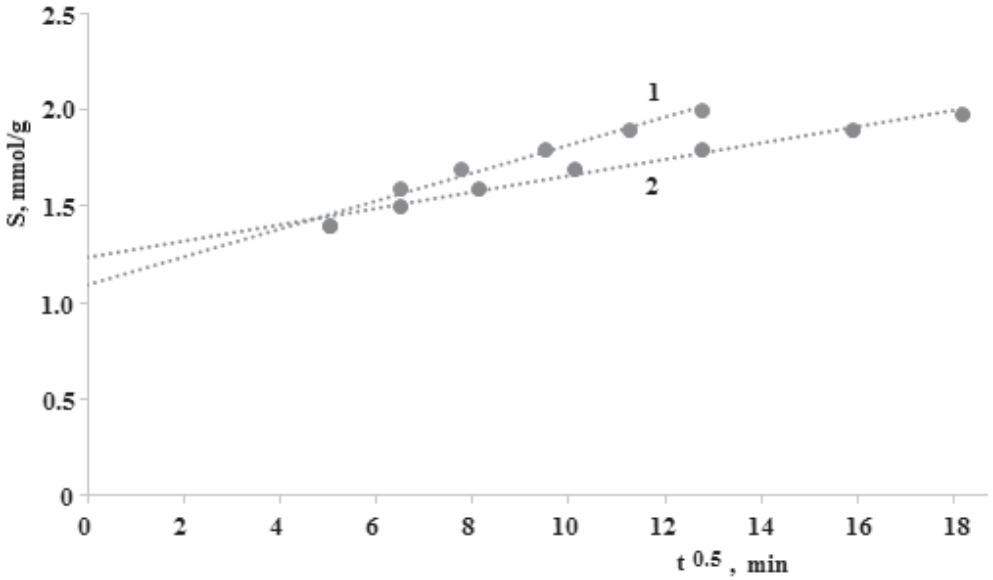

Figure 7-47. The $S = f(t^{0,5})$ graph for the sorption of 5-NO_2-salicylic aldehyde thiosemicarbazone on AV-17(Cl) -1 and AV-17(Cr) -2.

The analysis of the experimental and calculated data shows that both the sorption value and the sorption rate of HL on the composite AV-17(Cr) are slightly lower than on the AV -17(Cl). This can be explained by the fact that the particles of jarosite compounds block some of the pores of the sorbent. On the other hand, as it is known, the exchange of ligands in the Cr^{3+} compounds occurs very slowly.

Sorption isotherms of thiosemicarbazone sorption on AV-17(Cl) and AV-17(Cr). In order to determine the sorption capacity of HL on the AV-17(Cl) polymer and the AV-17(Cr) composite, sorption isotherms were obtained. The experiment was carried out as follows: 0.2 g of the sorbent was contacted with 50 ml HL solution of different concentrations at 25°C for 24 hours. The results obtained are shown in Figures 7-48 and 7-49. As can be seen from these figures, the form of the experimentally obtained isotherms does not correspond to the

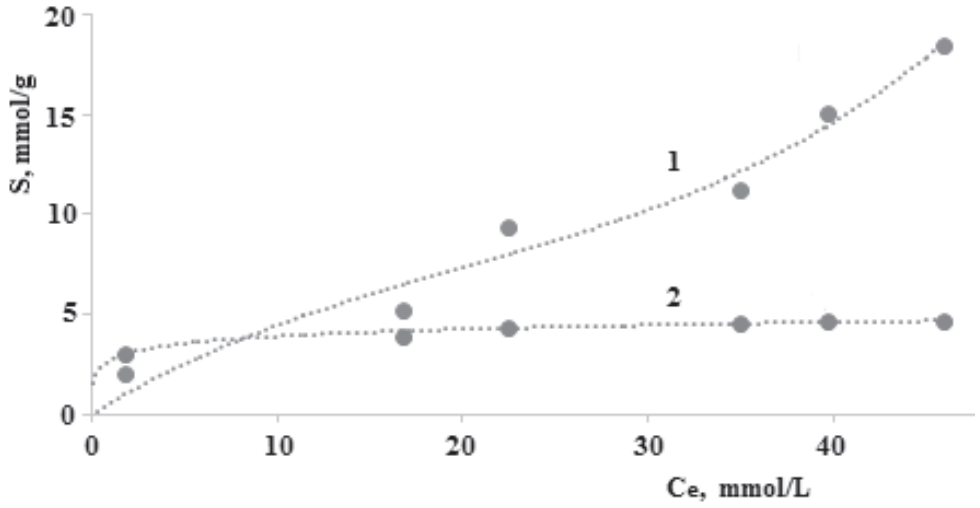

Figure 7-48. The 5-NO_2-salicylic aldehyde thiosemicarbazone sorption isotherm on AV-17(Cl): 1 – obtained experimentally and 2 – calculated according to the BET sorption model.

Freundlich, Langmuir or Sips sorption models. We have approximated the isotherms with the BET sorption model. Although the BET sorption model has been developed for gas or vapour sorption, it can be used with some approximation and in some sorption processes in solutions [159, 160].

Table 7-17. The values of the constants of BET sorption isotherm of HL on AV-17(Cl) and AV-17(Cr)

Sorbent	S∞, mol·g^{-1}	B, g mmol^{-1}	R^2	X^2
AV-17(Cl)	$5.43 \cdot 10^{-3}$	6572	0.9686	79.6379
AV-17(Cr)	$5.43 \cdot 10^{-3}$	3201	0.9874	52.7524

In this case, in the BET isotherm equation C_e/C_s is introduced instead of P/Ps, where P and Ps correspond to the equilibrium pressure and pressure of saturated vapour, and Ce and Cs - the equilibrium concentration and the concentration of the saturated solution. Thus, the BET equations (Eqs. (7-46) and (7-47)) were used.

Experimentally obtained isotherms data confirms that under similar conditions the HL sorption on AV-17(Cl) is slightly higher than on AV-17(Cr). For example, AV-17 (Cl) retains $18.5 \cdot 10^{-3}$ mmol HL/ g (Ce = 46 mmol/L), and AV-17 (Cr) retains 17.5. 10^{-3} mmol HL/g (Ce = 50 mmol/L. Using the value of the constant in Table 7-17, the isotherms of HL sorption on AV-17 (Cl) and AV-17 (Cr) were calculated (Figs.7-48 and 7-49). Although HL sorption on AV-17(Cl) is higher than on AV-17(Cr), the monolayer capacity on AV-17(Cl) is lower.

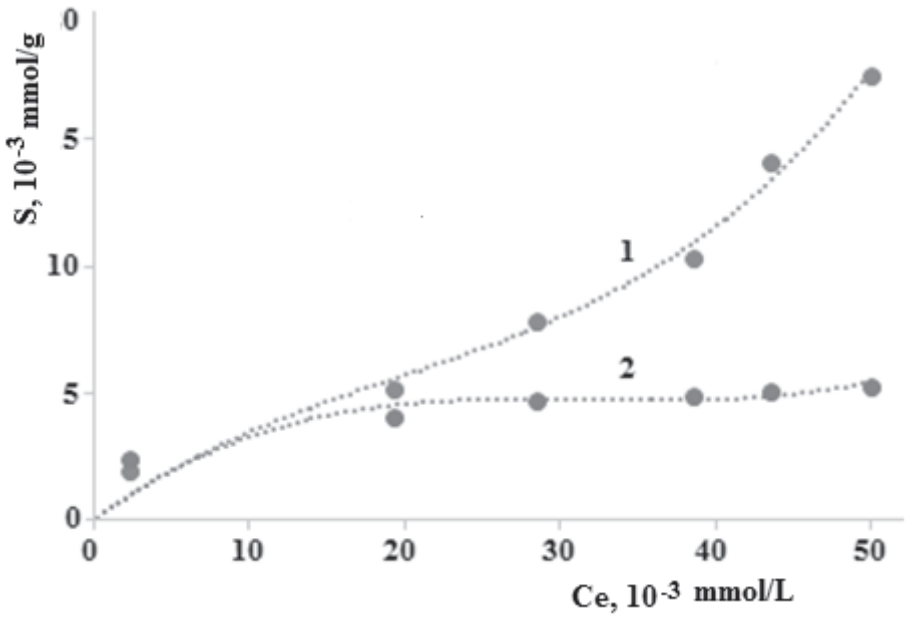

Figure 7-49. The 5-NO_2-salicylic aldehyde thiosemicarbazone sorption isotherm on AV-17(Cr): 1 – obtained experimentally and 2 – calculated according to the BET sorption model

Sorption of 3d metals on sorbents containing thiosemicarbazone. Biological activity is possessed by both thiosemicarbazones and their coordinative compounds with the cations of 3d metals. The formation of thiosemicarbazone coordinate compounds in the sorbent phase can be performed by two methods. 1. The sorbents are first loaded with thiosemicarbazone then with metal cations; and - 2.The sorbents are first loaded with metal cations, then with thiosemicarbazone. In this section, we present the results of the research on the formation of the coordinative compounds of some 3d cations with thiosemicarbazone incorporated in the sorbent phase. The sorbents (AV-17(Cl+HL), AV-17(Cr+HL)) were previously obtained by contacting 5 g of the AV-17(Cl) and AV-17(Cr) for 24 h with 0.5 L solution of 5-NO_2 -salicylic aldehyde thiosemicarbazone containing 5 mmol/L. The HL content in AV-17(Cl+HL) sorbent constituted 0.182 mmol/g or 43.66 mg/g, and in AV-17(Cr+HL) - 0.167 mmol/g or 40.01 mg/g. Samples of 0.4 g of sorbent were contacted with 100 mL of $CuSO_4$, $Co(NO_3)_2$, $ZnSO_4$, $NiSO_4$, $FeSO_4$ and $Fe(NO_3)_3$ solutions for 24 h at room temperature. After that, the sorption of the metal cations on the sorbents was determined. The choice of salts has been carried out in such a way as to exclude the formation of jarosite mineral compounds in the sorbent phase. As is known [58], bivalent cations as well as trivalent cations in the absence of sulfate anions, do not form jarosite mineral compounds in the polymer phase containing strongly basic groups. So, the cations examined can be retained by AV-17(Cl+HL) sorbent only as a result of their coordination with electron donor atoms (N, S, OH) of HL. The results of the metal cation sorption on AV-17(Cl+HL) and AV-17(Cr+HL are presented in Table 7-18. These results seem very interesting. First, we can state with certainty that the metal cations in the phase of AV-17 (Cl + HL) coordinate with the electron donor atoms of thiosemicarbazone. That is, in the polymer phase we have the immobilized coordinating compounds of thiosemicarbazone.

Table 7-18. The data of metal cations' sorption on AV-17(Cl+HL) or AV-17(Cr+HL)

Solution of	Sorbent	pH	Co*, mmol L^{-1}	S, mmol g^{-1}	S, mg g^{-1}
$ZnSO_4$	AV-17(Cl+HL) AV-17(Cr+HL)	5.98 4.54	10.55	0.056 0.190	3.72 12.62
$NiSO_4$	AV-17(Cl+HL) AV-17(Cr+HL)	6.16 4.67	5.67	0.081 0.096	4.75 5.64
$CuSO_4$	AV-17(Cl+HL) AV-17(Cr+HL)	4.72 4.06	9.90	0.018 0.072	1.14 4.58
$Co(NO_3)_2$	AV-17(Cl+HL) AV-17(Cr+HL)	5.02 4.70	6.17	0.205 0.214	12.08 12.61
$FeSO_4$	AV-17(Cl+HL) AV-17(Cr+HL)	3.85 3.52	2.50	0.038 0.038	2.12 2.12
$Fe(NO_3)_3$	AV-17(Cl+HL) AV-17(Cr+HL)	2.30 1.95	2.65	0.331 0.369	18.49 20.61

*Co is initial concentration

Most likely, metal cations coordinate with N and S atoms of thiosemicarbazone, forming chelate cycles [194], but some cations such as Fe^{3+} could also coordinate with the oxygen of the phenolic groups. This can explain the fact that Fe^{3+} cations are retained on polymers containing HL, much more than other cations (Tab.7-18). Regretfully, IR spectroscopy is less informative for investigated objects, and other spectroscopic methods are inapplicable. On the other hand, although the content of thiosemicarbazone in the AV-17(Cr+HL) phase is lower than in AV-17(Cl+HL), the sorption of metallic cations on AV-17(Cr+HL) is higher. So the existence of HL in the sorbent phase contributes to the retention of metal cations. Probably some of the metal cations are retained on AV-17(Cr+HL) as a result of their coordination with thiosemicarbazone, and other as a result of the cation exchange according to Equations (7-61) and (7-62).

$$2R_4N[Cr_3(OH)_6(SO_4)_2 + MSO_4 \leftrightarrow M[Cr_3(OH)_6(SO_4)_2]_2 + (R_4N)_2SO_4 \quad (7\text{-}61)$$

$$2H_3O[Cr_3(OH)_6(SO_4)_2] + M^{2+} \leftrightarrow M[Cr_3(OH)_6(SO_4)_2]_2 + 2H_3O^+ \quad (7\text{-}62)$$

Sorption thiosemicarbazone on Amberlite IRC-50 polymer loaded with 3d cations. For the study, a cross-linked ionic Amberlite IRC-50 polymer containing carboxylic groups was used. In the first stage, the polymer was charged with metal cations upon contacting of 0.4 g with 100 mL solution of $CuSO_4$, $Co(NO_3)_2$, $ZnSO_4$, $NiSO_4$, $FeSO_4$ and $Fe(NO_3)_3$ with respectively concentrations of 9.90; 9.80; 10.70; 5.67; 2.50 and 2.65 mmol/L at room temperature for 7 days. The metal content in the polymer samples is shown in Table 7-19. The samples of 0.2 g of polymer loaded with metal cations were contacted with 50 ml of thiosemicarbazone solution with the concentration of 3.182 mmol/L at room temperature for 7 days.

Table 7-19. Data on the sorption of metal cations on Amberlite IRC-50 and the sorption of the thiosemicarbazone on Amberlite IRC-50 loaded with metal cations

Solution	$CuSO_4$	$CuSO_4$	$Co(NO_3)_2$	$NiSO_4$	$ZnSO_4$	$FeSO_4$	$Fe_2(SO_4)_3$
Equilibrium pH	3.40	3.90	5.14	4.96	4.45	3.73	2.42
Metal content in polymer, mg g^{-1}	4.45	19.28	12.69	12.44	17.44	22.69	20.24
Equilibrium $Ce_{(HL)}$, mmol L^{-1}	2.828	2.929	2.929	3.080	2.029	3.080	3.080
$S_{(HL)}$, mmol g^{-1}	0.088	0.063	0.063	0.025	0.063	0.025	0.025
$S_{(HL)}$, mg g^{-1}	21.25	15.15	15.15	6.06	15.15	6.06	6.06

The data of Table 7-19 show that the sorption of thiosemicarbazone on the Amberlite IRC-50 polymer is the lower the higher is the metal content in the polymer. So, we can assume that thiosemicarbazone does not coordinate with the metal cations in the polymer phase. The decrease of thiosemicarbazone sorption with the increase in the metal content can be explained by the fact that the metal cations coordinating with the carboxylic groups lead to the additional crosslinking of the polymer chains. And this leads to a drastic decrease in the polymer pore size and, consequently, to a decrease in the diffusion of the thiosemicarbazone in the polymer phase. Previous results have shown [1], that the swelling in water of cross-linked carboxylic polymers containing Cu^{2+}, Cd^{2+} and Zn^{2+} cations is about 3 times lower than those containing Na^{+}. The effect of reducing the polymer swelling caused by the metal cation complexation is much higher than that caused by ethanol [1]. It should be noted that depending on the amount of divinylbenzene and the nature of the metal, the cations may be coordinated with a single or two (more often) carboxylic groups belonging to one or two polymeric chains. That is why there is no strict correlation between the metal content in the polymer phase and the sorption of thiosemicarbazone.

7.7. Chemical constructions in the polymer phase – a new way to obtain varied materials

Many technologies of concentration, separation and analytical determination of substances, purification of different types of water and gases are unthinkable without using the ionic cross-linked polymers containing strongly basic groups. The largest quantity of these polymers, a high tonnage product of the chemical industry, is used for water treatment at thermoelectric and nuclear stations. The main function of these polymers is the ion exchange process:

$R_4NA + B^- = R_4NB + A^-$, where R_4N^+ is the polymer matrix, A^- and B^- are anions. The biggest drawback of ionic cross-linked polymers holding strongly basic groups is the lack of selectivity of sorption of anions, especially the inorganic ones. This occurs because the ions sorption by the polymers is conditioned by Coulomb's electrostatic interactions. Smart technologies require new materials with selective sorption and catalytic properties. The question is whether these polymers could be transformed into materials with selective sorption and catalytic properties. At first glance, such polymers cannot be modified with metal compounds that would significantly change their physical and chemical properties. They do not contain in their matrix negatively charged or electron donor atoms and, theoretically, they are unable to interact with metallic cations. However, in our previous studies [27, 33, 53, 64, 84, 105, 123, 195], it was shown that in the phase of strongly basic cross-linked ionic polymers inorganic compounds of some metals (M) such as Fe^{3+}, Cr^{3+} Al^{3+}, Ga^{3+}, and In^{3+} can be syntheized. These compounds can be formed only in sulfate solutions, but not in those of nitrate or chloride. The metal compounds in the polymer phase are in the form of ultrafine particles which are located both inside and on the polymer phase in the form of the jarosite mineral type: $R_4N[M_3(OH)_6(SO_4)_2]$, where R_4N^+ are functional groups of the polymer. Depending on the pH of the solution of $M_2(SO_4)_3$, in the polymer phase some amount of $H_3O[M_3(OH)_6(SO_4)_2]$ also is formed. On heating in water media ($t \geq 80^oC$) synthetic $Na[Fe_3(OH)_6(SO_4)_2]$ is converted into α-FeOOH [46]. But jarosite type compounds in the polymer phase on boiling in water are converted into β-FeOOH ultradispersed particles in a superparamagnetic state [33, 64]. Using different procedures (several cycles of "Fe(III) sorption - heating in water" carried out) the particles sizes and morphology, their repartition on the surface and in the volume of the polymer granule, the composition of the "polymer-inorganic compound" structural units may be modified. With increasing iron content in the polymer phase, metallic compounds turn into relatively massive and magnetic ordered particles of β-FeOOH [33, 64]. Besides jarosite mineral type compounds in the phase of the strongly basic cross-linked ionic polymers can be synthesized BiOCl and Bi_2O_3 compounds [123, 124]. The composites formed by polymeric and metallic compounds are thermally stable up to 120°C, which is important for their application in different technological processes [64, 89]. The composites radically change the physical and chemical properties of strongly basic cross-linked ionic polymers. They can be used for simulations of biochemical mass transfer processes and as models with peculiar magnetic properties [55, 83] and be involved in redox processes [125, 196]. But most important is that they become adsorbents and catalysts [74] with selective properties.

In this section are presented the research results of the functionality modification of strongly basic cross-linked ionic polymers, through the composites synthesis in their phase by ion-molecular constructions. For investigation the commercial strongly basic cross-linked ionic polymers AV-17(Cl) and Varion-AD(Cl)) have been used. Composites AV-17(Cr) containing 20.1 mg Cr/g and Varion-AD(Cr) containing 35.7 mg Cr/g were obtained according to Ref. [197]. Composites AV-17(Fe) containing 19.6 mg Fe/g and Varion-AD(Fe) containing 21.9 mg Fe/g were obtained according to Ref. [197]. In the polymer phase, ultra-dispersed particles of the jarosite type compounds of $R_4N[Cr_3(OH)_6(SO_4)_2]$ and a small part of $H_3O[Cr_3(OH)_6(SO_4)_2]$, of $R_4N[Fe_3(OH)_6(SO_4)_2]$ and a part of $H_3O[Fe_3(OH)_6(SO_4)_2]$ were synthesized. As shown in Figure 7-50, the metal compounds in the phase of composites have very low crystallinity that was confirmed by X-ray diffraction analysis. Already it has been mentioned that the jarosite mineral type compounds are formed as layers of 3 or 6 octahedral cycles [58]. The OH^- groups are located in the equatorial plane, forming a bridge between metal ions, but SO_4^{2-} groups are located an axial position, each coordinate with 3 metal cations of 3 octahedra. Between the jarosite polymer layers, there are mobile R_4N^+ and $H_3O^+$and other cations retained by electrostatic interactions. In fact, the R_4N^+ groups are linked by the organic polymer chains and their mobility is limited by the chain's flexibility. This, together with the different degree of hydration of

mobile ions causes the formation in the polymer phase of jarosite type compounds with almost an absence of crystallinity. The natural jarosite has a high degree of crystallinity.

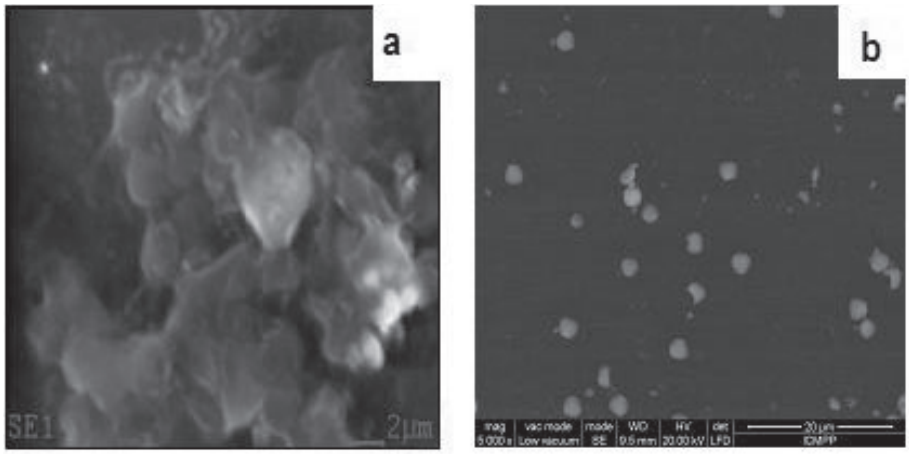

Figure 7-50. SEM images of the Cr(III)-containing (a) and Fe(III)-containing (b) compound particles on the surface of a polymer AV-17 granule.

The selective sorption properties of the composites are due to the SO_4^{2-} groups that may be substituted by tetrahedral anions such as XO_4^{2-} or XO_4^{3-} (CrO_4^{2-}, VO_4^{2-}, WO_4^{2-}, AsO_4^{3-}, PO_4^{3-} and others) according to Equations (7-63) and (7-64):

$$R_4N[M_3(OH)_6(SO_4)_2] + 2XO_4^{2-} = R_4N[M_3(OH)_6(XO_4)_2] + 2SO_4^{2-} \quad (7\text{-}63)$$

$$R_4N[M_3(OH)_6(SO_4)_2] + 2XO_4^{3-} = R_4N[M_3(OH)_6(XO_4)_2]^{2-} + 2SO_4^{2-} \quad (7\text{-}64)$$

Because not all of the R_4N^+ groups of the polymer enter the composition of the jarosite mineral type compounds the anions XO_4^{2-} and XO_4^{3-} can also be adsorbed by the polymer according to Equations (7-65) and (7-66):

$$2R_4NCl + XO_4^{2-} = (R_4N)_2XO_4 + 2Cl^- \quad (7\text{-}65)$$

$$3R_4NCl + XO4^{3-} = (R_4N)_3XO_4 + 3Cl\text{-} \quad (7\text{-}66)$$

But anions sorption according to Equations (7-65) and (7-66) is not characterised by selectivity because it is conditioned by Coulomb's electrostatic interactions, while the sorption according to Equations (7-63) and (7-64) is selective because it is conditioned by chemical donor-acceptor interactions. It should be noted that as a result of the sorption of anions according to Equation (7-64), the composite changes its functionality-it becomes able to adsorb cations (Ka^{n+}) according to Equation (7-67):

$$nR_4N[M_3(OH)_6(XO_4)_2]^{2-} + 2Ka^{n+} = \{R_4N[M_3(OH)_6(XO_4)_2]\}n(2Ka) \quad (7\text{-}67)$$

The researches [142] have shown that the composites, based on the polymer and the jarosite type compounds, are able to absorb not only the tetrahedral anions but also the anions of different configurations, such as NO_2^-, for example.

Investigation of selective adsorption of ions that can coordinate bidentate presents not only applied interest, but also a way to change the functionality of the composites. We prove this by researching NCS^- ions interactions with composite AV-17(Cr) and, for comparison, with AV-17(Cl). Sorption isotherms of NCS^- ions from KNCS solutions were obtained, containing 0.01 mol/L KNO_3, on the composites AV-17(Cr) and AV-17(Cr-NCS-Ag). The addition of KNO_3 to the KNCS solution almost completely eliminates the sorption of NSC^- ions as a result of ion exchange. For comparison, the sorption isotherm of NCS^- ions from KNCS solution on the AV-17(Cl) has also been obtained. Sorption took place at a temperature of 22 ^oC. The isotherms were calculated according to different sorption models: Langmuir (Eqs. (1-9) and (1-10)), Freundlich (Eqs. (1-6) and (1-7)). Sips (Eqs.(7-41) and (7-42)) and Dubinin-Radushkevich (Eqs.(7-43) to (7-45)). Besides the correlation coefficient of determination (R^2), the statistical analysis of errors was performed by the nonlinear Chi-square test (X^2) using Equation (4-7).

The experimental isotherm of NCS^- anions sorption on AV-17(Cl), obtained at the contact of the sorbent with the solution for 24 hours, is shown in Figure 7-51 (curve 1). As shown in Figure 7-51, in a large range of NCS^- ions concentration, on the sorption isotherm appears a plateau.

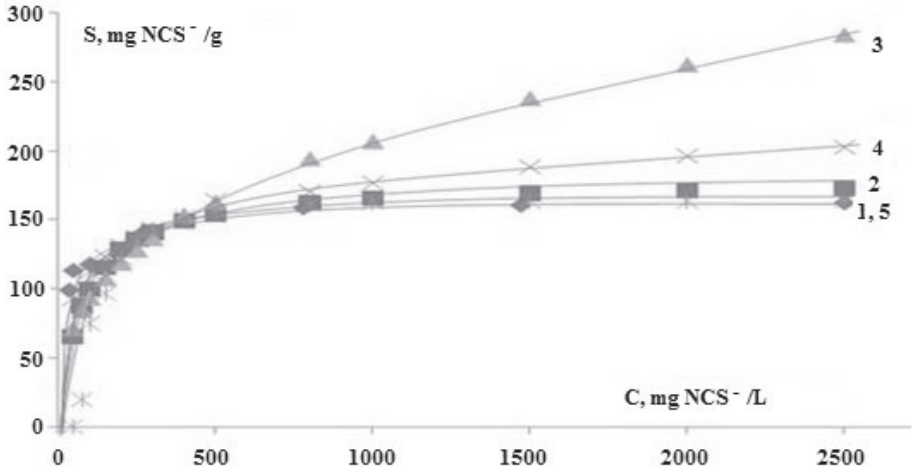

Figure 7-51. Equilibrium sorption isotherms of NCS^- ions on AV-17(Cl) in a large range of NCS^- concentration: obtained experimentally (1), calculated by Langmuir (2), Freundlich (3), Sips (4) and Dubinin-Radushkevich (5) sorption models

This is clearly seen in Figure 7-51. Perhaps in the systems with a great concentration of NCS- ions photocatalytic processes occor with the formation of the compounds of different species, in particular $(NCS)_2$ [198]. Because of this, the isotherm of Figure 7-51 in the low range of concentrations of NCS^- ions was also examined (Fig.7-52).

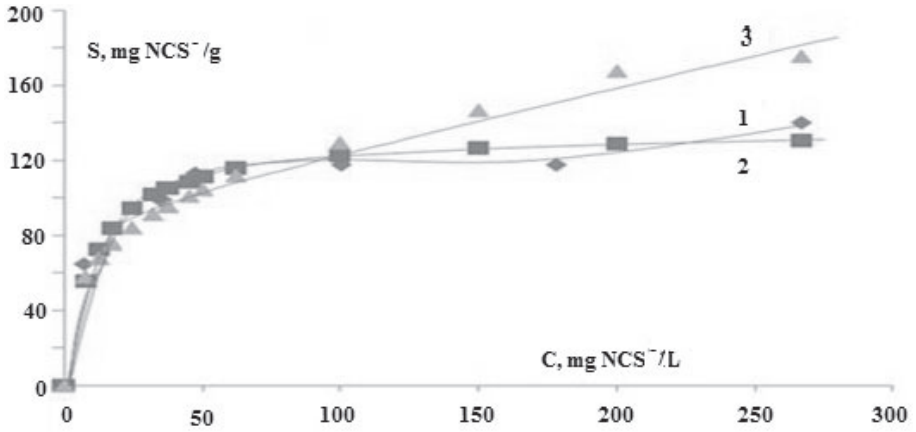

Figure 7-52. Equilibrium sorption isotherms of NCS^- ions on AV-17(Cl) in a low range of NCS^- concentration: obtained experimentally (1), calculated by Langmuir (2) and Freundlich (3) sorption models.

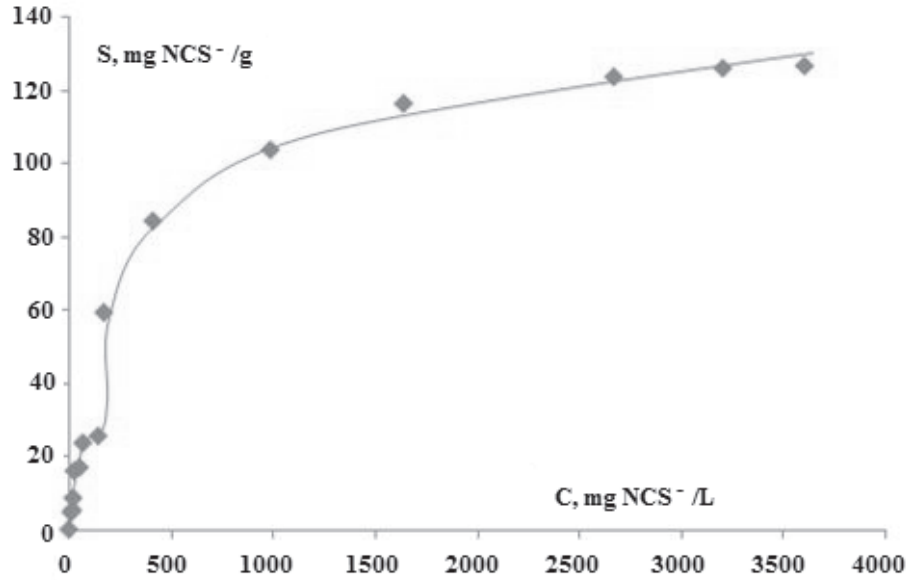

Figure 7-53. Nonequilibrium sorption isotherm of NCS^- ions on AV-17(Cr).

Both isotherms were constructed and calculated with the Langmuir, Freundlich, Sips and Dubinin-Radushkevich sorption models. The isotherms parameters and the value of R^2 and X^2 are listed in Table 7-20. The Figure 7-51 and Table 7-20 data, values of R^2 and non-linear Chi-square test X^2, show that the sorption isotherm, obtained in a wide range of the NCS^- ions concentration, is best described by Langmuir and Dubinin-Radushkevich (especially at the concentration higher than 100 mg NCS^-/L), sorption simulations. But at worst the isotherm is described by the Freundlich sorption model, especially at high concentrations of NCS^- ions.

Table 7-20. Parameters of the isotherms, calculated by the Langmuir, Freundlich, Sips and Dubinin-Radushkevich sorption models for sorption of NCS^- ions on AV-17(Cl) sorbent

Langmuir model	**S_L, mg/g**	**K_L, L/mg**		**R^2**	**X^2 (complete isotherm)**	**X^2(C_{NCS} > 100 mg/L)**
1. Large NCS^- concentration	177.8	0.013		0.9649	61.52	4.52
2. Low NCS^- concentration	135.9	0.092		0.9507	3.69	-
Freundlich model	**K_F**	**N**		**R^2**	**X^2 (complete isotherm)**	**X^2(C_{NCS} > 100 mg/L)**
1. Large NCS^- concentration	18.92	0.346		0.9936	131.44	88.9
2. Low NCS^- concentration	31.12	0.31		0.9944	9.61	-
Sips model	**S_S**	**K_S**	**1/n**	**R^2**	**X^2 (complete isotherm)**	**X^2(C_{NCS} > 100 mg/L)**
1. Large NCS^- concentration	333.3	0.103	0.346	0.9507	19.61	13.58
D.-R. model	**S_{D-R}**	**K_{D-R}**	**E, kJ/mol**	**R^2**	**X^2 (complete isotherm)**	**X^2(C_{NCS} > 100 mg/L)**
1. Large NCS^- concentration	164.02	0.002	15.82	0.9649	-	0.38

The isotherm, obtained at low concentrations of NCS^- ions (Fig. 7-52), is described by the Langmuir sorption model (Tab.7-20). The Freundlich sorption model does not adequately describes the isotherm, but the Dubinin-Radushkevich and Sips models, can not be used to describe the isotherm.

The fact that the sorption isotherm of NCS^- ions are best described by the Langmuir model, confirms that absolutely most of the active centres ($-N(CH_3)_3^+$) of the AV-17(Cl) sorbent are energetically equivalent and do not depend on their occupancy by the NCS^- anions. The value of E (free energy of adsorption, Eq. 7-44) of 15.86 kJ/mol (Tab.7-20) shows that the NCS^- ions sorption on the polymer AV-17(Cl) is determined by the anion exchange process. But a small part of sorption occurs involving chemical forces, especially at low concentration. The experimental isotherm of NCS^- anions sorption on AV-17(Cr), obtained at the contact of the sorbent with the solution for 24 hours, is shown in Figure 7-53. On this isotherm a plateau has also appeared at the low concentrations of the NCS^- ions in solution. The data in Figure 7-53 show that in similar conditions the sorption of NCS^- ions on the composite AV-17(Cr) is less than on the polymer AV-17(Cl). This seems strange at first. As we will see later, sorption on the AV-17(Cr) should be greater than on the AV-17(Cl). This divergence is due to the well-known fact that the exchange of ligands (in our case groups SO_4^{2-} with NCS^- ions) in complexes of chromium (III) takes place rather slowly. The complexes of chromium (III) are kinetically very stable. Sorption of the NCS^- ions on the polymer AV-17(Cl) occurs at a relatively fast rate according to Equation (7-68):

$$R_4NCl + NCS^- = R_4NNCS + Cl^- \quad (7\text{-}68)$$

The duration of the AV-17(Cr) composite contact with the solution of NCS^- during 24 h is not enough to achieve sorption equilibrium. Therefore, the isotherm is obtained in non-equilibrium conditions and it will be incorrect to calculate its parameters. The data of the isotherm, obtained at 96 h contact of AV-17(Cr) composite with a solution of NCS^- (Fig.7-54, Tab.7-21), have confirmed perfectly the above mentioned assumption. Indeed, on longer contact (96

hours against 48) of the AV-17(Cr) with solutions, containing KNCS and 0.01 mol L^{-1} KNO_3, the sorption of NCS^- becomes much higher than had been observed in the examined above cases.

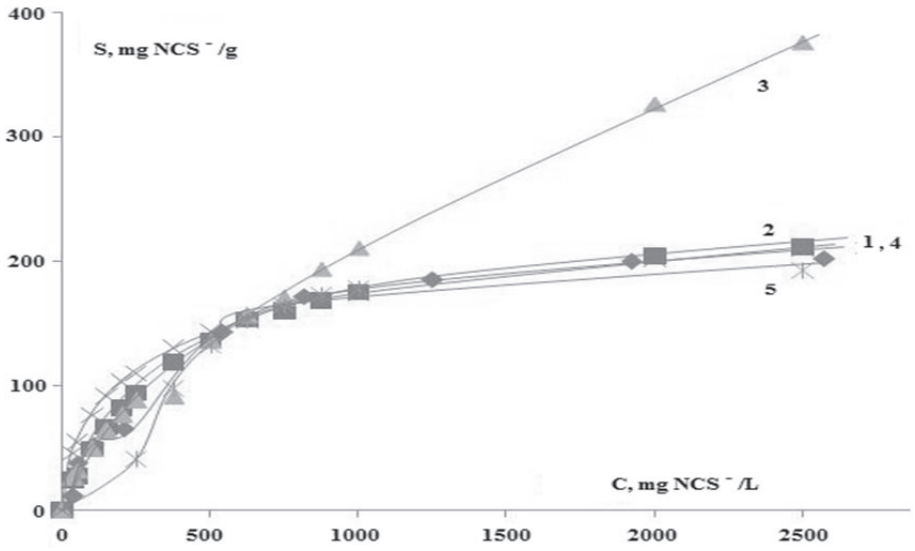

Figure 7-54. Equilibrium sorption isotherm of NCS^- ions on AV-17(Cr) in a large range of NCS^- concentration: obtained experimentally (1), calculated by Langmuir (2), Freundlich (3), Sips (4) and Dubinin-Radushkevich (5) sorption models.

The Figure 7-54 and Table 7-21 data show that the sorption isotherm, obtained in a wide range of the NCS^- concentration, is best described by the Langmuir and D-R (especially at the concentration of NCS^- higher than 500 mg L^{-1}) sorption models. The Sips sorption model gives a slightly inexact description, but the Freundlich model cannot adequately describe the experimentally obtained isotherm, especially at high concentration. The isotherm, obtained at low concentrations of NCS- (Fig.7-55, Tab.7-21), more adequately can be described by the D-R sorption model. The values of E of 3.1 and 57.8 kJ/mol confirmed that the NCS^- sorption on AV-17(Cr) is determined by physical processes at high concentration, and chemical processes - at low concentration of NCS^-.

Table 7-21. Parameters of the isotherms, calculated by the Langmuir, Freundlich, Sips and Dubinin-Radushkevich sorption models for sorption of NCS^- ions on AV-17(Cr) sorbent

Langmuir model	**S_L, mg/g**	**K_L, L/mg**		**R^2**	**X^2 (complete isotherm)**	**X^2(C_{NCS} > 100 mg/L)**
1. Large NCS^- concentration	45.1	0.0025		0.9885	9.91	-
2. Low NCS^- concentration	64.98	0.025		0.9661	18.3	-
Freundlich model	**K_F**	**1/n**		**R^2**	**X^2 (complete isotherm)**	**X^2(C_{NCS} > 100 mg/L)**
1. Large NCS^- concentration	2.718	0.63		0.9948	133.88	-
2. Low NCS^- concentration	4.263	0.562		0.9944	20.05	-
Sips model	**S_S**	**K_S**	**1/n**	**R^2**	**X^2 (complete isotherm)**	**X^2(C_{NCS} > 100 mg/L)**
1. Large NCS^- concentration	285.7	0.02	0.63	0.9885	1265.5	-
2. Low NCS^- concentration	123.45	0.052	0.562	0.9507	16.29	-
D.-R. model	**S_{D-R}**	**K_{D-R}**	**E, kJ/mol**	**R^2**	**X^2 (complete isotherm)**	**X^2(C_{NCS} > 100 mg/L)**
1. Large NCS^- concentration	195.39	0.0162	3.1	0.9885	-	1.06
2. Low NCS^- concentration	54.6	0.00015	57.8	0.9661	15.88	-

The complex interpretation of the isotherms show that they are obtained as a result of several processes, such as ion exchange, involving anions SCN^-, NO_3^-, SO_4^{2-} and, especially, different coordination modes of NCS^- with metal in the composite phase. Already it has been mentioned that NCS^- can coordinate with the metal via atoms N or S and can form bridges between metal atoms.

In order to elucidate the mode of coordination of the NCS^- with Cr^{3+} of the AV-17(Cr), an investigation was performed using FTIR spectroscopy. To confirm the IR spectra data spectra of other composites were also obtained, namely Varion-AD(Cr), AV-17(Fe) and Varion-AD(Fe).

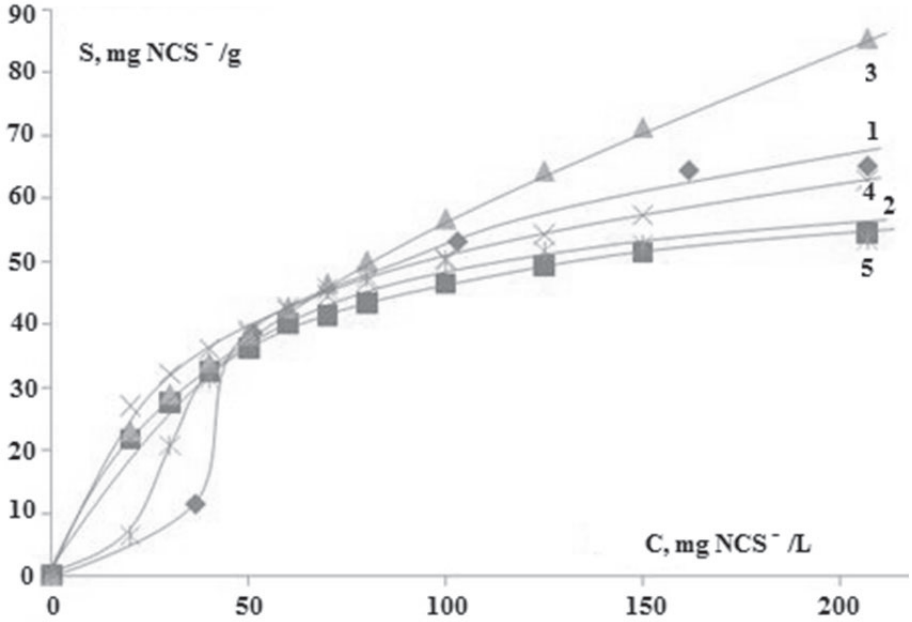

Figure 7-55. Equilibrium sorption isotherms of NCS^- ions on AV-17(Cr) in a low range of NCS^- concentration: obtained experimentally (1), calculated by Langmuir (2), Freundlich (3), Sips (4) and Dubinin-Radushkevich (5) sorption models.

Table 7-22. The IR spectroscopic data of the interaction of composites with various ligands and cations

Composite	Added anion or cation	ν(N≡C), cm^{-1}	Chemical bonds
AV-17(Cr)	NCS^-	2040 2090	Cr-NCS Cr-SCN
Varion-AD(Cr)	NCS^-	2040	Cr-NCS
AV-17(Fe)	NCS^-	2040 2140	Fe-NCS Fe-NCS-Fe
Varion-AD(Fe)	NCS^-	2040	Fe-NCS
AV-17(Fe)	NCO^-	2160 2225	Fe-NCO Fe-NCO-Fe
Varion-AD(Fe)	NCO^-	2140 2190	Fe-NCO Fe-NCO-Fe
Varion-AD(Cr)	NCS^-, Ag^+	2081 2146	Cr-NCS- Cr-NCS-Ag
AV-17(Fe)	NCS^-, Ag^+	2098 2140	Fe-SCN Fe-NCS-Ag
AV-17(Fe)	NCS^-, Cu^{2+}	2040 2140	Fe-NCS Fe-NCS-Cu
Varion-AD(Fe)	NCS^-, Ag^+	2080 2140	Fe-SCN Fe-NCS-Ag

The composite samples were previously washed on the filter with 0.1 M KNCS solution. IR spectra of the composites have also been obtained which were treated with the 0.01M solution of NaNCO. The NCO^- ligand has physical-chemical properties similar to NCS^- and absorption bands in the same segment of the IR spectrum. Interpretation of spectral absorption bands was performed according to Ref. [36]. In the IR spectra of all composites which were treated with the solution of KNCS or NaNCO, the absorption bands characteristic of SO_4^{2-} (about 1100 and 617 cm^{-1}) practically were absent, showing their substitution by other ligands. However, other absorption bands appeared. From the data in Table 7-22, it follows that NCS^- and NCO^- have interacted with the composites through the coordination of the metal with the N atom of the ligand. A small part of NCS^- has coordinated with Cr^{3+} of the AV-17(Cr) through the atom S.

In the composites AV-17(Fe) and Varion-AD(Fe) the ligands NCS^- and NCO^- have formed bridges (M-NCS -M or M-NCO-M) between the metal atoms. If taking into consideration that each NCS^- and NCO^- group with monodentate coordination, substitutes one of the oxygen bound SO_4^{2-} groups in jarosite type compound, it follows that 2 groups of

SO_4^{2-} should be substituted by $6NCS^-$ or $6NCO^-$ ions. Thus, the sorption of NCS^- and NCO- ions by the composites can be expressed by the following Equations (7-69) and (7-70):

$$R_4N[M_3(OH)_6(SO_4)_2] + 6NCS^- = R_4N[M_3(OH)_6(NCS)_6]^{2-} + 2SO_4^{2-} \quad (7\text{-}69)$$

$$R_4N[M_3(OH)_6(SO_4)_2] + 6NCO^- = R_4N[M_3(OH)_6(NCO)_6]^{2-} + 2SO_4^{2-} \quad (7\text{-}70)$$

As a result of the sorption of ligands according to Equations (7-69) and (7-70), the composites change their functionality – they become cation exchangers able to adsorb cations (Ka^{n+}) according to Equations (7-71) and (7-72):

$$nR_4N[M_3(OH)_6(NCS)_6]^{2-} + 2Ka^{n+} = \{R_4N[M_3(OH)_6(NCS)_6]\}_n(Ka)_2 \quad (7\text{-}71)$$

$$nR_4N[M_3(OH)_6(NCO)_6]^{2-} + 2Ka^{n+} = \{R_4N[M_3(OH)_6(NCO)_6]\}_n(Ka)_2 \quad (7\text{-}72)$$

Respectively, $\{R_4N[M_3(OH)_6(NCS)_6]\}_n(Ka)_2$ and $\{R_4N[M_3(OH)_6(NCO)_6]\}_n(Ka)_2$ composites can participate in the cation exchange processes. So, at the interaction of AV-17(Cr) or AV-17(Fe) with NCS^- or NCO^-- the new AV-17(Cr-NCS), AV-17(Cr-NCO), AV-17(Fe-NCS) and AV-17(Fe-NCO) composites are obtained. In these composites instead of AV-17 there can be any polymer containing strongly basic groups. And that is not all. If ligands NCS^- and $NCO^-$are coordinated monodentate through the atoms N, the S or O atoms are able to form new coordination bonds. Thus, the AV-17(Cr-NCS) and AV-17(Cr-NCO) or AV-17(Fe-NCS) and AV-17Fe-(NCO) have become selective sorbents for the sorption of heavy metal (Ag^+, Pb^{2+}, Hg^{2+} and others). Indeed, the above mentioned composites, being treated with solutions of $AgNO_3$ or $CuSO_4$, retain metal cations according to Equations (7-73) and (7-74):

$$\{R_4N[M_3(OH)_6(NCS)_6]\}_n(Ka)_2 + 6nAgNO_3 = \{R_4N[M_3(OH)_6(NCS)_6Ag_6]\}_n(NO_3)_{4n} + (Ka)_2(NO_3)_{2n} \quad (7\text{-}73)$$

$$\{R_4N[M_3(OH)_6(NCS)_6]\}_n(Ka)_2 + 6nCuSO_4 = \{R_4N[M_3(OH)_6(NCS)_6Cu_6]\}_n(SO_4)_{5n} + (Ka)_2(SO_4)_n \quad (7\text{-}74)$$

The existing coordinative nodes M-NCS-Ag and M-NCS-Cu are well shown in IR spectroscopy data (Tab.7-22). So, when AV-17(Cr-NCS), AV-17(Fe-NCS), AV-17(Cr-NCO) or AV-17(Fe-NCO) composites interact with Ag^+, Cu^{2+}, the new **AV-17(Cr-NCS-Ag), AV-17(Cr-NCO-Ag), AV-17(Fe-NCS-Cu)** and **AV-17(Fe-NCO-Cu)** composites are obtained. A lot of new composites can be obtained if instead Ag^+ and Cu^{2+} cations are other metal cations, able to form coordinate bonds. In the composites $\{R_4N[M_3(OH)_6(NCS)_6Ag_6]\}_n(NO_3)_{4n}$ and $\{R_4N[M_3(OH)_6(NCS)_6Cu_6]\}_n(SO_4)_{5n}$ the Cu^{2+}, Ag^+ cations are coordinatively unsaturated. Therefore, these cations may further coordinate the ions and molecules containing electron donor atoms, forming in the polymer phase various ionic-molecular constructions with special properties. For example, the composite AV-17(Cr-NCS-Ag) is able to absorb again a new portion of NCS^- ions through their coordination with Ag^+. This idea has been confirmed by the following investigation. The sorption isotherm of NCS ions on AV-17 (Cr-NCS-Ag) was obtained at a 48-hour contact of the composite with KNCS solutions (Fig. 7-56, curve 1).

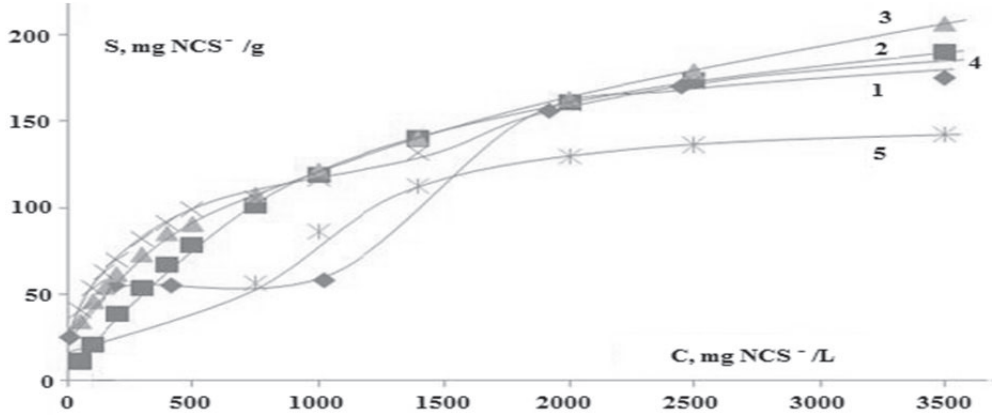

Figure 7-56. Equilibrium sorption isotherms of NCS^- on AV-17(Cr-NCS-Ag) in a large range of NCS^- concentration: obtained experimentally (1), calculated by Langmuir (2), Freundlich (3), Sips (4) and Dubinin-Radushkevich (5) sorption models.

The duration of composite contact with the solution has been taken taking into consideration that the rate of the coordination process of the NCS^- ligand with Ag^+ is rather high, incomparable with the ligand exchange rate in Cr^{3+}compounds. The Figure 7-56 and Table 7-23 data show that the isotherm, obtained in a wide range of the NCS^- concentration, is best described by the Sips and Langmuir sorption models but worst described by the D-R model.

Parameters of the isotherm obtained in a low range of NCS- ions concentration (Fig.7-57, Tab.7-23), are best described by the Freundlich and Sips sorption models.

Table 7-23. Parameters of the isotherms, calculated by the Langmuir, Freundlich, Sips and Dubinin-Radushkevich sorption models for sorption of NCS-ions on AV-17(Cr-NCS-Ag) sorbent

Langmuir model	**S_L, mg/g**	**K_L, L/mg**		**R^2**	**X^2 (complete isotherm)**	**X^2(C_{NCS} > 100 mg/L)**
1. Large NCS^- concentration	250	0.00091		0.9457	43.08	33.62
2. Low NCS^- concentration	43.1	0.04		0.9285	273	-
Freundlich model	**K_F**	**1/n**		**R^2**	**X^2 (complete isotherm)**	**X^2(C_{NCS} > 100 mg/L)**
1. Large NCS^- concentration	6.55	0.423		0.9457	49.85	39.44
2. Low NCS^- concentration	10.49	0.25		0.9756	101.73	-
Sips model	**S_S**	**K_S**	**1/n**	**R^2**	**X^2 (complete isotherm)**	**X^2(C_{NCS} > 100 mg/L)**
1. Large NCS^- concentration	746.3	0.011	0.423	0.9498	57.21	39.56
2. Low NCS^- concentration	245.7	0.0506	0.25	0.9756	127.0	-
D.-R. model	**S_{D-R}**	**K_{D-R}**	**E, kJ/mol**	**R^2**	**X^2 (complete isotherm)**	**X^2(C_{NCS} > 100 mg/L)**
1. Large NCS^- concentration	184.93	0.09129	2.34	0.9898	-	39.9
2. Low NCS^- concentration	39.646	0.000269	43.1	0.9385	278.93	-

Parameters of the isotherm obtained in a low range of NCS- ions concentration (Fig.7-57, Tab.7-23), are best described by the Freundlich and Sips sorption models.

Although the Dubinin-Radushkevich sorption model less adequately describes the sorption of NCS^- ions by the AV-17(Cr-NCS-Ag), the values of E (Tab.7-23), with a certain approximation, confirms that the sorption of anions is conditioned by the chemical forces, as well as the physical ones.

The results of this research demonstrate that by the construction of ionic-molecular combinations in the phase of ionic cross-linked polymers, we can obtain a wide variety of composites with special properties. This is important not only for sorption processes but also for multi-centre catalysis.

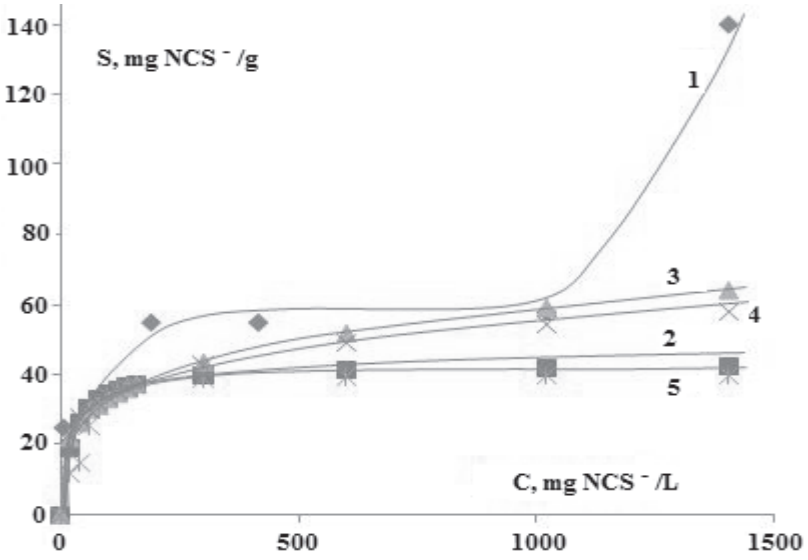

Figure 7-57. Equilibrium sorption isotherms of NCS^- on AV-17(Cr-NCS-Ag) in a low range of NCS^- concentration: obtained experimentally (1), calculated by Langmuir (2), Freundlich (3), Sips (4) and Dubinin-Radushkevich (5) sorption models.

7.8. Sorption properties of Bi(III)-containing polymer

7.8.1. Iodide ions sorption from solution

It is well known that iodine is a very important element for the normal functioning of the human organism. In many countries, the population suffers from iodine deficiencies in terms of their nutrient intake. Therefore, the obtaining of elemental iodine is an actual problem. There are two main sources of iodine: (i) marine flora and fauna and (ii) the water of oil wells. The iodine content in water from oil drilling is relatively high, ranging between 10-60 mg/L [199].

Basically, there are the two following methods of extraction of iodine from aqueous solutions: (i) extraction and (ii) sorption methods. Adsorption methods are based on the use of anion-exchangers. The process of iodide ions interaction with strongly basic anion exchangers was investigated in a number of scientific papers [199-203]. The authors have mentioned that sorption of iodide ions from different solutions by polymers containing strongly basic functional groups is over equivalent. Although sorption studies of iodide ions by strongly basic anion exchangers has been carried out for a long time, the sorbate-sorbent interaction mechanism is not yet fully elucidated. It is found that the sorption of iodide ions occurs as a result of the formation of polyiodide ions in the polymer phase. This process is performed by the anion exchange and chemical sorbate-sorbent interactions.

Studies of iodide ions adsorption on anion exchangers modified with metal compounds have not yet been done. It is necessary to perform such research not only to recover iodide ions from solutions but also in order to elucidate the mechanism of sorbate-sorbent interaction. It should also be noted that the polymers containing polyiodide ions can serve as sorbents for the removal of reductants from gaseous phases such as phosphine [204], hydrazine [205] and others.

In this investigation, the strongly basic anion exchangers AV-17(Cl) and Varion-AD(NO_3) [4] have been used. Polymer AV-17 modified with Bi(III) compounds also was investigated. The process of obtaining the sorbent AV-17(Bi) takes place according to the method described elsewhere [121]. The polymer modified with Bi(III) compounds contains crystalline BiOCl and amorphous BiOOH [124]. The Bi content in the prepared sorbent AV-17(Bi) was 25.3 mg Bi/g. Sorption of the iodide ions occurred in solutions containing (i) KI and (ii) a mixture of KI and KCl [206]. The investigation was carried out in static and dynamic conditions. In the static conditions, the polymer samples of 0.2 g were contacted with 50 mL of solution. When necessary, the pH value of the solution was adjusted using the solution of H_2SO_4 or NaOH.

Iodide ions sorption by AV-17(Cl) in the static conditions. The results showed that at the temperature of 19.5^{o}C the equilibrium sorption of iodide ions (in solutions containing 0.25 mg KI/mL) is reached at 10 minutes of contact with the polymer AV-17(Cl). It was also found that the sorption practically does not depend on the solution pH value in the range of 3-10.

Theoretically, iodide ions sorption on strongly basic anion exchangers should be a reversible process according to Equation (7-75):

$$R_4NCl + I^- \leftrightarrow R_4NI + Cl^- \quad (7\text{-}75)$$

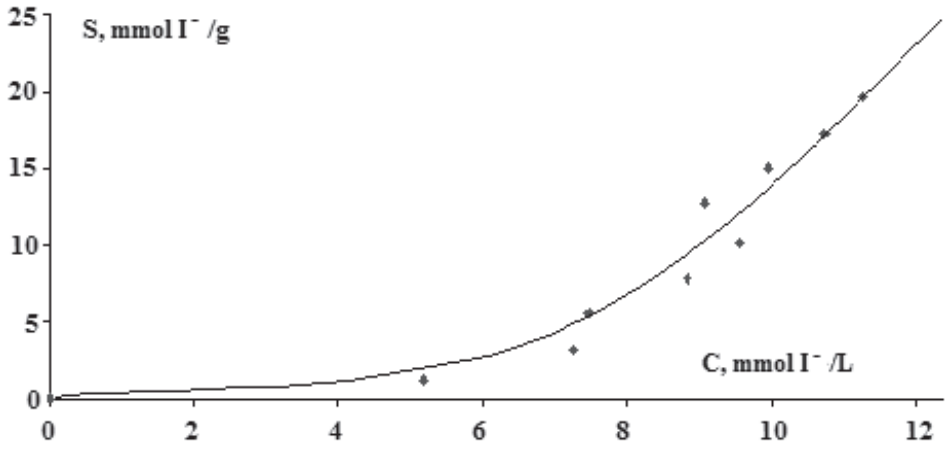

Figure 7-58. The isotherm of iodide ions' sorption from KI solutions on AV-17(Cl).

But the sorption isotherm obtained at 16.5^{o}C, shows that iodide ions retention on AV-17(Cl) from KI solution is not determined by the anion exchange process only (Fig.7-58). The shape of the sorption isotherm is similar to the BET isotherm. This indicates that in the polymer phase processes of condensation of iodide ions take place as a result of the forming of polyiodide ions $I(I_2)n^-$. This indicates that in the system containing polymer and KI solution, the redox processes take place, involving atmospheric oxygen. Polyiodide ions formation in the polymer phase is confirmed by the fact that the sorption value is much higher than the theoretical exchange capacity of the polymer. The isotherm parameters using the BET adsorption model were calculated by Equations (7-46) and (7-47). It is known that the BET

isotherm describes the adsorption of gases. But it can also be used to describe the sorption from solutions when in the sorbent phase the sorbate forms polymeric compounds [159].

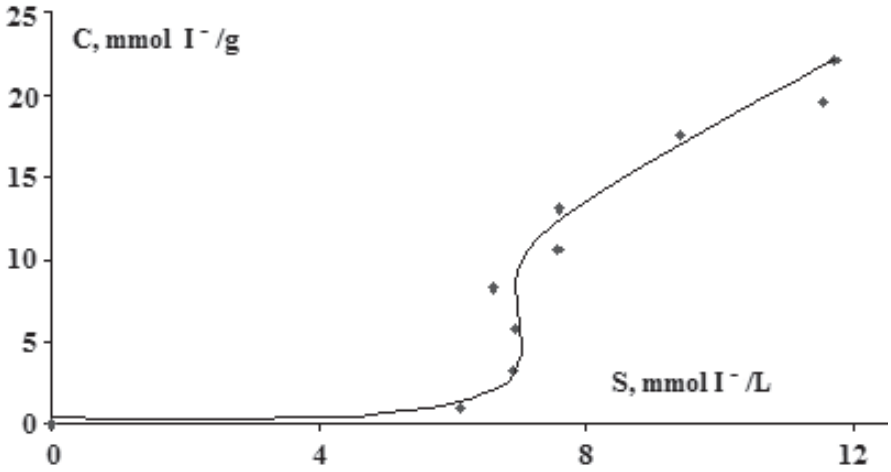

Figure 7-59. The isotherm of iodide ions' sorption on AV-17(Cl) from solutions containing KI and KCl.

The linear form of the experimentally obtained isotherm (Fig.7-58) with Cs = 13.4 mmol I^-/L, is shown in Figure 7-60, and the constants values in Table 7-24. As shown in Figure 7-58, the forming of the polyiodide ions in the polymer phase begins at concentrations higher than 7 mmol I^-/L. It would seem that sorption occurs in the outcome (Eq. (7-76)), i.e. in the result of the anion exchange:

$$R_4NI + nI_2 \leftrightarrow R_4NI(I_2)_n. \quad (7\text{-}76)$$

But the results of iodide ions sorption from solutions of KI with increased concentrations of KCl demonstrated that it is not so. The sorption isotherm of iodide ions from the KI solution containing 0.1 mol KCl/L on polymer AV-17(Cl) (at 16.5 ºC) is shown in Figure 7-59. The shape of this isotherm is similar to the shape of the sorption isotherm from KI solution in the absence of KCl (Fig.7-58). The linear form of the isotherm calculated using the BET model with Cs = 12.8 mmol I^-/L, is shown in Figure 7-60, and the constants values in Table 7-24. It is possible that in the polymer phase, the formation of I_2Cl^- ions and others [199] takes place.

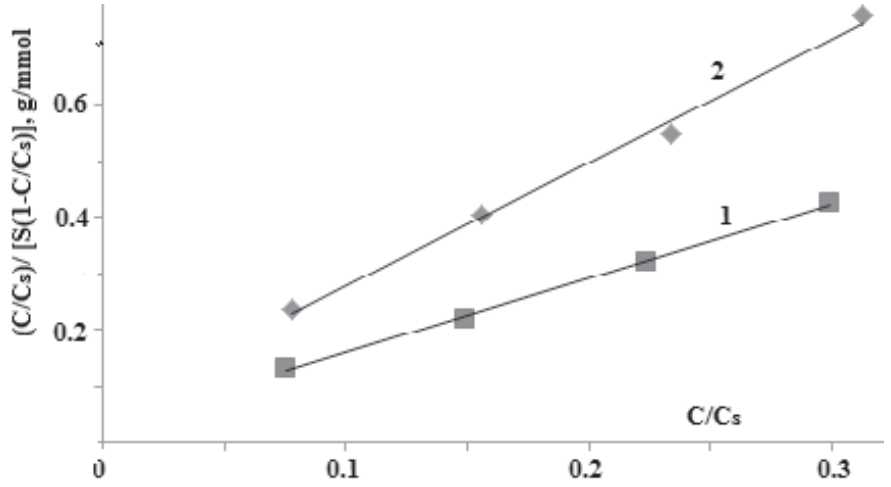

Figure 7-60. The linear BET isotherms of iodide ions' sorption on AV-17(Cl) from KI solutions (1) and solutions containing KI and KCl (2).

According to [199], sorption of the iodine-containing ions on the AV-17-8 increases in the following order:
$I^- < I_3^- < I_2Cl^-$.

Table 7-24. Isotherms constants of iodine ions' sorption on AV-17(Cl)

Sorbent	Solution	T, °C	pH	S_L, mmol/g	K_{BET}, g/mmol
AV-17(Cl)	KI	16.5	4.85–5.65	0.74	48.5
AB-17(Cl)	KI + KCl	16.0	4.66–5.95	0.46	33.8

The $S_L$value of iodine ions sorption from KI solution containing KCl is much lower in comparison with the solution without KCl (Tab.7-24). This means that in solutions with low concentrations of KI (C < 7 mmol KI/L), I^- ions are in competitions with the Cl^- ions. Given the much higher concentration of KCl than KI, iodide ions sorption that from solutions containing KCl is to be much lower than that from solutions without KCl, if sorption is to be determined by anion exchange. But the results show that sorption of iodide ions from solutions containing an excess of KCl is no lower than from solutions without KCl. These results suggest that a part of iodide ions and polyiodide is retained by AV-17(Cl) due to the anion exchange process and another as a result of chemical interaction with the polymer matrix.

It is known, that at low concentrations the BET isotherm turns to the Langmuir isotherm. Indeed, sorption of iodide ions at 19.5°C in solutions with low concentrations of KI on the polymer Varion-AD(NO_3^-) (strongly basic anion exchanger, analogue AV-17) is described by the Langmuir sorption model (Fig.7-61) according to Equation (1-9).

The constants S_L and K_L were calculated using a linear form of the Langmuir isotherm (Fig.7-62), performed according to Equation (1-10). The following values of the constants:

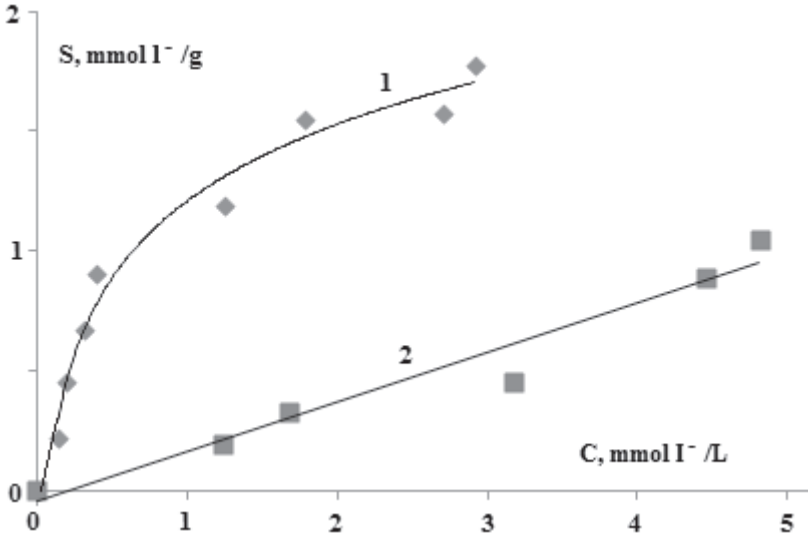

Figure 7-61. The isotherms of iodide ions' sorption by Varion-AD(NO_3) from KI solutions (1) and solutions containing KI and KCl (2).

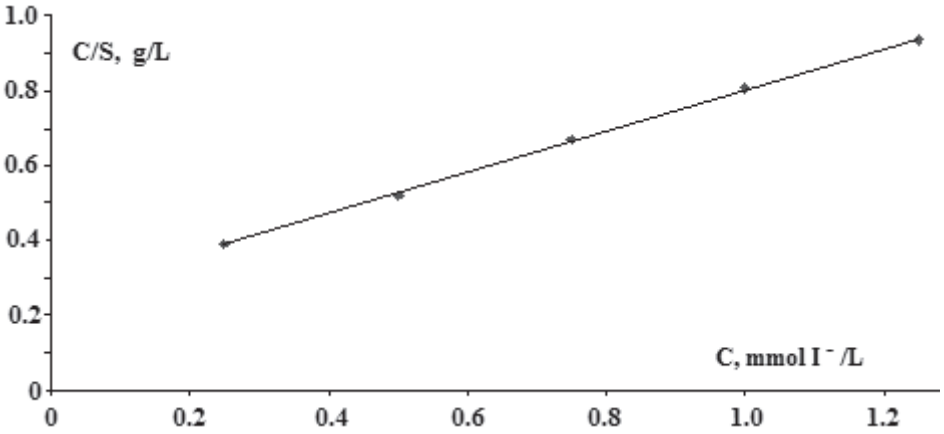

Figure 7-62. The linear Langmuir isotherm of iodide ions' sorption from KI solutions on Varion-AD(NO_3).

S_L = 1.84 mmol I^-/g and K_L = 2.134 L/mmol were obtained. The sorption isotherm of iodide ions from 0.1 M KCl solutions on Varion-AD, obtained at 19.5°C, is approximately described by the Henry sorption model (Fig.7-61) with K_H = 0.206 L/g.

Iodide ions sorption on AV-17(Bi) in the static conditions. As shown in Figure 7-63, the iodide ions sorption isotherm from KI solutions by sorbent AV-17(Bi), obtained at 12.5 ºC, also can be described by the BET sorption model. The isotherms of iodide ions sorption on AV-17(Bi) sorbent from solutions containing KI and KCl, obtained at 16°C and 60ºC (Fig.7-64), also correspond to the BET adsorption model. From linear BET isotherms (Fig.7-65) considering Cs = 23.2 mmol I^-/L (sorption from KI solutions), Cs = 21 mmol I-/L (sorption at 16°C from solutions containing KI and KCl) and Cs = 17 mmol I-/L (sorption at 60°C from solutions containing KI and KCl) were calculated constants shown in Table 7-25.

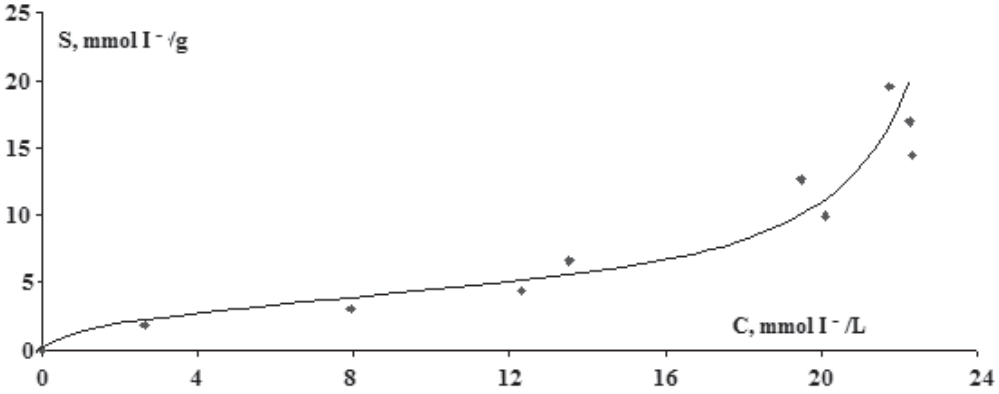

Figure 7-63. The isotherm of iodide ions sorption from KI solutions on AV-17(Bi).

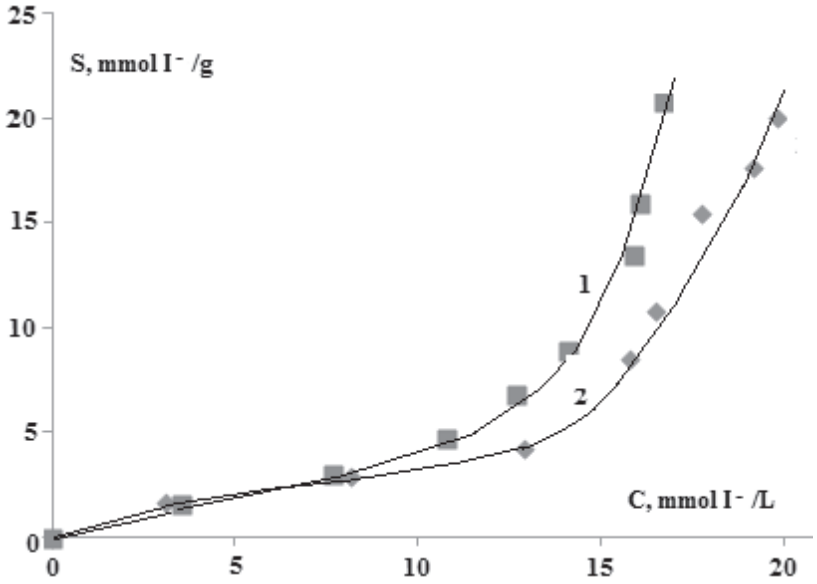

Figure 7-64. The isotherms of iodide ions sorption on AV-17(Bi) at 60ºC (1) and 16ºC (2) from solutions containing KI and KCl.

From the values of Figures 7-63 and 7-64, and S_L (Tab.7-25) we can see that the monolayer sorption capacity of the sorbent AV-17(Bi) is much higher than that of the polymer AV-17(Cl). It means that the compounds of Bi(III) in the polymer phase also are involved in the processes of iodide ions sorption. It is important to remark that the sorption of iodine ions slightly depends on the presence of an excess of KCl in the KI solution and on temperature. If data are compare from Figures 7-58 and 7-59, and Figures 7-63 and 7-64, we can see that the value of iodide ions sorption on AV-17(Cl) and AV-17(Bi) samples is almost the same. It would seem that in the similar conditions maximal iodide ions sorption on AV-17(Bi) must be

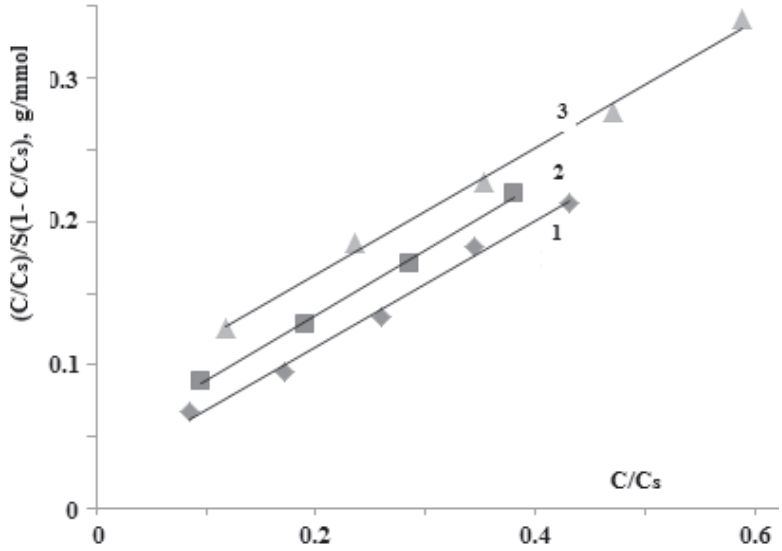

Figure 7-65. The linear BET isotherms of iodide ions sorption on AV-17(Bi) from KI solutions (1), from solutions containing KI and KCl at 16ºC (2) and at 60ºC.

larger than on the AV-17(Cl) because in the first sorbent there are R_4NNO_3 and Bi(III)-containing sorption centres and in the AV-17(Cl) there are only R_4NCl centres. It can be explained by the fact that a part of the Bi(III) compounds are situated on R_4NNO_3 groups and they block the access of iodine ions to them [124].

Iodide ions sorption on AV-17(Cl) and AV-17(Bi) in dynamic conditions. The solution of KI with an initial concentration of C_0 = 0.635 mg I^-/mL, pH_0 = 5.0 and a temperature of 14ºC has been passed through the column containing 2 g of polymer AV-17(Cl) with a flow of 4.46 mL/min. In the effluents, the concentration of I^- ions and the value of pH were measured. From the obtained experimental data, the dependencies C = f(V) and pH = f(V) were performed, where V is the volume of effluents. These dependencies are shown in Figure 7-66.

The dynamic sorption capacity (DSC), the total dynamic sorption capacity (TDSC) and the relative rate of sorption (W) were calculated from Figure 7-66 and are presented in Table 7-26. The values of these parameters are quite high. In Figure 7-66 it can be seen that the speed of the sorption of iodide ions is quite high. This confirms the high rate of sorption that has been observed in the static conditions. Sorption of iodide ions in 0.1M KCl solutions on polymer AV-17(Cl) at the same conditions of concentration of KI, temperature and initial pH, but at the flow rate of 5 mL/min, is lower than in the absence of KCl in a solution (Fig. 7-67, Tab. 7-26). But the relative rate of I- ions sorption from the solution containing an excess of KCl is slightly larger (Tab. 7-26). Although the affinity of the polymer to the iodide ions is much greater than to chloride ions, these ions (Cl^-) significantly affects I^- ions sorption. The pH value of effluents

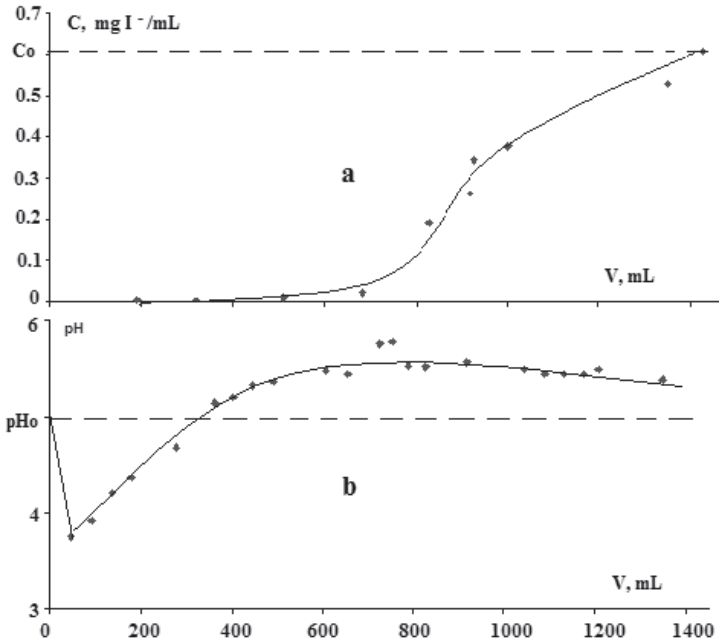

Figure 7-66. Breakthrough curves for sorption of iodine ions from KI solution on AV-17(Cl) (a) and the pH value of effluents during sorption (b).

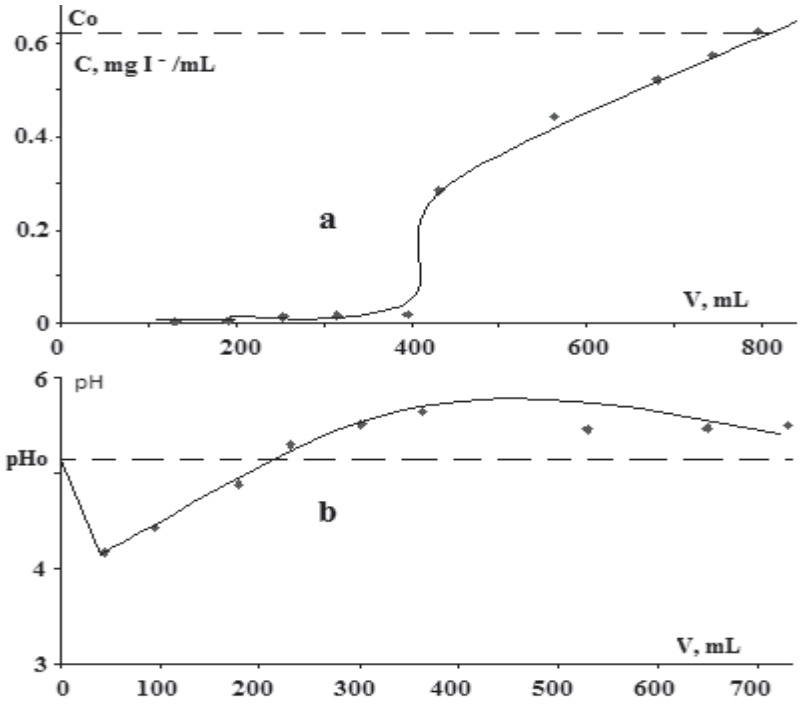

Figure 7-67. Breakthrough curve for sorption of iodide ions on AV-17(Cl) from KI solution containing KCl (a) and the pH value of effluents during sorption (b).

during iodide ions sorption on AV-17(Cl) from KI and KCl solution is presented in Figure 7-67(b). The breakthrough curves for the sorption of iodide ions from solutions (containing 0.635 mg I^-/mL) on sorbent AV-17(Bi) and the pH of the effluents (Figs. 7-68, 7-69 and 7-70) are similar to those obtained using polymer AV-17(Cl).

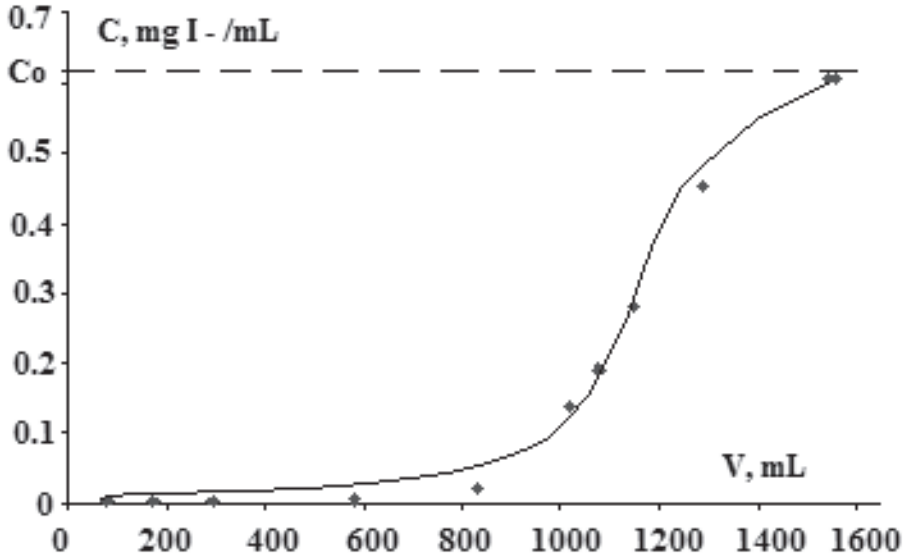

Figure 7-68. Breakthrough curve for sorption of iodide ions from KI solution on AV-17(Bi)

The values of the sorption parameters are higher than for sorption on AV-17(Cl) in almost the same conditions. The data in Table 7-27 show that the iodide ions sorption parameters from

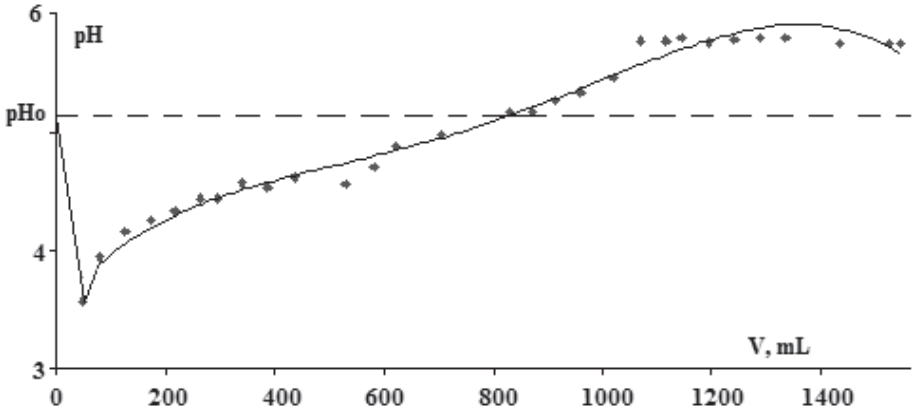

Figure 7-69. pH value of effluents during iodide ions sorption on AV-17(Bi) from KI

solutions containing KI and KCl on the sorbent AV-17(Bi) are lower than those from solutions in the absence of KCl. But they are quite high if takeing into consideration that the concentration of iodide ions is much lower than that of the chloride ions. This confirms that the selectivity for iodide ions sorption on AV-17(Bi) is greater than that on AV-17(Cl).

Comparing the curves from Figures 7-66(b), 7-67(b), 7-69 and 7-70(b), it was established that in the case of absorption from KI solutions and solutions containing KI and KCl, the variation in pH value in the effluents volume is almost the same for AV-17(Bi) or AB-17(Cl) samples. Probably, at the beginning of the process, the polymer retains OH^- ions from solution,

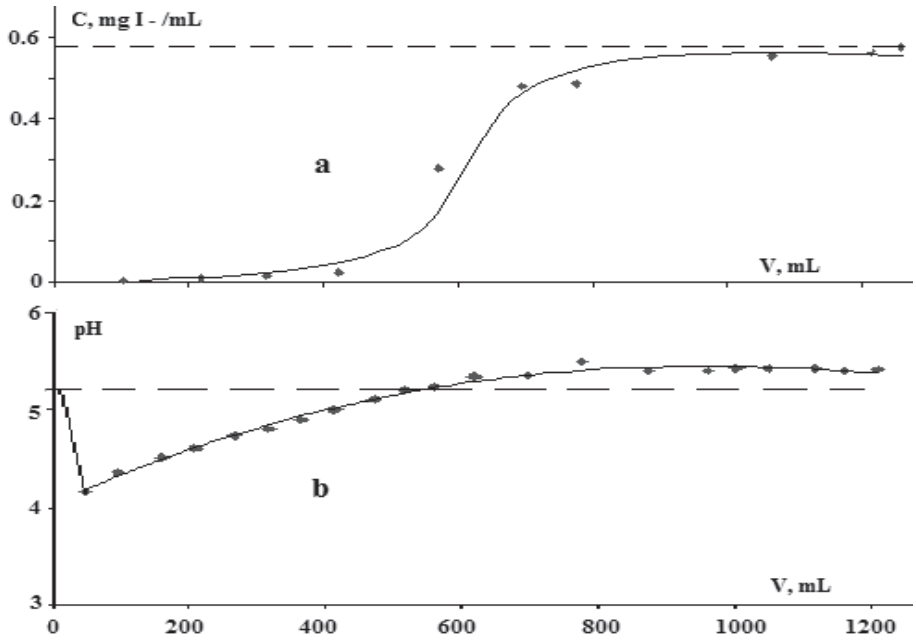

Figure 7-70. Breakthrough curve for sorption of iodide ions on AV-17(Bi) from solution containing KI and KCl (a), and the pH value of effluents during sorption (b).

Table 7-24. Isotherms constants of iodine ions sorption on AV-17(Cl)

Sorbent	Solution	T, ^oC	pH	S_∞, mmol/g	K_{BET}, g/mmol
AV-17(Cl)	KI	16.5	4.85–5.65	0.74	48.5
AB-17(Cl)	KI + KCl	16.0	4.66–5.95	0.46	33.8

Table 7-25. Isotherms constants of iodine ions' sorption on AV-17(Bi**)**

Sorbent	Solution	T, ^oC	pH	S_∞, mmol/g	K_{BET}, g/mmol
AV-17(Bi)	KI	12.5	5.0–6.15	2.23	15.2
AV-17(Bi)	KI + KCl	16.0	5.1–6.2	2.03	10.5
AV-17(Bi)	KI + KCl	60.0	4.54–6.1	1.87	7.8

thus decreasing the pH of the effluent. When promoting the sorption layer of iodide ions along the column, OH^- ions are displaced in the effluents, increasing its pH. This can be explained by the increase of pH value in the effluents, which becomes higher than the initial pH of the solution.

Table 7-26. Data of the iodide ions sorption in the dynamic conditions on AV-17(Cl)

Sorbent	Solution	T, °C	Flow rate, mL/min	DSC, mg I⁻/g	TDSC, mg I⁻/g	W, %
AV-17(Cl)	KI	14	4.46	212.72	314.28	67.7
AV-17(Cl)	KI + KCl	16	5.0	124.46	167.10	74.5

Table 7-27. Data of the iodide ions sorption in the dynamic conditions on AV-17(Cr)

Sorbent	Solution	T, °C	Flow rate, mL/min	DSC, mg I⁻/g	TDSC, mg I⁻/g	W, %
AV-17(Bi)	KI	16.5	4.9	263.52	377.62	69.8
AV-17(Bi)	KI + KCl	17.5	4.6	134.0	229.15	58.5

Note: Additional qualitative experiments showed that sorbent AV-17(Bi) is able to retain compounds of iodine (and bromine) from Valeni (Moldova) drilling waters.

7.8.2. Elimination of molecular iodine from the air.

In the body, radioactive iodine is rapidly absorbed into the blood and lymphatic systems. During the first hour 80-90% is adsorbed in the upper part of the small intestine. The accumulation of iodine in the organs decreases in the following order: thyroid gland, kidney, and liver. Less iodine accumulates in muscle tissues [207]. Excessive accumulation of radioactive iodine in the thyroid gland has serious negative health consequences: thyroid gland dysfunction, cancer risk and others. A method for removing radioactive iodine from the gas phase is known, consisting in the iodine-containing gas passing through a porous sorbent impregnated with an $AgNO_3$ salt. At the heart of the sorbent, silicon carbide with a porosity of 30-60% is proposed as a porous material. After impregnation with an $AgNO_3$ solution, the porous material is dried at a temperature of 100-150°C. The impregnation and drying operation is repeated several times. The storage of molecular iodine by the sorbent is carried out at 200°C [208]. During the retention of iodine, toxic NO_2 gas is released as a result of the reaction (Eq. (7-77)):

$$6AgNO_3 + 3I_2 \leftrightarrow 4AgI + 2AgIO_3 + 6NO_2 \quad (7\text{-}77)$$

Another process for the removal of iodine from gases [209] consists in the iodine-containing gas contacting the sorbent formed from metals selected from the group Cu, Ag, Pd, Bi, Pb, Sn or alloys of these metals with zinc. The iodine gas contacts the sorbent in the temperature range 125 ÷ 250 °C. As a result of the process, salt of insoluble metal iodide is formed [208]. Another process [209] for the sorption elimination of iodine from the air stream, consists in the air flow passing through the column containing the zeolite in which the sodium ions are substituted by silver and lead ions. The zeolite used is in the form of spherical or cylindrical granules of a diameter or length of several centimetres. Prior to use, the sorbent is activated at about 450 °C. The process of removing iodine from the air stream takes place at 14°C [209].

A new method is proposed [210] for the removal of molecular iodine (including radioactive iodine) from the air with the use of the strongly basic polymer modified with Bi(III) compounds**.** For research, the sorbent AV-17 (Bi) was used, obtained according to [121], which contained 43.5 mg Bi/g. A glass column with a diameter of 1.2 cm was used. The experiments were carried out using the system schematically shown in Figure 7-71. The molecular iodine was obtained by mixing 130 ml of a 0.1506 M KI solution with 15 ml of 2M H_2SO_4 solution

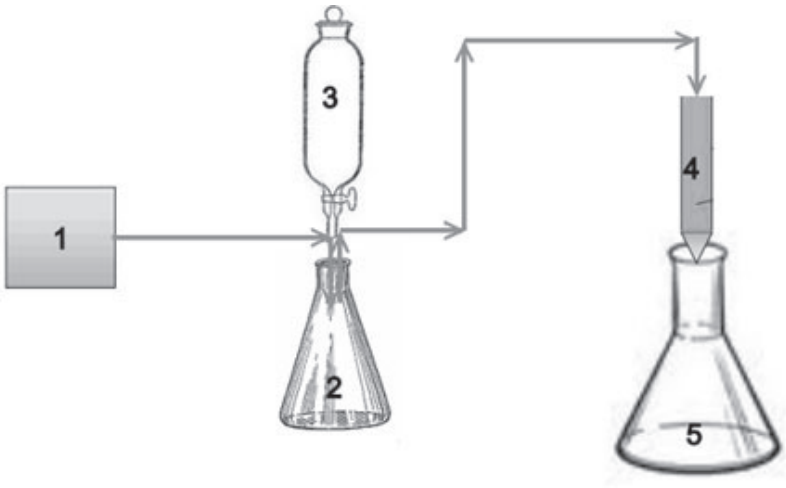

Figure 7-71. Installation scheme for the experiments: 1 – air pump, 2 – KI and H_2SO_4 solution, 3 – $KMnO_4$ solution, 4 – column with AV-17 (Bi), and 5 – starch solution.

and an excess of 0.1 M $KMnO_4$ solution at heating in the water bath. Transport of air containing iodine through the sorbent column was performed with an air pump. Detection and analysis of iodine were performed using the photocolorimetry method with a starch solution. From the experimental data, the coefficients of the Shylov equation were calculated: $\tau = K \cdot h - \tau_0$, where K is the protection coefficient (min/cm); h is the height of the sorbent layer in the column (cm); and τ_0 is the time of loss of protection (min).

Table 7-28. The experimental data for the molecular iodine removal from the air

Sorbent mass, g	h, the height of the sorbent layer in the column, cm	t, the duration of the process up to the occurrence of I_2 at the exit of the column, min
1.0	2.3	7.5
2.0	4,4	21.47
2.5	5.2	30.35
3.0	6.0	42.54
3.5	6.8	60.25
4.0	7.6	117.62

Air with a concentration of 1.5 mg I_2 /L and a speed of 1 L/min passed through the AV-17(Bi) sorbent column until the iodine appears at the exit of the column. The experiments were carried out varying the height (thickness) of the sorbent layer in the column. Each time, the duration of the iodine retention process in the column was fixed until it appeared at the exit of the column. The results are shown in Table 7-28. Data of Table 7-28 shows that the sorbent effectively removes iodine from the air. From the data of Table 7-28 the graph of the

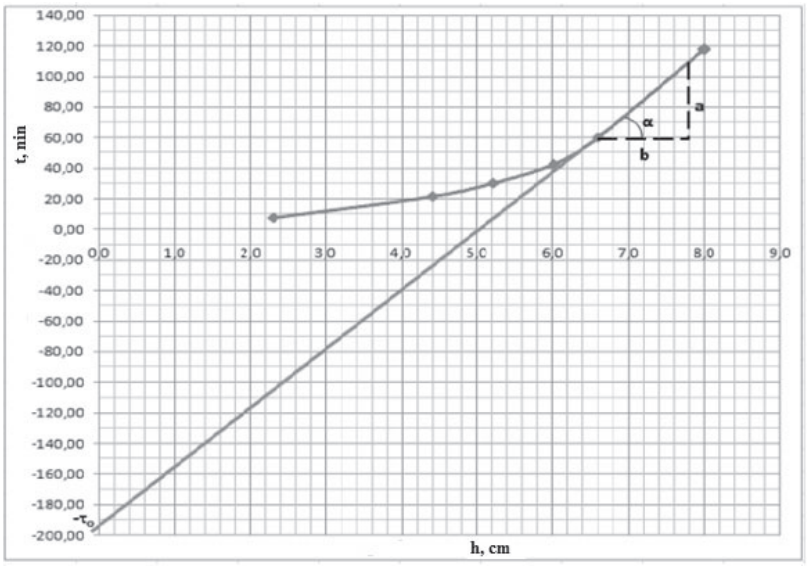

Figure. 7-72. The sorption time up to iodine output from the column depending on the thickness of the sorbent layer. Air flow rate 1 L/min.

dependence of the iodine retention time as a function of the height of the sorbent layer in the column (Fig.7-72) was plotted and the coefficients K (min/cm) and τ_0 (min) of the equation Shylov: $\tau = 41.67 \cdot h + 19$ were calculated. The obtained results prove that the AV-17(Bi) sorbent is effective in removing iodine from the air including radioactive iodine.

Cross-linked ionic polymers containing strongly basic groups have also been used for the elaboration of removal processes of H_2S from water [211] and air [212].

7.9. Unusual processes on polymers loaded with metallic compounds

7.9.1. Formation and destruction of Fe(III) compounds in the polymer phase.

The jarosite (alunite) mineral-type compounds in the polymer phase are amorphous or have a little degree of crystallinity and cannot be investigated using the X-ray diffraction method. On the other hand, it is expected that their formation conditions and their stability will differ from those of naturally or synthetically obtained jarosite. So, on heating in water (t >80 ^oC) synthetically obtained Fe-jarosite compounds are converted to highly dispersed particles of α-FeOOH in the superparamagnetic state [30]. In the phase of strongly basic anion exchangers, when boiling in water media, jarosite compounds may be converted into β-FeOOH in the superparamagnetic state or relatively massive magnetically ordered particles [33,76].

Native jarosite mineral is not so stable, partially being transformed into $Fe(OH)_3$ [58, 213].

It is necessary in order to apply Fe(III)-containing strongly basic anion exchangers as selective sorbents or catalysts to know their behaviour in different media and the sorption-desorption features of the Fe(III)-containing cations on such kind of polymers.

In the present section, there was a concomitant investigat ion of sorption and desorption processes of Fe(III)-containing cations on strongly basic anion exchanger [125]. For the investigation, commercial strongly basic anion exchangers AV-17 and Varion-AD in Cl^- form were used. For comparison, Fe(III)-containing cations sorption has been performed on some commercial strongly basic anion exchangers, sulfonic and carboxylic cation exchangers, and exchangers containing quaternary pyridinic nitrogen and donor atoms of electrons obtained at the ‘‘P. Poni’’Institute of Macromolecular Chemistry, Iasi, Romania.

For the preparation of the solution, $Fe_2(SO_4)_3 \cdot 9H_2O$ has been used. Dried samples (0.2 g) of the polymers were contacted with 100 mL of 0.02M, $Fe_2(SO_4)_3 \cdot 9H_2O$ or 7 g $Fe_2(SO_4)_3$/L solutions. The pH of the solution-sample system was maintained at 1.9 ± 0.1 by using either H_2SO_4 or KOH solutions. The sorption took place at 50 ±1.0^oC according to Ref. [72]. Except for some kinetics studies, the sample duration contact with the solution was 10 h. Following contact with the solution, the polymer samples were filtrated, washed with 50 mL distilled water, and dried at 50 ^oC for 3 h. The content of iron ions in the dried samples was determined by photocolorimetry [26], after desorption with 1M HCl solution. The error of determination constituted 0.3 mg Fe/g polymer. Some polymer samples (0.2 g) after sorption and washing with 50 mL distilled water were placed in 100-mL distilled acidulated water or 0.1M K_2SO_4 solution both with pH = 2 to investigate iron ions desorption at a different temperature. To determinate magnetic susceptibility, a Fe(III)-containing sample of AV-17 polymer was prepared. For that, 5 g of AV-17 was placed into 500 mL of $Fe_2(SO_4)_3$ (7 g/L) solution with pH = 1.9 and t = 52 ^oC for10 h. After sorption and washing with distilled water, samples were dried at 50^oC for 4 h. Paramagnetic susceptibility of Fe(III)-containing AV-17(Cl) was measured at room temperature using the Gouy method. The effective magnetic moment (μB-Bohr magneton) of iron ion in the polymer phase was calculated according to Ref.[214]:

$$\chi_g^{p+m} = \chi_g^{m} \cdot \omega + \chi_g^{p}(1 - \omega) \quad (7\text{-}78)$$

$$\chi_g^{m} = [\chi_g^{p+m} - \chi_g^{p}(1 - \omega)] / \omega \quad (7\text{-}79)$$

$$\chi_M^{m} = \chi_g^{m} \cdot M \quad (7\text{-}80)$$

$$\mu_{ef} = 2.84 (\chi_M^{m} \cdot T)^{1/2} \quad (7\text{-}81)$$

where χ_g^{p+m} is the mass (gram) magnetic susceptibility of the metal (ions) containing polymer, χ_g^{m} is the mass magnetic susceptibility of the metal in the polymer phase, ω is the mass part of the metal in the polymer phase, χ_M^{m} is the molar magnetic susceptibility of the metal, χ_g^{p} is the mass magnetic susceptibility of the polymer, M is the molar mass of the metal, T is the thermodynamic temperature, and μ_{ef} is the effective magnetic moment in Bohr magnetons (μB).

It was supposed that when a strongly basic anion exchanger is in contact with $Fe_2(SO_4)_3$ solution, the $[FeOH(H_2O)_5]^{2+}$ cations take part in the process formation of compounds in the polymer phase. It was shown [215] that the metallic cations sorption kinetics is determined by diffusion in the polymer phase.

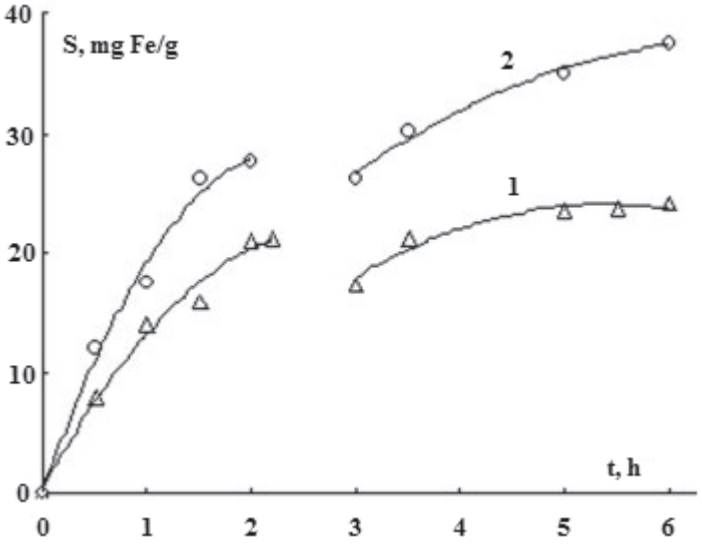

Figure 7-73. Kinetics curves of the Fe(III)-containing ions' sorption with interruption on AV-17 (1) and Varion-AD (2) at 50°C.

It is conditioned by the same charge sign of cations and of the ionized polymer functional groups and the high $Fe_2(SO_4)_3$ solution concentration ($2 \cdot 10^{-2}$M). It is known that if the sorption is determined by the internal diffusion, sorption will increase when the polymer is in contact with the solution again after process interruption by phase separation. However, as shown in Figure 7-73, after sorption process interruption for 24-h, there are fewer Fe(III)-containing cations than before. It means that when polymer contacts with $Fe_2(SO_4)_3$ solution, two concomitant processes take place: the formation of Fe(III)-containing compounds in its phase and their partial destruction. Partial destruction of the Fe(III)-containing compounds in aqueous medium has been confirmed by the next experiments. When Fe(III)-containing samples of the AV-17 polymer were introduced in acidulated water with pH 2.0 (diluted H_2SO_4) solution, desorption of iron cations has been observed (Fig. 7-74). Partial desorption of iron cations from Fe(III)-containing polymer takes place and in contact with electrolyte (0.1M K_2SO_4) solution with pH 2 (Fig. 7-75).

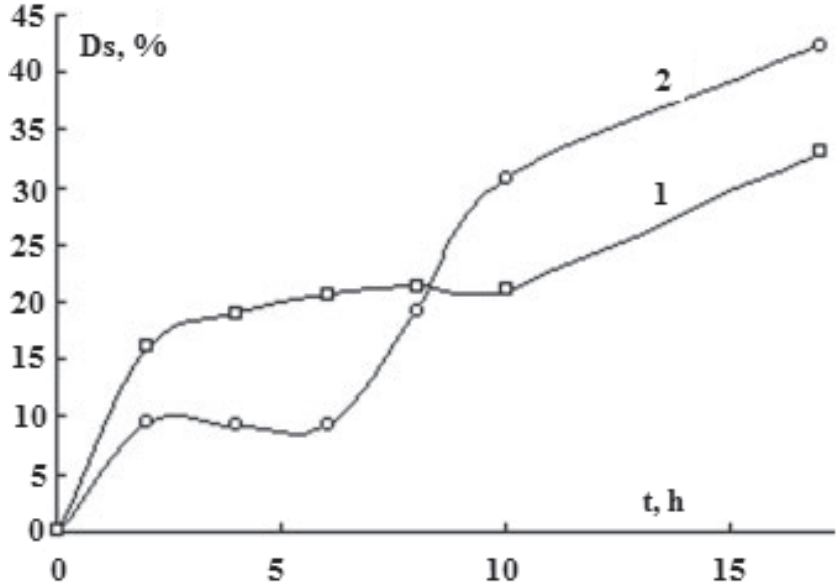

Figure 7-74. Desorption degree (Ds) of iron ions from Fe(III)-containing AV-17 in acidulated water (pH 2) at 50°C (1) and 9°C (2) as a function of polymer-water contact duration.

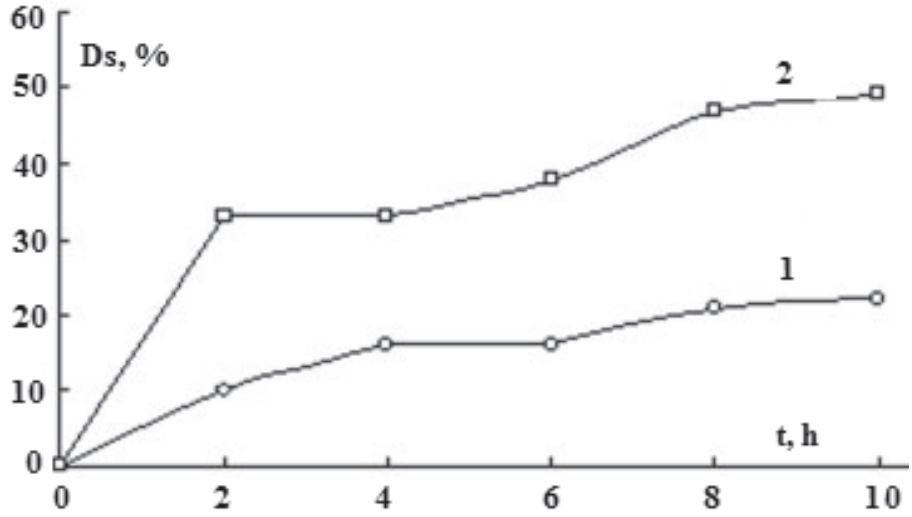

Figure 7-75. Desorption degree at 50°C of iron ions from Fe(III)-containing AV-17 in 0.1M K_2SO_4 solution with pH 2 (1) and from dried AV-17 in acidulated water (pH 2) (2) as a function of polymer-solution contact duration.

As shown in Figures 7-74 and 7-75, there is a plateau on desorption degree (Ds, %) as a function of a contact duration of the sample with acidulated water and K_2SO_4 solution. It may be attributed to a portion of the compounds that had been destructed in the polymer phase before introduction in solution. In this case, the desorption degree of iron cations from polymer samples at 50°C is more than 9°C. But with the increase of the contact duration of the Fe(III)-containing samples with acidulated water, the desorption degree at low temperature becomes higher (Fig.7-74). It means that Fe(III) compounds in the polymer phase are more stable at 50°C temperature. It may be that at this temperature the increasing of the structuration degree of the Fe(III) compounds takes place. The destruction of the Fe(III) compounds that have been obtained in the polymer phase at 50°C takes place when polymer samples remain after that in $Fe_2(SO_4)_3$ solution at room temperature (Fig.7-76). It confirms once more that with the decreasing of temperature the destruction degree of the Fe(III) compounds in the polymer phase increases. The structural stabilization of Fe(III) compounds in the polymer phase on heating is confirmed by the following results.

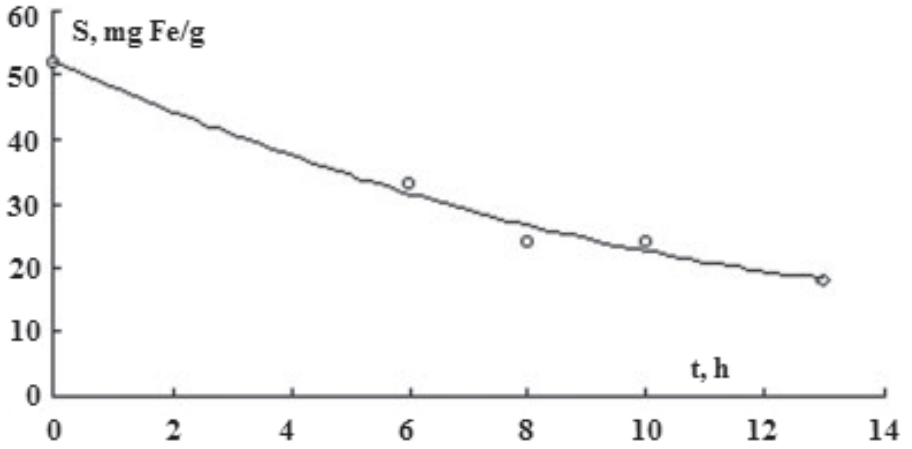

Figure 7-76. Desorption degree of iron ions from Fe(III)-containing AV-17 in $2 \cdot 10^{-2}$M $Fe_2(SO_4)_3$ solution (pH 1.9) at room temperature as a function of polymer-solution contact duration.

As shown in Figure 7-75, the desorption of iron ions in acidulated water at 50 °C from polymer samples being dried in air at 50°C during 4 h also takes place and the desorption degree is high. The electronic state of the iron ions in the dried polymer phase remains practically constant for a long time (at least 140 h), according to magnetic properties. The average effective magnetic moment of iron ion in the dried polymer sample at room temperature is 5.25 Bohr magnetons (μB). This magnetic moment is less than that of 5.9–6.0 μB for Fe^{3+} ion [216]. It means that in the polymer phase there exist antiferromagnetic interactions between iron ions in the jarosite compounds and paramagnetic particles, containing Fe^{3+}. The nature of the magnetical interactions in jarosite compounds is related in Ref. [83]. Supplementary investigations are needed to elucidate the reason for the instability of the Fe(III) compounds in the polymer phase. On the other hand, it can be mentioned that on sorption of some kinds of anions (NCS^- for example), Fe(III)-compounds in the polymer phase became stable.

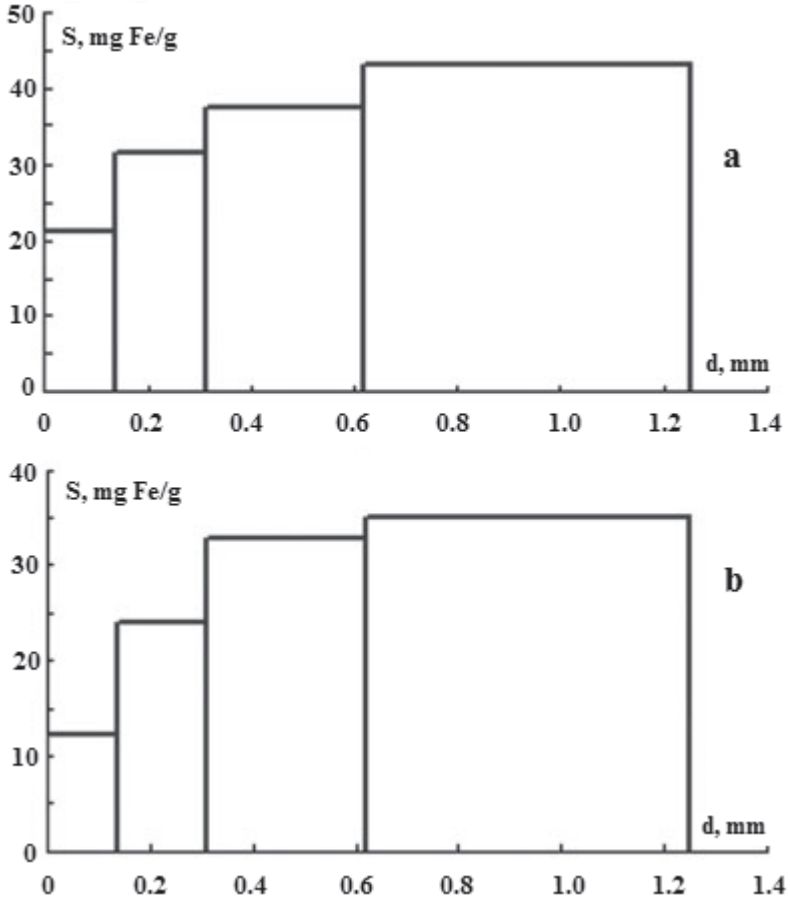

Figure 7-77. The Fe(III)-containing cations sorption dependence of AV-17 (a) and Varion-AD (b) granules sizes.

It is well known that sorption on solid sorbents depends on a specific area, and specific area depends on sorbent particle sizes. The smaller the particles sizes, the greater is the specific area and the sorption. As shown in Figure 7-77, sorption of Fe(III)-containing cations from $2 \cdot 10^{-2}$ M $Fe_2(SO_4)_3$ solution with pH 1.9 at 50°C during 12 h essentially depends on polymer granules sizes. But this dependence is unusual, as the larger the granules sizes, the greater is the sorption. This phenomenon may be explained only by taking into consideration the partial destruction of the Fe(III)-compounds in the polymer phase and iron ions diffusion from polymer granules. On the other hand, it means that Fe(III)-compounds formation takes place in the polymer granule volume.

It is obvious that the air contact surface of larger polymer granules is smaller than that of small granules. But the degree of destruction of the jarosite-type compounds in the polymer phase (desorption of Fe^{3+} cations) is inversely proportional to the specific surface of the granules. Therefore it can be said that the air contributes to the destruction of the jarosite compounds from the polymer phase.

Table 7-29. Values of sorption (S) from solutions of Fe(III)-containing cations (2×10^{-2} M $Fe_2(SO_4)_3$) by different polymers at 50°C

Polymer	Place of manufacture	Functional group	DVB, %	Granule diameter, mm	S, mg Fe/g
AV-17(Cl)	Russia	$-N^+(CH_3)_3$	8	0.4–1.2	47.5
AV-17-2P	Russia	$-N^+(CH_3)_3$	2	0.4–1.2	49.5
Varion-AD	Hungary	$-N^+(CH_3)_2C_2H_4OH$	8	0.3–1.1	46.5
Purolite A-400	England	$-N^+(CH_3)_3$	8	0.3–1.2	46.5
Amberlite IRA 410	USA	$-N^+(CH_3)_2C_2H_4OH$	8	0.3–1.2	45.0
4-VP-CH_2COOH	Romania	$\geq N^+CH_2COOH$	8	0.5	42.5
4-VP-CH_2CH_2COOH	Romania	$\geq N^+ CH_2CH_2COOH$	8	0.5	11.0

4-VP-CB	Romania	$\geq N^+CH_2C_6H_5$	8	0.5	10.0
4-VP-CE	Romania	$\geq N^+C_2H_5$	8	0.5	64.5
4-VP-AN	Romania	$\geq N^+ CH_2CH_2CN$	8	0.5	40.6
4- VP-AM	Romania	$\geq N^+ CH_2CH_2CONH_2$	8.	0.5	57.2
4-VP-MVC	Romania	$\geq N^+ CH_2CH_2COCH_3$	8	0.5	63.8
KB-2	Russia	>C-COOH | >C-COOH	2-3	0.3–1.0	95.6
KB-4	Russia	>CH-COOH	8	0.3–2.0	25.0
KB-4P2	Russia	>CH-COOH	2-3	0.25–1.0	26.0
Amberlite IRS-59	USA	>CH-COOH	8	0.3–1.2	35.0
KU-2	Ukraine	- SO_3H	8-10	0.3–1.5	48.5

Sorption of metallic cations on strongly basic anion exchangers is an unusual process. The chemistry of the metallic cation's sorption on such kinds of polymers completely differs from the one on carboxylic or sulfocation exchangers. Therefore, it is interesting to compare the sorption capacity of different kinds of exchangers toward Fe(III)-containing cations. For the investigation, polymer samples (0.2 g) interacted at 50°C for 12 h with $2 \cdot 10^{-2}$M $Fe_2(SO_4)_3$ solutions having pH 1.9. Characteristics of utilized commercial exchangers are given in Ref. [4]. Some of the polymer samples were obtained at the ''P Poni'' Institute of Macromolecular Chemistry (Iasi, Romania) by Dr Cornelia Luca and Dr Violeta Neagu. The obtained sorption capacities of the investigated polymers are listed in Table 7-29.

As shown in Table 7-29, the metallic cations sorption capacity of commercial strongly basic anion exchangers is comparable with the capacity of sulfate cation exchangers. The relatively small sorption capacity of the KB-4, KB-4P2, and Amberlite IRC-50 is due to the inability of carboxylic groups to form chelate complexes with iron cations. Carboxylic groups of the exchanger KB-2 are able to form chelate complexes with metallic cations and its sorption capacity is much greater. In the polymer phase containing pyridine quaternary nitrogen the formation of the jarosite type compounds takes place.

7.9.2. Fixation of atmospheric nitrogen and not only about it.

It is well known that some bacteria are able to fixate atmospheric nitrogen in soft conditions. It is also known that some metal compounds of iron can coordinate molecular nitrogen, but cannot turn into compounds [217- 219]. In industry, fixation of nitrogen from atmospheric air to obtain nitrite or nitrate compounds is a complicated process, which occurs in many steps and in rigid conditions. It seems incredible, but atmospheric nitrogen can be chemically converted into nitrate under ambient conditions and in a single technological stage. This is possible as a result of complex redox reactions involving ionic cross-linked polymers, containing strongly basic groups, during synthesis in their phase of jarosite mineral type compounds.

In the study of the Fe-jarosite formation in the polymer phase, the IR spectrum revealed a new intensive spectral line at 1283 cm^{-1}. According to Ref. [36], this absorption band belongs to the NO_3^- ions. The NO_3^- ions could not be in the polymer phase as a result of anion exchange if assuming that the used salt was contaminated with NO_3^-, because the solution concentration of $Fe_2(SO_4)_3$ which was contacted with the polymer was relatively high (4-8 g/L). It should be noted that an absorption band at 1283 cm^{-1} in the FT-IR spectrum of the polymer containing such compounds is extremely rarely observed because the SO_4^{2-} concentration in the system is incomparably high compared to the NO_3^- concentration.

This is one of the first works which points to the formation of nitrogen compounds in the system containing strongly basic cross-linked ionic polymer and $Fe_2(SO_4)_3$ [196].

The investigation of nitrite/nitrate formation by the system, containing strongly basic cross-linked polymer AV-17(Cl) and $Fe_2(SO_4)_3$ solution with pH 1.7-2.0 has been performed using the installation given in Figure 7-78. The AV-17(Cl) used is a commercial polymer, containing $-N(CH_3)_3Cl$ groups. The gel-type polymer has a polystyrene-divinylbenzene matrix and a full anion exchange capacity) of 3.5-4.2 mEq/g [4].

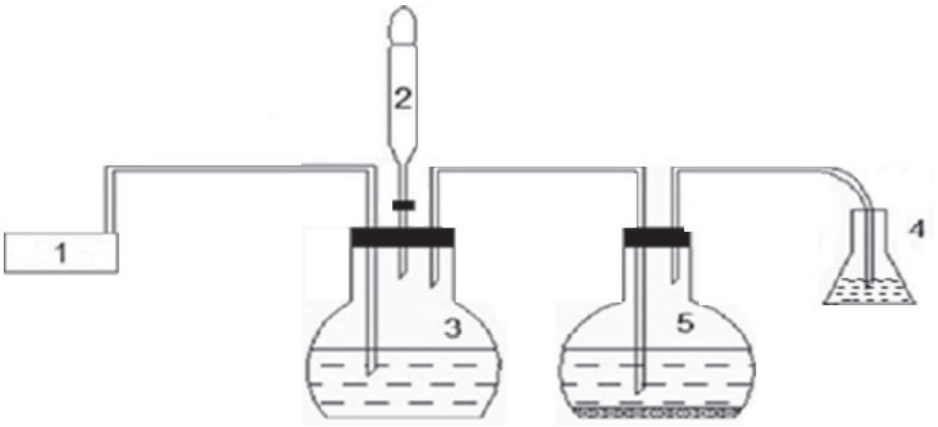

Figure 7-78. Scheme of the installation used for investigation of the nitrite/nitrate formation: 1 – air pump, 2 – separating funnel, 3 – reactor I, 4 – recipient, and 5 – reactor II.

The polymer AV-17(Cl) and solution of $Fe_2(SO_4)_3$ were inserted into reactor II. In reactor I $NaHCO_3$ was introduced to obtain CO_2, $KMnO_4$ to obtain O_2 or $Mn(OH)_2$ to absorb air oxygen. The separating funnel contained HCl acid solution to obtain CO_2 upon interaction with $NaHCO_3$. Air was bubbled through the system at a rate of 1 or 2 L / min. The recipient (4 in Fig.7-78) contains alkalized distilled water with pH 10. The system is air bubbled for 7 hours. After that, the ther content of Fe^{3+} and Fe^{2+} in the polymer phase and the content of nitrate and nitrite ions in the recipient were determinated.

To evaluate the influence of different factors (X_1- $Fe_2(SO_4)_3$, 2 -3 g/L; X_4- Na_2SO_4, 0.01-0.02 mEq/L; X_2- temperature, 40 – 50°C; (X_3- pH, 1.7-19; X_5- speed of air bubbling through the solution, 0-1 L/min; X_6- polymer mass, 0.2-0.4 g; X_7- polymer with solution contact duration, 5-7 h) on the Fe^{3+} and Fe^{2+} ions content in the polymer phase and on the $NO_2^-$and NO_3^- ions content in the recipient, the method of statistical mathematics was used. Parameters variation levels are indicated in brackets. The regression Equation (7-82), where Y is the content of NO_3^- relative to 1 g of polymer (mg NO_3^-/g) is as follows:

$$Y = 1.66 + 0.023X_1 - 0.46X_2 + 0.22X_3 - 0.042X_4 + 0.22X_5 - 0.62X_6 - 0.42X_7, \; b_{sig} = 0,18 \quad (7\text{-}82)$$

It was found that after the experiment is completed, the nitrite content in the recipient is very small but that of the nitrate ions is quite large. The increasing of $Fe_2(SO_4)_3$ concentration and solution pH influences positively the content of NO_3^- in the recipient and Fe^{3+} in the polymer phase. The greater the iron content in the polymer phase, the greater is the number of nitrate ions in the recipient. The rate of air bubbling through the solution of $Fe_2(SO_4)_3$ leads to the increase of NO_3^- ions content in the recipient. With the system temperature decreasing from 40 to 0°C, containing 0.25 g AV-17(Cl) and 100 mL solution with a concentration of 2.5 g $Fe_2(SO_4)_3$/L and pH 2.0 at a rate of air bubbling through the system of 2 L/min, after 7 h the content of NO_3^- ions in the recipient increased from 2.21 to 3.93 mg/g. As it is known, the solubility of air in water increases with the temperature decreasing. Undoubtedly some components of air are involved in the formation of nitrogen compounds, but it is unclear which of them (O_2, N_2 or CO_2) contribute to nitrogen compounds formation. To check whether oxygen participates in the formation of nitrogen compounds, we have performed experiments in the absence of oxygen, but in the presence of nitrogen and of carbon dioxide. In the same conditions, air was passed through the suspension of $Mn(OH)_2$ then through the system containing polymer and $Fe_2(SO_4)_3$ solution. In this case, the content of NO_3^- in water was much less. This means that oxygen from air is involved in the processes of nitrogen compound formation to demonstrate that atmospheric nitrogen is directly involved in the formation of nitrogen compounds in the system, and we have carried out additional experiments. Through the system containing 0.2 g of AV-17 polymer (from another factory) and 100 ml of the solution containing 8 g/L $Fe_2(SO_4)_3$, different gases were bubbled for 8 hours at 0 °C. Oxygen was obtained according to the reaction (7-83):

$$2KMnO_4 = K_2MnO_4 + MnO_2 + O_2 \quad (7\text{-}83)$$

And CO_2 was obtained from pure marble on interaction with pure HCl according to reaction (7-84):

$$CaCO_3 + 2HCl = CaCl_2 + H_2O + CO_2 \quad (7\text{-}84)$$

The experiment was performed in such a way that nitrogen (air) does not appear in the system. For comparison, an experiment was additionally carried out in the presence of air. The results are shown in Table 7-30. The data from Table 7-30 (where pHo and pHe are the pH of the water in the container respectively at the beginning and end of the experiment) clearly show that nitrogen-containing compounds are formed with the involvement of atmospheric nitrogen. The Fe^{2+} and Fe^{3+} content data in the polymer phase suggests that CO_2 influences the redox processes that take place in the system. There is no doubt that in the system, containing polymer and iron(III) sulfate, complex redox

processes occur. In addition, this is confirmed by the formation of Fe^{2+} ions in the system [125]. The Fe^{2+} ions are not able to form jarosite type compounds, therefore, in the result of the redox processes in the polymer phase decomposition of iron(III) compounds takes place. So, a part of Fe^{2+} ions passes from the polymer in the liquid phase. Experimental data confirm this. After interrupting the process of formation of the jarosite mineral type compounds by separating the polymer from the solution for 10 hours after 2.5 h and placing it again in solution, the content of Fe^{3+} in the polymer phase has decreased (Fig. 7-73] [125].

Table 7-30. The results obtained during the passage of different gases through the system

No exp.	Gas bubbled through the system	pHo	pHe	m (NO_3^-), mg/g	m (NO_2^- + NO_3^-), mg/g	m (Fe^{2+}), mg/g	m (Fe^{3+}), mg/g
1	O_2	10	10	0	0	3.20	7.57
2	CO_2	10	8.2	0	0	0.76	3.92
3	$O_2 + CO_2$	10	8.0	0	0	2.35	4.06
4	Air	10	8.1	1.75	1.80	0.68	3.66

Since in the solution of $Fe_2(SO_4)_3$, which has been in contact with the polymer, no NO_3^- ions were found, we consider that in the system, nitrogen oxides NOx were initially formed which, further were converted into nitric acid.

When the experiment was repeated after the iron was removed from the polymer used to obtain the nitrogen compounds in the previous experience, almost the same amount of NO_3^- ions was obtained. This means that functional groups (R_4N^+) of the polymer do not directly participate in the redox processes. Therefore, we believe that in the formation process of nitrogen compounds in the system nitrogen from the air participated. So, the system containing a strongly basic polymer and iron (III) sulphate solution is able to fix atmospheric nitrogen in soft conditions resulting in obtaining nitric acid in one technological step. In industry, as already mentioned, the fixation of atmospheric nitrogen with the formation of ammonia followed by nitric acid occurs in several technological stages and at high temperature and pressure.

Jarosite mineral type compounds in the polymer phase interact with oxygen and nitrogen from the air, forming nitrogen compounds. As a result of these redox processes occurring in the system, partial destruction of jarosite takes place. The investigation demonstrated [64]. that the functional groups of the polymer $-N(CH_3)^+$ are part of the composition of jarosite type compounds. But, the mobility of these groups is limited by the flexibility of the polymer chains. Therefore, both octahedra and octahedral cycles of the jarosite type compounds in the pores of different dimensions of the polymer are distorted. Probably in the polymer phase N_2, O_2, and also CO_2, interact in some cavities of cycles of the jarosite. The packaging of structural units in natural or synthetic jarosite is compact. Thus, the stability and reactivity of jarosite compounds in the polymer phase are different in natural or synthetic jarosite. Yet, does mineralogical science say anything about the interaction of the natural jarosite with the components of air? Whether such processes take place in the presence of the jarosite mineral in nature? We think that such processes occur in nature. Although it is difficult to detect the formation of nitrogen compounds, in contrast, the partial destruction of jarosite with the formation of $Fe(OH)_3$ (as a result of the Fe^{2+} formation, followed by air oxidation) is observed. According to Ref.[213], the jarosite mineral in nature is always accompanied by $Fe(OH)_3$ although we believe it would rather be one of the modifications of FeOOH. Using Mössbauer spectroscopy, we have investigated the freshly prepared sample and after nine months of storage in the air of the polymer AV-17(Cl) in the phase of which was synthesized $R_4N[Fe_3(OH)_6(SO_4)_2]$. The Mössbauer spectra were obtained at room temperature. The Mössbauer spectrum of the freshly prepared sample represents a single doublet with the following parameters: isomeric shift δ = 0.384 mm/s and quadrupole splitting ΔE_Q = 1.142 mm/s. The Mössbauer spectrum of the sample which was stored in the air up to nine months consists of two doublets which means that in the polymer phase the Fe^{3+} ions are in two different states. According to Ref.[65], a doublet (2 in Fig. 7-79) with ΔE_Q = 0.682 mm/s and δ = 0.520 mm/s belongs to $Fe(OH)_3$, and the other with ΔE_Q = 1.205 mm/s and δ = 0.492 mm/s (1 in Figure 7-79, belongs to the compound $R_4N[Fe_3(OH)_6(SO_4)_2]$ [64, 84]. We consider that the internal doublet of the spectrum rather belongs to one of a modification of FeOOH in a superparamagnetic state. Considering that the initial polymer was in the form of Cl^-, we can say that we have the β-FeOOH modification. According to Refs.[46, 220, 221], the formation of β-FeOOH occurs in the presence of Cl^- or F^- ions, although there are articles in which it is indicated that β-FeOOH can be formed also in their absence. Suzdalev [52] demonstrated that the spontaneous formation and transformation of α-, γ -Fe_2O_3 from one modification to another depend on the size of the particles. It is not excluded that α-, β-, δ-, γ- FeOOH formation takes place in the same way. So, it has been shown that the jarosite in the polymer phase, kept in the air, is also partially destroyed similar to the natural jarosite. But the natural jarosite and the jarosite in the polymer phase are not destroyed completely upon interaction with components of the air. This is clearly seen in the following research. The $Ga_2(SO_4)_3$ and $In_2(SO_4)_3$ solutions interact with ionic cross-linked polymers containing strongly basic groups. However $R_4N[Ga_3(OH)_6(SO_4)_2]$ and $R_4N[In_3(OH)_6(SO_4)_2]$ compounds in the polymer phase are more unstable than $R_4N[Fe_3(OH)_6(SO_4)_2]$ and especially more than $R_4N[Cr_3(OH)_6(SO_4)_2]$. As seen in Figures 7-80 and 7-81, sorption over

time of Ga(III)- or In(III)-containing cations on anion exchanger AV-17(Cl) from 0.01M $Ga_2(SO_4)_3$ or $In_2(SO_4)_3$ solutions goes through the maximum.

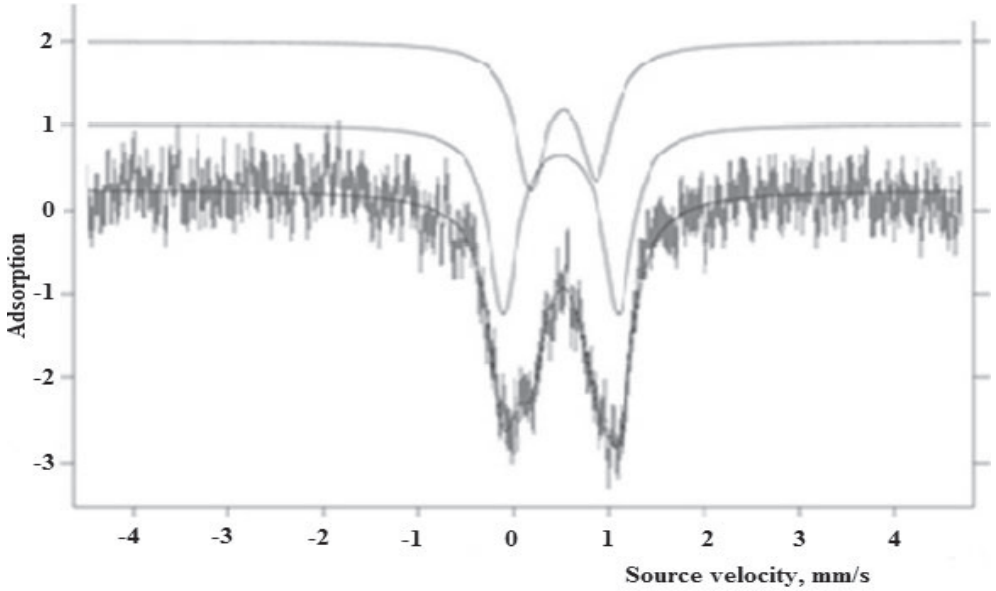

Figure 7-79. Mössbauer spectrum of the polymer sample, containing jarosite, which was kept in the air up to nine months: Fe-jarosite (1), and $Fe(OH)_3$ (2).

This fact shows that in time a part of the jarosite from the polymer phase is destroyed. The fact that the sorption of metal cations increases with temperature demonstrates that processes in the system are chemical and not physical. The interactions of jarosite type compounds with air components, take place on the surface of the polymer granules.

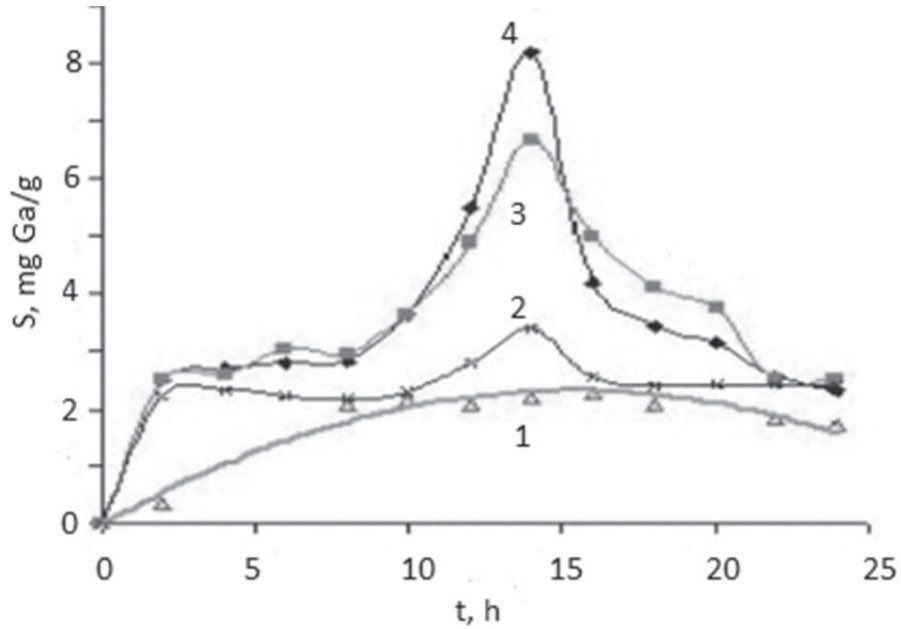

Figure 7-80. Kinetic curves of the Ga(III)-containing cations' sorption on AV-17(Cl) polymer. In the conditions of pH 2.0 and 17°C (1), pH 1.8 and 60°C (2), pH 2.0 and 60°C (3), and pH 2.0 and 60°C with interruption (4).

The histogram (Fig.7-82) clearly demonstrates that the retention of Ga^{3+} cations increases with increasing the specific surface of the polymer. As expected, the increasing of $Ga_2(SO_4)_3$ and Na_2SO_4 concentration, temperature and solution pH, results in increasing Ga(III)-containing cations sorption.

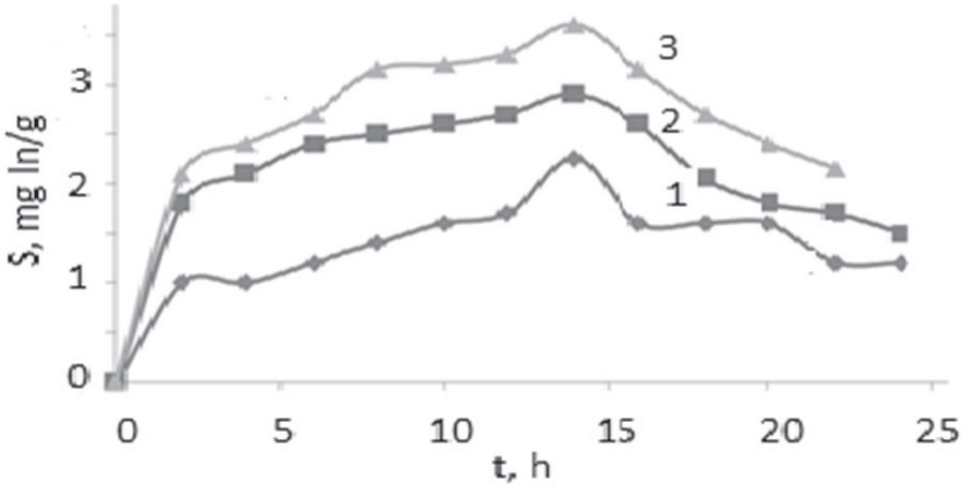

Figure 7-81. Kinetic curves of the In(III)-containing cations' sorption on AV-17 polymer at 22 (1), 54 (2) and 60°C (3).

Table 7-31. Optimizing the formation process of NO_3^- ions in water by the system containing AV-17(Cl) and solution of $Ga_2(SO_4)_3$

Step and number of experiment	X_1	X_2	X_3	X_4	X_6	X_7	Y, mg No_3^-/g
	-0.0002	-5	+ 0,1	- 0.015	+0,003	+1	
1	0.0123	45	1.9	0.010	0.018	6	-
2	0.0121	40	2.0	0.005	0.021	7	-
3	0.0119	35	2.1	0	0.024	8	4.96
4	0.0117	30	2,1	0	0,027	9	-
5	0.0115	25	2.1	0	0.030	10	7.78
6	0.0113	20	2.1	0	0.033	11	-
7	0.0111	20	2.1	0	0.036	12	15.53
8	0.0109	0	2.1	0	0.039	12	-
9	0.0105	0	2.1	0	0.042	12	15.53
10	0.0103	0	2.1	0	0.045	12	-
11	0.0101	0	2.1	0	0.048	12	4.96

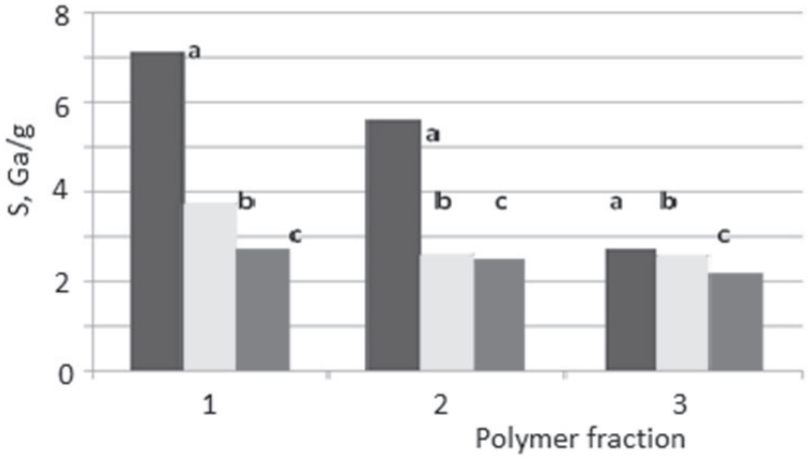

Figure 7-82. Histograms of Ga(III)-containing cations sorption depending on polymer granule diameter: 0.11-0.25 (1), 0.25-0.50 (2) and 0.50-1.2 mm (3) after 14 (a), 18 (b) and 24 h (3) polymer contacting with $Ga_2(SO_4)_3$ solution at 60°C.

The existence of Cl^- ions (KCl) in the solution and air bubbling through the system negatively influences the metal cations sorption. The influence of Cl^- ions is explained by the fact that they substituted SO_4^{2-} ions in the polymer phase. But it is known that compounds of the jarosite type are not formed in the absence of SO_4^{2-} ions. According to the regression equation, which expresses the degree of influence of various factors on the formation of nitrate ions, the factors that positively influence Ga^{3+} ion sorption influence negatively the formation of nitrate ions.

Coefficients of the regression equation allowed us to perform the experiment (Tab.7-31) to optimize the formation of nitrate ions in the recipient. In this experiment X_1 is the concentration of $Ga_2(SO_4)_3$ (g/L), X_2 is the temperature (^oC), X_3 is the pH of the solution, X_4 is- the concentration of Na_2SO_4 (mol/L), and X_6 is the duration of contact of the polymer with the solution (h). The air bubble rate through the system was constant and equal to 1 L/min. The data from Table 7-31 show that the nitrogen compounds are produced in a larger amount than in the solution of $Fe_2(SO_4)$. In the system, containing polymer AV-17(Cl) and $Ga_2(SO_4)_3$ solution, in the recipient (4 in Fig.7-78), 15.35 mg NO_3^- /g was found. The Cl^- ions in the solution contribute to the formation of nitrogen compounds and to the destruction of metal compounds in the polymer phase. Over time, the process of formation and destruction of Ga-jarosite and In-jarosite in the polymer phase occurs cyclically (Fig.7-83). From Figures 7-80, 7-81, 7-82 and 7-83, it is clear that the compounds of Ga(III) and In(III) in the polymer phase do not break down completely. This can be explained by the fact that not all of the octahedral cycles of the jarosite in the polymer phase participate in redox processes that lead to their destruction.

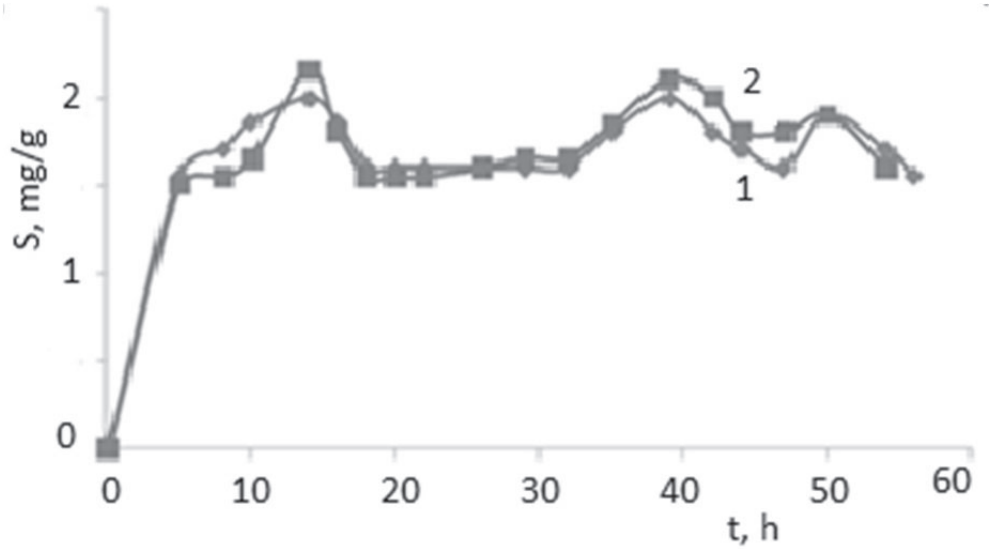

Figure 7-83. Kinetic curves of Ga(III)-containing (1) and In(III)-containing cations sorption (2) on AV-17 polymer at 60^{o}C.

The main effect of the mineral jarosite type compounds in the polymers phase is their interaction with the air components in nitrogen fixation, resulting in the formation of nitrates under very soft conditions of pressure and temperature. The mechanism of the redox processes in the polymer- $M_2(SO_4)_3$ solution system is very complicated and will remain for future investigation. At this stage, it can be assumed that atmospheric nitrogen and oxygen, getting in the cavity of distorted octahedral cycles of the jarosite compounds, leads to the formation of NOx oxides. On the other hand, the investigation of different factors that influence formation and destruction of the jarosite compounds may be useful to understand some processes occurring in mineralogy. Furthermore, these investigations could have an impact on understanding some processes that occurred on some planets. It is known that using Mössbauer spectroscopy, in 2004, jarosite was discovered on Mars by Opportunity, one of NASA's Mars Exploration Rovers. For scientists it was an argument that once water existed on Mars [222, 223]. The Mössbauer spectra of rocks on Mars show that jarosite mineral is accompanied by other iron compounds, including iron(II) and magnetic ordered phases (goethite α-FeOOH, hematite Fe_2O_3) [222, 224] It is known that jarosite mineral type compounds are formed in acid medium, but goethite and hematite are formed in a basic one. Therefore, we believe that the formation of goethite and hematite on the surface of Mars can be as a result of jarosite decomposition.

There are many publications about the possible destruction processes of jarosite on Mars [224, 225]. Could these processes, described in this article about the destruction of jarosite and the formation of nitrogen compounds, have occurred on Mars? As it is known, the Martian atmosphere contains small amounts of nitrogen compounds (N_2O, NH_3) [226, 227] and we assume that such a process would have taken place on Mars.

And finally, it must be said that processes of jarosite mineral type compounds and nitrogen compounds formation take place not only using polymer AV-17(Cl). Experiments have shown that they take place in systems, containing such strongly basic polymers as Purolite A-400, Dowx 1x8, Varion-AD and Ionenausta Uscher (III) as well.

REFERENCES

1. Gutsanu Vasile. (2013). *Unusual processes on ion exchangers*. Chişinau: CEP USM, (in Romanian).
2. Gutsanu, V. L. (1993). *Sorption and state of ions of certain metals in ion exchangers.* Thesis dis. Doctor habilitat in chemistry. Kishinev: KGU, (in Russian).
3. Gutsanu, V. L. (1974). *The influence of the nature of solvent and the ionic composition of solution on adsorption of Cu(II), Cd(II) and Zn(II) on ion exchangers*. Thesis dis. Doctor in chemistry. Kishinev: KGU, (in Russian).
4. Lurie, A. A. (1972). *Sorbents and chromatographic carriers*. Moscow: Nauka.
5. Gutsanu, V. L., & Dogaru, G. N. (1977). Sorption of metals on complexing ion exchangers in a wide range of pH. *Russian J. App. Chem*., 50, 2216-2220.
6. Gutsanu, V. L., & Muntyan, S. A. (1981). Sorption of Ni(II) and Co(II) by ion exchangers in a wide range of pH. *Russian J. App. Chem*., 54, 1035-.1040.
7. Gutsanu, V. L., Muntyan, S. A., & Turta, C. I. (1980). Sorption of iron (II) and iron (III) by ion exchangers in the tartrate solutions in a wide range of pH. *Proceedings of the Academy of Sciences of the Moldavian SSR, Series Biological and Chemical Sciences,* No.2, 73-79.
8. Gutsanu, V. L., Pushneak, A. N., & Migali, P. K. (1973). Sorption of copper by anion exchangers EDE-10P and AN-2FN from water-organic systems. *Proceedings of Higher Schools of the USSR. Chemistry and Chemical Technology*, 16, 55-.58.
9. Gutsanu, V. L., Pushneak, A. N., Migali, P.K., & Nguen Thi Niung. (1973). Sorption of Cu^{2+}, Cd^{2+}, Zn^{2+} ions on anion exchangers from water-acetone solutions. *Proceedings of the Academy of Sciences of the Moldavian SSR, Series Biological and Chemical Sciences,* No.6,79-.84.
10. Gutsanu, V. L., Pushneak, A. N., Migali, P. K., & Nguen Thi Niung. (1974). Sorption of Cu^{2+}, Cd^{2+}, Zn^{2+} ions on anion exchangers from water-ethanol solutions. *Proceedings of Higher Schools of the USSR. Non-ferrous metallurgy*, No.3, 33-.37.
11. Pushneak, A. N., & Gutsanu, V. L. (1976). Impact of ionic composition (SO_4^{2-} and NO_3^-) of solutions on metallic cations sorption by anion exchangers. *Proceedings of the Academy of Sciences of the Moldavian SSR, Series Biological and Chemical Sciences*, No.3, 67-70.
12. Gutsanu, V. L., & Dogaru, G. N. (1980). The anion effect on copper (II) complex-formation with anion exchanger EDE-10P. I. Assessing the impact of the anions on the sorption in weakly acidic solutions. *Zh. Fiz. Khim.*, 54, 2092-.2094.
13. Gutsanu, V. L., & Dogaru, G. N. (1980). The anion effect on copper (II) complex-formation with anion exchanger EDE-10P. II. Sorption of anions upon complexation. *Zh. Fiz. Khim.* 54, 2318-.2321.
14. Gutsanu, V. L., & Dogaru, G. N. (1981). The anion effect on copper (II) complex-formation with anion exchanger EDE-10P. III. Sorption from ammonia solutions. *Zh. Fiz. Khim*., 55, 2422-2424.
15. Gutsanu, V. L., & Dogaru, G. N. (1982). The anion effect on copper (II) complex-formation with anion exchanger EDE-10P. IV. Sorption of coper (II) from agueous-acetone solutions. *Zh. Fiz. Khim.*, 56, 2234-2238.
16. Gutsanu, V. L., & Dogaru, G. N. (1982). The anion effect on copper (II) complex-formation with anion exchanger EDE-10P. V. Sorption of anions upon complexation in agueous-acetone solutions. *Zh. Fiz. Khim*., 56, 2239-2242.
17. Pushneak, A. N., Gutsanu, V. L., & Migali, P. K. (1976). The change of pH in the systems "anion exchanger-electrolyte solution". *Proceedings of the Academy of Sciences of the Moldavian SSR, Series Biological and Chemical Sciences*, No.6, 69-72.
18. Safin, R. Sh., Gutsanu, V. L., & Vishnevskya, G. P. (1987). The anion effect on copper (II) complex-formation with anion exchanger EDE-10P. EPR spectra of the complexes obtained in a weakly acidic medium. *Zh. Fiz. Khim*., 61, 2134-2138.
19. Dogaru, G. N., & Gutsanu, V. L. (1981). Sorption of iron (III) from solutions of complex composition on cation exchanger KB-2. *Russian J. App. Chem.,* 54, 433-437.
20. Dogaru, G. N., & Gutsanu, V. L. (1977). Research on the optimization of Al(III) sorption on the cation exchanger KB-2. *Russian J. App. Chem.,* 50, 2379-2381.
21. Gutsanu, V. L., & Gafiichuk, V. A. (1986). Influence of concentration of Cl^- and SO_4^{2-} in solution on the sorption of Fe(III) on exchangers. *Zn. Phys.Khim*., 60, 1824-1826.
22. Gutsanu, V. L., & Gafiichuk, V. A. (1989). Evaluation of the factors that affect the sorption of iron (III) ions on ion exchangers. *Khimiya i Technologiya Vody. Soviet Journal of Water Chemistry and Technology,* 11, 584-588.
23. Gutsanu, V. L. (1990). Sorption and state of iron ions in ion exchange resins. (Review). *Soviet Journal of Water Chemistry and Technology,*, 12, 1074-1097.
24. Nalimov, V.V., & Chernova, N. A. (1965). *Statistical methods for the planning of extreme experiments*. Moscow: Nauka.
25. Bondar, A. (1973). *Mathematical modeling in chemical technology*. Kiev: Visha Shkola.
26. Marchenko, Z. (1972).*Photometrical determination of elements*. Moscow: Nauka.
27. Gutsanu, V. L., Turta, C. I., Gafiichuk, V. A., & Shofransky, V. N. (1988). Compounds of iron (III), which are

formed during the sorption on strongly basic anionite în the sulfate solution. *Zh. Fiz. Khim*., 62, 2415-2422.
28. Morais, P. S., & Skeff Neto, K. (1983). Spectroscopic characterization of superparamagnetic particles of thermolitic products of ferric sulphate hydrates. *Polyhedron*, 2, 875-880.
29. Hrynkiewcz, A. Z., Kubisz, I., & Kulgawczuk, D. S. (1965). Quadrupole splitting of the 14.4 keV gamma line of ^{57}Fe in iron sulphates of the jarosite group. *J. Inorg. Nucl. Chem.*, 27, 2513-2517.
30. Matashige Ohyabu, & Ohzabu Ujihira. (1981). I. A study of the precipitates formed by hydrolysis of Fe(III) nitrate solution conaining Na^+ and SO_4^{2-}. *J. Inorg. Nucl. Chem*., 43, 1948-1949.
31. Margulis, E. V., Savchenko, L. A., Shocarev, M. M., Beysekeeva, L. I., & Vershinina, S. I. (1973). Thermolizes of hydroxosulphates ($H_3OFe_3(OH)_6(SO_4)_2$ and $FeOHSO_4$). *Zh. Neorg. Khim*., 18, 1263-1269.
32. Margulis, E. V., Savchenko, L. A., Shocarev, M. M., Beysekeeva, L. I., & Vershinina, S. I. (1975). The thermal decomposition of the dual-basic jarosite type sulfates. *Zh. Neorg. Khim*., 20, 972-877.
33. Gutsanu, V., Gafiichuk, V., Shofransky, V., & Turta, C (2006). Nature of compounds formed in phase of strongly basic anion exchanger in contact with $Fe_2(SO_4)_3$ solutions. *J. App. Polym. Sci*., 99, 59-64.
34. Vishnevskaya, G. P., Volkov, A., Plachinda, A. S., Ramazanov, P. G., Reut, I. G., & Suzdalev, I. P. (1973). EPR spectra and paramagnetic relaxation of Fe(III) in ion exchange sulforesins. *Theor. Eksperim. Khim.,* 9, 409-914.
35. Prayor, U. (1979). *Free radicals in biology*. Moscow: Mir.
36. Nakamoto, K. (1991). *Infrared and Raman spectra of inorganic and coordination compounds.* Moscow: Mir.
37. Bellami, L. (1963). *Infrared spectra of complex molecules*. Moscow: Izd. In. Lit.
38. Semushkin, A. M., Yakovlev, V. A., & Ivanova, E. I. (1988). *Infrared spectra of ion-exchanger materials*. Leningrad: Khimiya.
39. Karrer, P. (1960).*Course of organic chemistry.* Leningrad: Khimiya.
40. Tulupov, P. E., & Grebeni, V. P. (1970). *Ion exchange and ion exchangers*. Leningrad: Nauka:
41. Ugleanskaya, V. A.; Zavialova, T. A, Romanenko, E. F.& Selemenev,V. F.(1983). *Teoria i praktika sorbtsionnykh protsessov*. Voronej: VGU. (Russia).
42. ToshioTakada, Masao Kiyama, Joshichika Banda, Tacachi Nakamura, Masauki Shida, Teruza Shinjo, & Jasuo Endon., (1964). Mossbauer study of α-, β- and γ-FEOOH. *J. Phys. Soc. Japan.*, 19, 1744-1746.
43. Rossiter, M. I. & Hoadgson, A. E. M. (1965). A Mössbauer study of ferric oxyhydroxide. *J. Inorg. Nucl. Chem.*, 27, 63-71.
44. Goncharov, G. N., Efimov, A. A., Kalyamin, A. V., & Tomilov, S. V. (1978). Investigation of the mechanism of hydrolytic precipitation in the hydrolysis of Fe(III) in nitrate solutions. *Zh. Obshchei. Khim*., 48, 2398-2408.
45. Rucosuev, M. N., Yazmin, I. I., Chikhachev, V.A., & Liubimtsev, V. A. (1971). Investigation of the structure and magnetic properties of the β-FeOOH in the dehydration process up to hematite. *Crystallography,* 16, 532-537.
46. Matashige Ohyabu, & Jusuke Ujihira. (1981). Study of the chemical states of chlorine and fluorine in akaganeite. *J. Inorg. Nucl. Chem*., 43, 3125-3129.
47. Nagai, N., Hosoito, N., Kiyama, M., Nakamura, T., Shida, M., Shinjo, P., … Endon, E. (1980). Presented at ICF, Kyoto, September–October 1980; Nagai, N.; Hosoito, N., Kiyama, M., Nakamura, T., Shida, M.; Shinjo, P., … Takada, T. (1982) presented at ICF, Tokyo and Dordrecht, 247-249.
48. Goncharov, G. N., Kalyamin, A. V., & Lurie, B. G. (1973). A study of ferromanganone nodule from the Pacific by the NGR method. *Dokl. Acad. Nauk. SSSR*, 212, 720-723.
49. Moreira, J. E., Knudsen, J. M., Delima, C. G., & Duefrense, A. (1073). Mössbauer and infrared spectrometric studies of some iron (III) precipitates. *Analit. Chim. Acta*, 63, 295-304.
50. Borggard, O. K. (1983). Extraction of amorphous iron oxides in EDTA from a mixture of akageneite (β-FeOOH) and amorphous iron oxides. *Acta. Chem. Scand.,* A27, 169-171.
51. Paterson, R. & Rahman, H. (1983). The ion exchange properties of crystalline inorganic oxide hydroxides, 1. β-FeOOH. *J. Colloid. Interface Sci.*, 94, 60-69.
52. Suzdalev, I. P. (1988). *Gamma resonance spectroscopy of proteins and model compounds*. Moscow: Nauka.
53. Gutsanu, V., Drutsa, R., & Rusu, V. (2001). Sorption of Fe(III) containing ions on strongly basic anion exchangers AV-17 and Varion-AD. *React. Funct. Polym*., 46 , 203–211.
54. Plachinda, A. S., Macarov, E. F., Alexeeva, S.I., & Egorov, E.V. (1976). On the dependence of chemical states of iron on their concentration in ion-exchange resin. *J. Inorg. Nucl. Chem*., 38, 859-861.
55. Fishtic, I.F., & Vataman, I.I. (1988). *Thermodynamics of the metallic ions hydrolysis*. Chisinau: Shtiintsa.
56. Palchevsky, V.V. (1976). *Complex-forming in redox systems, Vol. III*, Dushanbe: DGU.
57. Belozerskii, G.N., Baikov, M.V., Boldyrev, V.V. , Murin, A. N., Pavliuhin Y. T., & Sviridov, V. V. (1974). Study of the formation of ferrites from co-precipitated hydroxides by the NGR method. *Kinetika i Kataliz*, 15, 929-934. (Russia).
58. Arkhipenko, D.K., Devyatkina, E.T., & Palchik, N.A. (1978).*Crystallochemical particularities of synthetic jarosites*. Novosibirsk: Nauka. (Russia).
59. Freundlich, H. M. F. (1906). Überdie adsorption in iösungen. *Zeit. Phys. Chem*., 57(A), 385-470.
60. Bache, B.W., & Williams,E.G. A. (1971). Phosphate sorption index for soils. *J. Soil, Sci.*, 22, 89-301.
61. Mead, J. A. A. (1981). Comparison of the Langmuir, Freundlich and Temkin equations to describe phosphate adsorption properties of soils. *Aust. J. Soil Res*., 19, 333-342.
62. Langmuir, I. (1918). The adsorption of gases on plane surfaces of glass, mica and platinum. *J .Am. Chem. Soc*., 40, 1361-1403.

63. Holford, I. C. R. (1982). The comparative significance and utility of the Freundlich and Langmuir parameters for characterizing sorption and plant availability of phosphate in soil. *Aust. J. Soil Res*., 20, 233-242.
64. Gutsanua,V., Schitco, C., Lisa, G., & Turta, C. (2011). Ultra dispersed particles of Fe(III) compounds in the strongly basic cross-linked ionic polymer-precursors for new sorbents and catalysts. *Mater. Chem. Phys.,* 130, 854– 862.
65. Goldanskii, V.I. (1970). *Chemical applications of Mössbauer spectroscopy.* Moscow: Mir.
66. Rothstein, Y. R., Dyar, M. D., & Bishop, J. L. (2006). *37-th Annual Lunar and Planetary Science Conference, League City, Texas, March 13–17,* (abstract 1727).
67. Music, S., Krehula, S., & Popovic, S. (2004). Thermal decomposition of β-FeOOH. *Mater. Lett*., 58, 444.
68. Margulis, E.V., Savchenko, L. A., Shokarev, M.M., Beysekeeva, L. I., & Vershinina, F. I. (1975), Thermal decomposition of double basic (R^+, Fe^{3+}) - sulphates of jarosite type. *Zh. Neorg. Khim*., 20, 972-977.
69. Margulis, E.V., Savchenko, L. A., Shokarev, M. M., Beysekeeva, L.I., & Vershinina, F. I. (1973). Thermolysis of hydrosulphates ($H_3OFe_3(OH)_6(SO_4)_2$ and $FeOHSO_4$). *Zh. Neorg. Khim.,* 8, 1263-1269.
70. Frost, Ray L., Wills Rachael-Anne, Kloprogge, J. Theo., & Martens Wayde. (2006). Thermal decomposition of ammonium jarosite $(NH_4)Fe_3(SO_4)_2(OH)_6$. *J. Therm. Anal. Calorim*., 84, 489-496.
71. Freeman, E.S., & Caroll, B. (1958). The application of thermoanalytical techniques to reaction kinetics. The thermogravimetric evaluation of the decomposition of calcium oxalate monohydrate. *J. Phys. Chem*., 62, 394-397.
72. Gutsanu ,V., & Drutsa, R. (1977). Process for modified ionites obtained. Patent MD 810. *BOPI*, No.8, 24-25.
73. Gutsanu,V., & Drutsa, R. (2003).Process for regeneration of strongly basic anionites modified with Fe(III). Patent MD 2235. *BOPI*, 8, 22.
74. Gutsanu, V., & Rosca, I. (2005). Process for selective removal of cyanide, thiocyanate, cyanate ions from solutions. Patent MD 2746. *BIPI,* 4, 33.
75. Gutanu, V., Luca Cornelia, Turta, C., Neagu Violeta, Sofranschi, V., Cherdivarenco, M., & Simionescu, B. C. (1996). Ionic polymers. III. Sorption of Fe(lll) ions on new crosslinked ionic polymers based on 4-vinylpyridine:divinylbenzene copolymers. *J. App. Polym. Sci.,* 59, 1371-1377.
76. Gutsanu, V., Luca Cornelia, Neagu Violeta, Sofranschi, V., & Turta C. (1999). Iron(III) states in 4-vinylpyridine: Divinylbenzene copolymer modified by monochloracetic and acrylic acids. *React. Funct. Polym.,* 40, 123-128.
77. Mackey, L., & Collins, R.L. (1967). The Mössbauer effect of iron in ion exchange resin. *J. Inorg. Nucl. Chem.,* 29, 655-660.
78. Suzdalev, I. P., Plachinda, A. S., Makarov, E. F., & Dolgopolov, V. A. (1967). Investigation of ion-exchange resins using γ-resonance spectroscopy (Mössbauer effect). *Zh. Fiz. Khim.,* 41, 2831-2838.
79. Gutsanu, V. L., Turta, K. I. , Stukan, R. A., & Gafiichuk, V. A. (1985). Influence of the nature of the solvent on the Mössbauer spectra of Fe(III) adsorbed by the anionite EDE-10P from solutions of $FeCl_3$. *Zh. Fiz. Khim.,* 59, 693-696.
80. Luca, C., Barboiu,V., Petrariu, I., & Dima, M. (1980). Quaternary ammonium polyelectrolytes. IV. Addition reaction between poly(4-vinylpyridinium chloride) and electrophilic vinyl compounds. *J. Polym. Sci. Polym. Chem. Ed.,* 18, 2347-2355.
81. Shokarev, M.M., Margulis, E.V., Vershinina, F.I., Beysekeeva L.I., & Savchenko L.A. (1972) Infrared spectra of hydrosulphates and iron (III) hydrooxides . *Zh. Neorgan. Khim.,* 17, 2474-2479.
82. Matashige Ohyabu, & Yusuke Ujihira,Y. (1981).Study of the chemical states of chlorine and fluorine on akaganeite. *J. Inorg. Nucl. Chem*., 43, 3125-3129.
83. Townsend, M. G.; Longworth, G., & Roudaut, E. (1986). Triangular-spin, kagome plane in jarosites. *Phys. Rev. B*., 33, 4919-4926.
84. Drutsa, R., Gutsanu, V., & Rusu V. (2006). Sorption of Cr(III)-containing cations on strongly basic anion exchangers. *J. App. Polym. Sci*.,102, 3978-3985.
85. Boyd, G. E., Adamson, A. V., & Myers, L. S. (1947). The exchange adsorption of ions from aqueous solutions by organic zeolites. II. Kinetics. *J. Am. Chem. Soc*., 69, 2836-2648.
86. Kokotov, I. A., & Pasecinic, V. A. (1970). *Equilibrium and kinetics of ionic exchange*. Leningrad: Khimia.
87. Gutsanu, V., & Drutsa, R. (1998). Process for Cr(III) modification of the cross-linked polymers, containing R_4N^+ groups. Patent MD 1027. *BOPI*, 9, 23.
88. Gutsanu, V. , & Drutsa, R. (2003). Process for regeneration of strongly basic anionites modified with Cr(III). Patent MD 2234. *BOPI*, 8, 21.
89. Gutsanu,V., Tudorachi,N., & Lisa, G. (2013). The behavior of the AV-17(Cr) sorbent in various media. *Thermochim. Acta,* 574, 109-115.
90. Lisa, G., Apreutesei Wilson D., Scutaru, D., Tudorachi,N., & Hurduc, N. (2010). Investigation of thermal degradation of some ferrocene liquid crystals. *Thermochim. Acta,* 507–508, 49-59.
91. Fan,Y. Li. Y., & Ma, J. (2001). Physical and chemical stability of porous polystyrene-type beads with different degrees of crosslinking. *Polym. Degrad. Stabil*., 73, 163-167.
92. Jiang, K., Chen, S., Dong, P., & Liu, R. (2008). Synthesis of monodisperse crosslinked polystyrene microspheres. *Petrol. Sci*., 5 (4), 375–378.
93. Dragan, E.S., Dinu, M.V., Lisa, G., & Trochimczuk, A.W. (2009). Study on metal complexes of chelating resins bearing iminodiacetate groups. *Eur. Polym.*, *J.* 45, 2119-2130.

94. Frost, R. L., Wills, R-A., Weier, M. L., Musumeci, A. W., & Martens, W. (2005). Thermal decomposition of natural and synthetic plumbojarosites: importance in archeochemistry. *Thermochim. Acta,* 432 (1), 30-35.
95. Frost, R. L., Locke, A. J., & Wayde, W. N. (2008).Thermal analysis of beaverite in comparison with plumbojarosite. *J. Therm. Anal. Calorim*., 92 (3), 887-892.
96. Frost, R. L., Wills, R-A., Kloprogge, J. T., & Martens, W. N. (2006). Thermal degradation of hydronium jarosite $(H_3O)Fe_3(SO_4)_2(OH)_6$. *J. Therm. Anal. Calorim*. 83 (1), 213-218.
97. Tudorachi, N., & Chiriac, A. P. (2011). TGA/FTIR/MS study on thermal decomposition of poly(succinimide) and sodium poly(aspartate). *Polym. Testing,* 30, 397-407.
98. Cervantes-Uc, J. M., Cauich-Rodriguez, J. V., Vazquez-Torres, H., Garfias- Mesias, L. F., & Paul, D. R. (2007). Thermal degradation of commercially available organoclays studied by TGA-FTIR. *Thermochim. Acta,* 457, 92–102.
99. Kaljuvee, T., Edro, E., & Kuusik, R. (2007). Formation of volatile organic compounds at thermooxidation of solid fossil fuels. *Oil Shale*, 24 (2), 117-133.
100. Shao, D., Hutchinson, E. J., Heidbrink, J., Pan, W. P., &. Chou, C. L. (1994). Behavior of sulfur during coal pyrolysis. *J. Anal. Appl. Pyrolysis,* 30, 91-100.
101. Ferrasse, J. H., Chavez, S., Arlabosse, P., & Dupuy, N. (2003). Chemometrics as a tool for analysis of evolved gas during the thermal treatment of sewage sludge using coupled TG-FTIR. *Thermochim. Acta,* 404, 97-108.
102. Singare, P. U., Lokhande, R. S., & Madyal, R. S. (2010). Thermal degradation studies of polystyrene sulfonic and polyacrylic carboxylic cationites. *Russ. J. Gen. Chem.,* 80 (3), 527-532.
103. Yang, M., Tsukame, T., Saitoh, H., & Shibasaki,Y. (2000). Investigation of the thermal degradation mechanisms of poly(styrene-co-methacrylonitrile)s by ash pyrolysis and TG-FTIR measurements, *Polym. Degrad. Stabil.,* 67, 479-
489.
104. Drutsa, R., & Gutsanu, V. (2002). Obtaining selective sorbents for the sorption of food colorants from solutions. *Proceedings of the 1st International Symposium "Biochemistry and Biotechnology in the Food Industry"*. Chisinau: Tehnica-Info. 210-215. (In Romanian).
105. Gutsanu, V., & Drutsa, R. (2003). Pocess for modification with Al(III) compounds of the reticulate ionogenic polymers containing R_4N^+ groups. Patent MD 2241. *BOPI*, 8, 25.
106. Barry, T. Kilbourn. (1986). The role of the lanthanides in applied catalysis. *J. Less Common Metals,* 126, 101-106.
107. Koichi Mikami, Masahiro Terada, & Hiroshi Matsuzawa (2002). “Asymmetric” Catalysis by Lanthanide Complexes. *Angew. Chem. Internat. Ed*., 41, 3554-3572.
108. Allu Amarnath Reddy, Ashutosh Goel, Dilshat U. Tulyaganov, Mariana Sardo, Luis Mafra, Maria J. Pascual, … , & José M. F. Ferreira (2014). Thermal and mechanical stability of lanthanide-containing glass–ceramic sealants for solid oxide fuel cells. *J. Mater. Chem. A,* 2, 1834-1846.
109. Denkewicz, Jr., Raymond, P., Senderov, Ernest E., Grenier, Joseph W., & Souza, Therese (2001). Lanthanide halide water treatment compositions and methods. US Patent 6, 312,604.
110. Silvio Aime, Mauro Botta, Mauro Fasano, & Enzo Terreno (1988). Lanthanide (III) chelates for NMR biomedical applications. *Chem. Soc. Rev*., 27, 19-29.
111. Stephen Faulkner, Simon J. A. Pope, & Benjamin, P. Burton-Pye (2005). Lanthanide complexes for luminescence, imaging applications. *Appl. Spectrosc. Rev.,* 40, 1-31.
112. Marhol, M. (1985) *Ion exchangers in analytical chemistry*. Moscow: Мир.
113. Tatsuya Suzuki, Yasuhiko Fujii, Shin-ichi Koyama, & Masaki Ozawa (2008). Nuclide separation from spent nuclear fuels by using tertiary pyridine resin. *Prog. Nucl. Energ*., 50, 456-461.
114. Atsushi Ikeda, Tatsuya Suzuki, Masao Aida, Yasuhiko Fujii, Toshiaki Mitsugashira, Mitsuo Hara, & Masaki Ozawa (2005). A novel chromatographic separation technique using tertiary pyridine resin for the partitioning of trivalent actinides and lanthanides. *Prog. Nucl. Energ*., 47, 454 - 461.
115. Fausto Martelli, Sacha Abadie, Jean-Pierre Simonin, Rodolphe Vuilleumier, & Ricardo Spezia (2013). Lanthanoide (III) and actinoids (III) in water: Diffusion coefficients and hydration enthalpies from polarizable molecular dynamics simulations. *Pure Appl. Chem*., 85, 237-246.
116. Ho, Y. S., Ng, J. C. Y., & McKay, G. (2000). Kinetics of pollutant sorption by biosorbents: review. *Separ. Purif. Methods*, 29, 189-232.
117. Cheung, H. W., Ng, J. C. Y., & McKay, G. (2003). Kinetic analysis of the sorption of copper (II) ions on chitosan. *J. Chem.Technol. Biotechnol*., 78, 562-571.
118. Helfferich, F. (1962). *Ion exchangers.* Moscow: Izd. In. Lit.
119. Hall, K., Eagleton, L. C., Acrivos, A., & Vermeulen, T. (1966). Pore- and solid-diffusion kinetics in fixed-bed adsorption under constant-pattern conditions. *Ind. Eng. Chem. Fund*., 5, 212-223.
120. Gutsanu, V., & Cojocaru, L. (2005). Process for modification with Bi(III) compounds of the cross-linked ionic polymers containing highly basic groups. Patent MD 2706. *BOPI*, 2, 35,
121. Gutsanu, V., & Cojocaru, L. (2007). Process for obtaining selective sorbent containing Bi(III) compounds. Patent MD 3295. *BOPI*, 4, 42-43.

122. Gutsanu, V., & Cojocaru, L. (2008). Inorganic Bi(III) compounds in the phase of coss- linked polymers containing R_4N^+ groups. *Second International Conference on polymer blends,composites and gels, IPNs, membranes, polyelectrolites and gels: macro to nano scales 22-24 september, Kottayam Kerala, India,* 237-238.
123. Gutsanu, V., Cojocaru, L., Lisa, G., & Volodina, G. F. (2010) Ultrafine particles of Bismuth (III) compounds in the phase of crosslinked polymers: precursors for new sorbents and catalysts. *J. App. Polym. Sci.,*118, 2674-2681.
124. Gutsanu, V., Cojocaru, L., Lisa, G., & Volodina, G. F. (2012). Some metal compounds in the phase of crosslinked ionic polymer-precursors for new sorbents and catalysts. *J. App. Polym. Sci.,*124, 2582-2593.
125. Gutsanu, V. , Schitco,C., & Drutsa, R. (2008). Unforseen factors influencing Fe(III)- containing cations sorption on strongly basic anion exchangers. *J. App. Polym. Sc.,* 109, 2643-2647.
126. Scott, Keith M. (1990). Origin of alunite- and jarosite-group minerals in the Mt. Leyshon epithermal gold deposit northeast Queensland, Australia. *American Mineralogist*,75, 1176-1 181.
127. Dutrizac, J. E., & Kaiman, S. (1976). Synthesis and properties of jarosite-type compounds. *Can. Mineral*., 14, 151-158.
128. Dutrizac, J. E., & Chen, T. E. (2005). Factors affecting the precipitation of chromium(III) in jarosite-type compounds. *Metall. Materi. Trans*. *B*, 36, 33-42.
129. Dutrizac, J. E., & Chen, T. E. (2009). The behavior of Scandium, Yttrium and Uranium during jarosite precipitation. *Hydrometallurgy*, 98**,** 128-135.
130. Dutrizac, J. E., & Chen, T. E. (2003). Synthesis and properties of V^{3+} analogues of jarosite-group minerals. *Can. Mineral*., 41, 479-488.
131. Gutsanu, V., Lisa, G., Vizir, C., & Tudorachi N. (2014). Sorption and thermal properties of strongly basic cross-linked ionic polymer modified with Cr(III) compounds. *J. App. Polym. Sci.,* 41308. DOI: 10.1002/APP.41306.
132. Kannan, P., Biernacki, J. J., Visco Jr, D. P., & Lambert, W. J. (2009). Kinetics of thermal decomposition of expandable polystyrene in different gaseous environments. J Anal Appl Pyrol., 84, 139-144.
133. Friedman, H.L. (1964). Kinetics of thermal degradation of char-forming plastics from thermogravimetry. Application to a phenolic plastic., *J. Polym. Sci.,* 6, 183-195.
134. Vyazovkin, S.; Burnham, A. K.; Criado, J. M., Perez-Maqueda, L. A., Popescu, C., & Sbirrazzuoli, N. (2011). ICTAC kinetics committee recommendations for performing kinetic computations on thermal analysis data. *Thermochim. Acta,* 520, 1-19.
135. Niyazi Biçaak, & Bahire Filiz Şenkal (1998). Removal of nitrite ions from aqueous solutions by cross-linked polymer of ethylenediamine with epichlorohydrin. *React. Funct. Polym.,* 36, 71–77.
136. Yılmaz, Z., Kavakli Akkaş, P., Şen, M., & Güven, O. (2006). Removal of nitrite ions from aqueous solutions by poly(*N*,*N*-dimethylamino ethylmethacrylate) hydrogels. *J.App.Polym. Sci.,* 102, 6023–6027.
137. Gutsanu, V., Tutovan, E., Cotsofana, L., & Bulicanu, V. (2012). Nitrite ions sorption on strongly basic anion exchanger Purolite A-400 modified with Cr(III)-containing compounds. *Ion Exch. Lett.,* 5, 6-12.
138. STAS 11581-83. Produse de legume, fructe şi legume cu carne. Determinarea conţinutului de nitriţi şi nitraţi. Aprobat de Institutul Român de Standardizare. 1983, 02. 01, 4p (in Romanian).
139. Shuker, D. E. G. (1988). *The Chemistry of N-nitrosation in Nitrosamines.* In: *Nitrosamines: Toxicoligy and Microbiology*, edited by M. J.Hils. Cambridge: VCH Publishers.
140. Horöld S., Vorlop K-D., Tacke T., & Sell M. (1993). Development of catalysts for a selective nitrate and nitrite removal from drinking water. *Catalysis Today,* 17, 21-30.
142. Saba Samatya, Nalan Kabay, Ümran Yüksel, Müşerref Arda, Mithat Yüksel. (2006). Removal of nitrate from aqueous solution by nitrate selective ion exchange resins *React. Funct. Polym*., 66, 1206-1214.
142. Gutsanu, V., & Bulicanu, V. (2014). Removal of nitrate/nitrite ions by modified with metal-containing compounds strongly basic exchanger using response surface methodology. *Ion. Exch. Lett.*, 7, 1-5.
143. Gutsanu, V., & Bulicanu, V. (2015). Process for water purification from nitrates and nitrites. Patent MD 4318. *BOPI,* No.1, 33.
144. Roy, A. C., &.Datta S. K. (1985). Phosphate sorption isotherms for evaluating phosphorus requirement of wetland rice soils. *Plant. Soil.,* 86, 185-196.
145. Fernandes, M. L. V. , & Warren, G.P. (1994). Exchangeable and non-exchangeable phosphate sorption in Portuguese soils. *Fert. Res*., 37, 23-34.
146. Fox, R.L., & Kamprath, E.J. (1970). Phosphate sorption isotherms for evaluating the phosphate requirements of soils. *Soil Sci. Soc. Am. J*., 34, 911-916.
147. Rhodes, Edward R. (2006). Phosphate sorption isotherms for some Sierra Leone soils. *J. Sci. Food Agricult*., 26, 895-902.
148. Dye, C. (1995). Effect of citrate and tartrate on phosphate adsorption by amorphous ferric hydroxide. *Fert. Res.,* 40, 129-134.
149. Zongmin Ren, Lina Shao, & Gaosheng Zhang (2012). Adsorption of phosphate from aqueous solution using an iron-zirconium binary oxide sorbent. *Water, Air, Soil Pollut*., 223, 4221-4231.
150. Oliveira, M., Machado, A. V., & Nogueira, R. (2012). Phosphorus removal from eutrophic waters with an aluminum hybrid nanocomposite, *Water, Air, Soil Pollut*., 223, 4831- 4840.

151. Jae-Woo Choi, Seung-Yeon Lee, Sang-Hyup Lee, Ji-Eun Kim, Ki-Young Park, Dong-Ju Kim, & Seok-Won Hong (2012). Comparison of surface- modified adsorbents for phosphate removal. *Water, Air, Soil Pollut*., 223, 2881-2890.
152. Gutsanu, V. (2015). A composite containing Cr (III) compounds and its application to the selective sorption of phosphate ions. *IJSRSET,* 1, 367-378.
153. Elzinga, Evert J. & Sparks, Donald L. (2007). Phosphate adsorption onto hematite: An in situ ATR-FTIR investigation of the effect of pH and loading level on the mode of phosphate surface complexation. *Colloid. Interf. Sci*., 308, 53-70.
154. Zhongqi He, Wayne Honeycutt, Baoshan Xing, Richard W.McDowell, Perrz J.Pellechia, & Tieguan Zhang (2007). Solid-state Fourier transform infrared and ^{31}P nuclear magnetic resonance spectral features of phosphate compounds. *Soil Sci.,* 172, 501-515.
155. Weber, J. W. J. & Morris, J. C. (1963). Kinetics of adsorption on carbon from solution, *J. Sanit. Eng. Div. Am. Soc. Civil. Eng*., 89, 31-60.
156. Gerente, C., Leev. K. C., Le Cloirec, P., & McKay, G. (2007) Application of chitosan for the removal of metals from wastewaters by adsorption-mechanisms and models review, Crit. Rev. *Environ. Sci. Technol*., 37, 41– 127.
157. Foo, K. Y., & Hameed, B. H., (2010). Insights into the modeling adsorption isotherm systems. *Chem. Eng. J.,* 156, 2-10.
158. Brunauer, S., Emmett, P. H., & Teller, E., (1938). Adsorption of gases in multimolecular layers. *J. Am. Chem. Soc*., 60, 309-319.
159. Zelentsov, V. I., & Datsko, T. Y., (2012). Absorption models to describe the equilibrium in the aluminum oxyhydroxide - fluoride system. *Surf. Eng. App. Electrochem*., 48, 65-73.
160. Gutsanu, V., (2014). Iodine ions sorption on polymer AV- 17(Cl) and sorbent AV-17(Bi). *Chem. J. Mold*., 9, 90-98
161. Tania, V. Fernandes, T. V., Karel J. Keesman, K. J., Grietje Zeeman G., & Jules, B. van Lier, (2012). Effect of ammonia on the anaerobic hydrolysis of cellulose and tributyrin. *Biomass and Bioenergy*, 47, 316-323.
162. Lobanov, S.A. (2007). *Technology of separation and recycling of ammonia nitrogen from wastewater of the chemical plants*. Abstract Ph. D. dis., Permi (in Russia.).
163. Nebukhina, I.A.; Simonova, N.N., & Rvachev, I.S., (2015). Effect of organic compounds on the efficiency of removal of ammonium ions from wastewater by oxidation. *Questions Modern Sci. Pract., Vernadsky University*. DOI: 10.17277/voprosy, pp.028-033, 2015, (Russian Journal).
164. Shou-Qing Ni & Jian Zhang (2013). Anaerobic ammonium oxidation: from laboratory to full-scale application. *BioMed Research International*. 2013, 469360. DOI:10.1155/2013/469360.
165. Long-Fei Ren, Shou-Qing Ni, Cui Liu, Shuang Liang, Bo Zhang, Qiang Kong, & Ning Guo (2015). Effect of zero-valent iron on the start-up performance of anaerobic ammonium oxidation (anammox) process. *Environ. Sci. Pollut. Res*., 22, 2925-2934.
166. Nozhevnikova, A.N., Litty, Yu.V., & Zubov, M.G. (2015). Biotechnology of wastewater treatment with the effective removal nitrogen due to the participation of anammox-bacteria, developed for the 2014 Winter Olympics in Sochi. , *Ecological Engineering and Environment Protection,* No 2, 24-29.
167. Litty, Yu.V. (2012). *Anaerobic oxidation of ammonium and methanogenesis in the systems of aerobic wastewater treatment with immobilization microorganisms*. Abstract Ph.D. dis., Moscow State University M.V. Lomonosov.
168. Kazakova, E. (2011). *Removal of nitrogen by means of micro-organisms chemoautotrophic return flow treatment facilities of sewage sludge.* Abstract Ph.D. dis., Scientific-Rresearch Inst. VODGEO, Moscow.
169. Rajinikanth Rajagopal, Daniel, I. Masse, & Gursharan Singh. (2013). A critical review on inhibition of anaerobic digestion process by excess ammonia. *Bioresource Technology,* 143, 632-641.
170. Sprynskyy, M., Lebedynets, M., Terzyk, Artur P., Kowalczyk, P., Namie´snik J., & Buszewski, B. (2005). Ammoniumsorption from aqueous solutions by the natural zeolite Transcarpathian clinoptilolite studied under dynamic conditions. *J. Colloid Interface Sci*., 284, 408–415.
171. Lebedynets, M., Sprynskyy, M., Sakhnyuk, I., Zbytniewski, R., Golembiewski, R., & Buszewski, B. (2004). Adsorption of ammonium ions onto a natural zeolite: Transcarpathian clinoptilolite. *Adsorption Sci.Technology*, 22, 731-741.
172. Kucic, D., Markic, M., & Briški F. ((2012). Ammonium adsorption on natural zeolite (clinoptilolite): adsorption isotherms and kinetics modeling. *The Holistic Approach to Environment,* 2, 145-158.
173. Malyovannyi, M., Sakalova, G., Chornomaz N., & Oleh Nahurskyy, O. (2013). Water sorption purification from ammonium pollution. *Chemistry Chem. technology*, 7, 355-358.
174. Donghui Wen, Yuh-Shan Ho, Shuguang Xie and Xiaoyan Tang, ((2006). Mechanism of the adsorption of ammonium ions from aqueous solution by a Chinese natural zeolite. *Separation Sci.Technology*, 41, 3485–3498.
175. Khosravi, A., Esmhosseini, M., Jalili J., & Khezri, S. (2012). Optimization of ammonium removal from waste water by natural zeolite using central composite design approach. *J. Incl. Phenom. Macrocycl. Chem*., 74, 383-390.
176. Gupta, V.K., Salegh, H., Yari, M., Shahryari-ghoshekandi, R., Maazinejad, B., & Chahardori, M. (2015). Removal of ammonium ions from wastewater. A shot review in development of efficient methods. *Global J. Environ. Sci. Manage*, 1, 149-158.

177. Ola, I. El-Shafey, Nady, A. Fathy, & Thoria, A. El-Nabarawy (2014). Sorption of ammonium ions onto natural and modified Egyptian kaolinites: Kinetic and equilibrium studies. *Advan. Phys. Chem*., 2014, Article ID 935854, 12 pages, 2014. DOI:10.1155/2014/935854.
178. Alias Mohd Yusofa, Lee Kian Keata, Zaharah Ibrahimb, Zaiton Abdul Majida, & Nik Ahmad Nizamb (2010). Kinetic and equilibrium studies of the removal of ammonium ions from aqueous solution by rice husk ash-synthesized zeolite Y and powdered and granulated forms of mordenite, *J. Hazard. Mater*., 174, 380-385.
179. Marina Azevedo Souza, Susana Johann, Luciana Alves Rodriques dos Santos Lima, Fernanda Fraga Campos, Isolda Castro Mendes , Heloisa Beraldo,..., & Carlos Leomar Zani (2013). The antimicrobial activity of lapocol and its thiosemicarbazone and semicarbazone derivates. *Mem. Inst. Oswaldo Cruz*., 108, 342-351.
180. Özlen Güzel, Nalan Terzioğlu, Gültaze Çapan, & Aydın Salman. (2009). Synthesis and biological evaluation of new 5-methyl-*N*-(3-oxo-1-thia-4-azaspiro[4.5]-dec-4-yl)-3-phenyl-1*H*-indole-2-carboxamide derivatives. *ARKIVOC*. Issue 12, 98-110. DOI: http://dx.doi.org/10.3998/ark.5550190.0007.c12.
181. Negi Parul, Nandy Subhangkar & Mahato Arun. (2012). Antimicrobial activity of different thiosemicarbazone compounds against microbial pathogens. *IRJP*. 3, 350-363.
182. Velezheva, V., Brennan., Ivanov, P., Kornienko, A., Lyubimov, S., Kazarian, K., Nikonenko, B., Majorov, K., & Apt, A. (2011). Synthesis and biological evaluation of substituted 4-rylthiazol-2-amino derivatives as potent growth inhibitors of replicating *Mycobacterium tuberculosis* $H_{37}R_V$. *Bioorg. Med. Chem. Lett*., 21, 5589–5593.
183. Rosu, T., Gulea, A., Nicolae, A., & Georgescu, R. (2007). Complexes of 3d metal ions with thiosemicarbazones: synthesis and antimicrobial activity. *Molecules,* 12, 782-796.
184. Patel, A.L., & Chaudhary M. J. (2012). Synthesis, characterization and antimicrobial studies on bivalent copper, nickel and cobalt complexes of thiosemicarbazone. *Int .J. Chem.Tech. Res*., 4, 918-924.
185. Pahonțu, E., Ilieș, D-C., Shova, S. , Paraschivescu, C., Badea, M., Gulea, A., & Roșu, T. (2015). Synthesis, characterization, crystal structure and antimicrobial activity of copper (II) complexes with the Schiff base derived from 2-hydroxy-4-methoxybenzaldehyde. *Molecules,* 20, 5771- 5792.
186. Pahontu, E., Julea, F., Rosu, T., Purcarea, V., Chumakov, Y., Petrenco. P., & Gulea, A. (2015). Antibacterial, antifungal and *in vitro* antileukaemia activity of metal complexes with thiosemicarbazones. *J. Cell. Mol. Med.,* 19, 865-878.
187. Shivare, S., & Gautam, M. D. (2011). Synthesis, characterization and microbial study of complexes of Cu(II) and Ni(II) with thiosemicarbazone*. J. Chem. Pharm. Res*., 3, 682-688.
188. Patel, H. D., Divatia, S. M. & Clercq, E. (2013). Synthesis of some novel thiosemicarbazone derivates having anti-cancer, anti-HIV as well as anti-bacterial activity. *Ind. J. Chem*., 52 B, 535-545.
189. Tahmeena Khana, Rumana Ahmad, Seema Joshia, & Khan, A. R. (2015). Anticancer potential of metal thiosemicarbazone complexes: A review. *Der Chemica Sinica*. 6, 1-11.
190. Paden, K. A., Gellineau, H. A., Jung-Eun Ahn, MacMillan, S. N., & Wilson, J. J. (2017). Bis(thiosemicarbazone) complexes of cobalt(III). Synthesis, characterization, and anticancer potential*. Inorg. Chem*., 56, 6609–6623.
191. Asiri, A. M., & Khan, S. A. (2010). Palladium(II) complexes of NS donor ligands derived from steroidal thiosemicarbazones as antibacterial agents. *Molecules*, 15, 4784-4791.
192. Roman, O., & Gutsanu, V. (2018). Thiosemicarbazone immobilized on cross-linked ionic polymers. *Res. J. Live Sci. Bioinformatics, Pharmaceutical Che. Sci.,* 4, page No 225. DOI - 10.26479/2018.0402.17.
193. Kreshkov, A.P. (1965). *Fundamentals of Analytical Chemistry*. *V.2*. Moskow: Khimia.
194. Graur, V. (2015). Synthesis, structure and biological activity of N(4)-allyl-3-thiosemicarbazones and their coordination compounds with some 3d metals. *Studia Universitatis Moldavie.* 6, 130-141.
195. Gutsanu, V. (2008). Ultrafine particles of inorganic compounds in the phase of strongly basic exchangers, *Second Internatonal Conference on polymer blends, composites and gels, IPNs,embranes, polyelectrolites and gels: macro to Nano scales 22-24 september, Kottayam Kerala, India,* 129.
196. Gutsanu, V. (2013).Unforeseeable processes in the systems containing strongly basic cross linked ionic polymer and $Fe_2(SO_4)_3$ solution. *Adv. Chem. Sci*., 2, 96-99.
197. Gutsanu, V. (2015). Ionic-molecular constructions in the polymer phase - a new way to obtain different materials with selective properties. *IJIRSET,* 4, 8989 - 9001.
198. Eremin, L. P., Poleschuk, O.H., Babovskaya, L.A., & Egorov, N. B. (1999). Investigation of the mechanism of photolysis of solid inorganic thiocyanate using semi-empirical quantum-chemical calculations. *Bulletin of Tambov State Pedagogical University. Series of natural and exact sciences.* 7, 21-26 (in Russian).
199. Stroeva, E. V. (2004). *Physico-chemical bases of extracting iodine from solutions of highly mineralized Orenburg gas condensate*. Ph.D. thesis, Mendeleev MCT University, Moscow.
200. Myagkoy, O. N., Krasova, K. N., Serdiucova, M. I., & Meleshko, B. P. (1974). *Theory and practice of the sorption processes.* Voronezh State University: Voronezh. (in Russian).
201. Myagkoy, O. N., & Serdiucova, M. I. (1977). *Theory and practice of the sorption processes*. Voronezh State University: Voronezh. (in Russian).
202. Myagkoy, O.N.; Serdiucova, M.I., & Seryacenko, L. A. (1981). *Theory and practice of the sorption processes.* Voronezh State University: Voronezh. (in Russian).
203. Serdiucova, M. I. (1984). *Theory and practice of the sorption processes*. Voronezh State University: Voronezh. (in Russian).
204. Vulih, A.I., & Dubinina, E. G. (1976). *Redox macromolecular compounds*. Khimia: Leningrad (in Russian).

205. Myagkoy, O. N., Serdiucova, M. I., & Perunova, N.A. (1980). *Theory and practice of the sorption processes*. Voronezh State University: Voronezh. (in Russian).
206. Gutsanu, V. (2014). Iodine ions sorption on polymer AV-17(Cl) and sorbent AV-17(Bi). Chem. J. Moldova. 9, 90-98.
207. Vasilenko, I. Ja., & Vasilenko, O. I. (2003). Radioactive iodine. *Energy: Economics, Technology and Ecology*, No. 5, 57-62.
208. Rovny, S. I., Piatin, N. P., & Istomin, I. A. (2006). Sorbent for the capture of radioactive iodine from the gas phase. Патент RU 2288514.
209. Metalidi, M., Koliadin, A.B., Beznosiuk, V. I., & Fedorov , Yu. S. (2011). Method for cleaning gas streams from iodine. Patent RU 2414280.
210. Gutsanu, V., & Copusciu Iu. (2015). Proces for air purification from iodine. *BOPI*, No 2, 26.
211. Gutsanu, V. (2013). Process for recovery of sulphide and hydrogenosulphide ions from solutions. Patent MD 4241. *BOPI,* No.7, 26.
212. Gutsanu, V. (2016). Process for air purification from sulphureted hydrogen. Patent MD 4400. *BOPI*, No.2, 31.
213. Betehtin, A. G., (2010) *Mineralogy course*. Moscow: Book House "University".
214. Gutsanu, V. L., Turta, C. I., Ropot, V. M., & Dogary, Gh. N. (1977). Magnetic properties of low-copper anion exchangers AV-16G, AN-2FN and EDE-10P. *Zh. Fiz. Khim*., 51, 1513-1516.
215. Gutanu, V., Rusu, V., & Druta, R. (2003). Kinetics of sorption of Fe(III) hydroxocations by strongly basic anion exchangers. *Revista Chim*., 54, 359-65 (in Romanian).
216. Day, C., & Selbin, I. (1969). *Theoretical Inorganic Chemistry*. Moscow: Khimiya.
217. Betley, T. A., & Peters, J. C. (2003). Dinitrogen chemistry from trigonally coordinated iron and cobalt platforms. *J. Am. Chem. Soc.,* 125, 10782-10783.
218. Smith, J. M., Sadique, A. R., Cundari, T. R., Rodgers, K. R., Lukat-Rodgers, G.; Lachicotte, J., ..., & Holland, P. L. (2006). Studies of llow-coordinate iron dinitrogen complexes. *J. Am. Chem. Soc*., 128, 756-769.
219. Mankad, N. P., Whited, M. T., & Peters, J.C. (2007). Terminal FeI… N_2 and FeII…HC interactions supported by tris(phosphino)silyl ligands. *Amgew. Chem.,* 119**,** 5870-5873.
220. Šarić, A., Musić, S., Nomura, K., & Popović, S.(1998). Microstructural properties of Fe-oxide powders obtained by precipitation from $FeCl_3$ solutions. *Mater. Sci. Engin. B*., 56, 43-52.
221. Musić, S., Krehula, S., Popović, S., & Skoko, Ź. (2003).Some factors influencing forced hydrolysis of $FeCl_3$ solutions. *Mater. Lett*.**,** 57*,* 1096-1102
222. Madden, M. E. E., Bodnar, R. J., & Rimstidt, J. D. (2004). Jarosites as an indicator of water-limited chemical weathering on Mars. *Nature*, 431**,** 821-823.
223. Rull, F., Fleischer, I., Maretinez-Frias, J., San, A., Upadhyay, C., & Klingelhofer, G. (2008). Raman and Mössbauer spectroscopic characterization of sulfate minerals from the Mars analogue sites at Rio Tinto and Jaroso Ravine, Spain. *Lunar and Planetary Science*. XXXIX**,** 1616.pdf.
224. Zolotov, M. Y., & Shock, E. L. (2005). Formation of jarosite-bearing deposits through aqueous oxidation of pyrite at Meridiani Planum. *Geophys. Res. Let*., 32**,** 1-5.
225. Navrotsky, A., Forray, F. L., & Drouet, Ch. (2005). Jarosite Stability on Mars. *Icarus,* 176, 250-253.
226. Villanueva, G. L.,Mumma, M. J., Novac, R. E., Radeva, Y. L., Kaufl, H.U., Smette, Tokunaga A., ..., & Hartogh, P. (2013). A Sensitive search for organics (CH_4, CH_3OH, H_2CO, C_2H_6, C_2H_2, C_2H_4), hydroperoxyl (HO_2), nitrogen compounds (N_2O, NH_3, HCN) and chlorine species (HCl, CH_3Cl) on Mars using Ground-based High-resolution Infrared Spectroscopy. *Icarus*, 223**,** 11-27.
227. Mahaffy, P. R., Webster, Ch. R., Atreya, S. K., Franz, H., Wong, M., Conrad, P.G., ... , & Trainr, M. (2013). Abundance and isotopic composition of gases in the Martian Atmosphere from the Curiosity Rover. *Science*, 341**,** 263-266.

ANNEXE

A brief description of the parameters of Mössbauer spectroscopy [1-3].

1. Isomeric shift (δ). Isomer shift (**δ**) is sometimes called the chemical shift, especially in the older literature. The isomeric shift of the spectral line is conditioned by the interaction of the Coulomb type forces of the atomic nucleus charge with the surrounding electrons. The analytical expression of the isomeric shift is as follows:

$$\delta = (2\pi Ze^2/5)(R_e^2 - R_g^2)\,[|\Psi_s(0)|_b^2 - |\Psi_s(0)_a|^2] \qquad \text{(a-1)}$$

where: *Ze* is the nucleus charge, *e* is the electron charge, R_e^2 and R_g^2 are the effective nuclear charge radius of the excited state and ground state, $[\Psi s^2(0)]_a$ and $[\Psi s^2(0)]_b$ are the electron density on the nucleus surface of source(a) and sample (b).

From equation (1) it follows that **δ** is a function of the difference between the radius of the nucleus in the excited and fundamental state and of the difference in the electronic density on the atomic nucleus of the sorbent and of the source. Only the electrons of the **s** type have a density on the atomic nucleus different from zero. The electron density of **p**, **d** or **f** electrons on the surface of the atomic nucleus is null. Electronic density on the atomic nucleus surface of electrons **1s** does not differ essentially from that of electrons **2s**. An essential change in the electronic density on the nucleus is caused by the **3s** type electrons which are sensitive to the entourage of the atom. It is believed that this change is caused by the effect of shielding electrons of type **3s** by **d**-type electrons.

To each adsorbent (M**ö**ssbauer nucleus) there corresponds a certain source of γ-rays. The most commonly used system is the ^{57}Co γ-ray source and the ^{57}Fe absorber.

If the temperature of the adsorbent differs from the source temperature, the value of **δ** also depends on the temperature. For substances containing ^{57}Fe in the temperature range of 80-300 K, the temperature-dependent isomeric shift varies up to 0.08 mm/s (1 mm/s = $8.8\cdot10^{-8}$ eV; 1 eV = $1.60217733*10^{-19}$ Joule).

For ^{57}Fe, $R_e^2 < R_g^2$ and for ^{119}Sn $R_e^2 > R_g^2$. The more electrons of type **p** and **d** contained in the atom, the higher is the shielding degree of electrons of type **s** and the lower the $|\Psi_s(0)|_b^2$. So in iron compounds with the higher degree of covalency of chemical bonds, **δ** is lower and in ionic compounds - larger. For iron compounds with high spin **δ** is higher than for the compounds with a low spin state. The isomeric shift is a relative magnitude, so it is necessary to indicate the reference substance. This is usually sodium nitroprusside: $Na_2[Fe^{III}CN)_5NO]*2H_2O$.

The **δ** value for Fe^{3+} in the compounds generally ranges up to 0.9 mm/s, and for Fe^{2+} - from 1.0 to 1.8 mm/s.

2. Quadrupole splitting (ΔE_Q). Quadrupole splitting of Mössbauer lines is caused by interaction of the quadrupole moment (**eQ**) of the nucleus with the electric field gradient (**EFG**) created by the asymmetric distribution of the electric entourage. Nuclei having a nuclear spin (**I**) equal to zero and 1/2 are spherical, and their quadrupole moment is zero. Nuclei having I > 1/2 have a quadrupole moment different from zero. The nucleus of the ^{57}Fe atom in the ground state has I = 1/2 and, therefore, eQ = 0, and in the excited state I = 3/2 and $eQ \neq 0$.

The eQ interaction with EFG leads to partial splitting of nuclear energy levels (2I + 1). EFG occurs because of: a) the asymmetric distribution of the electrons of own atom (ion), and b) the asymmetric distribution of the electrons of the ligands. The energy of quadrupolar interactions is calculated with Equation (a-2):

$$E_o = (1/4)\,V_{zz}\,e^2Q[3m^2 - I(I+1)/3I^2 - I(I+1)] \qquad \text{(a-2)}$$

where: **eQ** is quadrupole moment; **m**- projection of the nuclear spin **I** on the **Z** axis, which can have values from + **I** to **-I**; $\mathbf{V_{zz} = \partial^2 v/\partial^2 z}$ - the electrical gradient component in the direction of the **Z** axis, and **v**- the potential of the electric field.

The ΔE_Q is calculated with Equation (a-3):

$$\Delta E_Q = Qe^2q\,(1+\eta^2/3)^{1/2}\,(1-\gamma_\infty) \qquad \text{(a-3)}$$

where: **q** is electric field gradient; **$(1-\gamma_\infty)$** - antishielding factor; and **η** - antisymmetry parameter.

The + or - sign of **q** is determined from the M**ö**ssbauer spectrum obtained by applying an external magnetic field greater than 30 kOe.

The quadrupole splitting is conditioned both by the symmetry of the electron distribution of the investigated atom, as well as of the ligands. The contribution to ΔE_Q of the electrons of the atom with the asymmetrical distribution is greater than the asymmetry of the distribution of the electrons (charges) of the ligands.

The Fe^{3+} ion has the **$3d^5$** electron configuration, and the electron distribution is symmetrical. If the distribution of ligand charges is symmetrical ($FeCl_4^-$), then for Fe^{3+} in compounds $\Delta E_Q = 0$ and the M**ö**ssbauer spectrum will contain only one spectral line (Fig. a-.1b) However, if the ion complex contains different ligands ($[Fe(OH)_2Cl_2]^-$), then $\Delta E_Q \neq 0$ and the spectrum consists of two spectral lines (Fig.a-1c).

In all the Fe^{2+} compounds a quadrupole splitting occurs because an electron of $3d^6$ leads to the asymmetry of the electrical charges distribution around the nucleus and $\Delta E_Q \neq 0$. Therefore, M**ö**ssbauer spectra of compounds of Fe^{2+} contain two spectral lines (i.e. they have a doublet form) (Fig.a-1c).

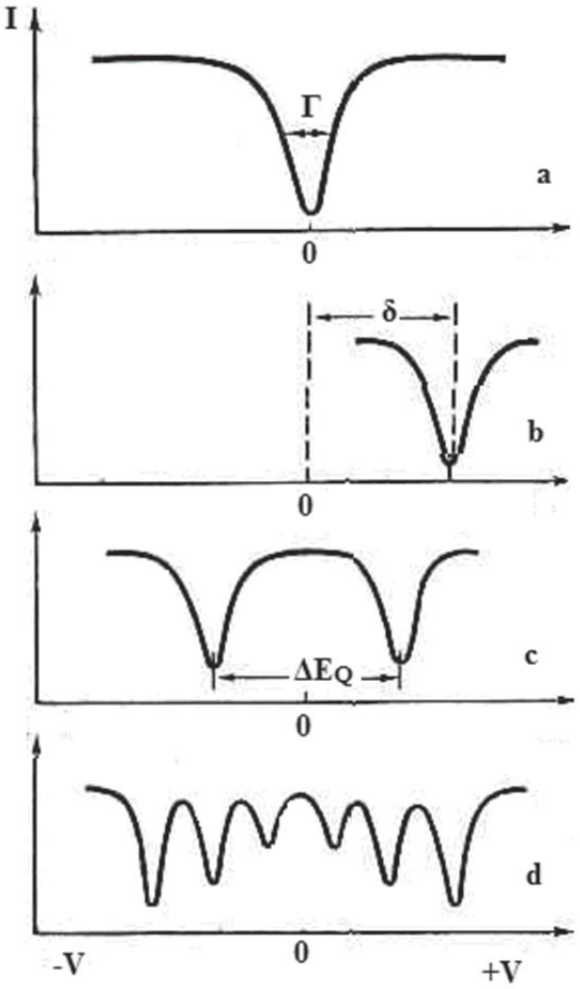

Figure a-1. The Mossbauer spectra and their parameters.

In Fe^{3+} compounds, the ΔE_Q value usually ranges from 0 to 0.9 mm/s, but there are also compounds for which ΔE_Q is greater than 1 mm/s. In Fe^{2+} compounds the ΔE_Q varies from 1.5 to 3.7 mm/s.

3. Magnetic hyperfine splitting (magnetic hyperfine structure). The hyperfine magnetic structure appears as a result of the interaction of the nuclear magnetic moment (**μ**) with the magnetic field (H) on the nucleus (internal field) that is created by its atom itself. As a result of these interactions, the energy levels of the nucleus in the ground and excited states are split. In this case, the energy levels are described with Equation (a-4):

$$E_m = \mu m_I H/I = g\mu_n m_I H \qquad \text{(a-4)}$$

where: **μ** is the magnetic moment of the nucleus; **μ_n** – the nuclear magneton; **g-** the gyromagnetic constant; **m_I = I, I-1, …., -I** –(the magnetic quantum number of the nucleus); **H -** the intensity of the magnetic field around the nucleus; and **I -** the spin of the nucleus in the considered state of energy.

As a result of these interactions, the energy levels of the nucleus in the ground and excited state are split into **2I+1** components. The M**ö**ssbauer spectrum of ^{57}Fe, in this case, has a hyperfine structure consisting of 6 lines of different intensity (Fig.a-1d).

From the spectrum in the form of sextet is calculated the effective intensity of the internal magnetic field around the nucleus ($\mathbf{H_{ef}}$), a useful parameter of the M**ö**ssbauer spectroscopy.

4. The width of the spectral lines (Γ). The width of the spectral line (**Γ,** mm/s) assumes the width of the half height of the peak (Fig.a-1a). The theoretical width of the spectral line for Fe is

$\mathbf{\Gamma_o} = 4.6*10^{-9}\mathbf{eV}$ or $\mathbf{\Gamma_o} = 0.095$ mm/s. Instead, the experimental spectral line is much larger.

In the case of a doubled spectrum, peaks could be asymmetric. This is why the width of the line on the left ($\mathbf{\Gamma_l}$) and the line on the right ($\mathbf{\Gamma_r}$) of the spectrum is measured. One of the causes of peak asymmetry is the vibration of the nucleus (atom, ion) Mössbauer in the plane and normal on the surface of the solid body [4]. The width of the spectral line ($\Delta\mathbf{\Gamma} = \mathbf{\Gamma_{exp.}} - \mathbf{\Gamma_{teor.}}$) is caused by several factors:

- Diffusion of the M**ö**ssbauer atom (ion) on the surface and/or in the solid body volume.
- Spin-spin relaxation or spin-lattice relaxation.
- Superposition of several spectral lines of different states of the M**ö**ssbauer atom.
- The thickness of the adsorbent layer.
- Functionality of the apparatus.

Ion exchangers have proven to be good physical models for research of the relaxation processes using M**ö**ssbauer spectroscopy [5]. In the case of spin-spin relaxation, the form of the spectrum does not change with temperature variation, but changes with the variation in the concentration of M**ö**ssbauer atoms in the sample of the absorber. If the shape of the spectrum changes with temperature variation but does not change with the variation in the concentration of M**ö**ssbauer atoms, then spin-lattice relaxation occurs.

From the width data of the spectral lines, we can determine the diffusion coefficient of the M**ö**ssbauer atoms in the ropy and solid systems [2, 6] and the duration of the localization of the atoms (ions) on the active centres of the sorbent, the ion exchanger [7].

a) For diffusion in viscous media:

$$\Delta\Gamma = 2E_o^2D/\hbar c^2 = 2\hbar x^2D \qquad \text{(a-5)}$$

where: $\mathbf{E_o}$ is the gamma-ray energy; $\mathbf{D = kT/6\pi\eta R\eta}$ - diffusion coefficient; $\mathbf{x - E_o/\hbar c, \hbar = h/2}$,

c - the speed of light in a vacuum; **h** - Planck's constant; **k** - Boltzmann's constant; **T** - thermodynamic temperature; **η** - viscosity of medium; and **R** - the radius of the spherical particle that diffuses.

b) For jump diffusion:

$$\Delta\Gamma = 2\hbar/\tau;\ \tau \approx b^2/6D^2 \ [2] \qquad \text{(a-6)}$$

where: **τ** is the particle localization time on the active centre of the sorbent; **b** - the distance between the active centres of the sorbent on which the jump occurs (the length of the jump); and

D – the diffusion coefficient by a jump.

For ^{57}Fe ions a width in the spectral line is observed the $\tau \leq 10^{-7}$s and $D > 19^{-9}$ cm/c [2].

5. The Mössbauer effect probability (f ') for absorbent. The probability of the M**ö**ssbauer effect, together with the width of the spectral line (**Γ**), is of particular importance for studying the dynamics (parameters related to thermal fluctuations) of ions (atoms) in compounds. In the most general form, the probability of the M**ö**ssbauer effect for the absorbent can be expressed by the following formula (a-7):

$$f' = \exp(-\langle X^2\rangle / \lambda_o^2) \qquad \text{(a-7)}$$

where: $\langle X^2 \rangle$ is the square of the vibration projection of the nucleus in the γ-ray propagation direction; and λ_o^2 is the square of the characteristic wavelength of the γ-ray.

In the Debye solid body model the temperature dependence is described by Equation (a-8):

$$(f)_T = \exp\{- 6R/k\theta[0.25 + (T/\theta)^2 \int_0^x \frac{xdx}{e^x - 1}]\} \quad \text{(a-8)}$$

where: $\mathbf{x = \theta/T}$; **R**- recoil energy of the lattice; **θ** - Debye characteristic temperature ($\mathbf{k\theta = h\nu_{max}}$.); **k** - Boltzmann's constant; and $\mathbf{\nu_{max}}$- the upper limit of the particle (atom, ion) vibration frequency.

With the temperature increase of the absorbent, $\langle X^2 \rangle$ increases and **f** decreases. The M**ö**ssbauer spectrum cannot be obtained if the probability of the effect is zero. Therefore, the M**ö**ssbauer spectrum of low viscosity solutions cannot be obtained. This allows us to determine whether the sorbate-sorbent interactions are of a physical or chemical nature. If the cations (Fe^{2+}, Fe^{3+} and others) are retained by the ion exchangers as a result of the Coulomb interactions, then their mobility in a wetted sorbent in the water is large and the probability of the M**ö**ssbauer effect is zero. In this case, at temperatures higher than the melting temperature of the ice, the M**ö**ssbauer spectrum cannot be obtained. However, if the cations are retained by the ion exchangers as a result of coordination with the atoms of the functional groups, then the M**ö**ssbauer spectrum of the polymer sample wetted in water will be obtained at any temperature.

If the cations are retained by the ion exchanger both as a result of ion exchange and as a result of complex formation, then on the graph **f**, depending on the temperature of the wetted sample, a sharp change will occur at about 0^oC. The M**ö**ssbauer effect probability may also depend on the degree of cross-linking of the polymer. The cation coordinated with the electron donor atoms in the polymer matrix will vibrate on the axis of the chemical bond, but if the polymer is moistened it will vibrate along with the polymer chain. Thus, the M**ö**ssbauer effect will have two components. Sometimes metal cations in the polymer phase form inorganic compounds in the form of particles [8,9]. If the particles are very small, then they can diffuse in liquid in the wet polymer and at temperatures higher than the freezing temperature of the solvent, the M**ö**ssbauer spectrum will not be obtained. But after drying the polymer the spectrum will be obtained [8].

References

1. Goldansky, V.I. (1970). *Chemical Applications of Mossbauer Spectroscopy*. Moscow: Mir.
2. Turta, C. (2003). *Introduction to gamma resonance spectroscopy (Mossbauer Spectroscopy)*. Chisinau: CEP USM. (In Romanian).
3. Barb, D. (1972). *The Mossbauer effect and its applications*. Bucharest:ARSR. (In Romanian).
4. Goldarsky, V.I., Makarov, E. F.,Stucan, R. A.,Sumarokova, T. N., Truhtanov, V. A., & Khrapov, V.V. (1964). Features of the Mössbauer effect for tin compounds with a coordinate number of six. Dokl. AN.SSSR. 136, 400 – 403.
5. Suzdalev, I. P., Afanasyev, A. M., Plachinda, A.S., Goldarsky, V.I., & Makarov, E. F. (1968). Study of the spin-lattice structure of Mössbauer spectra of Fe^{3+}. *J. Experiment. Theoret. Phys.* 55, 1752 - 1765.
6. Johanson, A (1969). Mossbaue spectra of ^{57}Fe in ion exchange resins. *J. Inorg. Nucl. Chem*., 31, 3273 - 3285.
7. Suzdalev, I. P., Plachinda, A.S., Makarov, E. F., & Dolgopolov, V.A. (1967). Investigation of ion-exchange resins using γ-resonance spectroscopy (the Mossbauer effect). *Zn. Phis. Khim*., 42, 2831- 2837.
8. Gutsanu, V.L., Stukan, R.A., Turta, C.I., & Gafiichuk, V.A. Mössbauer spectra of iron(III) ions sorbed by the anion exchanger EDE-10P and AV-17 from solutions of various salts. *Zn, Phis. Khim*. 60, 936 -940.
9. Gutsanu,V., Schitco, C., Lisa, G., & Turta, C. (2011). Ultra-dispersed particles of Fe(III) compounds in the strongly basic cross-linked ionic polymer-precursors for new sorbents and catalysts. *Mater. Chem. Phys.,* 130, 853– 861.